SEDIMENTOLOGY, GEOCHEMISTRY, VOLCANOLOGY AND BASIN EVOLUTION OF THE SOLDIERS CAP GROUP, EASTERN SUCCESSION, MT ISA INLIER, NORTHWEST QUEENSLAND, AUSTRALIA.

Owen J. Hatton
B.Applied Science-Applied Geology (Hons)
University of Technology, Sydney

UNIVERSITY OF TASMANIA

Submitted as fulfillment of the requirements for the degree
of Doctor of Philosophy

CODES SRC
Centre for Ore Deposit Research

School of Earth Sciences
University of Tasmania
April 2004

Declaration

This thesis contains no material that has been accepted for the award of a degree or diploma at any other institution. To the best of the authors knowledge, this thesis contains no material previously written or published by another person, except where due reference is given in the text. All referenced material is listed at the back of the thesis.

Owen J. Hatton

Date: 20/04/2004

Authority of Access

This thesis is not to be made available for copying or loan for a period of no less than eighteen (18) months from the date of this statement. Following that time the thesis may be made available for limited loan or photocopying in accordance with the *Copyright Act* of 1968.

Owen J. Hatton

Date: 20/04/2004

ABSTRACT

The Soldiers Cap Group is a polydeformed, complexly altered and highly metamorphosed volcanosedimentary terrane which represents the easternmost extent of outcropping lithologies of the informal Maronan Supergroup, in the Mesoproterozoic Eastern Succession of the Mt Isa Inlier, northwestern Queensland, Australia. The Maronan Supergroup is a regionally important sequence hosting a range of base and precious metals deposits. This study presents the results of a detailed program of field mapping and sampling, whole rock and isotopic geochemistry, undertaken to 'look through' the deformation, alteration and metamorphism to determine the primary sedimentological, volcanological and geochemical processes, and define detrital source areas and orientations of the host basin of the upper Soldiers Cap Group. Although the Soldiers Cap Group is interpreted as extending well south and west of the Williams Batholith, this thesis is only based upon the area of extensive outcrop to the north and east of the batholith.

A revision of the lithostratigraphy of the upper Soldiers Cap Group along genetic lines has resulted in the definition of 3 major and 5 minor sub-units within the Mt Norna Quartzite. Sedimentological structures preserved in quartzites, psammites and psammopelites include swaley- and hummocky-bedforms, climbing ripples, hummocky cross stratification, rip-up clasts, trough cross-bedding, extremely thickly- bedded quartzites, and cycles of massive quartzite. When these are placed into the new lithostratigraphic framework for the upper Soldiers Cap Group, the sedimentary processes of deposition are defined as storm generated currents above storm wave-base inducing oscillatory flow which then continued below storm wave-base as sand rich turbidity currents (tempestites). Once thought to be a deeper water turbidite sequence, this new interpretation places the environment of deposition for the upper Soldiers Cap Group at a narrow, storm-dominated shelf. A probable shallowing upward succession is suggested by a marked change from the underlying turbidites with classical Bouma sequences of the Llewellyn Creek Formation to the debris flow and turbidity current dominated basal Mt Norna Quartzite. Similarly in the mid Mt Norna Quartzite there is a discrete change in the sedimentological environment from turbidity current to tempestite dominated units. The sedimentology of the overlying Toole Creek Volcanics was not as well studied

due to poor outcrop. However, the presence of similar sedimentary structures in the Toole Creek Volcanics suggests the continuation throughout the upper part of the sequence, of the processes occurring in the mid Soldiers Cap Group.

Despite the lower amphibolite facies metamorphic grade and numerous regional alteration events, metabasalts and metadolerites of the upper Soldiers Cap Group have numerous well preserved contact relationships with adjacent metasedimentary lithologies. These include stratigraphically well constrained, brecciated (peperites), planar and diffuse contacts, all of which are indicative of synsedimentary sill emplacement. Within parts of the upper Soldiers Cap Group, distinctive volcanic structures including pillowed flows and in-situ hyaloclastites represent a sequence of synsedimentary flows. The geochemical signature of these mafic rocks defines them as ferrobasalts ($\geq$ 12wt% FeO_t) with continental tholeiite affinities derived from partial melting of an N-MORB source, with an unquantified degree of crustal contamination. Fe-enrichment in the Soldiers Cap Group is always associated with increased Ti, P and Zr. Mafic units with a well defined Fe-Ti-P fractionation trend, interpreted as representing crystallization of Ti-magnetite and apatite, occur in the Weatherly Creek Syncline. Lower Fe-Ti-P units occur in the Pumpkin Gully Syncline where early fractionation of Fe-Ti-P phases was suppressed. Units with intermediate Fe-Ti-P values in the Toole Creek Syncline require the mixing of magmas from at least two magma chambers with differing fractionation histories. Ferrobasalt sequences are generally produced in discrete, high level chambers separated from the main magma source in active tectonic environments, where composition is controlled by the rate of magma resupply, redox conditions (fO_2), size of the magma chamber and cooling rates. In the case of the Soldiers Cap Group the more Fe-enriched sequence of the Weatherly Creek Syncline represents a closed magma chamber, with limited magma resupply where fO_2 controlled magnetite fractionation. Conversely, the Pumpkin Gully Syncline sequence represents a smaller, more open, magma chamber in which resupply was an important process. Selected immobile and rare earth elements were used to define a geochemical 'fingerprint' for the Soldiers Cap Group metatholeiites that is distinct from other Mt Isa Inlier basalts and could be of use in future exploration.

Detailed geological mapping, combined with petrographic and whole-rock geochemical studies of two mineralised and barren, unusually apatite+Mn-garnet rich, stratigraphically well-constrained, laterally extensive iron formations, allowed a confident interpretation of their genesis. Concordant contact relationships with surrounding units, rare erosional contacts, an uncommon P-Mn rich mineralogy and predeformational quartz-epidote±carbonate(±garnet) alteration haloes, all indicate that they are the product of primary, hydrothermally derived, chemical sedimentation. Multivariate statistics were used to define groups of elements with strong interelement correlations, which were then refined by bivariate plots. This method defined mixed hydrothermal detrital and minor hydrogeneous components. The hydrothermal component comprised two stages, a relatively simple Fe-Si stage and a more complex P-Mn-Eu-Ca bearing stage. Detrital input was largely from extrabasinal mafic sources located presently to the east of the Soldiers Cap Group. Minor hydrogeneous uptake of (Pb+Zn)-Mn also occurred. Positive Eu anomalism and distinct chondrite normalised REE patterns represent reduced, acidic, Fe-P-Mn rich hydrothermal fluids with temperatures of $\geq 250°C$. To account for these features, large scale convection cells in overpressured sections of the sedimentary pile are proposed. These were driven by the intrusion of fractionating Fe-rich magma chambers into the lower parts of the basin. These generally metal-poor aquifers were breached by renewed movement on extensional faults resulting in fluid expulsion along these structures to the sediment-water interface, where they mixed with cold oxidised seawater in restricted, relatively quiescent seafloor depressions. The anomalous P-Fe-Mn rich geochemical signature similar to that of exhalites associated with base-metals mineralization globally (Sullivan, Canada and Broken Hill Australia) has important implications for future exploration within the Maronan Supergroup.

U-Pb dating of detrital zircons from three samples covering ~4km of stratigraphic thickness from the basal Mt Norna Quartzite to the mid Toole Creek Volcanics, by the recently developed Laser Ablation Inductively Coupled Plasma Mass Spectrometry (LA-ICP MS) method, provided insights into possible source terranes for the Soldiers Cap Group. Pb^{207}/Pb^{206} probability plots define several zircon populations. The dominant age inheritance is represented by a *ca.* 1750 Ma peak consistent with a source from Mt Isa Inlier Cover Sequence 2 volcanosedimentary units. Possible contributing sequences include the 1760-1720 Ma Mary Kathleen

Group, the *ca.*1740 Ma Mt Fort Constantine Volcanics, and units of the similarly aged Ballara Quartzite, Marraba Volcanics and Mitakoodi Quartzite. Other detrital populations include a *ca.*1970 Ma population interpreted as representing zircons from the earliest rifting events in the Mt Isa Inlier, a *ca.*1860 Ma peak consistent with Barramundi Basement equivalents in the Eastern Succession, a *ca.*1790 Ma aged population likely sourced from the Argylla Formation, *ca.*1680 Ma 'Maronan Supergroup' aged zircons, and a *ca.*1580 Ma population representing metamorphic overgrowths. The *ca.*1790 Ma population, present in other samples, is absent from the upper Mt Norna Quartzite suggesting changes in extrabasinal erosion patterns. Age populations present in all samples include a *ca.*2450 Ma Archaean peak which has a poorly constrained source within the region and likely represents significant recycling of grains. These age dates suggest that much of the material for the Soldiers Cap Group could be derived from Eastern Succession units and that the Maronan Supergroup was likely formed proximal to the eastern margin of the ancient Mt Isa Inlier.

Basin scale structural controls in comparable volcanosedimentary sequences are commonly unraveled using isopachs or balanced cross section methods. Strong deformation and the current subvertical orientation of the stratigraphy largely prevented this in the Soldiers Cap Group. The approach taken in this study was to combine sedimentology with palinspastically reconstructed palaeoflow markers, volcanology, detrital zircon data and interpretations of iron formation genesis to determine the orientation and nature of the host basin to the Soldiers Cap Group at Mt Norna Quartzite-Toole Creek Volcanics time. Based upon mapped thickness and lithostratigraphic changes, map scale faults in the Weatherly Creek Syncline area (Lomas Creek Faults, Mt Norna Fault) are now interpreted as synsedimentary faults. Reconstructed palaeocurrent markers interpreted to represent shore-normal flow and detrital zircon U-Pb provenance data, concur, indicating a broadly south-southeast deepening basin. The Lomas Creek Faults are now interpreted as the result of renewed extension in the upper part of a classical 'sag-phase' of an intracontinental rift. Faulting was possibly initially controlled by a larger scale fault, represented by the modern Cloncurry Overthrust. To account for mapped thickness changes in the mid-Mt Norna Quartzite, extension was likely transferred to an as yet unidentified fault to the southeast of the study area.

Comparisons to other Proterozoic terranes worldwide show that there are at least two close geological analogues for the Soldiers Cap Group. These are the Aldridge Formation, Belt-Purcell Basin, B.C. Canada, host to the massive Sullivan Pb-Zn deposit and the Etheridge Group, Georgetown Inlier, northeast Queensland, Australia. Analogous features include several basin-wide extension events associated with hydrothermal activity and linked to voluminous Fe-tholeiite magmatism, chemical sedimentation, input of coarser sediment, and synsedimentary faulting. These three basins may represent an as yet unrecognized variant on the accepted genetic evolution of the sag-phase of intracontinental rift basins. This analogy has important implications for future exploration, with a 'hybrid' empirical model drawing on both BHT and SEDEX models being proposed for use in the Soldiers Cap Group.

Yesterday I was with my 4 year old nephew who complained that he was too tired to walk up a rock, could I carry him? Having my arms full with everything he insisted we take to the rock, I declined his request. He complained saying "That's not fair!"
I replied "Well mate.. life's not fair."
"What's life?", he asked. I had to think about it for a moment
..."when you breathe in and you breathe out you are living, and when you breathe and open your eyes, your mind and your heart you are living life".

He looked at me and with arms outstretched and eyes wide open he drew a deep breath in and exhaled all the way out and said "There, see... I lived life real good - will you carry me now?"

Vikki Simpson (The Waifs)
8 Dec 2002

For my sister, gran & dad

Acknowledgements

Table of Contents

Chapter One- Introduction

Chapter Two- Overview of the Regional Geological Setting of the Mt Isa Inlier and Eastern Succession, NW Queensland

Chapter Three- Sedimentology of the upper Soldiers Cap Group

Chapter Four-U-Pb detrital zircon age constraints on source terranes for the Soldiers Cap Group, Eastern Succession, Mount Isa Inlier, Northwest Queensland, Australia.

Chapter Five- Volcanology of basaltic units of the upper Soldiers Cap Group

Chapter Six- Geochemistry of ferrobasalts of the upper Soldiers Cap Group

Chapter 7- Soldiers Cap Group iron formations (Mt Isa Inlier, Australia) as windows into the hydrothermal evolution of a base-metal bearing, Proterozoic, rift basin.

Chapter Eight- Basin geometry, palaeocurrent studies and the development and nature of large-scale faults

Chapter Nine- Comparison of the Soldiers Cap Group to the Aldridge Formation, B.C. Canada, and the Etheridge Group, Georgetown Inlier NE Qld and implications for base-metal exploration

Chapter 10- Conclusions and Recommendations for future........260-266
Work

APPENDICES

List of Figures

List of Tables

List of Commonly Used Abbreviations

SCG= Soldiers Cap Group
LCF= Llewellyn Creek Formation
MNQ= Mt Norna Quartzite
TCV= Toole Creek Volcanics
WCS= Weatherly Creek Syncline
TCS= Toole Creek Syncline
PGS= Pumpkin Gully Syncline
WCIF= Weatherly Creek Iron Formation
MNIF= Mt Norna Iron Formation
MSG= Maronan Supergroup

List of Appendices

Appendix One: rock catalogue(copy kept at Utas)
Appendix Two: palaeocurrent data (raw and corrected)
Appendix Three: whole rock geochemistry results
Appendix Four: LA-ICPMS U/Pb dating results
Appendix Five: Hatton & Davidson 2004 (reprint of paper in Australian Journal of Earth Sciences)

NB:Originals of traverse, drill hole and sedimentological logs are available from the author on request

Chapter One- Introduction

1.1 Preamble

Classic models for the Proterozoic intracontinental rift basins of Australia are
characterized by an early 'rift phase' of shallow water sedimentation and voluminous
volcanism which evolves to deeper-water sedimentary fill and lesser volcanism of the
'sag phase' (*eg.* Etheridge *et al.* 1987). However, other rift basins do display renewed
magmatic activity in the later phases of development. For instance looking globally,
the Mesoproterozoic Belt-Purcell Basin of western Canada in which siliciclastic
sediments of the Aldridge Formation are exposed, includes up to 30% of the
stratigraphic sequence as synsedimentary mafic sills (Moyie Sills-Anderson &
Goodfellow 2000) which have a temporal and spatial association with the movement
of hydrothermal fluids at various stages in the basin evolution.

This thesis examines this concept in detail using the Soldiers Cap Group, a well
preserved rift-basin remnant in the Proterozoic Mt Isa Inlier, northwest Queensland,
Australia (Fig.1.1). The Soldiers Cap Group is considered to largely consist of sag-
phase sediments overlying the syn-rift Fullarton River Group, host to the large
Broken Hill-type Cannington Pb-Zn-Ag deposit (Beardsmore *et al.* 1987; Bodon
1998, Walters & Bailey 1998). Additionally, the Soldiers Cap Group contains a
major mafic intrusive-extrusive package, the Toole Creek Volcanics which lies
stratigraphically above volcanosedimentary piles of the Mt Norna Quartzite and

Llewellyn Creek Formation. There is also evidence of stratigraphically widespread hydrothermal activity, in the form of Fe-P rich horizons with subeconomic base metals mineralisation. Fortunately, the Soldiers Cap Group represents one of the texturally best preserved segments of the basin. It is therefore an ideal place to study the relationships between magmatism, sedimentation, hydrothermal activity and overall basin development in a rejuvenated rift setting.

The Eastern Succession of the Mt Isa Inlier, including the Soldiers Cap Group, is a medium-grade metamorphic terrane (greenschist-amphibolite) which has undergone several discrete deformation events. The present study aims to 'look through' the deformation, metamorphism and alteration and use detailed sedimentology, volcanology, petrography, whole-rock and isotope geochemistry and reconstructions of palaeoflow data to unravel the geological history of the Soldiers Cap Group. This interpretation will then be used to investigate the processes in the upper Soldiers Cap Group and compare this with other global analogues, particularly the Belt-Purcell Basin of western Canada. The implications for Pb-Zn exploration in the region and the similarly aged Georgetown Inlier, northeast Queensland, Australia were also considered.

1.2 Research Aims

1.2.1 Major Aims

The main project aims were:-

(1) Ascertain timing, relationships to adjacent lithologies, methods of deposition and geochemical signature of the mafic units within the Soldiers Cap Group;

(2) Use detailed sedimentology, detrital zircon U-Pb dating and palinspastic reconstructions of palaeoflow data to identify the geometry, timing and nature of any primary basinal features;

(3) Resolve the nature of the iron-oxide rich sediment horizons via detailed mapping, geochemistry and petrography and relate any hydrothermal activity to other events in the basin;

(4) Formulate a local basin-scale model for the development of the upper Soldiers Cap Group;

(5) Evaluate the Aldridge Formation, Belt-Purcell Basin, B.C. Canada, host to the massive Sullivan (Fe)-Pb-Zn deposit as a possible analogue to the Soldiers Cap Group

1.2.2 Secondary Aims

Secondary lines of investigation arising from the primary aims include:-

(1) revision of the lithostratigraphy of the Soldiers Cap Group along genetic/sedimentological lines;

(2) recommendations for future exploration in the Soldiers Cap Group based upon comparisons with the Aldridge Formation and also Etheridge Group, Georgetown Inlier

(3) define a geochemical fingerprint which could be used to define lateral equivalents to Soldiers Cap Group mafics and iron formations in future drilling under cover

1.3 Work Methods

1.3.1 Field Work

No set 'study area' was defined, instead areas where there was a reasonable degree of exposure, and hence the possibility for mapping and focused sampling were studied during two field seasons of 5 months and one shorter one of 6 weeks, largely controlled by the Northern Australian monsoon season (November-April). As a result of this methodology, not all areas of the outcropping Soldiers Cap Group could be studied in equal detail. Therefore, the broad area of the Soldiers Cap Group studied extended to the northeast and southeast of the town of Cloncurry, northwest Queensland, Australia (Figs.1.1 & 1.2). The approximate boundaries are the Williams Batholith in the south, the Cloncurry Fault in the west and the northernmost extent of outcropping Soldiers Cap Group in the Pumpkin Gully Syncline. To the east cover of the Eromanga Basin obscures outcrop and this is the area in which interpretations of geophysical data and drill core became important in interpreting extensions of the Soldiers Cap Group undercover.

Field methods used were predominantly detailed traversing and reconnaissance mapping controlled by airphotos, GPS, tape and compass. Detailed aeromagnetic, gravity images and stereographic airphoto pairs provided by BHP Minerals were hand-interpreted as an aid to delineating the structural patterns and stratigraphy of the upper Soldiers Cap Group. From this two large scale maps (Fig.1.2b; 1:15000 & 1:25000) were drafted covering the outcropping area of the Pumpkin Gully Syncline (Map Sheet Two), and the majority of the Weatherly Creek Syncline (Map Sheet One). Smaller scale maps were drafted based upon detailed mapping of two of the iron-oxide rich horizons (Ch.7).
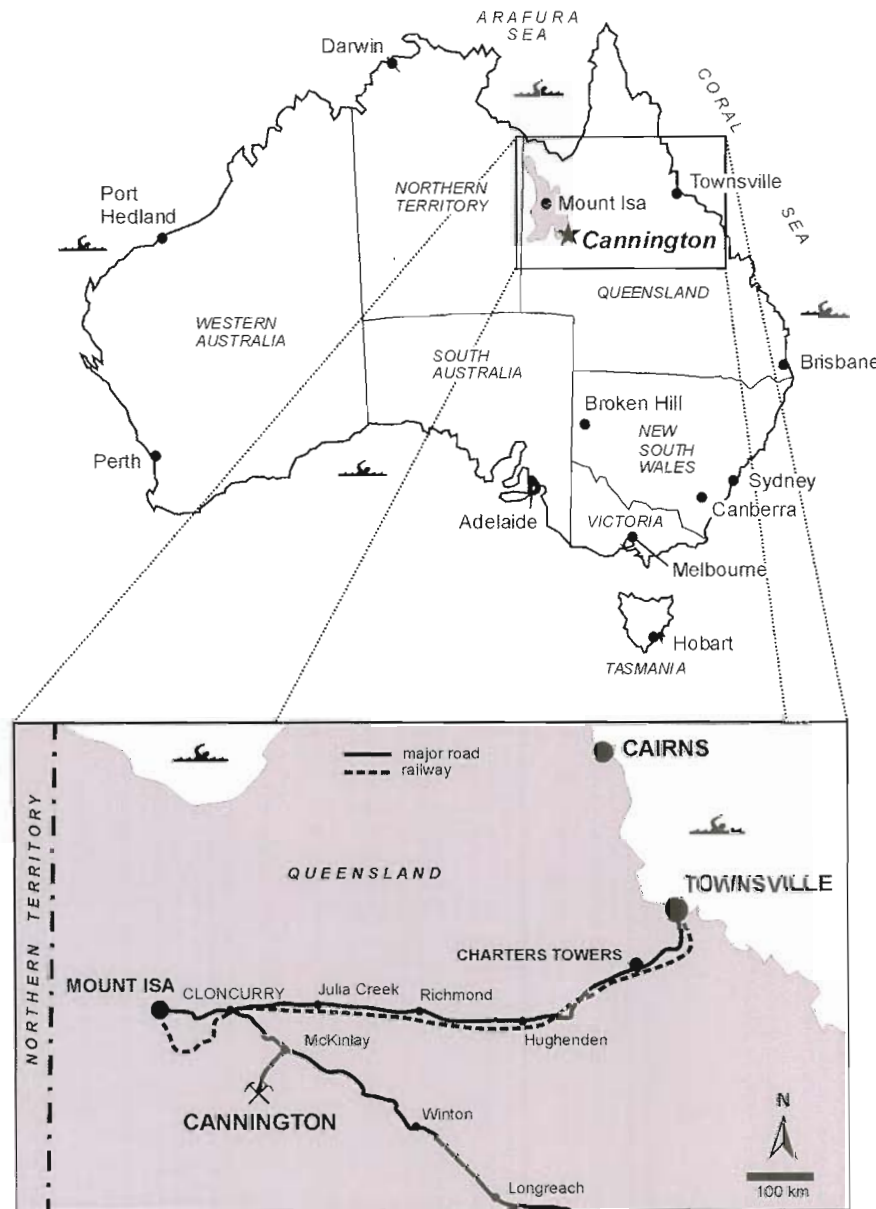
Figure 1.1: Location diagram showing the interpreted extent of the Mt Isa Inlier, major population centres and infrastructure in northwestern Queensland, Australia. Taken with permission from Bodon (2003). Interpreted position of the Mt Isa Inlier shown in the upper map of Australia with light grey shading.

Diamond drill core from relevant BHP Minerals exploration drilling was logged in detail, along with core from the now closed Monakoff mine (refer to Map Sheet Two for locations). Due to the general lack of relevant drill core intercepting unmineralised, unaltered units, the primary source of geological information was

from detailed traversing and mapping. Logs of the drillholes referred to in this thesis can be obtained on request from the author.

1.3.2 Laboratory Work

The main phases of laboratory work involved XRF and ICP-MS whole rock and radiogenic isotope geochemistry, and description of polished and cover slipped thin sections of numerous samples from the Soldiers Cap Group. All geochemical and isotopic results are attached as Appendices 3 &4. All samples quoted in the thesis are held in the University of Tasmania rock store and archive at the Sandy Bay campus, Hobart and are listed in Appendix 1.

1.4 Previous Work

1.4.1 Geological Mapping

Earliest mapping of the Soldiers Cap Group was done by Honman *et al.*(1939) and Carter *et al.*(1961). The published 1:100 000 Cloncurry sheet of Ryburn *et al.*(1987) and the northernmost part of 1:100 000 Mt Angelay geological sheet covers the entire field area. Other published maps covering the field area are Loosveld (1987) 'Structural Geology of the Central Soldiers Cap Group' 1:100 000; Williams (1997) 1:25 000 'Geology of the Western Pumpkin Gully Syncline' and detailed structural maps of the Weatherly Creek Syncline-Snake Creek Anticline area by Lewthwaite (2000). Maps drafted by BHP (*cf.*Arnold 1983) geologists also much of the study area. The abovementioned mapping while giving excellent control on the broad stratigraphy, structure and geology of the area, did not fully address several points considered crucial to this study.
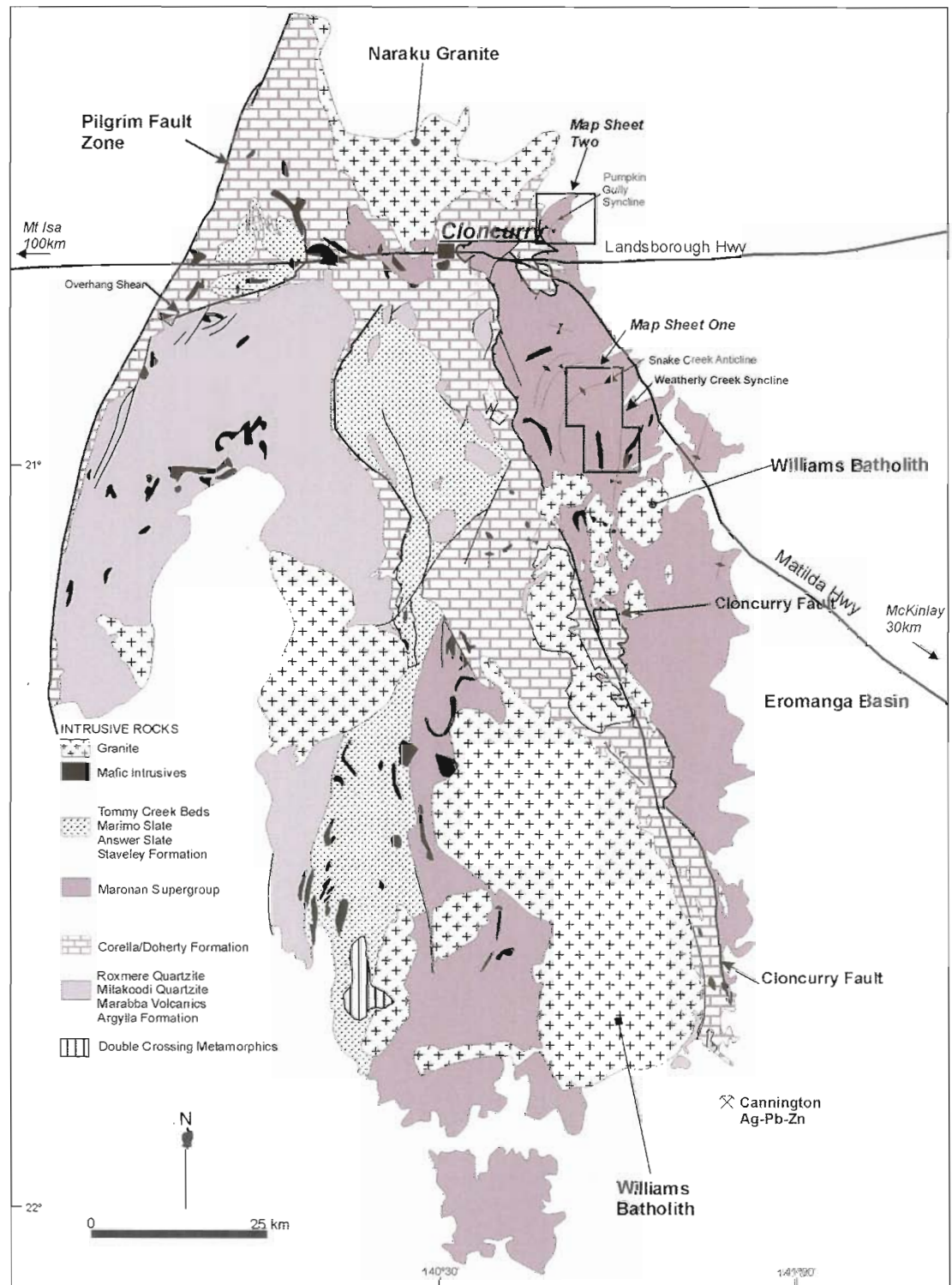
Figure 1.2: Location diagram depicting the location of the field study area (solid outline) relative to the major tectonostratigraphic units in the Eastern Succession (modified from Betts *et al.* 2000). Also depicting the location of the two main map sheets The major highways in the area are also shown as a solid line with distances to the nearest towns marked.

Namely, there is little published information on sedimentology, palaeoflow, the emplacement environment of the mafic units and the geology of iron-oxide rich horizons. Consequently, much of this existing data, particularly the structural elements, were integrated with new data into the present study.

1.4.2 Geochemistry

Compared to other regions of the Mt Isa Inlier, published whole rock geochemical data on Soldiers Cap Group lithologies is comparatively sparse. Early authors include Glikson *et al.* (1976) and Wyborn & Blake (1982) who mainly studied the various mafic units of the Eastern Succession. A more comprehensive database incorporating much of this earlier data, can be found in the AGSO Rockchem database. Recently published Soldiers Cap Group geochemical data includes that of Williams (1998); Davidson (1998; *cf.*Davidson *et al.* 2001); Adshead (1995) and Giles 2001. All of these studies focused largely on either mafic units immediately associated with metal deposits (*ie.* Monakoff, Pegmont, Cannington & Osborne) or were regionally oriented with wide spaced sample localities. Therefore the opportunity existed to undertake a detailed geochemical sampling program across the Soldiers Cap Group within the well confined stratigraphic, sedimentological and volcanological framework defined in this study.

Isotope geochemistry in the region has largely been confined to regional or deposit scale studies involving U-Pb dating of zircons by SHRIMP and LA ICP-MS (Page & Sun 1998; Giles 2000; Belousova *et al* 2001; this study Ch.4). Again, this provided significant scope for detailed local scale detrital zircon studies using the relatively cheap, quick turnaround LA ICP-MS method.

8

1.4.3 Exploration

Various companies have held numerous exploration leases over the field area since the early 1970's. Companies holding leases at various times include Esso Minerals, Shell Minerals, MIM, BHP Minerals, Normandy, Noranda, Utah Development Co., Placer, Great Central Mines and Eagle Resources. BHP Minerals are perhaps the most useful to the current investigation, having held a large part of the field area under their Cloncurry Authorities to Prospect in the1980's (Arnold 1983). This investigated most of the outcropping areas of the Soldiers Cap Group, exploring for base metal and copper-gold mineralisation. This also provided high resolution aeromagnetic, gravimetric and geological surveys of the study area which were used as a base to much of this investigation.

Chapter Two- Overview of the Regional Geological Setting of the Mt Isa Inlier and Eastern Succession

2.1 Regional Geology Overview

The Mt. Isa Inlier of northwest Queensland is composed of Palaeo-Meso Proterozoic rocks interpreted by numerous authors as a sequential product of intracontinental rifting, deposition of rift related sediments, syn-rift volcanism, and deformation over the period *ca.*1900-1500 Ma (Etheridge *et al.* 1987; O'Dea *et al.*1997). The McArthur Basin, older basement of the Murphy Inlier and younger sediment cover of the South Nicholson Basin surrounds the Inlier to the northwest. To the south and east, younger Phanerozoic sediments of the Eromanga, Carpentaria and Georgina Basins cover the eastern extension of the Inlier (Fig.2.1b).

The Mt Isa Inlier can be separated into three major tectonostratigraphic zones on the basis of boundary faults, lithology, metamorphic grade, deformation style and tectonostratigraphic setting (Fig.2.1a). Westernmost is the Western Succession, central is the oldest Kalkadoon-Leichardt Block and the youngest division is the easternmost Eastern Succession, containing the Soldiers Cap Group (Fig.2.1a &b). The Mt. Isa Inlier is an important metallogenic province containing world class ore deposits (Fig.2.1b) of several differing styles, including stratiform sediment-hosted (SEDEX) Zn-Pb-Ag deposits (Mt.Isa, Century), Cu-Au-Fe oxide deposits (Ernest Henry), U-REE deposits (Mary Kathleen), ironstone hosted Cu-Au deposits (Osborne, Starra), and the massive Broken Hill-type Cannington Ag-Pb-Zn deposit and the sub-economic Pb-Zn (Pegmont). Much of the metallogeny and geology of the Eastern Succession is succinctly summarised in Williams (1998).
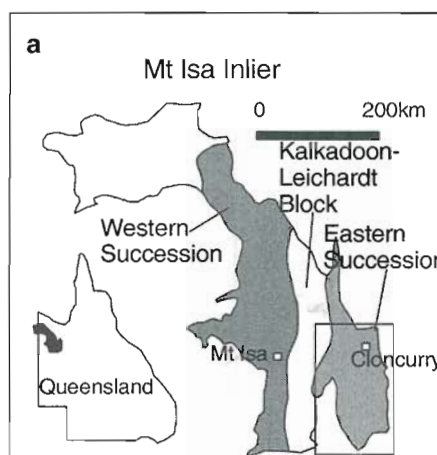
Figure 2.1a: tectonostratigraphic divisions of the Mt Isa Inlier and location within Queensland Also showing the area of Fig.2.1b, which outlines the geology of the study area.

2.2 Regional Lithostratigraphy

2.2.1 Mt Isa Inlier Lithostratigraphy

The stratigraphy of the Mt Isa Inlier was first divided into three major *Cover Sequences* by Blake (1987:Fig.2.2). In this scheme, deformed, metamorphosed basement (Barramundi Basement 1870-1890 Ma) is overlain by Cover Sequences 1-3 each representing a different stage of rift development (Fig.2.2). Recent U-Pb zircon dating by several authors (Page 1981; Page & Sweet 1998; Page & Sun 1998; Belousova *et al.* 2001) has further constrained the relative ages of these tectonostratigraphic units. Cover Sequence 1, comprising mostly felsic volcanics, was given an age of 1875-1850 Ma (Fig.2.2). Cover Sequence 2 comprised sedimentary and bi-modal volcanic rocks and was given an age of 1790-1760 Ma (Fig.2.2). Cover Sequence 3 was made up of sedimentary and lesser bi-modal volcanic rocks of 1680-1670 Ma age (Fig.2.2).

O'Dea *et al.* (1997) proposed a subdivision of the 3rd cover sequence of Blake (1987) to allow for a fourth younger cover sequence, however, they kept the first two the

same as those of Blake (1987). After recent dating (Page & Sun 1998), the age of the

Soldiers Cap Group has been revised and many workers in the region consider it to

be part of Cover Sequence 3 of the Blake (1987) scheme.

2.2.2 Maronan Supergroup Lithostratigraphy

Until recently, lithostratigraphic relations within the Soldiers Cap Group have been

unclear, mainly because there was little reliable geochronological data to confirm

absolute stratigraphic positions. One of the first attempts to define the

lithostratigraphy is found in Carter *et al.* (1961). They named the current Soldiers

Cap Group the Soldiers Cap Formation, which had three informal divisions, from

youngest to oldest: 1- interbedded metabasalt, chert and slate, 2- interbedded

quartzite and metabasalt and 3- and a high metamorphic grade pelitic sequence.

Derrick *et al.* (1976e) formally re-defined the Soldiers Cap Formation as the Soldiers

Cap Group, which comprised the informal formations of Carter *et al.* (1961) renamed

as the Toole Creek Volcanics, Mt. Norna Quartzite and the Llewellyn Creek

Formation respectively. Arnold (1983) produced a complex stratigraphy scheme for

the Soldiers Cap Group based upon mapping for an exploration program for base and

precious metals. The results of this study have necessitated some modifications to the

existing lithostratigraphic schema for the Soldiers Cap Group, these are discussed in

Chapter 3.

Beardsmore *et al.* (1988)(*cf.* Beardsmore 1992; Newbery 1990) made the first major

revision of the stratigraphy of the Soldiers Cap Belt of earlier authors. They proposed

the informal Maronan Supergroup (Fig.2.1b), which contained the Soldiers Cap

12

Group and the newly named Fullarton River Group, which was partly

undifferentiated Soldiers Cap Group and partly Kuridala Formation of earlier authors.
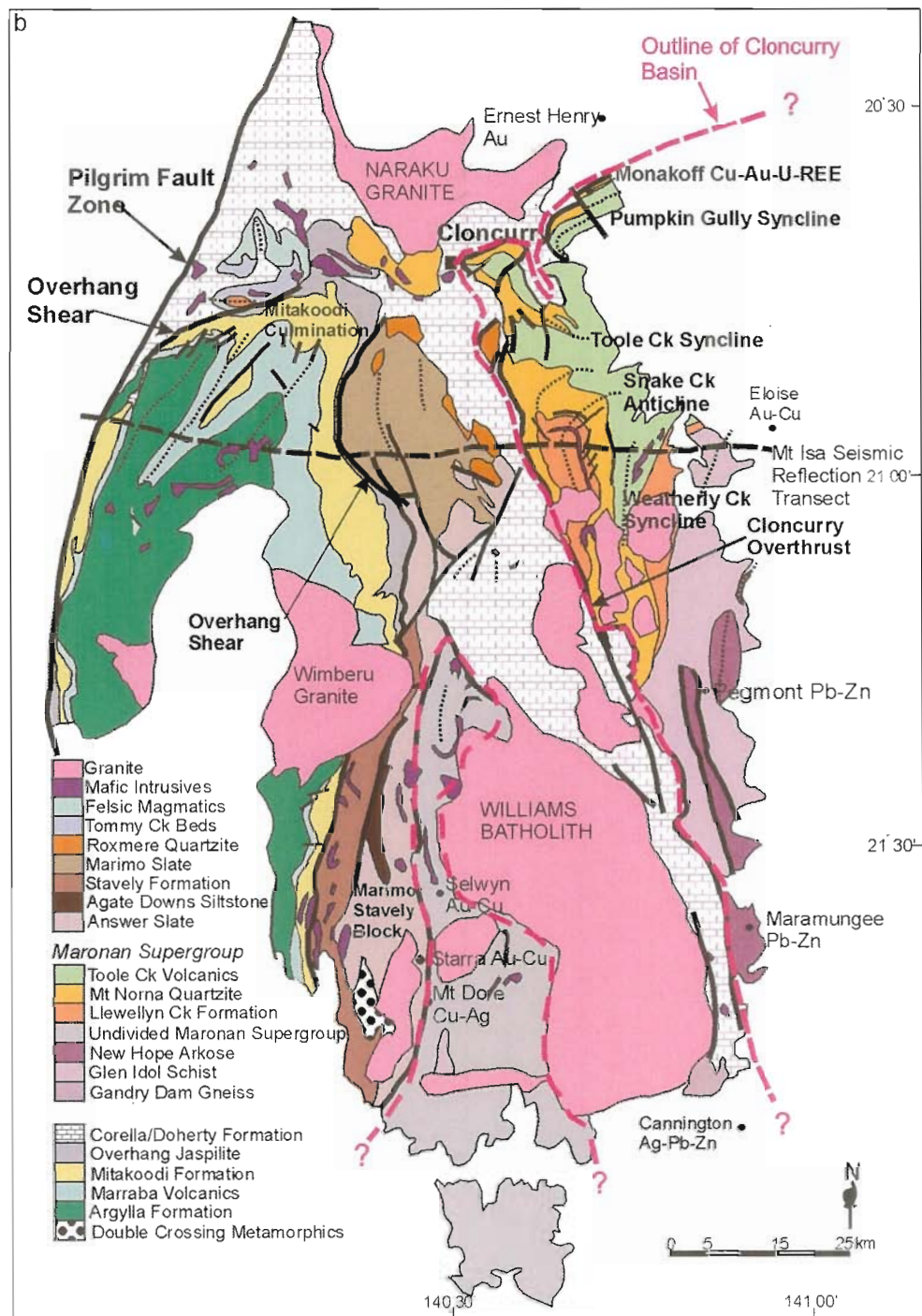
Figure 2.1b: Simplified Eastern Succession tectonostratigraphic elements and geological units (modified from Betts *et al.* 1999). Also shown are the broad extent of the study area and the inferred limits of the Cloncurry Basin of Newbery (1990).

The designation of the Maronan Supergroup by Beardsmore et al.(1988) necessitated

abolition of the Kuridala Formation that had persisted in common usage by workers

The designation of the Maronan Supergroup by Beardsmore et al.(1988) necessitated abolition of the Kuridala Formation that had persisted in common usage by workers in the area since Carter *et al.* (1961). Beardsmore *et al.* (1988) proposed that the Kuridala Formation become part of the lower Soldiers Cap Group (Llewellyn Creek Formation), and upper Fullarton River Group (New Hope Arkose). Following this revision of Beardsmore et al. (1988), the stratigraphy of the Soldiers Cap Group itself remained largely unchanged from that presented by Derrick et al. (1976e). Additionally, Beardsmore (1992) based upon regional scale lithostratigraphy (*cf.* Newbery 1990,) placed the Maronan Supergroup stratigraphically below the Malbon and Tewinga Groups, with a poorly defined, possibly tectonic, contact with the overlying calc-silicate breccias of the Mary Kathleen Group.

Early writers (*eg.* Derrick *et al.* 1976; Glikson 1972; Plumb *et al.* 1980), correlated the Soldiers Cap Group both temporally and spatially, with the Malbon, Tewinga and Haslingden Groups, placing it below the Mary Kathleen Group (Cover Sequence 2), with a maximum age for the Soldiers Cap Group of *ca.*1780 Ma. Dating of intrusive and volcanic rocks (Page 1978; 1981; 1983) provided some geochronological information but there was still no clear correlation between rocks either within the Eastern Succession or across the rest of the Inlier.

Recent geochronological work, notably that of Page and Sun (1997; 1998; *cf.* Belousova *et al.* 2001; Fig.2.2; Ch.4) and Page & MacCready (1997), presented U-Pb SHRIMP dates from zircons in the Fullarton River Group. These include a detrital maximum depositional ages of 1677±9 from the Gandry Dam Gneiss, and from the Soldiers Cap Group, a meta-rhyolite-crystallisation age of 1654±4 Ma and maximum depositional age of 1658±8 Ma.
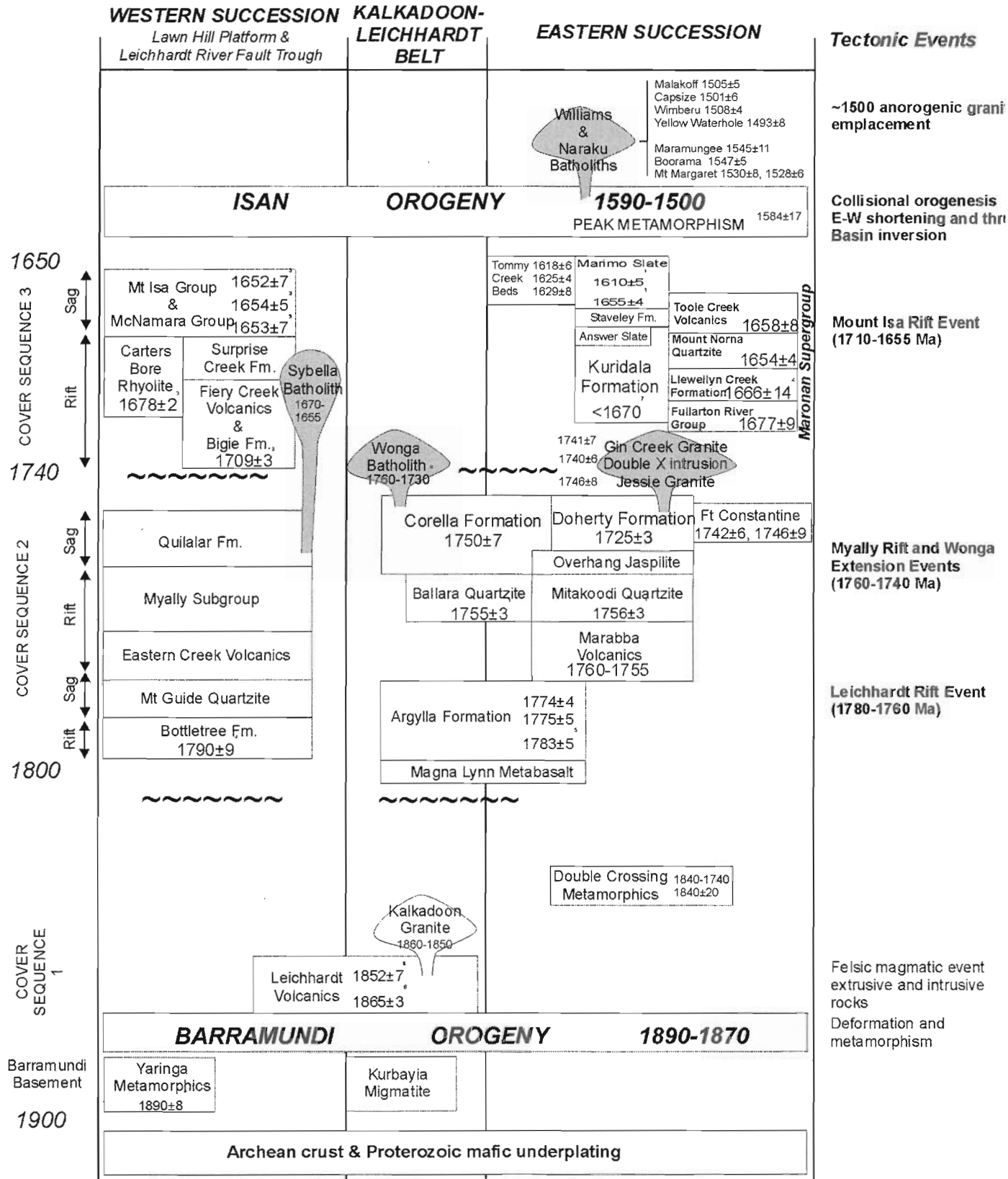
Figure 2.2: Tectonostratigraphic framework of the Mt Isa Inlier including the Eastern Succession (modified after Betts *et al.* 1997; O'Dea *et al.* 1997; Page & Sun 1998; Page & Sweet 1998; Bodon 2002). 1-Page *et al.*1997; 2- Giles (2000); 3-Page & Sweet 1998; 4-Connors & Page (1995);5-Page(1983); 6-Page & Williams (1988); 7-Page (1998) ; 8-Pearson *et al.* (1992). All other ages are from Page & Sun (1998) or referenced in the text.

The age of the Maronan Supergroup based upon this recently produced dating, between 1710-1650 Ma in age. This age correlates the Soldiers Cap Group temporally with rocks of the Mt. Isa Group. Based upon other regional dating outlined in Figure 2.2 the Soldiers Cap Group is interpreted as being in tectonic contact with the breccias of the Corella and Doherty Formations (1740-1750 Ma; Fig.2.1b; Fig.2.2). Giles (2000) noted a conformable contact with calcsilicates of the Mary Kathleen Group at an undisclosed location in the Cloncurry region. No such contacts were noted by the author in the study area or nearby regions of Mary Kathleen Group calcsilicate breccias (L.Marshall pers.comm. 2001).

Another temporal correlation possible on the basis of this dating is the Maronan Supergroup to the Willyama Supergroup in the Broken Hill-Olary Block. Page & Laing (1992) produced U-Pb SHRIMP dates from zircons in the host rock of the Broken Hill Pb-Zn-Ag orebody, defining a maximum age of deposition of 1690±5 Ma, clearly within the age overlap given for the age of deposition of Eastern Succession rocks.

The Maronan Supergroup is also broadly correlative in age, tectonostratigraphic setting and lithologies, with the Etheridge Group of the Georgetown Inlier which has ages of mafic and felsic magmatism 1690-1670 Ma (Black *et al.* 1998). Laing (1996) noted these temporal and geological correlations and proposed the Diamantina Orogeny which spans the period *ca.* 1680-1500 Ma and encompasses the Mt Isa Inlier, Georgetown Inlier and Broken Hill Block. Sedimentation within this Diamantina Orogeny began at *ca.*1750 Ma followed by waning volcanism and sedimentation until peak metamorphism and deformation at *ca.* 1610-1580 Ma.

Subsequent deformation (1580-1530 Ma) and granite emplacement occurred between 1520-1480 Ma (Laing 1996). Lister *et al.* (1997) proposed an alternative to this by referring to a ~1590 Ma rifting event they termed the Hiltaba Event. This had an area of influence from the Mt Isa Inlier to the Broken Hill Block and further than the Diamantina Orogen into the Gawler Craton. Lister *et al.* (1997) proposed the Hiltaba Event involved subduction at a tectonic margin and concomitant volcanism in the Eastern Succession and extension in the Western Succession. Giles *et al.* (2002) also noted the temporal and spatial correlation between the various Proterozoic 'intracontinental basins' of Australia and suggested they were the result of far-field influences of subduction processes on the southern margin of the craton.

2.3 Tectonostratigraphic Setting and Development

2.3.1 Mt Isa Inlier

Early workers (Carter *et al.* 1961) suggested there were two sedimentary sequences, the Western and Eastern Successions, separated by the older central basement block. Detailed mapping by the Bureau of Mineral Resources and the Geological Survey of Queensland (Derrick *et al.* 1976a-e, 1977a,b; Glikson *et al.* 1976) resulted in a newer model, in which the older basement sequence was the product of a fault bounded rift they termed the Leichardt River Fault Trough. The associated volcanosedimentary sequences were interpreted as the result of various phases of rifting.

As mentioned above the Mt Isa Inlier can be separated into three major tectonostratigraphic zones (Fig.2.1a; Fig.2.2). The oldest and central Kalkadoon-Leichardt Block is composed of granites, felsic volcanics and basement metamorphosed and deformed during the *ca.*1890-1840 Ma Barramundi Orogeny

(Fig.2.2; Etheridge *et al.*1987; Page & Williams 1988). 'Barramundi Basement' is represented in outcrop by small areas of gneiss in the Kalkadoon-Leichardt Block, and deformed granitoids of the Kalkadoon Batholith (Wyborn *et al.* 1988). Inferred equivalents to Barramundi Basement in the Eastern Succession are the Double Crossing Metamorphics dated recently at 1840±20 Ma (Fig.2.2; Page & Sun 1998). Limited geochemical data led Glikson *et al.* (1976) to propose that basalts of the Eastern Fold Belt with geochemical ocean floor tholeiite affinities were produced at a continental margin. Wyborn and Blake (1982), on the basis of consideration of available data, proposed the rifting that produced the Inlier was ensialic. Etheridge *et al.* (1987) furthered this by proposing the involvement of crustal extension by small-scale convection, underplating and rifting due to crust-mantle delamination following the ideas of Kröner (1983).

This incipient rifting event in the Mt. Isa Inlier is thought to have involved crustal doming intersecting a rift triple junction in the stable crust of the Northern Australian Craton (Etheridge *et al.*1987; Newbery 1990; O'Dea *et al.* 1997; O'Dea & Lister 1995). Giles *et al.* (2002) have suggested that the different rifting and volcanosedimentary depositional events within the Mt Isa Inlier are the result of far-field tectonics related to subduction on the southern margin of the Northern Australian Craton.

The onset of mantle melting is thought to have begun at *ca.*2000 Ma and rifting began between 1950-1900 Ma, with a duration of approximately 100 Ma implied for the initial extensional phase (Fig.2.2; Etheridge *et al.* 1987). Page & Williams (1988) dated the closure of this event, represented by the Barramundi Orogeny at 1890-1870

Ma (Fig.2.2) suggesting a relatively short duration for this earliest event. Crustal extension ensued with the production of long linear basins with bounding longitudinal faults that produced half-graben tilt blocks (Newbery 1990). These half-graben tilt blocks combined with the orientation of the rift arms, would have been the major control on the geometry of sedimentary basins, with each rift arm assumed to have taken part in different rifting events.

Initial rifting led to the production of bi-modal volcanics and rift-sag volcanosedimentary units of Cover Sequence 1 (Fig.2.2; Blake 1987; O'Dea et al. 1997; Etheridge et al. 1987). Betts & Lister (2001) renamed this earliest *ca.*1800-1755 Ma east-west rifting event, the *Leichardt Rift Event* (LRE; Fig.2.2) and the resultant basin the Leichardt Superbasin. Concurrent with extension, silicic sedimentation and mafic volcanism were important in the development of the Leichardt Superbasin. Voluminous continental tholeiites of the Eastern Ck Volcanics are associated with the LRE and are inferred to be the product of hot mantle plumes (Wilson *et al.* 1995; O'Dea *et al.* 1997).

The deposition of shallow marine sediments in the Leichardt Superbasin records the *Myally Rift Event* (MRE; Fig.2.2), a series of intermittent rifting and episodic subsidence events (O'Dea *et al.* 1997; Betts 1997; Betts *et al.*1999; Lister *et al.* 1999). Deposition of shallow marine sediments of the Myally Subgroup and Quilalar Formation (O'Dea *et al.* 1997; Jackson *et al.* 1990) indicates that a shallow water carbonate system transgressed the existing older Kalkadoon-Leichardt Block.

The next major extensional episode was the *Mt Isa Rift Event* (MIRE) which

occurred between *ca.*1710-1655Ma (Fig.2.2; Page & Sweet 1998; O'Dea *et al.*1997).

The MIRE involved the deposition of shallow marine and fluvial siliciclastics

deposited into a southeast-deepening basin (Betts 1997; Betts & Lister 2001). Betts

et al. (1999) proposed that the MIRE involved northwest-southeast directed crustal

extension, and that it was completed by *ca.*1650 Ma (*cf.* Page & Sweet 1998). Early

LRE mainly north-south oriented faults were reactivated at various stages during

both the MIRE and the later Isan Orogeny (Betts *et al.*1999; Lister *et al.* 1999).

Two distinct models have been proposed recently for the evolution of the Mt Isa Rift

Event. Scott *et al.* (2000) (*cf.* Southgate *et al.* 2000) proposed the 'strike-slip' model.

This involved extension in the *Isa Superbasin* occurring as a result of the creation of

accommodation space via transtension within the craton as a result of subduction and

orogeny along the southern margin. This model is based upon detailed sequence

stratigraphic work across the Mt Isa Inlier that has defined several new

supersequences in the Isa Superbasin (Domagala *et al.* 2000; Bradshaw *et al.* 2000;

Southgate *et al.* 2000). Much of the evidence for these supersequences comes from

integrated seismic, drilling, dating and palaeomagnetic data from across the Mt Isa

Inlier.

Betts & Lister (2000) disputed this model and proposed the 'episodic rift-sag model'

involving three broad rift events in the Isa Superbasin. Their Stage I was active

rifting and crustal extension that produced a series of half-grabens initiated on a

framework of earlier basement blocks. Complex interaction with earlier faults

segregated many of the east-west oriented Leichardt Rift Event half grabens. During

this stage bi-modal volcanism and emergent domes and calderas were formed. Stage

II involved a change from rift to sag dominated extension involving the deposition of transgressive sequences, with wedge shaped geometries and defined thickness changes. Stage III was in the form of 'classic' sag phase rifting, driven by asymmetrical lithospheric thinning (Betts *et al.* 1999) that prompted the main depocentre to relocate to the Lawn Hill Platform.

Whilst both models are well constrained and detailed, neither has provided much insight into how these various rifting events may have affected the tectonostratigraphic evolution of the Eastern Succession. Little published evidence exists that the Eastern Succession and Western Succession ever formed a continuous, synchronous basin (Betts *et al.* 2000, *cf.* Southgate *et al.* 2000) and hence it is difficult to place the Maronan Supergroup within published tectonostratigraphic models.

During the period *ca.*1600-1500 Ma the Mt Isa Inlier underwent basin closure, deformation and metamorphism during the Isan Orogeny (Fig.2.2). This orogeny involved several discrete predominantly east-west compressional events with deformation of the weakened crust producing a variety of folds, thrusts and several generations of structural fabrics in the Eastern Succession (Passchier 1986; Loosveld 1992; MacCready *et al.*1998).

2.3.2 Eastern Succession Tectonostratigraphic Development

The earliest rift event in the Eastern Succession, inferred as equivalent to the Leichardt Rift Event in the Western Succession, is represented by felsic volcanics of the Argylla Formation and flood basalts of the Magna Lynn Metabasalt (Fig.2.2;Blake and Stewart 1992; Betts *et al.* 1997). The end of this rift event in the

Eastern Succession is represented by the mafic volcanics and siliciclastic sediments of the Marabba Volcanics (Fig.2.1b; 2.2) (Betts *et al.* 1997). Overlying the Marabba Volcanics are the rocks that represent the *ca.* 1740-1760 Ma Myally Rift Event. In the Eastern Succession these are the Mitakoodi Quartzite and parts of the Corella Formation (Fig.2.1b; 2.2). Earliest mafic volcanism in the Eastern Succession at this time, is the Marabba Volcanics, which are overlain by the clastic sediments, and rhyolites of the Mitakoodi Quartzite (Fig.2.1b; 2.2). The Mitakoodi Quartzite is believed to be synchronous with the post-rift Quilalar Formation in the Western Succession (Potma 1996; Betts *et al.* 1999). Extension at this time in the Eastern Succession is interpreted to be NW-SE on the basis of stratigraphic markers in the Mitakoodi Quartzite (Betts *et al.* 1997).

The next rift event in the Eastern Succession is represented by a period of extension evidenced by south dipping normal faults, the Wonga Extension Event in the Wonga-Shinfield Zone, located off the western edge of Figure 2.1b (Passchier 1986; Williams 1989; Passchier & Williams 1989). Syn-tectonic granites and dolerites intruded the Wonga-Shinfield Zone and are interpreted as weakening the crust to produce the ductile fabrics and intense metasomatism observed (Oliver et al. 1991; Betts et al. 1999,1998). O'Dea et al. (1997) proposed a link between the Wonga Extension and E-W extension in the Western Succession. Betts et al. (1997) disputed this and proposed that it was related to the N-S extension in the Myally Rift Event.

The next rift event was the Mt Isa Rift Event (MIRE). Although there are rocks of the MIRE age in the Eastern Succession, as mentioned above the relationship between the Western and Eastern Successions at this stage of the Inlier's evolution remains unclear.

Thermal relaxation of the crust *ca.* 1700 Ma is interpreted as inducing 'sag-phase' rifting in the Eastern Succession. This produced the immature sediments of the lower Maronan Supergroup (Fullarton River Group) (Beardsmore *et al.* 1987) derived from syn-depositional felsic volcanics and deposited in the Cloncurry Basin (Newbery 1990). Assuming the upper Maronan Supergroup (Soldiers Cap Group) has an age of 1677±9 Ma (Page & Sun 1998) source areas for Maronan Supergroup rocks vary from the oldest possible (*ca.* 1875-1865 Leichardt Volcanics Page 1978; 1983) to the 1720±7 Ma Doherty Formation, or the older Argylla Formation (1783±5 Ma Page 1983), all located both presently and anciently to the west (Fig.2.1b). Beardsmore *et al.* (1988; *cf.* Wyborn and Blake 1982) suggested an older basement block to the east based upon grain size indicators in the Soldiers Cap Group.

Bi-modal volcanism associated with sedimentation and iron-formation hosted (Pegmont) and base metal Broken Hill-Type deposits (Cannington) suggest widespread metalliferous basinal brine production associated with early Maronan Supergroup deposition.

Lessening of tectonic activity and ongoing sag subsidence led to the development of mature sediments represented by the Soldiers Cap Group, Marimo Slate and Staveley Formation (Marimo-Staveley Block). Growth faults, their associated fault blocks and the orientation of the previously active rift arm(s), are thought to have played an important part in the development of both basin geometries and the formation of regional unconformities at this stage, and may have provided pathways for mineralising fluids (Derrick 1982; Newbery 1990; O'Dea *et al.* 1997). The Maronan Supergroup and Stavely Formation may be the result of concurrent rift-sag events, or

deposition in separate sub-basins. Giles & MacCready (1997) suggested that the Soldiers Cap Group was deposited to the east of the Marimo-Staveley Block (Fig.2.1b), the eastern margin controlled by the present day Cloncurry Overthrust (Fig.2.1b) with basin fill provided from the erosion of older half-graben tilt blocks.

As mentioned above, during the period *ca.*1600-1500 Ma the Mt Isa Inlier was subject to considerable deformation and metamorphism during the Isan Orogeny (Fig.2.2). This involved several discrete predominantly east-west compressional events, with deformation of the crust weakened by metamorphism and granite intrusion producing a variety of folds, thrusts and several generations of structural fabrics in the Eastern Succession outlined below (2.4) (Passchier 1986; Loosveld 1992; MacCready *et al.*1998). I-type granitoids of the Williams and Naraku Batholiths intruded the region at *ca.*1500 Ma (Wyborn *et al.*1988; Wyborn 1998).

2.4 Structural and Metamorphic Geology

2.4.1 Structural Evolution of the Soldiers Cap Group

This study has not been as detailed as some recent structural and metamorphic work on the Soldiers Cap Group (Lewthwaite 2000; Loosveld 1988; Mares 1998). However, as outlined in the project aims, 'looking through' deformation necessitated an understanding of the structural evolution of the area. To this end the fabric catalogue used in this study is outlined below in Table 2.1. This was based largely upon previously published models (Ryburn *et al.* 1987; Loosveld 1988; Lewthwaite 2000) and field observations of the author.

The first deformation event (D_1) was developed via east-west oriented thrusting of the Soldiers Cap Group over the Mary Kathleen Group, producing thrusts and tight folding (F_1). D_1 (F_1) folds are tight to isoclinal, often with transposed bedding planes and rootless intrafolial folds. D_1 has produced at least two, and in some areas three foliations, referred to as S_1. S_1 varies in orientation and form throughout the study (Pollard *et al.* 1996) area from a slaty cleavage through to a gneissosity.

Deformation Event	Fabric Elements	Description
D_1	$S_0 \, S_1 \, S^0_1$	S_1= weak foliation, sub-parallel to bedding (S_0), transposed bedding and rootless intrafolial folds common. S^0_1= weak intersection lineation
D_2	$S_2 \, L^2_2$	S_2= strong regional penetrative cleavage-schistosity
$D_{2.5}$	$S_{2.5}$	$S_{2.5}$= where observed, is a weak crenulation of S_2
$D_{3ductile}$	S_{3d}	S_{3d}= very weak slaty cleavage
$D_{3brittle}$	S_{3b}	S_{3b}= weak crenulation or slaty cleavage
D_4	S_4	S_4= weak shear fabric and cleavage adjacent to D_4 faults and shears

Table 2.1: fabric catalogue used in this study, based largely on limited field observations and work of previous authors in the region.

D_1 structures developed in the Soldiers Cap Group include bedding parallel foliation in the Pumpkin Gully area related to the Pumpkin Gully Thrust (Fig.1b; Williams 1998) and the Cloncurry Overthrust (Fig.2.1b), interpreted as an active surface during D_1 (Giles & MacCready 1997). The Toole Creek Syncline (Fig.2.1b) and the Snake Creek Anticline (Fig.2.1b) were interpreted by Loosveld (1989) and Lewthwaite (2000) as D_1 structures. Other authors have defined the Snake Creek Anticline as a D_2 fold (Fig.2.1b; Rubenach & Barker 1998), a composite D_1 and D_2 structure (Ryburn *et al.* 1987) or as $D_{2.5}$ influenced (Bell & Hickey 1996; New 1993).

D_2 produced large, regional scale features, with F_2 folds (Weatherly Creek Syncline, Mick Creek Anticline, Pumpkin Gully Syncline; Fig.2.1b; Map Sheet One) being tight to isoclinal, steep to upright and with amplitudes considerably larger than F_1 folds. S_2 varies from a differentiation cleavage to a coarse schistosity in the pelitic units. L^2_2 mineral elongation varies from shallow-moderate plunging, approximately parallel to F_2 fold axes to steeply plunging, down dip of S_2.

Bell & Hickey (1996) proposed $D_{2.5}$, lying between D_2 and D_3, that produced structures at a high angle to D_2 and later D_3 structures. Notable features of $D_{2.5}$ deformation are that it is not homogeneous over the Eastern Fold Belt and may only be recognisable where favourably oriented with respect to earlier structures. $D_{2.5}$ where observed in the Soldiers Cap Group, has refolded D_2 folds and produced a shallowly dipping crenulation cleavage.

$D_{3ductile}$ (Blake & Stewart 1992) is interpreted as being an approximately E-W compression similar to that which produced D_2 folds, and hence D_3 structures are often intensified $D_2/D_{2.5}$ foliations. F_3 folds plunge northeast-northwest, are steeply inclined and have a moderately spaced axial planar cleavage. The remobilisation of the F_2 Pumpkin Gully Syncline in the nose area is interpreted as a $D_{3ductile}$ feature. Evidence of $D_{3brittle}$ (Blake & Stewart 1992) occurs in many of the north to northeast trending faults that dissect both D_2 folds and produce a weak crenulation of earlier fabrics or a weak cleavage. Many of the north to northeast trending faults within the Weatherly Ck Syncline area are interpreted as $D_{3brittle}$ reactivations of earlier syn-depositional faults (discussed in detail in Chapter 8).

Subsequent (D_4) deformation of the Eastern Fold Belt produced a complex series of faults and shear zones, often with long and complex movement histories. These include large scale structures such as the Cloncurry Fault. The Cloncurry Fault postdates the Cloncurry Overthrust and also postdates Saxby Granite intrusion (Giles & MacCready 1997).

2.4.2 Metamorphic Evolution of the Soldiers Cap Group

Within the Maronan Supergroup and adjacent units the peak metamorphic grade developed ranges from upper-greenschist (epidote-amphibolite transition in the Soldiers Cap Group) in the Cloncurry area to upper-amphibolite facies in the southern extent around Cannington and the Selwyn Range (Jaques *et al.* 1982; Ryburn *et al.* 1987). Several authors (Lister *et al.* 1996; Rubenach & Barker 1996; Pollard *et al.* 1995) have suggested M_1, which is either a separate metamorphic event that is pre-D_1, involving high T/low P metamorphism, or alternatively involving a fall in temperature in the P-T-t pathway on the way to peak metamorphism at M_2. M_1 would appear to be only locally developed across the Eastern Succession (Pollard *et al.* 1995).

The peak of regional high T-low P metamorphism, M_2, occurred during D_2 (Page & Bell 1986; Page 1993; Oliver 1995). M_2, based upon geothermometry and geobarometry, had approximate P-T conditions of 4 kb and 630°C and a geothermal gradient of 45-50° C/km (Loosveld 1988; Oliver 1995; Jaques *et al.* 1995). Metamorphic zircon selvedges from rocks in the Soldiers Cap Group were recently dated at 1584±17 Ma (Page & Sun 1998), which is interpreted to represent peak metamorphism (M_2). Perkins & Wyborn (1996) obtained a date of ~1590 Ma using Ar^{40}/Ar^{39} dating on metamorphic actinolite from Osborne. These dates overlap with

the depositional ages of some units within the Eastern Succession, notably the Tommy Ck Block, and are *ca.* 60 Ma earlier than peak metamorphism in parts of the Western Succession (Connors & Page 1995).

Peak metamorphism within the Soldiers Cap Group itself is less clear with Rubenach & Barker (1998) proposing that metamorphism within the Snake Ck Anticline area involved as many as two pre-D_2 (M_2) metamorphic events. According to Rubenach & Barker (1998) the geothermal gradient in the Snake Ck Anticline area may have been as high as 80° C/km (*cf.* Loosveld 1989 ~41°C/km). On the basis of this they proposed that segments of the Soldiers Cap Group may have experienced inhomogeneous, pre-D_2 high grade metamorphic conditions. Some corroborating field evidence from this study exists in the markedly sharp change in metamorphic grade across the stratigraphically well constrained Llewellyn Ck Formation-Mt Norna Quartzite contact.

2.5 Regional Metasomatism

The Eastern Succession has undergone extensive post-peak metamorphic alteration that displays a distinct spatial and temporal relationship with the post D_2 felsic intrusives of the Williams and Naraku Batholiths and the Cloncurry Fault (Fig.2.1b; Laing 1998; Williams 1998; Mark 1999). The alteration is interpreted as occurring when the rocks were still hot (<400°C), is related to late ductile shears and was progressively retrograde in temperature (Williams & Blake 1993).

Na-metasomatism (Williams & Blake 1993); plagioclase±quartz±actinolite±diopside ±scapolite assemblage, and minor K-feldspar±aluminosilicate alteration of pelitic sequences within the Eastern Succession (Rubenach & Foster 1997) is the earliest of

these metasomatic events. This sodic-calcic metasomatism is interpreted as the product of $NaCl\text{-}CaCl_2$ fluids at 400-500°C, and 20-40 wt% NaCl salinity (Williams & Blake 1993).

Later albitisation (albite±pyroxene±quartz±magnetite) assemblages formed in retrograde zones within D_3 shear zones (Williams & Blake 1993). These albitisation events became successively more Na-rich, also with hematite replacing magnetite. This event is thought to be the product of >400°C, high salinity, $NaCl\text{-}KCl\text{-}CaCl_2$ fluids (Williams & Blake 1993). Very late albitisation also forms within the central zones of complex structures such as the Snake Ck Anticline and overprints D_4 structures (Rubenach & Barker 1998).

The youngest metasomatic event within the Eastern Succession is K-feldspar±hematite±magnetite±epidote, 'red-rock' feldspathisation, commonly associated with brittle structures and silicification throughout the Soldiers Cap Group (Williams & Blake 1993). Associated with this alteration is a late silicification-phyllosilicate (Rubenach & Barker 1998) alteration composed of quartz±muscovite±chlorite±K-feldspar, found commonly as selvedges to the red-rock alteration.

All these metasomatic events are closely controlled and localised by both large and small scale dilational and brittle fractures (Williams & Blake 1993). Dependent upon age, most mineralisation within the Eastern Succession displays these regional metasomatic events overprinted by or overprinting various deposit scale alteration styles (eg. Ernest Henry, Eloise, Williams 1998).

2.6 Eastern Succession Intrusive History

The largest intrusions within the Eastern Succession are the felsic I-type granitic intrusives of the Naraku and Williams Batholiths (Fig.2.1b). These are interpreted to be the product of three broad intrusive ages. The first event occurred at ca.1750-1730 Ma (Wyborn et al. 1988; Page & Sun 1998) and comprises the Gin Creek Granite, and other smaller unnamed granites. The second episode of intrusion was at ca.1545-1530 Ma (Page & Sun 1998) and involved the Maramungee Granite and smaller Mt Margaret intrusives east of the Cloncurry Fault (Fig.2.1b; Wyborn 1998). The third intrusive event is related to the 1510-1485 Ma aged Malakoff, Capsize, Wimberu and Yellow Waterhole Granites (Fig.2.2).

Wyborn (1998) interpreted these as having been intruded after D_2 but noted that D_3 and D_4 structures showed clear crosscutting relations. As mentioned above there is some discrepancy with ages of crystallization of the Maramungee and Boorama Granites and peak metamorphism/deformation.

On the basis of the geochemistry, mineralogy and lithology, Wyborn (1998) defined the Williams and Naraku Batholiths as the product of a source emplaced in the lower crust at *ca.* 2500-2200 Ma and they were considered not to have the hallmarks of magmas produced as a result of subduction. Mark (1999) proposed that underplating of mafic material into mid crustal levels underneath the Mt Isa Inlier produced the granites of the Mt Angelay igneous complex located to the south of the Williams and Naraku Batholiths south of the area of Figure 2.1b. Several large mafic bodies underlying the Eastern Succession (Mt Isa Deep Seismic Transect ~ Goncharov *et al.*1998) provide evidence to support this model.

2.7 Regional Mineralisation

The Cloncurry district has a protracted history as a producing mineral field and as a result there are a multitude of recorded mineral occurrences. Overall they can be divided into three economically important groups $Pb\pm Zn\pm Ag$; U-REE; $Cu\pm Au\pm Co\pm Ag$ ($\pm$Fe-Oxide) (Williams 1998; Fig.2.1b).

The first group is perhaps the most economically important and includes the Broken Hill-type Ag-Pb-Zn resource at Cannington (Fig.2.1b; 45 Mt @ 12% Pb, 5% Zn and 520 g/t Ag). Cannington is generally accepted as exhibiting many similarities to the giant Broken Hill deposit, notably high metamorphic grade and an association with various quartz-garnet-magnetite, gahnite and other Ca-Fe-Mn rich lithologies (Bodon 2003, Giles 2000). Of somewhat lesser economic value is Dugald River (38 Mt @ 13%Zn, 2.1% Pb and 43 g/t Ag). Other $Pb\pm Zn\pm Ag$ occurrences within the Maronan Supergroup include the ironstone hosted subeconomic Pegmont deposit (Newbery 1991; Fig.2.1b; 11 Mt @ 8.45% Pb, 3.7% Zn and 11 g/t Ag) and the skarn-like Maramungee and Maronan deposits. All of these deposits define a mineralised corridor between Maronan and Cannington within the lower part of the Maronan Supergroup.

The only economically significant example of the second group, U-REE is Mary Kathleen, hosted in a selectively replaced carbonate unit of the Mary Kathleen Group (Derrick 1977a). Mary Kathleen mineralisation has been dated at 1550±15 Ma (Page 1983) which is younger than adjacent granites but still coeval with deformation and metamorphism. The ironstone hosted Hot Rocks prospect to the east of Cloncurry contains sub-economic U-REE grades.

The third group, Cu±Au±Co±Ag (±Fe-Oxide) are considerably more numerous than the other styles of mineralisation and include the producing Cu-Au deposits at Ernest Henry (167 Mt @ 1.1%Cu and 0.54 g/t Au) and Eloise (3.2 Mt @ 5.8@ Cu, 1.5 g/t Au and 19 g/t Ag). Au rich deposits of this style include Tick Hill (470 000 t @ 27g/t Au), Gilded Rose, Mt Freda and Lorena (Davidson 1998, Davidson *et al.* 2002, Williams 1998).

The Cu-Au-(Fe oxide) association is prevalent in the Cloncurry region with several examples of economic mineralisation. The most notable feature of these deposits is the close association with Fe-oxide rich metasediments, or 'ironstones' and their often complex alteration and mineralisation histories. The three best examples are Starra (Fig.2.1b; 6.9 Mt @ 4.8g/t Au and 1.65% Cu), Osborne (Fig.2.1b; 11.35 Mt @ 3.04% Cu and 1.28g/t Au) and Monakoff (Fig.2.1b; 1 Mt @ 1.5% Cu, 0.5g/t Au,Ba,U,F,REE) (Davidson 1996; Williams 1998). Many of these deposits have a close spatial association with the felsic intrusives of the Williams and Naraku Batholiths (Fig.2.1b), although little to no mineralisation is hosted within the granitoids. The majority of the Cu-Au association deposits are controlled by brittle or brittle-ductile structures that were active during the Isan Orogeny (Williams 1998).

Comprehensive data on fluid-rock interaction for the Eastern Succession is not available, however evidence suggests that ore fluids related to the various metasomatic events, were high-T (>500°C), had very high salinities, were post D_2, high-K, and developed at shallow levels (Beardsmore 1992; Williams 1998; Wyborn 1998). Oxygen isotope data suggests that the fluids are either of a magmatic or metamorphic origin, possibly extensively modified by reactions with host lithologies and have traveled considerable distance along structural conduits (Beardsmore 1992; Williams 1998; Mark 1999).

Chapter Three- Sedimentology of the upper Soldiers Cap Group

3.1 Introduction

The upper Soldiers Cap Group comprises a thick, multiply deformed, upper greenschist to amphibolite metamorphic grade, sequence of quartzites, pelites, psammites and psammopelites. In spite of the high metamorphic grade, complex deformation and alteration history, numerous sedimentary structures and palaeoflow markers are well preserved, and by 'looking through' the structure and metamorphism detailed sedimentological data was able to be gathered.

In this study the upper Soldiers Cap Group has been examined using sedimentary sections up to several kilometres long (Map Sheet One), creek traversing and detailed geological mapping (1:25000 scale) of areas of extensive outcrop. The majority of the data has been collected along the western limb of the Weatherly Creek Syncline within the Mt Norna Quartzite and lower Toole Creek Volcanics. This was due to good continuity of section, good outcrop and the local lack of complex alteration overprints compared to other parts of the Soldiers Cap Group, which lead the author to believe it represents a relatively intact segment of the ancient basin from which reliable geological data could be gathered. Other sedimentological data was collected during detailed mapping (1:15000 scale) of the Pumpkin Gully Syncline and larger scale reconnaissance mapping of the greater area of Soldiers Cap Group outcrop.
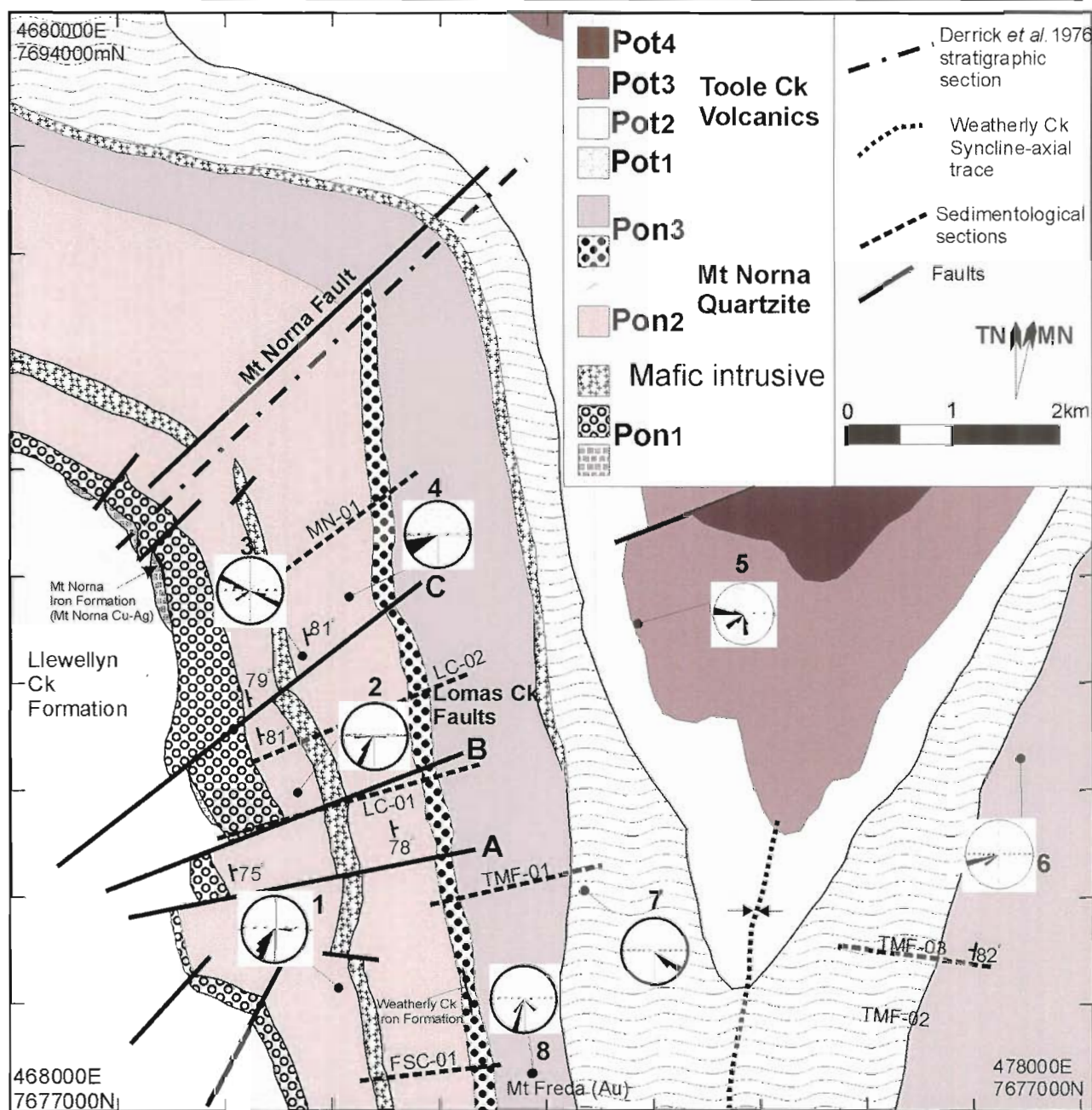
Figure 3.1: Simplified geology of the Weatherly Creek Syncline area depicting major sedimentological facies associations in the clastic sediment dominated Mt Norna Quartzite and mafic dominated Toole Creek Volcanics defined using mapping and sections from the present study combined with earlier authors mapping. Group 2 and 3 bimodal palaeocurrents depicted represent wave generated ripple crests.

3.2 Lithostratigraphy
3.2.1 Previous Interpretations

Previous stratigraphic schemes are those of Derrick *et al.* (1976e) [*cf.* Ryburn

et al. (1987), Cloncurry 1:100 000 sheet], and one constructed by BHP

Minerals as part of various exploration joint ventures in the Cloncurry

Authorities to Prospect (Arnold 1983).

The lithostratigraphy of Derrick *et al.* (1976e; Table 3.1) was constructed based upon a type section (Fig.3.1) that started at GR 651482E 7785000N and extended for some 10km to GR 750895E 7687100N across the Llewellyn Creek Formation (hereafter LCF), Mt Norna Quartzite (hereafter MNQ) and Toole Creek Volcanics (hereafter TCV). The Derrick et al. (1976 e; *cf.* Ryburn *et al.* 1987) stratigraphy works well over the upper Soldiers Cap Group, with the exception of the MNQ, where it does not separate the major subdivisions that are apparent within this unit.

The Arnold (1983) stratigraphy involved a more detailed subdivision of the MNQ, with 3 major and 8 minor units defined. This subdivision of the MNQ was mainly based upon certain levels of the unit being interpreted as prospective for lithologically controlled base metal and copper-gold mineralisation. These subdivisions are best exposed along the original type section of Derrick *et al.* (1976e) and are not readily observable elsewhere. The MNQ was divided into the three gross units of *Pon₁*, *Pon₂* and *Pon₃* and subdivisions of *Pon₁* and *Pon₃* (Table 3.1). This stratigraphy of Arnold has merits but is generally over complicated, with too many irrelevant subdivisions, particularly in the case of the MNQ.

35

Llewellyn Creek Formation	Mt Norna Quartzite	Toole Creek Volcanics
Derrick et al. 1976(e)	*Derrick et al. 1976(e)*	*Derrick et al. 1976(e) & Arnold (1983)*
Pol- Pelitic schist (garnet-staurolite-andalusite), phyllite and greywacke, *Pol$_d$–* amphibolite, metabasalt, metadolerite	*Pon$_1$-* Iron Formation *Pon$_d$–* amphibolite, metabasalt, metadolerite *Pon-* undifferentiated quartzite, greywacke, siltstone, chert and limestone	*Pot-* undifferentiated amphibolite, siltstone, phyllite and slate *Pot$_4$-* quartzite, phyllite, chert and siltstone *Pot$_3$-* amphibolite, metabasalt and metadolerite with minor undifferentiated metasediments *Pot$_2$-* fine grained quartzite and metasiltstone, chert and minor metabasalt *Pot$_1$-* amphibolite, metabasalt and metadolerite *Pot$_{1j}$-* banded iron formation-various stratigraphic levels
Arnold (1983)	*Arnold (1983)*	
Pol- arenites, siltstones, shales, phyllites, garnet-staurolite-andalusite schists, minor amphibolite	*Pon$_3$-* undivided metasediments, amphibolites and carbonaceous shales *Pon$_{3d}$-* labile arenites, siltstones, shales and subordinate amphibolites and carbonaceous sediments *Pon$_{3c}$-* quartz arenites, siltstones, shales and subordinate amphibolites *Pon$_{3b}$-* amphibolite, arenites, siltstones and minor BIF *Pon$_{3a}$-* arenites, siltstones, minor qtz arenites and minor amphibolites and schists *Pon$_2$-* labile arenites, siltstones, greywackes, minor amphibolite and schist *Pon$_{1c}$-* quartz arenite, minor BIF and labile arenite *Pon$_{1b}$-* quartz arenites, greywackes, siltstones, shales, phyllites and schists *Pon$_{1a}$-* amphibolite and rare plagiogranites	

Table 3.1: Lithostratigraphies of Derrick *et al.* (1976e) and Arnold (1983) presented for comparison with Table 3.2, lithostratigraphy outlined in this study
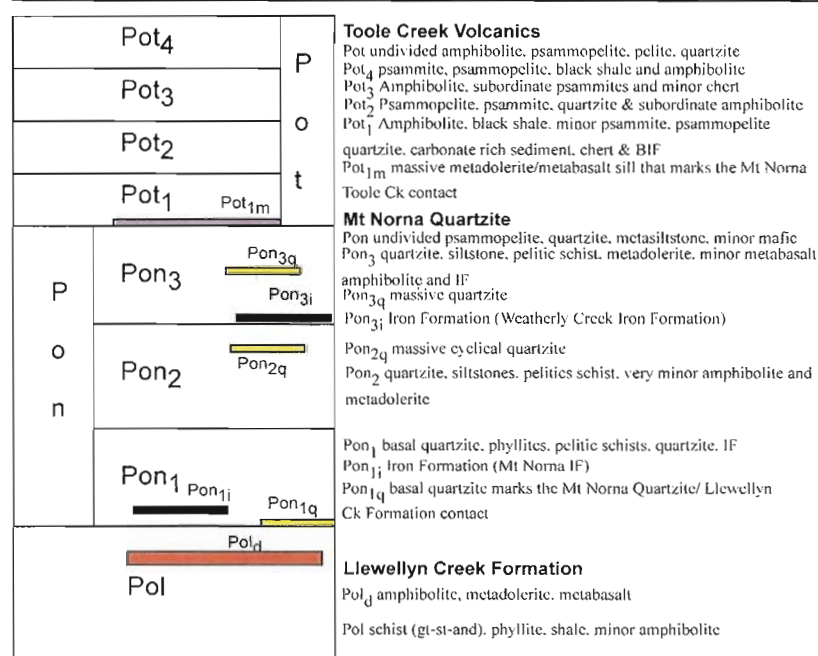
Figure 3.2: Stratigraphic column defined and used during the present study, refer to Table 3.1 and 3.2 and text for detail.

3.2.2 Current Lithostratigraphy

Traversing and mapping completed across the TCV and MNQ during the 1999 field season has necessitated revision, modification and amalgamation of previously published lithostratigraphies of the upper Soldiers Cap Group (Fig.3.2; Table 3.1). This revision is based on map scale correlations of completed traverses, sections, mapping at 1:25000 scale, and detailed airphoto and geophysical (aeromagnetics and gravity) interpretations.

The LCF remains unchanged from that of Derrick *et al.* (1976e), with the LCF/MNQ contact marked by the first appearance of the intermittent but consistent along strike, massive, thickly bedded quartzite of Pon_{1q} and/or massive quartzites of Pon_{1q} (Fig. 3.2; Table 3.2).

Lithostratigraphic Units	Overall Thickness	Lithology	Boundary Definitions
Pon_3 ($Pon3_q$, $Pon3_i$)	250-750m	Quartzite, psammite, pelite, metadolerite, amphibolite, massive quartzite (Pon_{3q}) and minor metabasalt and IF (Pon_{3i})	Top marked by increase in mafics including the first coherent metabasalt and/or a ~50m thick amphibolite. Rare ~5% black shales
Pon_2 (Pon_{2q})	1000-2000m	Quartzite, pelitic schist, psammite, psammopelite, variably altered metabasalt-metadolerite, amphibolite	Top defined by the first appearance of massive stacked, cyclical quartzites (Pon_{2q}) and Hummocky Cross Stratification
Pon_1 (Pon_{1q}, Pon_{1i})	1000-2600m	Interbedded pelitic schist and massive quartzite (Pon_{1q}), minor interbedded psammopelites, IF (Pon_{1i}) and polymict breccias	Base defined by massive quartzite (Pon_{1q}, Pon_1), top defined by increase in massive quartzite and mafics

Table 3.2: Descriptions of revised (this study) Mt Norna Quartzite lithostratigraphy, omitting quartzite beds and iron formations. (IF=Iron Formations).

In the locality of Mt Norna itself the transition from the LCF to the MNQ and TCV is difficult to reconcile due to a marked decrease in metamorphic grade, suggesting that the LCF-MNQ contact may represent a tectonic contact.

The composite metamorphic isograds mapped across the LCF-MNQ boundary in the Mt Norna area by Rubenach & Barker (1998) locally transgress bedding. They interpreted to represent multiple metamorphic mineral growth over the period from early-D_1 to syn-D_4. Similarly, Giles & MacCready (1997) proposed a method within the existing structural framework of refolding of earlier isograds which produced the observed offset in isograds in the Weatherly Creek Syncline/Snake Creek Anticline area. Loosveld (1988) proposed a method of equilibration of isograds in fold nappes following peak metamorphism to produce the offset of the higher grade domain in the Snake Creek Anticline. Away from zones of high strain such as the interpreted hinge of the Snake Creek Anticline in the Mt Norna area, the LCF-MNQ contact is

38

conformable and mappable for several kilometres along strike. The author therefore sees no need to revise the stratigraphy of the lower Soldiers Cap Group to include a tectonic contact.

The major revision to published lithostratigraphy is within the MNQ and is largely a refinement of the Arnold (1983) scheme, outlined above in Table 3.2 and depicted in Figure 3.2. The stratigraphy of the TCV was not significantly altered although some later internal reports from BHP Minerals suggested the subdivision of *Pot₁* into *Pot₁ₐ* and *Pot₁ᵦ*, with the former being an amphibolite dominated subunit and the latter shale dominated. This suggestion has not been adopted based upon a lack of supporting geological evidence.

A change resulting from the modification of stratigraphy in this study is the MNQ-TCV contact (*Pon₃-Pot₁*; Fig. 3.2; Table 3.2) which is now marked by a ~50m thick metadolerite sill (*Pot₁ₘ*; Fig.3.2; Table 3.2; *cf.* Derrick *et al.* 1976e; Ryburn *et al.* 1987) with some intrusive contacts (Ch.5), or the first coherent metabasalt flows and sills (Ch.5). This unit is present across much of the map area (Fig.3.1; Map Sheet One) and is consistently found at a similar stratigraphic level throughout and so provides a reliable stratigraphic marker.

3.3 Previous Sedimentological Interpretations

The lower Maronan Supergroup (Fullarton River Group-see Ch.2), was interpreted by Beardsmore *et al.* (1988) as a shallow to moderate water depth shelf-shore sequence intercalated with bi-modal volcanics deposited during a phase of active rifting.

The overlying Soldiers Cap Group has long been interpreted as the only deep marine, turbidite sequence within the Eastern Succession. For detail on regional and local stratigraphy refer to Figure 2.1. Most authors interpret the Soldiers Cap Group as the product of the progressively westward deepening, maturing Cloncurry Basin of Newbery (1990; Fig.2.2), (*cf.* Beardsmore *et al.* 1988; Blake 1987; Loosveld 1987).

The Fullarton River Group-Soldiers Cap Group transition is marked by the interpreted conformable contact of the New Hope Arkose with the LCF (Beardsmore *et al.*1988). Sedimentary structures preserved in the LCF include graded bedding, scour and fill structures, load casts, minor ripple cross-stratification, fluid escape structures and partial to complete Bouma sequences (Derrick *et al.* 1976e; Beardsmore *et al.* 1988; Newbery 1990; Beardsmore 1992; Ryburn *et al.* 1987). The interpreted palaeoenvironment is that of a deep-water shelf (Beardsmore *et al.* 1988; *cf.* Blake 1987). Loosveld (1988) noted shallow water sedimentary structures (hummocky cross stratification) within the LCF and suggested that it may have been a reworked turbidite sequence deposited on a moderately sloping inner shelf.

The MNQ has been interpreted as representing a moderate to low energy environment, possibly a medial-distal turbidite fan (Beardsmore *et al.* 1988; *cf.* Blake 1987). Loosveld (1988) interpreted the lack of scours and wackes to indicate that the MNQ was deposited in a moderate energy environment such as a distal turbidite fan. The TCV were interpreted as being the result of mature clastic sedimentation at an indeterminate water depth by Beardsmore *et al.* 1988 (*cf.* Blake 1987). In summary most authors (Blake 1987;

Beardsmore e*t al.* 1988; Glikson & Derrick 1970; Derrick *et al.* 1976e; Loosveld 1988; Newbery 1990) proposed that the LCF-MNQ-TCV transition is a conformable upwards facing sequence recording a deepening marine environment within the medial-distal parts of a 'classical' submarine fan system.

3.4 Sedimentary Nomenclature and Petrography

Given the grade of metamorphism and large degree of recrystallisation that has affected the Soldiers Cap Group, standard metamorphic nomenclature has been used in lithofacies titles. The petrogaphic and lithofacies descriptions below use standard sedimentary grain size nomenclature (psammite, psammopelite and pelite) to infer a pre-metamorphic grain size wherever possible. Previous authors (Derrick 1976e; Arnold 1983), have used the terms ortho-quartzite to describe the medium-coarse grained equigranular units in the sequence. In keeping with the standard metamorphic nomenclature used for the petrography and sedimentary lithofacies titles outlined below, these units are referred to as quartzites. Metasediment is a 'generic' term used here to describe all units of interpreted sedimentary origin and includes psammites, psammopelites and quartzites.

Examination of thin sections from the upper SCG shows the petrography of the quartzites to be relatively uniform across the study area. This generally comprises subhedral quartz with common recrystallised/annealed boundaries, and undulose extinction (Fig.3.3a), elongate euhedral-subhedral biotite and chlorite, often controlled by structural foliations (Fig.3.3b).
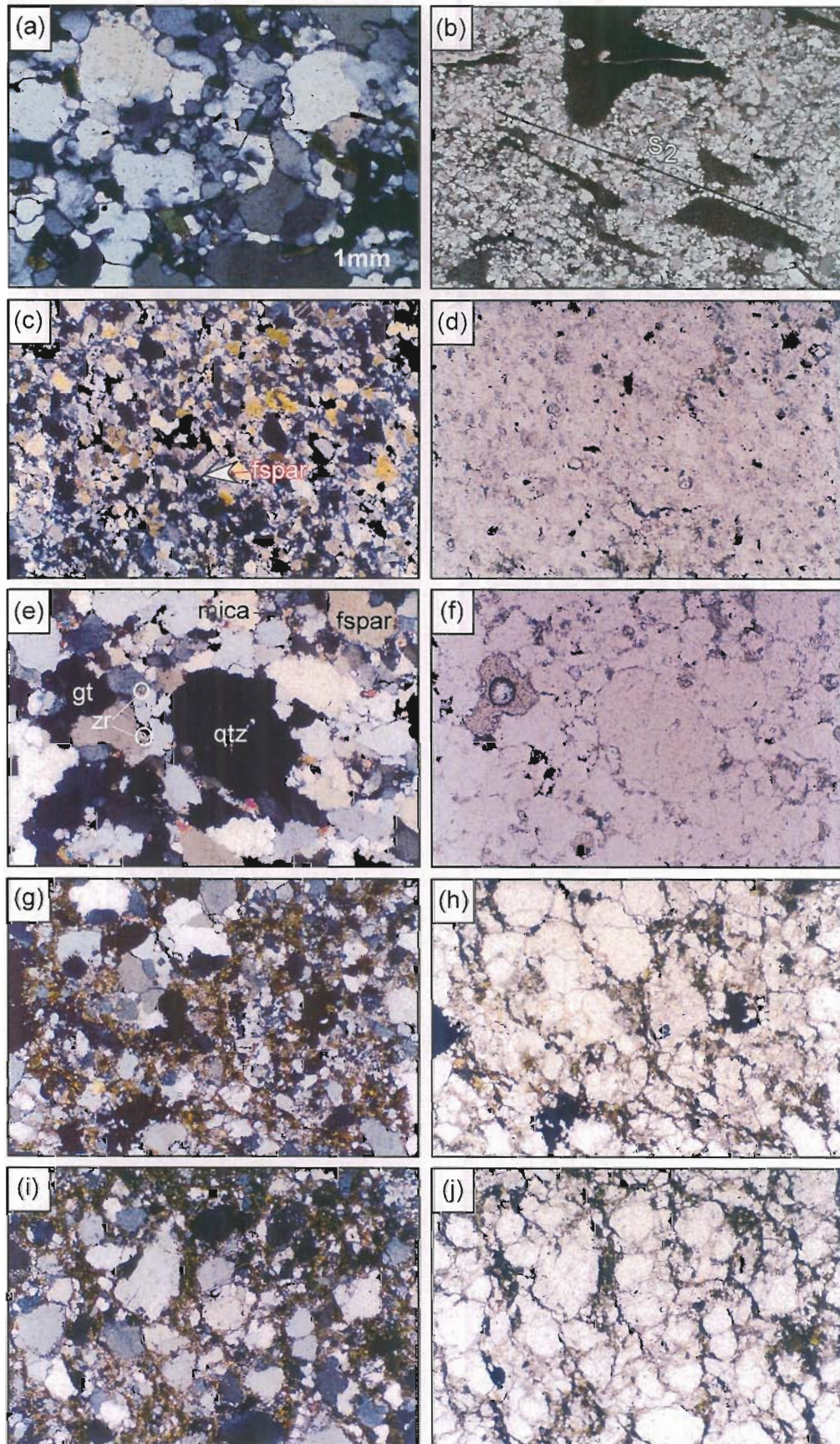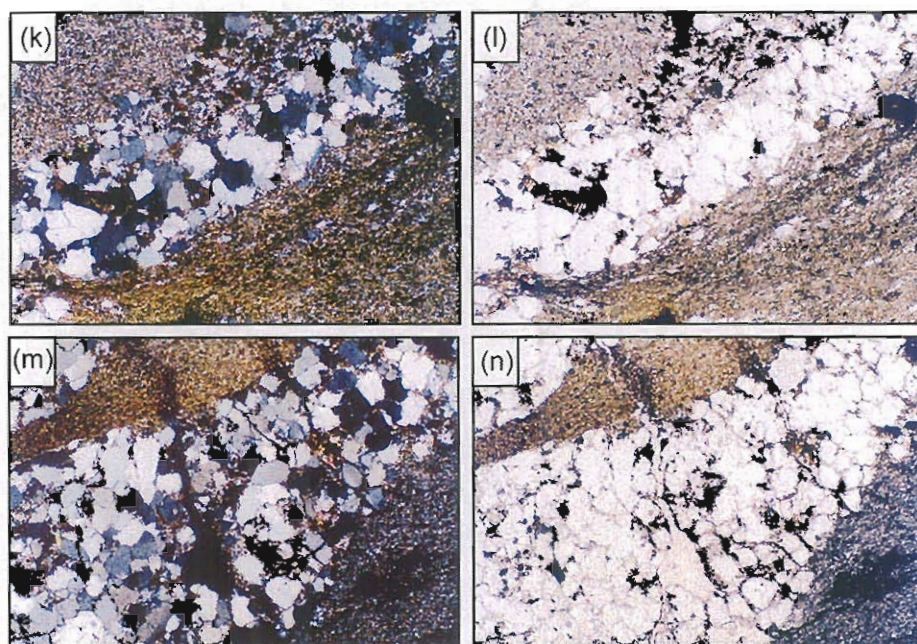
Figure 3.3: (a) photomicrograph (crossed polars) of Basal Quartzite (zircon dating sample (BQ-012) showing the annealed and recrystallised nature and lack of complex sodic-calcic alteration overprints; (b) photomicrograph of Polymictic Breccia Facies (crossed polars) siltstone clasts in quartz-phyllosilicate matrix which is aligned parallel to the dominant local and regional foliation (WC-73); (c) crossed polars image of psammopelite from Quartzo-pelite Facies Association(PG-89); (d) uncrossed polars image of (c); (e) crossed polars image of sample from base of clast supported massive quartzite body lower MNQ (WC-67), Quartzo-Pelite Facies Association, note detrital zircons and rounded garnet at left of image; (f) uncrossed polars image of (e); (g) intermediate matrix supported quartzite, phyllosilicate matrix (biotite-chlorite) with quartz-feldspar-zircon-ilmenite clasts, crossed polars (WC-60); (h) intermediate matrix supported quartzite, phyllosilicate matrix (biotite-chlorite) with quartz-feldspar-zircon-ilmenite clasts, uncrossed polars (WC-63); (i) intermediate matrix supported quartzite, phyllosilicate matrix (biotite-chlorite) with quartz-feldspar-zircon-ilmenite clasts crossed polars (WC-63); (j) intermediate matrix supported quartzite, phyllosilicate matrix (biotite-chlorite) with quartz-feldspar-zircon-ilmenite clasts uncrossed polars; (k) crossed polars images of Polymictic Breccia Facies from the Basal Quartzite Facies, lower MNQ (WC-73). Note the elongated phyllosilicate 'clumps', marked by 'PC', parallel to foliations and recrystallised quartz crystals and interstitial muscovite-biotite-chlorite in the matrix; (l) uncrossed polars image of (k) Polymictic Breccia Facies from the Basal Quartzite Facies, lower MNQ. Note the elongated phyllosilicate 'clumps' parallel to foliations and recrystallised quartz crystals and interstitial muscovite-biotite-chlorite in the matrix; (m) crossed polars images of Polymictic Breccia Facies from the Basal Quartzite Facies, lower MNQ (WC-73). Again Note the elongated phyllosilicate 'clumps' parallel to foliations and recrystallised quartz crystals and interstitial muscovite-biotite-chlorite in the matrix; (n) uncrossed polars images of (m) Polymictic Breccia Facies from the Basal Quartzite Facies, lower MNQ. NB: all images in this Figure have a 2mm wide field of view.

43
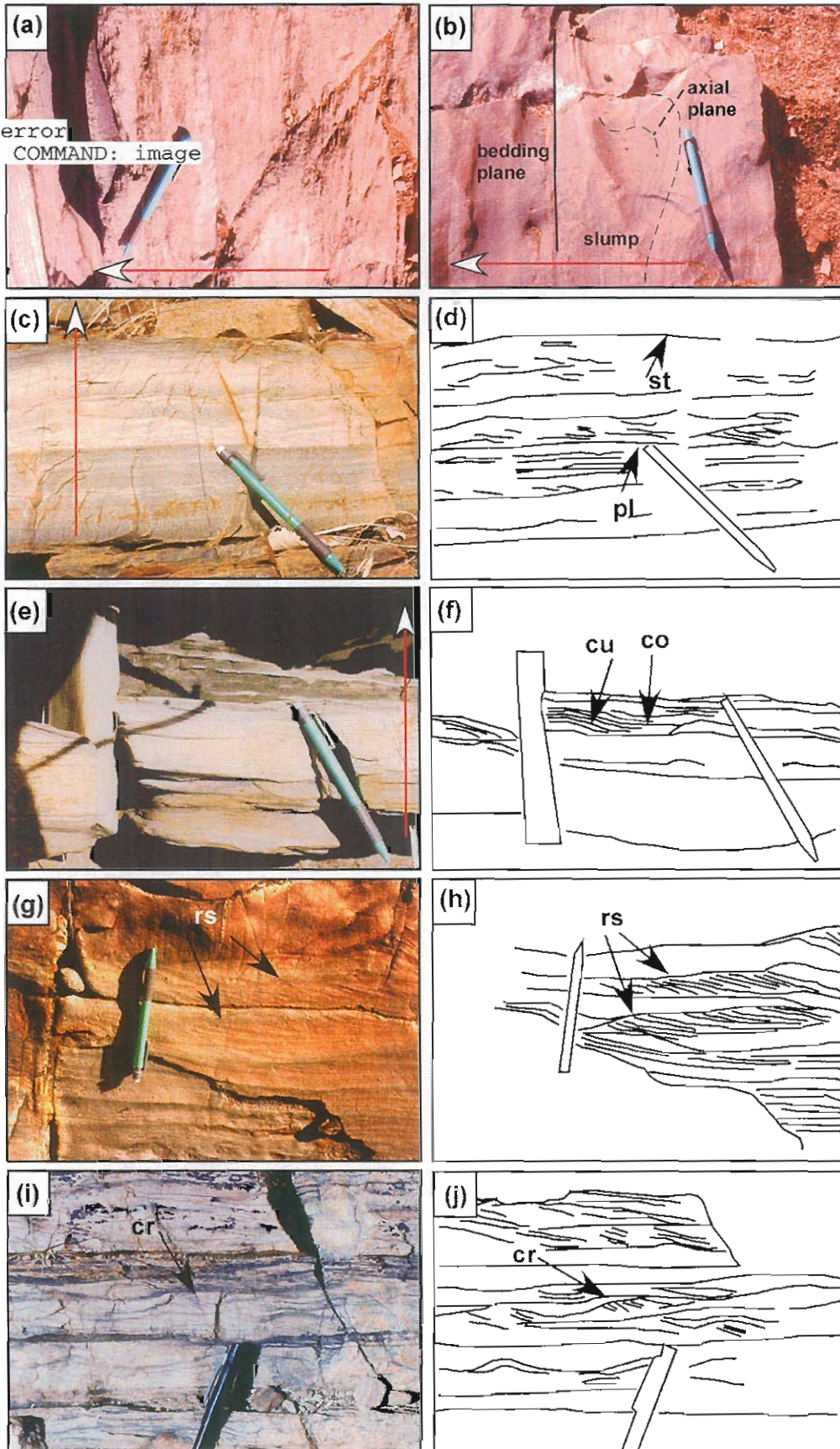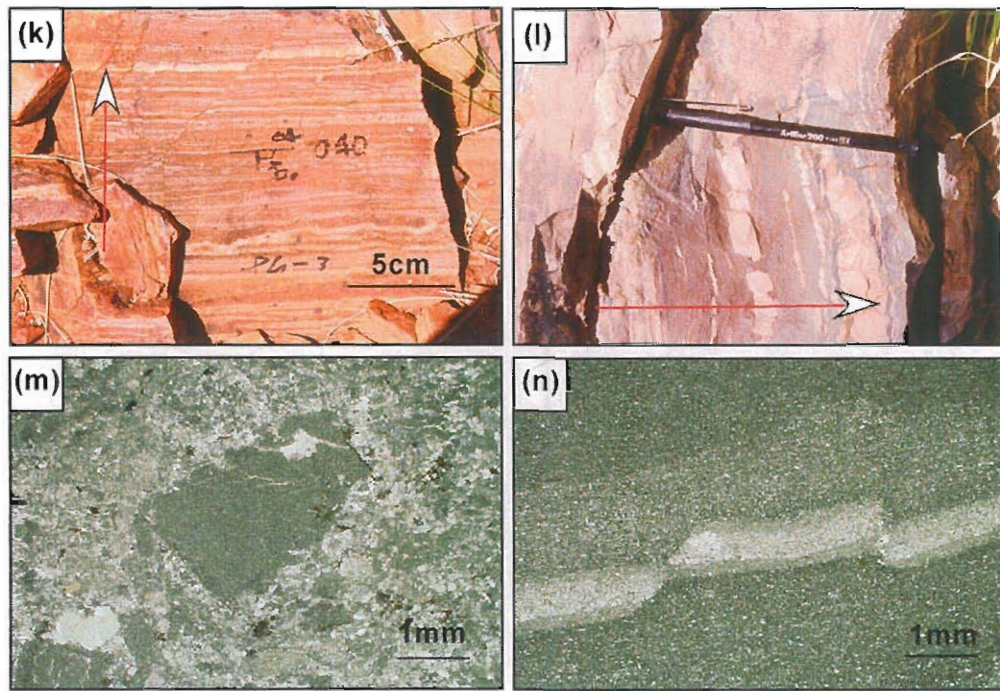
Figure 3.5: Images of load structures and ripple forms in the Quartzo-Pelite Facies Association
and the Swale-Ripple Facies Association (a) flame structures, Massive Quartzite Facies, wayup
to left of image; (b) slump front in Massive Quartzite Facies, way up to left and north to bottom
of the image; (c) Swaley Psammite Facies showing sequence from planar laminated ('pl') and
sharp base to swaley top('st'); (d) line sketch depicting the major surfaces in (c); (e) concave-up
('cu')and convex-up('co') swaley bedform, Swaley Psammite Facies, adjacent to location
of (c-d); (f) line sketch depicting the major surfaces in (e); (g) reactivation surfaces ('rs') in
quartzite of the Rippled Psammite Facies, stratigraphic way up to top of image; (h) line sketch
of (g) depicting the major surfaces; (i) climbing ripples ('cr') in Rippled Psammite Facies;
(j) line sketch of (i) depicting the major surfaces;(k) Laminated Psammopelite Facies, Pumpkin
Gully Syncline; (l) Disrupted Facies adjacent to the Telegraph Fault, Pumpkin Gully Syncline;
(m) Photomicrograph crossed polars oflarge subrounded clast of Laminated Psammopelite
(metasiltstone) in chaotic phyllosilicatematrix Disrupted Facies; (n) Photomicrograph of
synsedimentary faulting in Disrupted Facies. (NB: red arrows in all figures define interpreted
way-up).

Detailed studies of the metamorphic paragenesis of the area are available in Lewthwaite (2000; *cf.* Rubenach & Barker 1998). Localised quartz-epidote and later feldspar±haematite and magnetite are related to alteration associated with basaltic units (Ch.5).

Several outcrops of quartzite at the base of the MNQ are spatially associated with zones of late regional albitisation within the Snake Ck Anticline (*cf.* Rubenach & Barker 1997). Samples from the basal MNQ (Thickly Bedded Quartzite Lithofacies) used in the detrital zircon studies (BQ-012; Ch.4), have distinctive quartzite metamorphic textures (Fig.3.3a;), and relict sedimentary grain arrangements, relict ripple forms (Fig.3.4a-b) and sharp, mappable contacts with surrounding units. This suggests that they are a product of metamorphism and deformation of a primary fabric and not later alteration.

Clast-matrix relationships within the quartzites are also relatively uniform across the study area with a clast assemblage in order of occurrence of quartz, feldspar, garnet, zircon, ilmenite (Fig.3.3g-j). Textures range from clast supported (Fig.3.3e-f), to matrix supported with a greater percentage of phyllosilicates between quartz-feldspar clasts (Fig.3.3g-j) suggesting a protolith with a clay mineral rich matrix.

In thin section psammopelite units comprise metamorphic biotite-chlorite, sillimanite and rare garnets and detrital feldspars with rare feldspar overgrowths on crystal rims (Fig.3.3b-d). Petrographically these facies are all very similar, with remnant bedding defined by biotite and chlorite, and structural grain by uncommon elongated quartz grains. Pelitic schists within

the sequence have few preserved primary textures and are now composed of a

very fine-grained assemblage of biotite-chlorite-quartz-feldspar which are

aligned parallel to the dominant foliation.

3.5 Sedimentary Lithofacies and Lithofacies Associations

The metasedimentary rocks of the upper Soldiers Cap Group are here

subdivided into nine lithofacies on the basis of grain size, bed form, bed

thickness, preserved sedimentary structures and spatial relationships observed

in detailed sections. Additionally, they are grouped into four lithofacies

associations. These are summarised in Table 3.3 and described in detail

below. The sequence, distribution and relationships between lithofacies and

facies associations is outlined below and depicted in Figures 3.6 and 3.7.

Metabasaltic units and iron formations, whilst forming an integral part of the

sedimentary pile, are discussed in detail in Chapter 5 and Chapter 6

respectively.

3.5.1 Basal Quartzite Facies Association

Graded Quartzite Facies

Description

This facies consists of thickly-bedded (0.5-3m thick) medium-coarse grained

quartzites. Both normally graded and massive beds have sharp upper and

lower contacts. Important sedimentary structures within this facies are swale

and hummock bed tops that generally occur on massive beds. These bedforms

are up to 0.5 high and have 0.5-2m trough-trough wavelengths. Rare internal

laminations were observed in some swaley beds, that followed the bed form

and consisted of sets >0.5m thick. Rare asymmetrical current ripples with

wavelengths from 0.05-0.08m and amplitudes from 0.05-0.01m, occur on

some bed tops. Massive quartzite beds occasionally contain rounded

intraformational clasts 'intraclasts' (Fig.3.4c-d ; Fig.3.7~100-200m). These

intraclasts comprise coherent siltstone with remnant lamination, are rounded

to subrounded and up to 0.2m long (longest axis) and are aligned sub-parallel

to host bedding. There is no internal stratification or organisation of these

intraclasts vertically or laterally within the beds and clast density is low.

Interpretation

Features such as normal grading and asymmetrical current ripples suggest

deposition from a low density, medium energy turbidity current (Lowe 1982).

However, the floating clasts described here create some difficulty in

interpreting this facies as the product of a turbidity flow. Kneller & Branney

(1995) suggests that this style of clast is formed by aggradation on a flow

surface in a quasi-steady turbidity current, clast deposition occurs when

sediment supply is outstripped by flow rate. This facies is interpreted here as

the result of a steady or near steady turbidity flow with a migrating laminar

flow surface on which the intraclasts 'rode' to their current positions. The

presence of swale and hummock bedforms and rare associated internal

laminations, similar to those in the Swaley Facies Association outlined below,

suggest a significant component of storm current reworking at or near storm

wave base.

Thickly Bedded Quartzite Facies

Description

This facies comprises thick to extremely thickly bedded (2-25m), massive, medium- to coarse-grained quartzites. Minor interbeds of medium- to coarse-grained psammite with rare remnant bedding, between 1-4m thick occur between thinner quartzite beds. Both the quartzite and sandstone are massive and internally structureless. These quartzites are considered to be primary as opposed to alteration products based on preservation of many primary sedimentary structures including matrix clast-relationships and occasional detrital grains in adjacent units (*eg.*Fig.3.4a-b).

Interpretation

A detailed summary of the problems of interpreting thick massive sands in subaqueous sequences is given by Haines *et al.* (2001; *cf.* Kneller 1995). They interpreted beds with very similar features to this lithofacies as the product of high density turbidity currents. Other common environments for thick massive sands include 'classical turbidites' (Bouma 1962) or sandy debris flows (Shanmugam 1997; 2002). Shanmugam (2002) proposed that many units previously interpreted as high density turbidites were actually the product of sandy debris flows. This concurs with the underlying Graded Quartzite Lithofacies and associated Polymictic Breccia Facies, both of which infer an active sedimentary environment conducive to the production of debris flows. Debris flow is defined here as a mixture of granular debris, in this case adjacent 'lithologies', and water flowing downslope, likely along a channel (Allen 1985)

Polymictic Breccia Facies

Description

Polymictic breccia consisting of locally derived clasts (siltstone, sandstone and rare iron formation), ranging in size from 0.005-0.05m (long axis), in a medium- to fine-grained silty màtrix. Estimated thickness of individual intervals is between 0.5-3m. Clasts and phyllosilicates in the matrix are aligned parallel to the dominant structural foliation and recrystallisation during peak metamorphism has destroyed many primary textures. In thin section this facies is composed of a fine-grained quartz-muscovite-chlorite groundmass with two distinct clast types chaotically distributed (Fig.3.3k-n); 1- fine grained quartz-plagioclase 'pelite'; 2- medium grained quartz-plagioclase-chlorite-muscovite 'psammite'. These clasts are largely derivatives of the underlying Graded Quartzite and Thickly Bedded Quartzite Facies. This breccia occurs both stratigraphically above and below the Mt Norna Iron Formation as (Ch.7) and also at smaller exhalite occurrences along strike (Fig.3.7; ~300m). Contact relations are generally unclear due to poor outcrop, however the breccia is mappable along strike at Mt Norna for approximately 70m.

Interpretation

The location of this unit within the lower MNQ at a well defined stratigraphic position and the close association with iron formations allows confident interpretation as a distinct, albeit minor, lithofacies. However, the strong structural, metamorphic and alteration overprint presents difficulties in defining the true degree of rounding of the clasts and any inference of transport distance or mechanisms. Stratigraphic and spatial proximity to the

Mt Norna iron formation infers a close relation to hydrothermal processes (Ch.7). The presence of clasts of underlying lithologies and inferred conformable contacts with surrounding units suggests that this breccia is effectively in-situ or at the least proximal to source. This facies may be analogous to the sedimentary breccias observed in the Aldridge Formation, British Columbia Canada, interpreted as the result of expulsion of overpressured basin fluids along extensional structures depositing in the subsurface and at surface (Höy *et al.* 2000; Turner *et al.* 2000). Definitive conclusions are difficult, but based upon the evidence available, this facies is interpreted as the result of a mixture of sedimentary and hydrothermal processes closely related to the deposition of the Mt Norna iron formation (*cf.* Ch.7).

3.5.2 Quartzo-pelite facies association

Quartzite Facies

Description

This facies consists of 1-3m thick massive to normally graded beds of quartzite which have conformable contacts with the associated Pelitic Facies (Fig.3.4e). Sedimentary structures observed include small scale (0.05-0.2m) concordant trough cross bedding that comprises solitary sets >0.6m thick. Planar cross lamination consists of small-scale (0.05-0.15m) grouped sets. Small-scale (>0.1m) angular-subangular rip-up clasts of underlying siltstone at the bases of massive quartzite beds are also present but not common. Swaley and hummocky bedforms are common on massive and normally graded, thicker beds (Fig.3.4e). A representative section of this lithofacies and the Pelite Facies is depicted in Fig.3.6a (FSC-01)

Interpretation

Normal grading, rip-up clasts and planar cross lamination are all features

indicative of deposition from a medium energy turbidity current (Lowe 1982).

The association with the Pelitic Facies outlined below reinforces this

interpretation. The common presence of swaley and hummocky bedforms

similar to those in the Basal Quartzite Facies Association and Swaley Facies

Association is interpreted as the product of storm generated oscillatory

currents.

Pelitic Facies

Description

This facies comprises thin- to thickly-bedded (0.1-3m) very-fine- to medium-

grained pelitic schists. No relict sedimentary structures were observed, as

structural and metamorphic overprints have destroyed primary textures,

however, this material is in places interbedded with and has sharp contacts

with quartzites of the Graded Quartzite Facies (Fig.3.7; Fig.3.6 FSC-01).

There is no direct link between the thickness of these units and the associated

quartzites.

Interpretation

The obliteration of any remnant structures by metamorphism and deformation

makes interpretation of this facies difficult. However, the close association

with beds of the Quartzite Facies and the presence of rip-up clasts of this

facies preserved in adjacent units suggests that these pelites are the result of

ambient pelagic sedimentation and additional suspensional sedimentation,

associated with turbidity currents.

3.5.3 Swale-Ripple Facies Association

Massive Quartzite Facies

Description

This facies consists of medium-coarse grained, laminated to very thickly

bedded (0.05-7m) cycles of quartzite. A representative section for this facies

is shown in Fig.3.6a (FSC-02). Bed contacts range from sharp to gradational

and separate intervals of planar laminated and massive quartzite. A range of

bedforms are present, from massive to laminated, normally graded, planar

beds and massive beds with swale and hummock tops (Fig.3.4g). Beds with

swales and hummocks present range from 1-7m thick and have sharp bases

and tops. Swale (trough-trough) wavelengths are from 0.4-1.4m and

amplitudes from 0.05-0.25m (trough-adjacent hummock). Trough cross-

bedding is present as solitary concordant small scale sets (>0.2m thick). Soft

sediment and dewatering structures including slumps and flame structures are

common within finer grained beds (Fig.3.5a-b). Roughly circular siliceous

concretions up to 0.75m in diameter occur rarely on some massive bed bases.

The most diagnostic feature of this facies is the repetition over 10-50m, of a

cycle with a massive, thick, planar basal quartzite, overlain by a sequence of

planar laminated and massive quartzite, rare trough cross-bedded quartzites

and swaley and hummocky quartzites described above (Fig.3.4g). There is no

clearly defined upward change in grain size (Fig.3.6a-TSC-01 1200-1700m).

Interpretation

As with the other quartzite-dominated facies within this sequence, the

difficulty is determining a debris flow vs. turbidity current origin. On the basis

of normal grading, trough cross-bedding and dewatering/liquefaction features,

and the overall lack of features indicative of sandy debris flows outlined by

Shanmugam (1997) and found in the Basal Quartzite Facies, this facies is

interpreted as a product of cyclical turbidity currents. The vergence of slump

folds have similar unreconstructed orientations (see below) and point to a

relatively uniform local palaeoslope of around 10-15°. Oscillatory currents,

again likely storm generated, are inferred to produce the swaley and

hummocky topography on the massive quartzite beds.

Swaley Psammite Facies

Description

This facies comprises medium-grained, laminated to thinly-bedded (0.05-

0.35m) sandstone. Beds have sharp bases and distinctive swaley and

hummocky geometry commonly with internal laminations (Fig.3.5c-f;

Fig.3.6b FMF-01 7-9m). Swales and hummocks have wavelengths of 0.2-

0.4m and amplitudes of 0.08-0.15m. Internal laminae consist of grouped sets

0.1-0.15m thick, that commonly consist of convex up and concave-up swale

and hummock form laminae that intersect and truncate at low angles (>15°;

Fig.3.5c-f). Parallel lamination underlies the internal cross-laminae and rare

rippled fine-grained tops are also present (Fig.3.5c-d). No sole marks were

observed in this facies.

Interpretation

Based upon the intersecting low-angle cross laminae and swaley and

hummocky bedforms, similar to those described by numerous previous

authors (DeCelles & Cavazza 1991; Dott & Bourgeois 1982; Harms et al.

1982; Hunter & Clifton 1982; Walker et al.1983; Duke 1985) this facies is

55

interpreted as the product of a storm generated oscillatory current, that

produces characteristic hummocky cross stratification (HCS; Dott &

Bourgeois 1982; Walker et al. 1983). The presence of HCS confirms the

preservation of sedimentation which occurred at or above storm-wave base

(Harms et al. 1975).Several facies schemes (Dott & Bourgeois 1982; Walker

et al. 1983) and conceptual models (*eg.* Nottvedt & Kreisa 1987; Myrow &

Southard 1996) exist for storm generated sequences of fine-medium grained

sandstones. Walker et al. (1983) constructed the BPHFXM facies model, B=

massive-graded/sharp base; P= parallel lamination; H=hummocky cross

stratification; F=flat lamination; X=cross lamination; M=bioturbated

mudstones. Within this facies model the Swaley Psammite Facies sequence in

the SCG is best described as PH(X) with X rarely present. Following Walker

et al. (1983) the sequence described here is intepreted as the product of

unidirectional currents P (parallel laminations) grading into H (hummocky

cross stratification) produced by peak storm activity-oscillatory currents and

X (rippled) beds as reworking by waning storm energy. The Walker *et*

al.(1983) facies scheme was preferred for the upper SCG due to the lack of

interbedded mudstone, a major component of the Dott & Bourgeois (1982)

facies model, and the presence of parallel lamination underlying HCS within

this facies.

Rippled Psammite Facies

Description

This facies consists of medium-grained, thinly-bedded to laminated (0.05-

0.35m) sandstone (Fig.3.6b FMF-01 2-4m). Beds are generally sharp-based

and internally laminated. Preserved structures include asymmetrical ripples

(wavelength 0.05-0.1m, amplitude 0.01-0.08m) at the top of thin beds.

Climbing ripples (Fig.3.5i-j) are common in this facies and consist of ripple

sets of wavelength 0.012-0.2m, amplitude 0.05-0.1m and uniform angles of

climb of approximately 10-12°. Small scale (>0.10m) sets of planar cross-

beds are commonly truncated by high angle reactivation surfaces (Fig.3.5g-h).

Interpretation

The climbing ripple, planar laminations and reactivation surfaces of this facies

are interpreted as the product of a steady flow of increasing velocity and

constant sediment supply, possibly a density flow. The lack of a change in the

angle of climb of the climbing ripples discounts any decrease in flow strength

and concomitant increase in sediment supply.
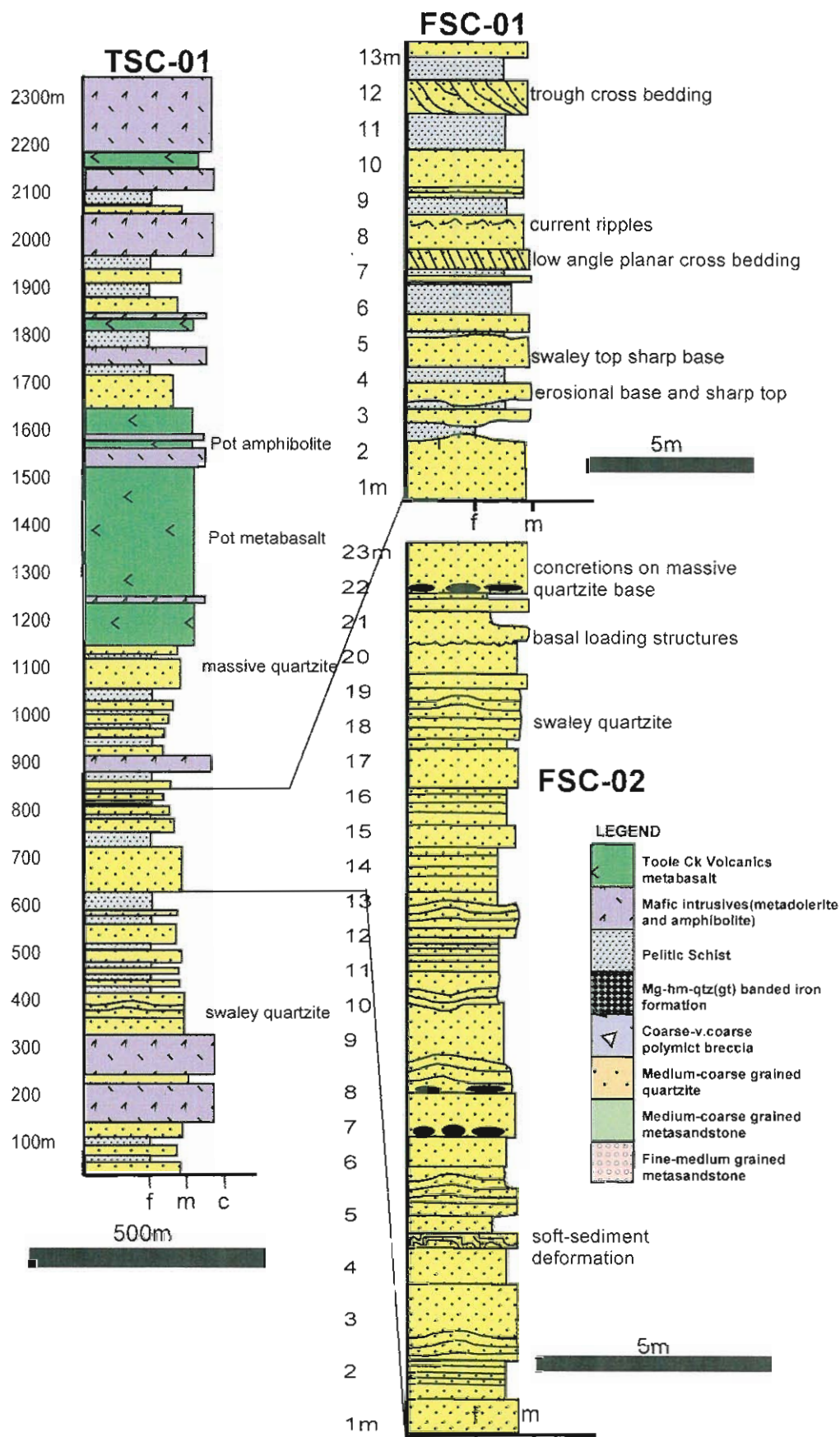
Figure 3.6a: Schematic regional sedimentological log (TSC-01) and more detailed relevant facies sections- FSC-01 & FSC-02. Facies sections represent segments of regional traverse logs mapped at a more detailed scale. For section locations refer to Figure 3.1 and Map Sheet One.

62
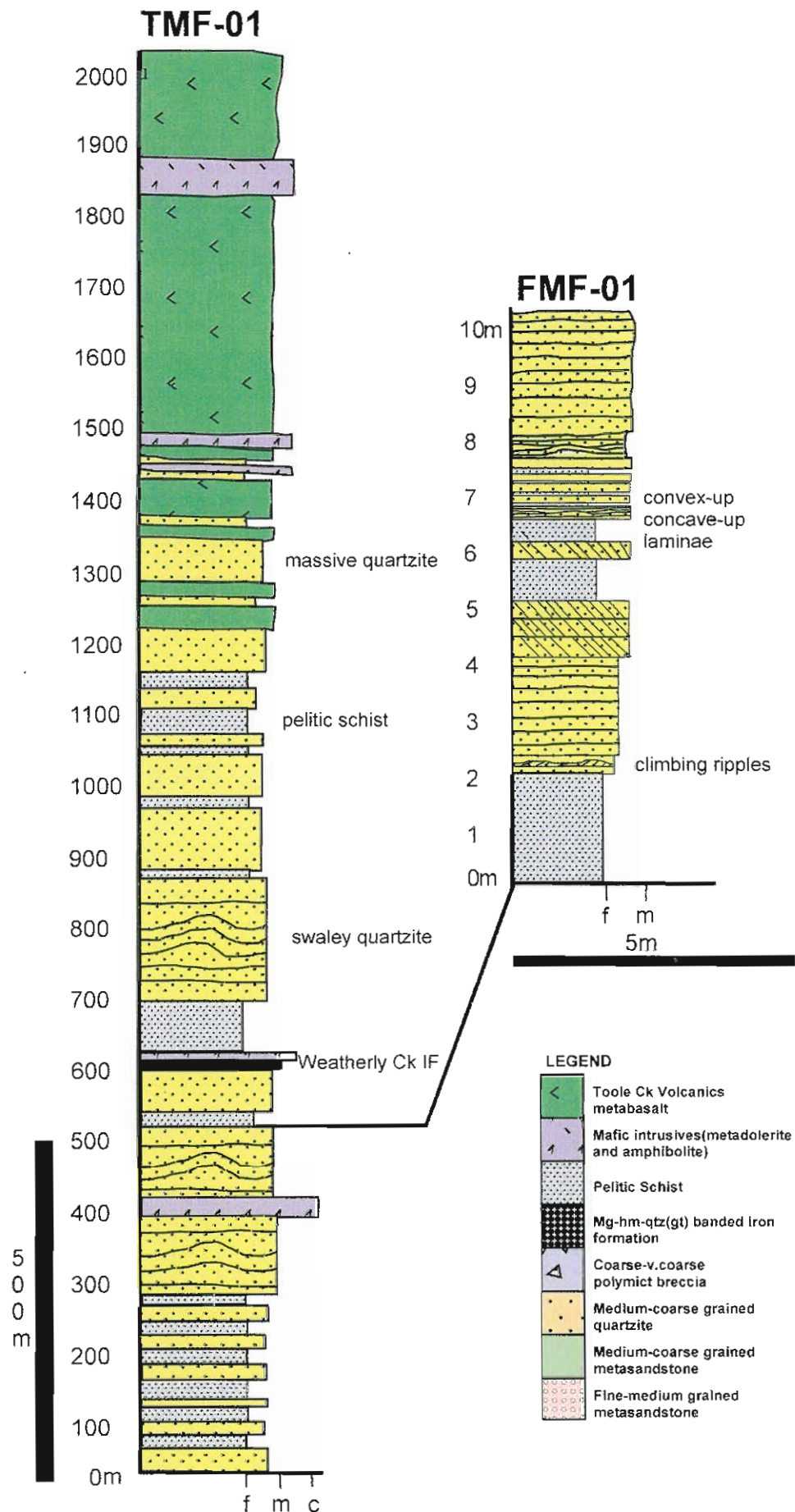
Figure 3.6b: Schematic regional sedimentological log (TMF-01) and relevant facies log (FMF-01) depicting the relationship between the Rippled Psammite Facies and Swaley Psammite Facies.

3.5.4 Psammo-pelitic facies association

Laminated Psammopelite Facies

Description

This facies is composed of a repetitive sequence of fine- to medium-grained, laminated to thinly-bedded sandstone/siltstones (Fig.3.5k) interbedded with mafic intrusives interpreted by the author as synsedimentary (Ch.5). Rare sedimentary structures include small scale synsedimentary faulting, and very rare small-scale planar cross-bedding. This facies is restricted to the Pumpkin Gully Syncline. Very rare carbonacaeous laminae are present.

Interpretation

Limited outcrop makes confident interpretation difficult however based upon the internal features and associations with surrounding units an environment of deposition can be proposed. The fine grained and laminated nature of this facies suggests sustained low energy undirectional currents. The association with Quartzite Facies and Pelite Facies and presence of small scale cross bedding suggests a turbidity current origin. The presence of carbonate implies that it may be shallow water.

Disrupted Facies

Description

This facies comprises disrupted beds of fine- to very coarse-grained brecciated sandstone, siltstone and minor iron formations in a fine grained matrix (Fig.3.5l-n). Locally continuous beds up to 5m thick have sharp conformable contacts with overlying coherent laminated sandstone/siltstone and underlying iron formations.

The distribution of this facies is largely controlled by proximity to the northerly striking Telegraph Fault (Map Sheet Two; Ch.7), with the maximum thickness of approximately 15m at the end of the body closest to the fault and 2-5m along strike further to the west. This breccia is not present to the east of the Telegraph Fault in the vicinity of the Monakoff deposit. Breccia fabrics range from rounded, milled and altered locally derived clasts (0.05-0.8m long axis) in a fine-grained matrix, to large (0.8m; Fig.3.5l-m) clasts with intact bedding and lamination in a fine-grained matrix. The basal contact of several thick beds contains rip-up clasts of underlying iron formations. Thin section and hand specimens display a series of complex textures including syn-sedimentary faulting (Fig.3.5l-n), load cast structures and slumping/deformation of sedimentary bedding. As with the Laminated Psammopelite Facies, the Disrupted Facies is restricted to the Pumpkin Gully Syncline.

Interpretation

The close proximity of this facies to the Telegraph Fault and control by this fault on the distribution of this facies points to the two being genetically linked. The presence of locally derived rip-up clasts (iron formations) and conformable contacts with adjacent lithologies suggest that this breccia is primary and not a result of complex structural overprinting by structures such as the D_1 Pumpkin Gully Thrust (Williams 1997). The interpretation of the Telegraph Fault as a reactivated synsedimentary fault and the presence of rip-up clasts of local material allows this breccia to be interpreted as a style of talus breccia shedding off the Telegraph Fault.

3.6 Distribution and abundance of facies associations

The facies and facies associations described above were defined based upon genetic sedimentological and stratigraphic grounds and conform to and form a part of the lithostratigraphy, defined above (Fig.3.2; Table 3.2). The distribution and relative percentage of these associations is as follows and is also depicted as an interpreted surface distribution in Figure 3.1 and as a composite stratigraphic column, that includes more detailed representative logs of important sedimentological facies for the Weatherly Creek Syncline area (Fig.3.6 and 3.7).

The Basal Quartzite Facies Association is restricted to the basal parts of the SCG, is wholly contained within Pon_1 and within this unit is laterally extensive and mappable across the Weatherly Creek Syncline area (Fig.3.1; Map Sheet One). This facies association was not observed within the Pumpkin Gully Syncline or in the Toole Creek Syncline area.

The Quartzo-Pelite Facies Association is present in lithostratigraphic units Pon_1-Pon_3 as a major constituent (~75-80%) and as a moderate component (20-30%) of Pot_1-Pot_4 where it is intercalated with metabasalts and metadolerite sills and flows (Ch.5), sporadic shales iron formations and metasomatic ironstones. Notably, hummock and swale bedforms are rare above Pot_2. This facies association was observed in the Pumpkin Gully Syncline and the distribution there is discussed below.

The Swaley Facies Association is present from the mid-MNQ to lower TCV (Pon_2-Pot_1) where it comprises up to 30% of the stratigraphic column, and is

63

laterally contiguous and mappable along strike for up to 700m. The cyclical quartzites of the Massive Quartzite Facies are present from the mid-MNQ, where an increase in volumetric dominance over the Quartzo-pelite Facies Association marks the *Pon$_2$-Pon$_3$* contact. This facies association was not observed within the Pumpkin Gully Syncline.

The stratigraphy and geology of the Pumpkin Gully Syncline is interpreted as being correlative with that of the Weatherly Creek Syncline, with MNQ overlain by TCV younging from N-S in the former (see Map Sheet Two; *cf.* Ryburn *et al.*1987). However, there are some subtle differences in sedimentology which necessitated the creation of a separate facies association, the Psammo-pelite Facies Association, in the Pumpkin Gully Syncline. Within the Pumpkin Gully Syncline this comprises ~20% of the sequence and is intercalated with elements of the Quartzo-pelite Facies Association, sporadic ironstone and iron formations, and numerous synsedimentary mafic sills of the TCV and upper MNQ (Ch.5). Distribution of this facies association is strongly controlled by several structural elements, the inferred D1 Pumpkin Gully Thrust (Williams 1997) and the north-south striking Telegraph Fault that dissects the fold forms of the Pumpkin Gully Syncline (Map Sheet Two).

3.7 Environments of Deposition

Environmental reconstructions of Australian Proterozoic sequences such as the SCG are complicated by the general lack of body and trace fossils and often complex tectonic and alteration overprints. As mentioned above, previous authors have interpreted the SCG sequence as analogous to published deep marine, prograding turbidite fan models (*eg.*Shanmugam &

Moiola 1991; Mutti & Ricci Lucchi 1972; Walker 1978). If this were so, the

Thickly Bedded Quartzite Lithofacies, and possibly the Swaley Facies

Association would represent channel deposits in the proximal turbidite fan

region, and the Quartzo-pelite Facies Association the medial-distal turbidite

fan lobes. The arrangement of facies and facies associations should thus

reflect 'classic' prograding turbiditic fan lobes *ie.* stacked, thickening and

coarsening upward turbidite bodies, with decreasing pelite up sequence

(Shanmugam & Moiola 1991; Mutti & Ricci Lucchi 1972; Walker 1978).

Whilst the appearance of greater thicknesses of the cyclical quartzites of the

Massive Quartzite lithofaces at the base of *Pon$_3$* may superficially appear to

represent upwards thickening, schematic sedimentary sections (Fig.3.6 and

3.7) do not show marked thickening and coarsening upward sequences on the

scale of <100m that are normally consistent with ancient turbiditic fan lobes

(Shanmugam & Moiola 1995). In addition, there is no evidence for the

thinning and fining upward sequences, on the scale of several 10's of metres

indicative of channel abandonment in prograding lobes (Mutti & Ricchi-

Lucchi 1972). All the facies associations presented here are mappable across

the study area and the lateral extent of several 100's of metres, planar nature

and lack of definitive evidence for aggradation of the quartzite bodies is

markedly different from the lensoidal and laterally restricted geometries of

modern prograding deep-water turbidite fans. The observed combination and

distribution of facies and facies associations presented here, suggests that the

SCG was deposited by processes other than those which operate in the

prograding turbidite fan systems proposed by previous workers in the area.

It should be noted that this study does not discount altogether the presence of

a classical turbidite fan in the SCG. As mentioned above this study was

focused on the Mt Norna Quartzite and lower Toole Creek Volcanics with no sedimentological data collected from the Llewellyn Creek Formation. Sedimentary relationships between the Llewellyn Creek Formation and Mt Norna Quartzite are unconstrained within the present study. The possibility remains that this stratigraphically lower unit represents a deeper water turbidite sequence as suggested by previous authors.

Sedimentary structures in the SCG, including rippled tops of massive quartzite beds, 'floating' clasts, quartzites with sharp bases, planar laminated massive quartzites and climbing ripples, all indicate deposition from high-energy, turbidity and density flows. Distinctive swaley and hummocky bedforms, low angle truncations of of concave-up cross bedding (HCS) suggest a significant component of wave-associated oscillatory currents.

There are several examples in the ancient rock record of 'turbidite-like' storm influenced sequences that are similar to the upper Soldiers Cap Group. Laajoki & Korkiakoski (1988) studied a 'turbidite-tempestite' transition in Proterozoic amphibolite facies rocks in Finland. Tempestites in this study were defined as the product of sedimentation directly related to storm-wave action. They also noted several facies markedly similar to those in the Soldiers Cap Group. These were massive sands, underlying 'background' turbidites and thinner, hummocky-cross stratified (HCS) beds. They inferred the environment of deposition as the outer to middle parts of a broad, steep shelf and/or the upper slope of a narrow shelf.

Roep & Linthout (1989) studied a sequence of thickening and thinning upward, hummocky-cross stratified and wave-rippled 'laminites' in early Proterozoic andalusite-cordierite quartzites in Sweden. In comparison with existing models for storm dominated shelves, they inferred a wave dominated shelf with lobe-like tongues of sand deposited from the upper shelf out into deeper water.

Hamblin & Walker (1979) studied a Jurassic storm-dominated shelf with a sequence similar to that described here for the upper Soldiers Cap Group. This comprised a series of deeper water turbidites overlain by storm generated and beach and fluvial facies. This sequence was interpreted as being emplaced by turbidity currents that were immediately re-worked by storm currents. They inferred that the turbidite section of the sequence was emplaced below storm-wave base (SWB) as density currents generated by loading of the substrate by storm events above-SWB. The Soldiers Cap Group is analogous to this sequence except that it does not have the transition from shallow marine to fluvial facies that is observed by Hamblin & Walker (1979). It has a weak-moderate storm influence, in the form of swaley-hummocky bedding, throughout.

The link proposed by Hamblin & Walker (1979) between storm-loading of shelf sediments and density currents has been proposed by several other authors. Duke *et al.* (1991) proposed storm wave loading of inner shelf sediments as a method to produce a density flow of sand that continues below-SWB also as a turbulent current. Walker (1984; *cf.* Myrow & Southard 1996) proposed that cyclic storm-loading could produce turbulent currents at or

above SWB that then travel downslope below-SWB.

Based upon the individual lithofacies, facies associations and facies sequence presented here, predictive models and similarities to other sequences (Hamblin & Walker 1979; Einsele & Seilacher 1982; Walker 1984; Nottvedt & Kreisa 1987; Laajoki & Korkiakoski 1988; Roep & Linthout 1989; Myrow & Southard 1996), the upper Soldiers Cap Group palaeoenvironment is interpreted as a shallow, moderate slope, storm influenced proximal-medial shelf. The true lateral extent of this system is indeterminate due to the structural complexity of the area. However, the present mapped extent of lithofacies and facies associations, suggests it was at least 10km wide (Fig.3.1). The facies association sequence outlined above indicates an early period of high energy sand rich turbidity and debris flows intercalated with hydrothermal events represented by the Mt Norna Iron Formation (Ch.7), with a minor storm overprint, represented by the Basal Quartzite Facies Association. Following this was a period of deposition of lower energy turbidity currents, with a minor storm current overprint, and some mafic intrusion (Ch.5), represented by the Quartzo-pelite Facies Association. Loading of the upper parts of the shelf by periodic larger storm events produced density and turbidity currents, 'tempestites' (Einsele & Seilacher 1982), that travelled down the regional palaeoslope, producing the Swale-Ripple Facies Association (Fig.3.8). Quartzites and psammopelites with HCS represent preserved individual storm events within the sequence. The oscillatory nature of the storm currents would have produced a range of sediment transport directions, from shore-normal to shore-parallel (Fig.3.8). The implications of this are discussed below with respect to data collected

from palaeoflow markers. The presence of swale-hummock bedforms throughout the remainder of the sedimentary pile suggests that oscillatory currents remain an important sediment re-working mechanism in the upper MNQ and TCV.
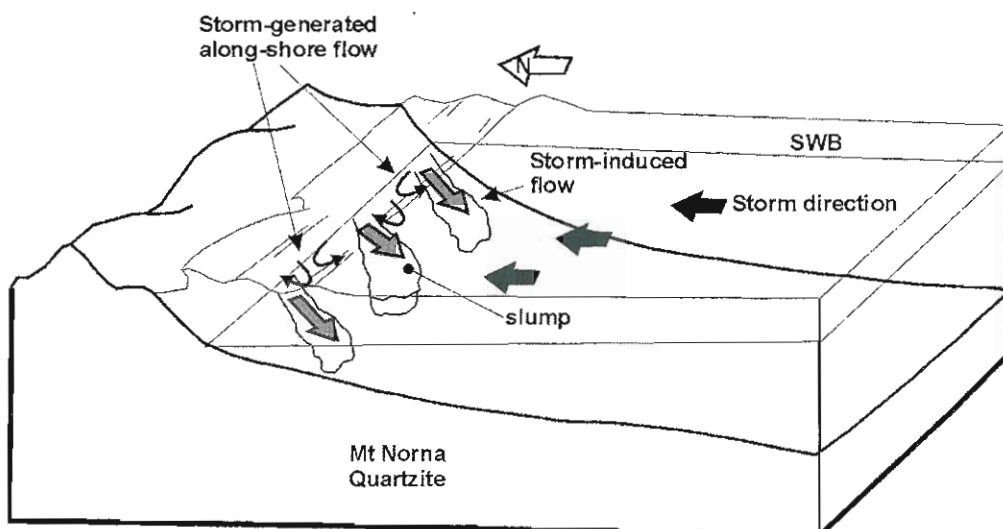
Figure 3.8: Schematic block diagram depicting the interpreted environment of deposition at Mt Norna Quartzite in the Soldiers Cap Group.

The ambiguity inherent in Proterozoic palaeoenvironmental interpretation combined with the lack of well constrained examples of similar age makes definitive estimations of water depth difficult. Models and examples that are available suggest that storm wave base and production of tempestites on modern and some ancient continental margins can occur between 2 and >100m of water depth (Hamblin & Walker 1979; Vincent 1986; DeCelles & Cavazza 1991; Snedden & Nummedal 1991; Swift & Thorne 1991; Hequette & Hill 1995).

The intercalation of dominantly turbidite-like units of the Quartzo-Pelite Facies Association, mafic sills and flows, poorly exposed and understood black shales, and minor iron formations suggests a more quiescent, possibly deeper water environment for the mid-upper TCV.

The Psammo-pelite Facies Association is areally restricted to the Pumpkin Gully Syncline and has a similar sequence and interpreted environment of deposition to the rest of the Soldiers Cap Group. In this case however, the lack of swaley and hummocky bedforms and the presence of rare carbonaceous laminae suggest deposition by turbidity currents in shallow water unaffected by wave associated oscillatory currents.

3.8 Palaeoflow Indicators

The documentation of palaeoflow indicators is placed here, following the reconstruction of the sedimentary environment, as interpretations of palaeoflow and basin geometries are largely dependent on sedimentological interpretations.

3.8.1 Data Collection and Methods

There is no published attempt to reconstruct part or all of the Maronan Supergroup using palaeoflow indicators. Ripple crests, cross bed foresets and rare slump fronts were measured across the study area and unfolded to define palaeoslope at the time of deposition of a ~10km long segment of the upper SCG.

Fifty-four data points were collected from areas of continuous well exposed outcrop along detailed sedimentological sections, creek traverses and during regional reconnaissance mapping across the Weatherly Creek Syncline and Toole Creek Syncline. These areas ranged in size from a single outcrop of 5-10m^2 to areas of well exposed pavements in creek cuttings 100-200m long and 20-50m wide. Whilst there was a comparable number of possible data

points available from the SCG in the Pumpkin Gully Syncline, the less well understood and complex structural history precluded an attempted reconstruction of this area.

Palaeocurrents were measured as inclination and azimuth, from the maximum angle of foresets of planar cross-bedding, ripple cross-laminations (Fig.3.5 c-d and g-j), HCS laminae (Fig.3.5e-f); trough cross beds, strike of ripple crests (Fig.3.5g-j- palaeoflow taken as normal to crest). Where present, the vergence direction and orientation of the axial plane of slump folds within bedding planes (Fig.3.5b) were measured and palaeoflow was taken as a combination of fold axis trend and vergence (Sharp *et al.* 2000). Where possible, numerous measurements were taken from the same outcrop or area of outcrop. Raw and reconstructed data are presented in tabular form in Appendix 6. Accounting for the subvertical dip of beds and complex structural history, care was taken to be certain that measurements were taken away from zones of high strain identified through mapping, aeromagnetic images and airphotos. Given the steeply dipping nature of the beds, the plunges of the measurements are considered to be less accurate than the azimuths. Prinicipally for this reason, the latter are referred to in this discussion (*cf.* Miall 1990; Potter & Pettijohn 1977). Rare measured vergence and axial planes of slump fronts, when combined with palaeoflow indicators, provided better constrained information on both palaeoslope angle and orientation of the palaeoshore.

Tempestite sequences characteristic of shelf environments, (Nottvedt & Kreisa 1987; Myrow & Southard 1996), will have a wide range of possible palaeoflow orientations. This is largely a result of the interaction of the

oscillatory storm currents and coexisting coastal sediment flow patterns such as longshore drift and rip currents. The lack of tool and sole marks which are often combined with bioturbation effects in the reconstruction of the palaeogeography of many HCS sequences (*eg.* De Celles & Cavazza 1992; Hequette & Hill 1995; Seilacher 1982), limits the degree of confidence available to the interpretations presented here. However, several studies (Hequette & Hill 1995; Nottvedt & Kreisa 1987; Myrow & Southard 1996), show that preserved palaeocurrents in tempestites can be representative of ancient flow patterns.

Within the 'turbidite-like' part of the tempestite sequence sedimentary structures indicative of unidirectional flow, such as trough-cross beds, planar cross-laminations, ripple foresets and particularly slumps, provide the clearest and most reliable palaeoflow markers. These would all generally be at high angles to the shoreline (Bouma 1962; Allen 1968). Studies show that palaeocurrents within the storm dominated part of the sequence (HCS) are generally either normal to shoreline (Myrow & Southard 1996) or parallel to slightly oblique to shoreline (Driese *et al.* 1991; Snedden & Nummedal 1991; Hequette & Hill 1995) or conceivably a combination of both in varying degrees (Myrow & Southard 1996). Ripple crests of wave generated features proximal to the shoreline are likely to be oriented parallel to shore while those more distal are likely to be normal (Aigner 1985; Driese *et al.*1991). Confident palinspastic reconstruction of the Weatherly Creek Syncline is difficult given the polydeformational history of the area. Two broad assumptions were made before reconstruction was attempted based upon a simplification of the various structural models proposed for the area (Ch.2;

Table 2.1; Ryburn *et al.* 1987; Loosveld 1988; *cf.* Lewthwaite 2000). This involved, 1- D_1 east-west thrusting of Soldiers Cap Group nappes over Mary Kathleen Group calcsilicates but resulted in no significant rotation of strata except at or near thrust fold noses (Laing 1998; Williams 1997); 2- tight, upright folding during D_2 as the major rotational event producing large features such as the Weatherly Creek Syncline.

Reconstructions were undertaken following as closely as possible the rotation methods suggested by Ramsay (1961) on equal angle stereonets. This assumed an average plunge of approximately 65°N for the Weatherly Creek Syncline. This was inferred from data presented on the Ryburn *et al.* 1987 1:100 000 scale geological map and a similar more detailed map presented by Loosveld (1988), and some measurements taken by the author. The plunge was removed by rotating poles to bedding through 65° to the vertical. The new bedding orientation was then brought to horizontal before reading off the reconstructed palaeocurrent azimuth. Given the lack of control on the style of folding *ie.* flexural versus slip and the high degree of shortening in the region (>80%; Loosveld 1988), errors on the unfolded measurements would be large (Ramsay 1961) and so it should be stressed that the reconstructed azimuths only provide a 'best-estimate' of the palaeoflow regime of the basin. Obvious complexity also arises from the overprint of tight, upright D_2, and subsequent folding and faulting/shearing (D_3-D_4) on possible earlier D_1 thrust nappes and non-cylindrical behaviour of small scale fold hinges. Therefore these measurements were considered as a useful adjunct to the rest of the detailed geological data gathered in this study (*ie.* U-Pb detrital zircon ages-Ch.4) as opposed to 'first-order' data.

3.8.2 Results

Unfolding of the palaeoflow measurements via the methods outlined above

shows that the flow within the segment of the SCG studied here was

segregated into several discrete populations, Groups 1-8 (Fig.3.1), which

represent a series of measurements from individual outcrop or creek section

and are generally from the same sedimentary facies. Raw and reconstructed

palaeocurrent data are tabulated in Appendix Two.

Palaeocurrent Group	Sedimentary Lithofacies, Facies Association/ Lithostratigraphic Unit	Sedimentary Structures	Interpretation
1	Swale-Ripple Facies Association/Pon_3	HCS x-laminae and ripple crests	Storm generated currents
2	Quartzo-pelite Facies Association/Pon_2	Planar x-lamination foresets, ripple crests	Turbidity currents/tempestites
3	Swale-Ripple Facies Association/Pon_2	HCS x-laminae, ripple crests	Storm generated currents
4	Quartzo-pelite Facies Association/Pon_2	Planar x-lamination foresets	Turbidity currents/tempestites
5	Quartzo-pelite Facies Association/Pot_3	Planar x-lamination foresets	Turbidity currents/tempestites
6	Quartzo-pelite Facies Association/Pon_3	Planar x-lamination foresets	Turbidity currents/tempestites
7	Quartzo-pelite Facies Association/Pot_1	Planar x-lamination foresets	Turbidity currents/tempestites
8	Swale-Ripple Facies Association/Pon_3	Planar x-lamination foresets, slump fronts	Turbidity currents/tempestites

Table 3.3: Summary of the sedimentological, stratigraphic distribution and interpreted deposition mechanism of palaeocurrents measured as part of this study.

These groups can be combined into two dominant populations that are

separated geographically by a set of northeasterly striking faults, the Lomas

Creek Faults (Fig.3.1; *cf.*Arnold 1983). The population to the north of the

faults, is made up of ripple crests and planar cross-laminations in turbidity

current dominated facies (Groups 2 and 4), and reconstructed ripple crests and

ripple cross laminations in HCS dominated facies (Group 3). Note that the

bipolar populations in Figure 3.9 (2 and 3) represent the strike of ripple crests,

not a possible tidal population (see below). Within the turbidite dominated palaeoflow markers of Group 2, ripple crests are oriented east-west and planar cross-laminations are oriented southeasterly. Group 3, which were measured on wave current produced features, have a ripple crest population oriented northwest-southeast and a HCS laminae population oriented southwesterly. Group 4, measured on planar cross laminations are oriented largely southwest.

South of the Lomas Creek Faults, Group 1 is composed of southwesterly oriented HCS cross laminations in psammopelites and slump fronts in quartzites with a minor easterly HCS ripple component. Group 8, measured on planar cross laminations in turbidity flows, were oriented south-southeast, with slump fronts in massive quartzites oriented to the southwest. Group 7, made up of planar cross-laminae also in turbidity generated units when reconstructed define a southeasterly trend.

3.8.3 Palaeoenvironmental implications of reconstructed palaeoflow markers

Hamblin & Walker (1979) proposed that palaeocurrents which were the product of storm-generated currents, such as the SCG tempestites, were likely to follow palaeobathymetry at an intermediate angle to the local shoreline into a localised depocentre. Other authors (Snedden & Nummedal 1991; Driese *et al.* 1991; Myrow & Southard 1996) proposed that storm currents can flow parallel to oblique to shore, and still generate seaward flowing turbidity currents.
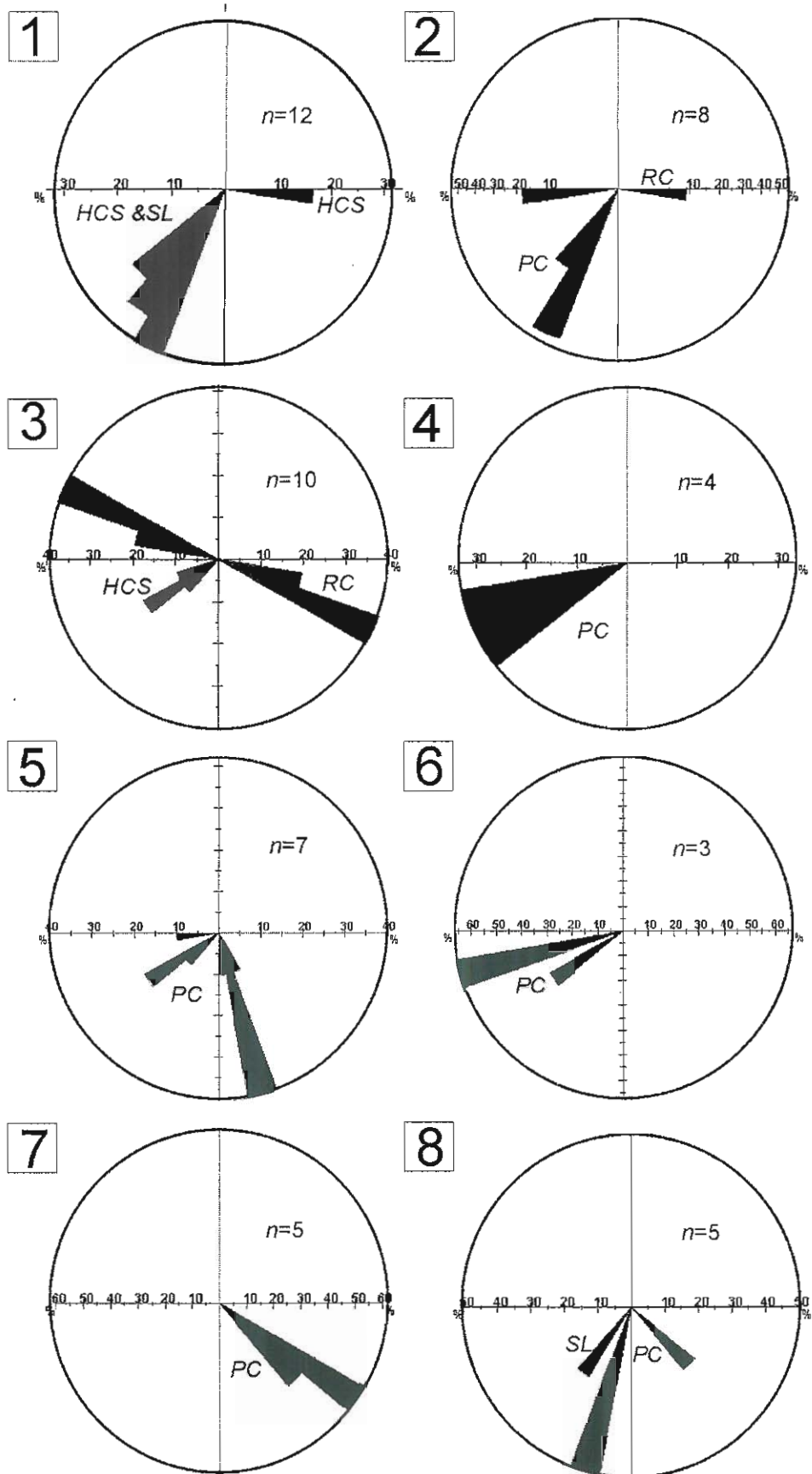
Figure 3.9: Reconstructed palaeocurrents from the western limb of the Weatherly Creek Syncline, refer to Figure 3.1 for locations of Groups 1-8. *PC=planar cross laminations; SL=slimps; HCS=hummocky cross sratification; RC=ripple crests.*

Other possible influences on the direction of tempestite flow patterns include, overprint of storm waves on existing geostrophic current flow patterns (Duke 1990; Duke *et al.*1991; Myrow & Southard 1996) and related longshore and/or rip currents (Myrow & Southard 1996). Preservation of HCS structures is largely controlled by the rate of sediment fallout from suspension and the intensity of the storm current and can represent either the shoreward movement or seaward movement during storm events (Hequette & Hill 1995; Myrow & Southard 1996), and generally during the peak of storm activity (*cf.* Einsele & Seilacher 1982; Seilacher 1982). Therefore, the recognition of fair-weather alongshore currents which represent 'background' sedimentation around the storm events will be very difficult. The lack of bimodal palaeoflow patterns, combined with the lack of distinctive sedimentary features such as flaser bedding, precludes the interpretation of a tidal influence on the sequence.

South of the Lomas Creek Faults (Fig.3.1), Groups 1 and 8 contain slumps which, when reconstructed, are aligned south-southwest implying that the local shoreline was oriented east-west or northwest-southeast. Within these two groups storm generated currents in Group 1 are aligned east-west as well as south, inferring components of both along-shore and off-shore transport. Similarly, Group 8 turbidity current features are aligned close to the slump front, indicating offshore transport. Turbidity current markers from overlying sediments of *Pot₁* in Group 7 are oriented to the southeast implying a slight change in sediment transport following the intrusion of voluminous mafic sills of the upper MNQ-lower TCV.

North of the Lomas Creek Faults the lack of measured slump fronts hinders interpretations of shoreline orientation. Following the rationale of Driese *et al.* (1991; *cf.* Aigner 1985) ripple crests associated with proximal storm currents will be approximately parallel to shoreline so the markers in Group 3 imply a broadly east-west oriented local shoreline. Additionally, turbidity current markers are oriented southwest, supports a shoreline orientation similar to that south of the Lomas Creek Faults with downslope flow slightly oblique to shore.

The Lomas Creek Faults exert a significant control on the palaeoflow, stratigraphy and lithology of the mid-upper Soldiers Cap Group. Possible reasons for and implications of this control are discussed in more detail in Chapter 8. Possible sources for the Soldiers Cap Group based upon U-Pb detrital dating of zircons and controls on basin orientation will be discussed next.

Chapter Four-U-Pb detrital zircon age constraints on source terranes for the Soldiers Cap Group

4.1 Introduction

For this study U-Pb isotopic ages of detrital zircons collected from geologically well constrained samples of the upper Soldiers Cap Group were obtained by the recently developed Laser Ablation Inductively Coupled Plasma Mass Spectrometry (LA-ICP MS) method (Allen *et al.* 2001; Feng *et al.* 1993; Fryer *et al.* 1993; Hirata & Nesbitt 1995; Garbenschonberg & Arpe 1997; Palin *et al.* 2000; Scott & Gauthier 1996). The main aim of this study was to delimit the previously poorly defined source terrane of the Soldiers Cap Group, constrain basin geometry and outline the depositional history in the area.

4.2 Eastern Succession Geochronology: Previous Work

Recent work on Eastern Succession geochronology, (Belousova *et al.* 2001; *cf.* Giles 2000; Page and Sun 1998;), provides a substantial U-Pb zircon age database (Fig.11). Maronan Supergroup dates from Page & Sun (1998) include a maximum depositional age of 1677±9 Ma for the Gandry Dam Gneiss; a rhyolite crystallisation age of 1654±4 Ma from undifferentiated Soldiers Cap Group and maximum depositional ages of 1693±5 &1654±4 Ma from Mt Norna Quartzite. These dates constrain the Soldiers Cap Group to between 1690-1650 Ma in age considerably younger than previously thought (*cf.* Ch.2). Inherited detrital populations analysed by Page & Sun (1998) in the Soldiers Cap Group include:- samples from Gandry Dam Gneiss at

Cannington with two distinct detrital populations at 1750-1770 Ma and 2520-2565 Ma; two further felsic gneiss (Gandry Dam Gneiss) samples from Cannington with Archaean and 1715±5 Ma provenances; felsic volcanics from Gandry Dam Gneiss 45km north of Cannington with 2550-2320 Ma and 1830 Ma populations (Fig.4.1);.Mt Norna Quartzite to the south of the area of the present study which returned detrital populations of Archaean age, 1780, 1770, 1740 and 1850 Ma. Felsic volcanic samples from the Boomara Horst of what has been mapped as undifferentiated Soldiers Cap Group (*cf.* Wilson & Grimes 1986), some 100km to the north of the area of this study, provided formation ages of 1775±4 & 1774±4 Ma. Clearly this places these units stratigraphically lower than the Soldiers Cap Group and Page & Sun (1998) interpreted them as stratigraphically equivalent to the Argylla Formation.

Belousova *et al.* (2001) dated numerous samples from the Soldiers Cap Group taken from outcrop, under cover and also recent detritus shed from outcrop, using multi-collector LA-ICP MS to determine U-Pb ages and Hf isotopic data for zircons. This study defined four broad stages of crustal evolution and orogenesis in the Eastern Succession; Stage 1 (2550-2320 Ma) involved crustal genesis and reworking; Stage 2 (1950-1825 Ma) intracontinental rifting terminated by orogenesis; Stage 3 (1800-1600 Ma) rifting, significant reworking of older crust and juvenile input again terminated by orogeny; Stage 4 (1590-1420 Ma) dominated by "older crustal input". The Soldiers Cap Group falls within their Stage 3 of rifting and reworking of older crustal elements.
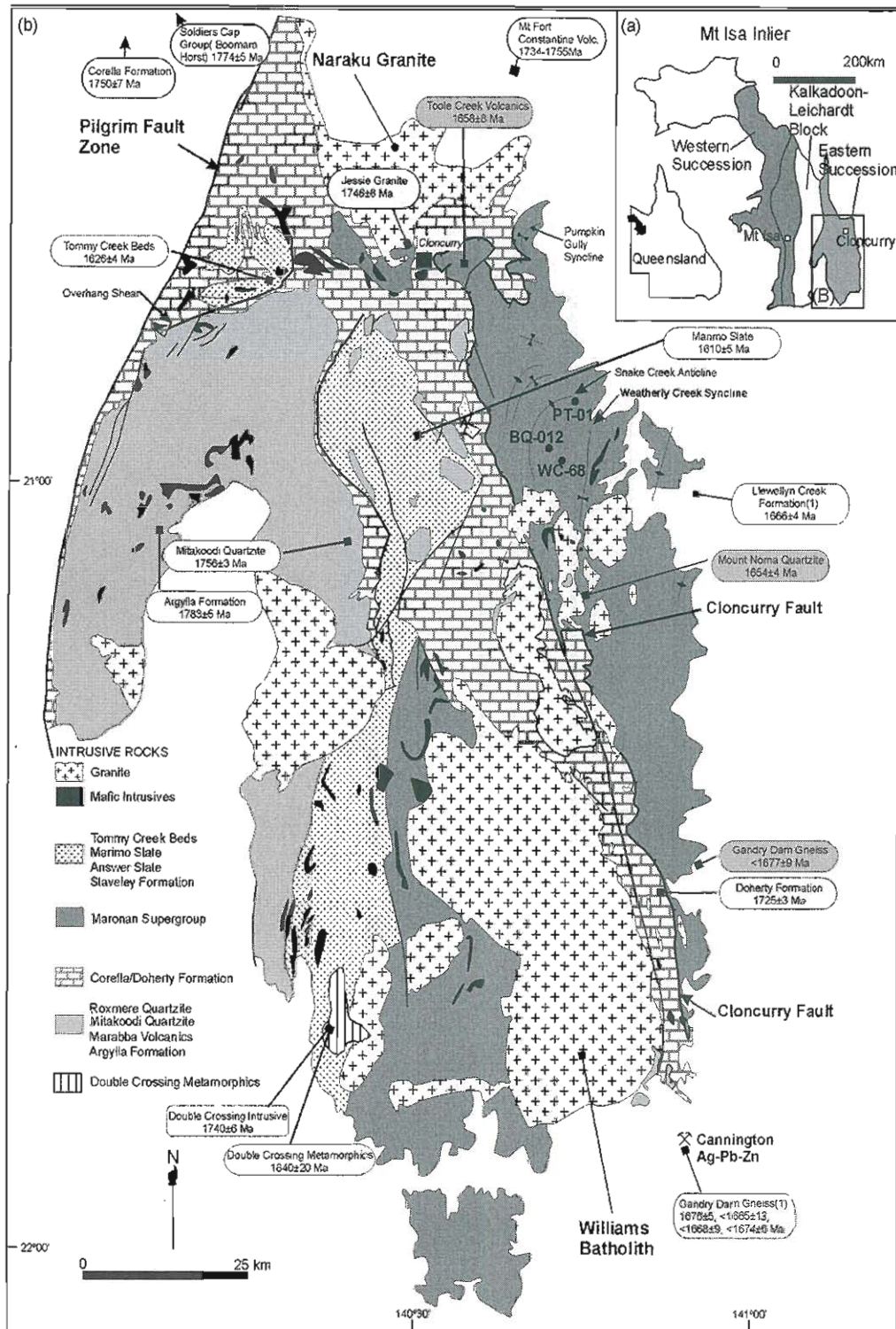
Figure 4.1: (a) Tectonostratigraphic divisions of the Mt Isa Inlier, NW Queensland Australia; (b) Simplified Eastern Succession regional geology (modified after Betts *et al.*2000). Samples in this study and recent geochronology displayed. Age dates in grey boxes sourced from Page and Sun 1998; 1-Giles 2000, all others from Page 1983; Hill *et al.*1995 or are referenced in the text.

Giles (2003) dated by SHRIMP methods, a sample from units mapped as

Llewellyn Creek Formation (GR 76690000mN 487000E). This study defined

an Archean-Palaeoproterozoic population, a 1750-1700 Ma population and a

1680-1640 Ma grouping which defined a maximum depositional age of

1666±14 Ma for the Soldiers Cap Group which falls within the errors of the

ages defined by Page & Sun (1998).

4.3 Analytical Methods

4.3.1 Sample Locations

Sample *BQ-012* (Fig 11; Map Sheet One AMG-GR 468476E 7687893N) from

the lowermost Mt Norna Quartzite (Basal Quartzite Facies Association, *Pon₁*),

comprises a medium grained, massive to weakly laminated quartzite,

interpreted as the product of sand rich debris flows (Ch.3; Hatton *et al.* 2000).

Sample *WC-68* (Fig.11; Map Sheet One AMG-GR 470660E 768024N) was

taken from the mid-upper Mt Norna Quartzite (Quartzo-pelite Facies

Association-*Pon₂*) from a planar-laminated quartzite bed top interpreted as the

product of a storm reworked, turbidity current (Hatton *et al.* 2000). Sample

PT-01 (Fig 11; Map Sheet One AMG-GR 468231E 7696675N) was taken

from a massive quartzite bed within the mid-Toole Creek Volcanics (Quartzo-

pelite Facies Association-*Pot₂*) interpreted as the product of storm-generated

turbidity currents.

4.3.2 Zircon separation and preparation

Samples were crushed in a tungsten-carbide jaw crusher to gravel size (2-4

mm) prior to milling in a chrome-steel mill to 0.05-0.5mm. Samples were then

sieved, the fine-sand fraction (63-125 μm) was collected and the less dense

fractions panned off. The zircons were separated from the fine sand fraction

via conventional heavy-liquid separation techniques using tetrabromoethane.

The heavy mineral fractions were then extensively washed, dried and magnetically separated using a Franz magnetic separator. Between 50-100 zircons 40μm long or greater were randomly selected from each heavy mineral separate. The selected zircons were mounted in epoxy blocks and polished using a diamond lap. The grains were examined to determine zoning and morphology using the backscatter detector of the Environmental Scanning Electron Microscope (ESEM) at the Central Science Laboratory, University of Tasmania. Prior to and following the ESEM and LA-ICP MS sessions the samples were ultrasonically cleaned to remove surface contamination.

4.3.3 Laser ablation ICPMS method

The use of Laser Ablation Inductively Coupled Plasma Mass Spectrometry (LA-ICPMS) for U-Pb dating of detrital zircons has been applied in several geochronological studies worldwide (*eg.* Machado & Gauthier 1996; Machado *et al.* 1996; Palin *et al.* 2000; Belousova *et al.* 2001; Berry *et al.* 2001). The principle advantage of LA-ICPMS for isotopic analysis of zircons is the rapid sample throughput which allows a detrital population (~60 grains) to be characterized in a single analytical session (~10 hours). Laser microprobes operate with spot diameters comparable to ion microprobes (30-50 μm) but the laser drills into the grain at a considerably greater rate, degrading spatial resolution with depth into the grain during analysis and inducing artificial U-Pb fractionation. This is partially compensated by collecting the LA-ICPMS data in time resolved mode so that zones with different U-Pb ratios can be identified and the data reduced accordingly.

4.3.4 Instrument operating parameters

U-Th-Pb isotopic compositions of zircons were measured using an Agilent HP4500 ICPMS coupled with a Merchantek 266nm Nd:YAG laser at the Centre for Ore Deposit Research, University of Tasmania, under the supervision of the author and Dr. Marc Norman. Isotopic masses collected were ^{238}U, ^{235}U, ^{232}Th, ^{208}Pb, ^{207}Pb, ^{206}Pb, ^{204}Pb and ^{202}Hg. Zircons were analysed with a 30μm diameter beam, a laser repetition rate of 5 Hz, and a power setting of 0.2 mJ. The ICPMS was operated in time-resolved mode, collecting one point per mass per sweep of the mass range with a dwell time of 10 msec/mass. Each analysis consisted of measurement of gas background count rates on each mass for 60 sec prior to ablation, followed by 60 sec of ablation (Fig.4.2a-d). Each analysis was followed by a 2 minute washout period during which signal intensity returned to background level before another analysis run commenced.

4.3.5 Data collection, reduction, correction and presentation

Sample runs consisted of 12 unknowns bracketed by two sets of 4 standards. A total of 233 analyses of unknown zircons were taken from the three samples (*WC-68 n=56; PT-01 n=60; BQ-012 n=117*). Four analyses of an in-house zircon standard from the Blind Gabbro, Snowy Mountains, NSW (Collins 1998), were analysed using the same analytical conditions as the unknowns at the beginning of the day, after every 12 unknowns, and at the end of the day (Appendix 4). The measured ^{206}Pb/^{238}U, ^{207}Pb/^{235}U, and ^{207}Pb/^{206}Pb ratios of each set of 12 unknowns were corrected to the bracketing standard analyses using accepted values of the Blind Gabbro zircons obtained by SHRIMP (^{206}Pb/^{238}U=0.06585±0.0005; ^{207}Pb/^{206}Pb=0.05554±0.0004;

^{207}Pb/^{235}U=0.50427; ^{206}Pb/^{238}U age= 411±5 Ma; W. Collins *pers. comm.*

2001). Zircons from the Blind Gabbro were chosen as a calibration standard

due to their concordant U-Pb age, extremely rare inheritance, low common

Pb, and relatively high abundance of U, Th, and radiogenic Pb. Additionally,

no reliable Proterozoic standards were available to the author at the time of

analysis. Typically, one spot analysis was obtained per grain. Where grain

size allowed, 2-3 consecutive analyses were obtained on a single grain. The

raw data is presented in Excel format in Appendix Four as a hard copy and on

CD.
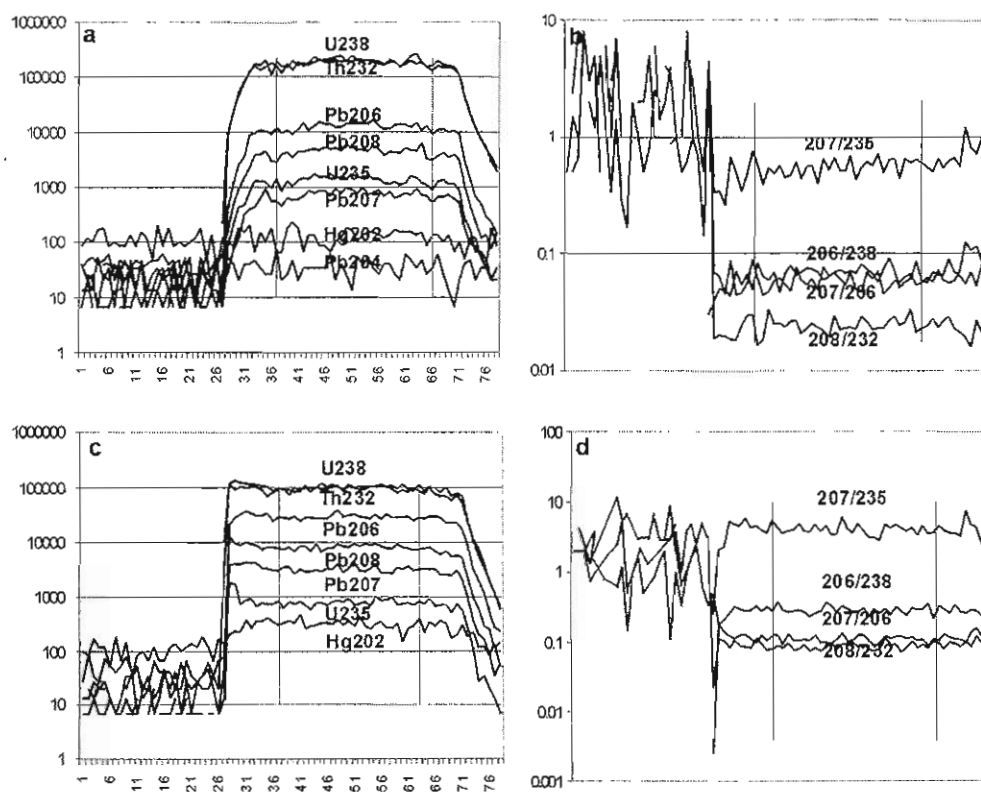
Figure 4.2: (a) counts per second (cps) vs. time graph depicting U-Th-Pb counts for an analysis of the standard (Blind Gabbro), the interval of integrated data is marked; (b) U-Th-Pb ratios vs. time for the same standard analysis as (a); (c) cps vs. time plot of U-Th-Pb for unknown zircon from sample BQ-012, as with the standards the integration interval is shown; (d) U-Th-Pb ratios vs. time for the same analysis as (c).

Data were reduced using the LAMTRACE program (van Achterbach *et al.* 2001) with the assistance of Dr. Marc Norman (presently at the Australian National University, Canberra). Each time-resolved spectra was examined and net count rates for each mass were obtained by subtracting average background intensities (counts per second) from average signal intensities taken ~15 sec after beginning of ablation when the signal had stabilized (Fig.4.2). Under the operating conditions used for this study, homogeneous grains with low common Pb from the Blind Gabbro produced near-steady signals with no resolvable change in $^{206}Pb/^{238}U$ or $^{207}Pb/^{235}U$ signal intensities during the analysis (Fig.4.2a-d).

Figure 4.3: $^{207}Pb/^{206}Pb$ probability plot for analyses of standard (Blind Gabbro) used in calibration of results.

Figure 4.4: U-Pb Concordia plot for all samples analysed of the standard (Blind Gabbro) with upper intercept quoted at 2σ. Age from SHRIMP dating is 411±5 Ma (W.Collins *pers.comm.* 2001).
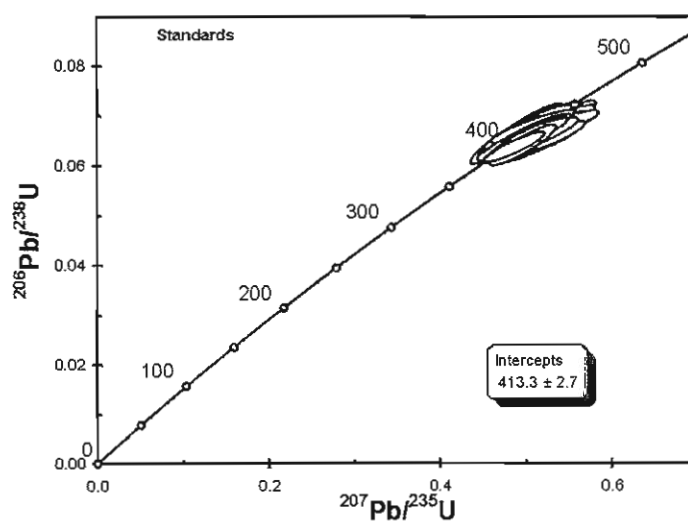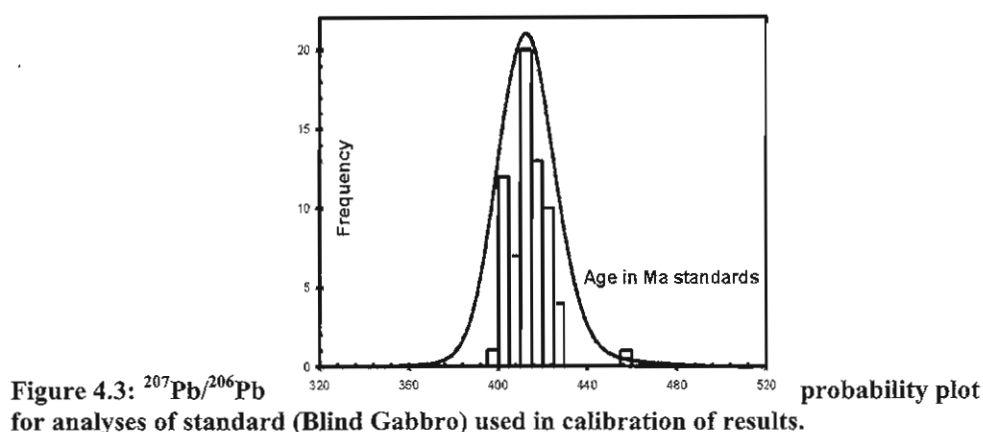
Analytical precision of LA-ICPMS zircon analyses is primarily a function of count rate, which is controlled by spot diameter, abundance of U and Th, and age of the grain. Individual spot analyses of the Blind Gabbro typically produced precisions of 2-3% (2σ) on the measured $^{206}Pb/^{238}U$ ratios. An indication of this analytical precision is the tight distribution of apparent ages of Blind Gabbro zircons, producing a $^{207}Pb/^{206}Pb$ age and upper concordia intercept of 413±3 Ma (2σ; calculated using ISOPLOT v.2.00 Ludwig 1999) for the 67 analyses used for calibration (Fig.4.3; Fig.4.4) which is well within the errors of the unpublished SHRIMP age of 411±5 Ma.

Where zones with widely differing U-Pb isotopic ratios were apparent in the time-resolved spectra of individual Soldiers Cap Group grains these analyses were discarded. Although numerous grains were zoned at the microscale, relatively few grains in the sample population studied here showed this effect, with the vast majority of grains appearing essentially internally homogeneous in U-Pb isotopic compositions within the uncertainties of each analysis. Five grains showed distinct evidence of zoning in their U-Pb spectra and were discarded from age calculations.

The LA-ICPMS technique has a similar source profile to the SHRIMP method but because of noise and isotopic overlaps cannot accurately measure $^{204}Pb/^{206}Pb$ at very low levels of ^{204}Pb. Li *et al.* (2000) made a special attempt to measure ^{204}Pb in zircons using LA-ICPMS. They found $^{206}Pb/^{204}Pb$ was >3000 ($^{204}Pb/^{206}Pb$ < 0.00033) for all spots on the Precambrian zircons analysed in their study. This matches our analytical experience that ^{204}Pb peaks are too low to measure accurately with LA-ICPMS (Fig.4:2c-d) but are

also too low to significantly change the age of the grain within the errors.

Many papers based upon SHRIMP dating do not use ^{204}Pb as an indicator of

common Pb. The counting statistics are generally so poor that either the ^{208}Pb

or ^{207}Pb method are commonly used (Muir *et al.* 1994; Cawood *et al.* 1999).

The ^{208}Pb method was used here instead of a direct correction using ^{204}Pb (*cf.*

Cummings & Richards 1975; Machado and Gauthier 1996) to avoid

uncertainties associated with potential interferences from ^{204}Hg, and the large

errors associated with the low count rates for ^{204}Pb in most of these samples.

Analyses of the Blind Gabbro standard indicative of significant amounts of

common Pb were excluded from the calibration although these were

exceedingly rare in the dataset. Using the ^{208}Pb method high common Pb was

detected in a further seven grains and these were discarded from the sample

population.

Laser induced fractionation was a particular problem in this study and has

been observed in other LA-ICPMS studies (*eg.* Horn *et al.* 2000) and is one

of the restrictions of the method. Data was routinely obtained for ^{206}Pb/^{238}U,

^{207}Pb/^{235}U and ^{208}Pb/^{232}Th, but these ratios were only used as a first pass

filter to estimate discordance and also to identify grains with high common

Pb. The U/Pb fraction was monitored using standards during this study

(Blind Gabbro) but this failed to adequately describe the individual

fractionation in over 50% of grains.

Therefore, due to laser induced fractionation effects and the presence of

significant common Pb in several samples, all subsequent discussion in this

paper refers only to ^{207}Pb/^{206}Pb ages. These were calculated from a

population of common Pb corrected samples. This ratio is interpreted as largely independent of these effects and has been used by several authors in detrital studies of other regions (*eg.* Machado & Gauthier 1996; Berry *et.al* 2001; Sircombe 2001; *cf.* Raetz *et al.* 2002). Due to high MSWD's (mean square of weighted deviates) for the three samples calculated using ISOPLOT (v.2.0; Ludwig 1999; Appendix 4) and probabilites of fit close to 0 (Appendix 4), simple weighted means were considered to be unrepresentative and therefore were not used in age estimations. Additionally, the high MSWD and low probability of fit points to the zircon data representing more than one age population (Giles 2003).

Following the methods of previous authors in similar studies (*eg.*Berry *et.al* 2001; Raetz *et al.* 2002; Giles 2003) age groupings and provenance were determined using probability plots (Fig.4.6). Cumulative probability graphs draw attention to zircon ages in a collective 'pool', represented by distinct peaks (Fig.4.6; Raetz *et al.* 2002). Plotting these ages outlines a spectrum of zircon forming events which have affected a sample population. In the case of this study being the ages of provenance terranes and/or later events which have reset zircon systematics. Probability plots were made for the entire sample population and individual samples by the summation of a set of assumed normally distributed, corrected $^{207}Pb/^{206}Pb$ ages. This was done using the ISOPLOT program (v 2.00; Ludwig 1999). Assuming that the peaks on these plots approximate the mode of a zircon forming event (Raetz *et al.* 2002), in this case a detrital provenance, approximate ages were taken from discrete peaks, rounded to the nearest 10 Ma and quoted as *ca.* ages (Fig.4.6). These plots do not allow an exact age determination or estimation

of error (Raetz *et al.* 2002), however ages within 2σ (30 Ma) of the *ca.* age can effectively be considered possible provenance sources. Based upon the limitations of this method and the generally large errors inherited from the analytical method, no maximum or minimum ages of deposition will be presented. Raetz *et al.* (2002) also caution against interpretation of subtle peaks on 'shoulders' of probability graphs as they can represent overlapping normally distributed populations producing aritificial distributions and/or represent younger Pb-loss.

The effect of Pb loss in zircons is to broaden the peaks in the age spectra with tailing or skewing to younger ages (Li *et al.* 2000). Using the LAM-ICP-MS method, Pb loss at intermediate ages cannot be detected by measuring discordance and individual zircon ages represent minimum ages of zircon growth. However, clustering of grain ages is the key indicator of the age of important zircon forming events since Pb loss should disperse grain ages (Li *et al.* 2000; Knudsen *et al.* 1997). A knowledge of any previous regional geochronology is also important in defining Pb-loss. In the Soldiers Cap Group potential Pb-loss events such as peak metamorphic ages are well constrained in Page & Sun (1998). Zircon is effectively a closed system below 900°C, so Pb loss will generally only occur as a result of large scale crustal thermal and exhumation events related to orogeny, alteration or hydrothermal fluid activity (Rubin *et al.* 1989; Lee *et al.* 1997; Mezger & Krogstad 1997). Even though no obvious zircon overgrowths were observed during this study, $^{207}Pb/^{206}Pb$ probability graph populations show a small grouping of grains with *ca.*1580 Ma Isan Orogeny ages which can be linked to peak regional metamorphism (*eg.* Fig.4.6; 1584±17 Ma of Page & Sun 1998). The lack of

ages younger than this *ca.* 1580 Ma grouping (Fig.4.6) suggests that the

majority of the zircons analysed have not suffered significant lead loss.

Additionally, the relatively well constrained, consistent and coherent peaks in

Figures 4.6 and 4.7 a-c combined with known age data from the region,

suggests that these peaks represent detrital inheritances.

4.4 Results
4.4.1 Zircon Morphology

Grain sizes of zircons separated from the Soldiers Cap Group samples ranged

from 35-250μm long and averaged 40-50μm wide (Fig.4.5). Grains with

fractures, along which common Pb is commonly found were very rare in the

sample set. Three zircon morphology groups can be defined and are present in

varying proportions in the samples (Table 4.1). The first (Group 1) are

subhedral, subangular grains that are commonly zoned (Fig.4.5a) and have

aspect ratios of 2-3. The second (Group 2) are typically massive, well rounded

grains that are fragments of larger grains (Fig.4.5b) and have aspect ratios of

1-2. Group 3 comprises elongate, prismatic, subhedral, subrounded grains that

are often concentrically zoned (Fig.4.5c) and have aspect ratios of 4-5.

Microscale zoning within the grains ranges from well developed concentric

<1-5μm wide zones, to homogeneous cores surrounded by concentric zoning,

to complexly zoned cores surrounded by concentric zoning. Grains with

unequivocal metamorphic overgrowths were not observed during the ESEM

or LA ICPMS sessions.

Figure 4.5: ESEM photomicrographs with scales in microns, of representative zircons from the three main morphology groups: (a) Group One (b) Group Two (c) Group Three.

	Group 1	Group 2	Group 3
	number	*number*	*number*
WC-68	32	12	12
PT-01	26	10	24
BQ-012	55	38	24

Table 4.1: Numerical populations in the analysed sample population of the three zircon morphology Groups.

Zircon morphology can suggest different styles of growth during the history

of the crystal (Pupin 1980). Primary zircons that are the product of

magmatism usually have strong oscillatory zoning and good crystal form and

moderate to high aspect ratios (Poldevaart 1956), such as seen in Groups 1 and 3. This zoning is related to the chemistry and temperature of the crystallising medium (Pupin 1980). Zircons that have been subjected to either metamorphic or hydrothermal overprints typically have corroded and/or overgrown rims of clear, unzoned zircon (Wayne *et al.* 1992; Rubin *et al.*1989; *cf.* Page & Sun 1998), unequivocal examples of these were not observed within this sample set when examined by ESEM. Detrital zircons commonly show the results of mechanical attrition such as rounding and fragmentation of grains and moderate-low aspect ratios as seen in Group 2, are often interpreted as a result of transport in an active sedimentary system.

4.4.2 U-Pb data

After data reduction and correction following the methods outlined above, a total of 221 sample points from three samples (*BQ-012, WC-68 & PT-01*) were available to be used in age calculations and provenance determination. When the common-Pb corrected data for each sample is plotted on a cumulative probability graph (Fig.4.6) three main coherent populations were defined: (1) a dominant *ca.* 1750Ma peak which represents Proterozoic aged detrital provenance; (2) a *ca.*2450Ma Archaean population (3) a *ca.*1790 Ma population. As mentioned above, Raetz *et al.* (2002) advise against the use of secondary peaks on probability graphs. However, the subtle shoulder on Figure 4.6 to the right of the main *ca.*1750 Ma peak is a discrete feature which may represent a combined peak resulting from the superposition of *ca.*1860 Ma and *ca.*1970 Ma population peaks or mixing of two separate provenances (*cf.* Sambridge & Compston 1994).
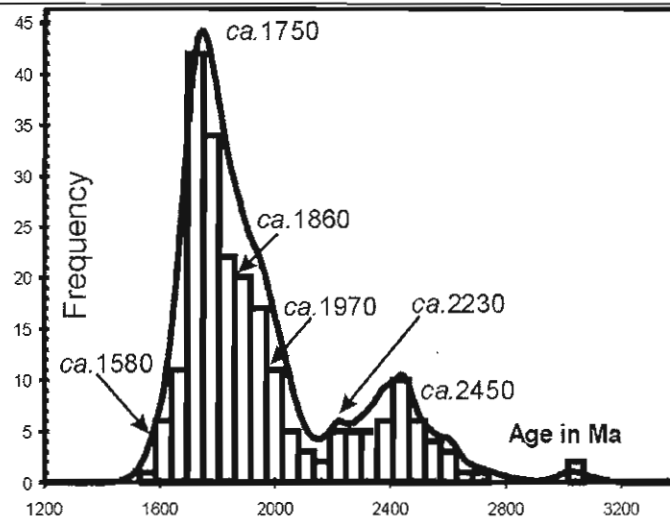
Figure 4.6: Probability graph (Age in Ma vs. frequency) for all corrected zircon analyses in this study. Detrital zircon provenance populations defined as approximate ages rounded to the nearest 10Ma. Plotted using ISOPLOT v.2.0 (Ludwig 1999).

Neither of these populations will be discounted as geologically meaningless as lithologies of *ca.*1860 Ma age do exist in the Mt Isa Inlier and so represent a possible detrital source. However, less weight will be placed upon the interpretations resultant from these peaks. Other secondary populations include a *ca.*1580 Ma grouping likely the product of peak regional metamorphism (Fig.4.6; Page & Sun 1998), a *ca.*1680 Ma population which is within overlaps of Maronan Supergroup ages (Page & Sun 1998), and two smaller Archaean populations *ca.*2230 Ma and *ca.*2500 Ma present as shoulders on the main Archaean peak (Fig.4.6). Zircons of all morphology Groups are present in all three samples. Table 4.2 outlines the presence of each relative to the two major age peaks. The distribution of the main age populations in the samples will now be discussed in stratigraphic order from oldest to youngest.

Sample BQ-012

The 110 corrected analyses in sample *BQ-012* have a marked bimodal distribution on probability plots (Fig.4.7c). This distribution defines a *ca.*1750 Ma population and a combined Archaean population with components of the *ca.*2230 Ma and *ca.*2450 Ma populations. A subtle peak on the right shoulder of the main peak (Fig.4.7c) likely represents superposed *ca.*1860 Ma and *ca.*1970 Ma peaks (Fig.4.6). The dominant *ca.*1750 Ma Proterozoic age population is present as grains from morphology Group 1 and 3, and Archaean ages from Group 2 (Table 4.2).

Sample WC-68

A total of 54 sample points were available after data reduction/correction from *WC-68*. Probability plots define two major populations. The first is a *ca.*1790 Ma which is not represented in the spectra of *BQ-012* or *PT-01*. The second is a *ca.*2450 Ma Archaean population with a minor older *ca.*2620 Ma population. The subtle combined *ca.*1860 Ma and *ca.*1970 Ma peak on the right 'shoulder' of *BQ-012* and *PT*-01 is absent in *WC-68*. Zircons of this peak are from morphology Group 2. The majority of the *ca.*1750 Ma ages were from zircons of morphology Groups 1 and 3 and the Archaean ages from Group 2 (Table 4.2).

Age Peaks	ca.1750	a.1790 Ma	ca.2450 Ma
Zircon	Morphology	Group	
PT-01	1 and 3	1 and 3	2
WC-68	1 and 3	1 and 3	2
BQ-012	1 and 3	1 and 3	2

Table 4.2: Summary of the broad distribution of grain morphology groups in the two major populations.
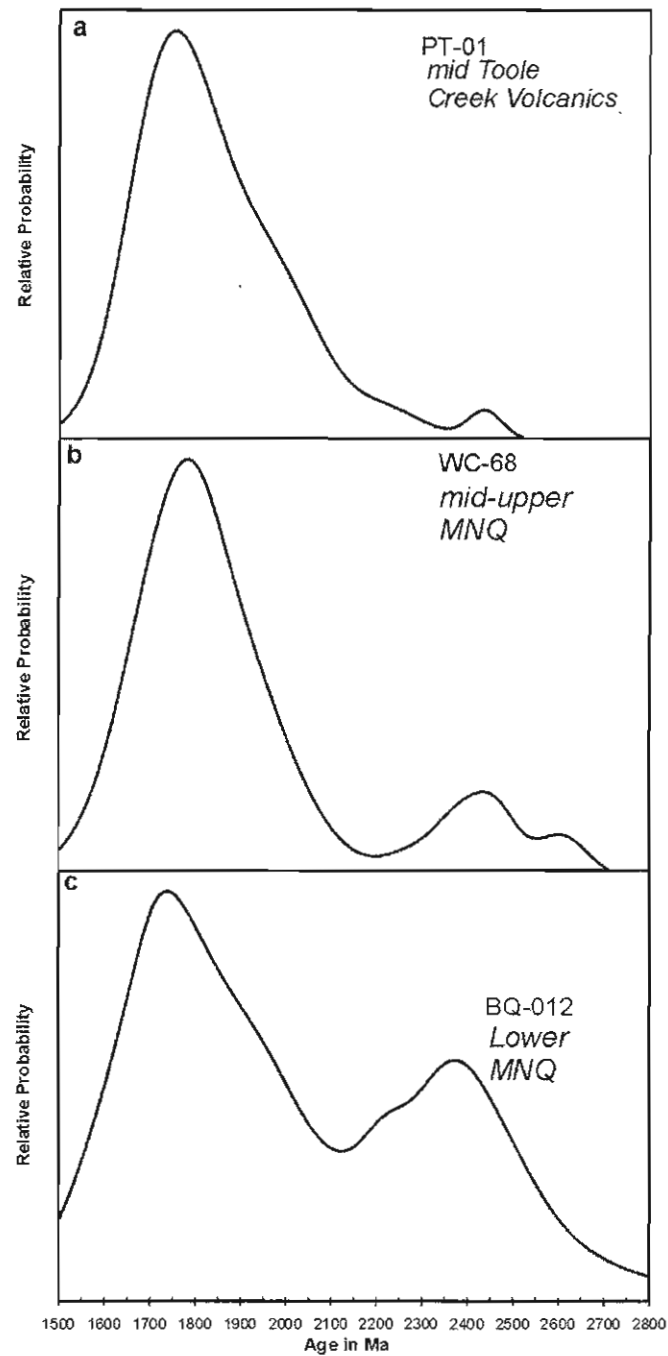
Figure 4.7: U-Pb detrital zircon probability graphs for the three samples taken from the Soldiers Cap Group in stratigraphic order from (c) upwards. Calculated using ISOPLOT v.2.05. Note the subtle peaks in *BQ-012* and *PT-01* on the shoulder of the main peak.

Sample PT-01

From a total of 57 analyses sample *PT-01* has a similar corrected $^{207}Pb/^{206}Pb$ age data spread to *BQ-012* with a major *ca.*1750 Ma and a small Archaean-Paleaeproterozoic *ca.*2450 Ma population. Similar to *BQ-012* a subtle combined *ca.*1860 Ma and *ca.*1970 Ma peak is present. Zircons from Group 2 make up the bulk of this secondary population. A similar age spread relative to grain morphology as *WC-68* was observed in this sample (Table 4.2).

4.5 Zircon Provenance

The common subrounded-subangular morphology of the zircons (Fig.4.5) and a general lack of metamorphic or hydrothermal overgrowths, suggests that $^{207}Pb/^{206}Pb$ age data presented as probability graphs here, represent detrital zircon populations defining source terranes. Whilst the age peaks were present in all zircon morphology groups, there is some correlation between zircon morphology and age. The rounded and fragmented grains of morphology Group 2 provides the bulk of the Archaean and older ages, and the prismatic and zoned zircons of Groups 1 and 3 provide the bulk of the *ca.*1750 Ma and *ca.*1790 Ma age population.

Within the Eastern Succession there are several units that may have provided detrital zircons for the numerically dominant *ca.*1750 Ma age population in the three samples. Page & Sun (1998) dated calcsilicates from Corella Formation to the north of the study area at 1750±7 Ma (Fig.4.1; Fig.4.8) and felsic-intermediate Mt Fort Constantine Volcanics north of the Pumpkin Gully Syncline at 1734-1755 Ma. (Fig.4.1; Fig.4.8) They also noted provenance of Corella Formation and Mt Fort Constantine Volcanics age in Mt Norna

Quartzite samples. The Jessie Granite, a small S-type microgranite dated at

1746±8Ma (Page & Sun 1998; Fig.4.1; Fig.4.8), mafics of the Marraba

Volcanics and sediments of the Ballara Quartzite and Mitakoodi Quartzite

may also have been potential sources (Fig.4.1; Fig.4.8).

Figure 4.8 (previous page): Diagram depicting the tectonostratigraphy of the Mt Isa Inlier and the interpreted sources for the Soldiers Cap Group zircon provenances which have reliable age dates. Magenta/red defines the most likely sources for the *ca.*1750 Ma population and yellow the enigmatic secondary *ca.*1860 Ma population. Modified from Bodon (2002; *cf.* Betts *et al.* 1997; O'Dea *et al.* 1997; Page & Sun 1998; Page & Sweet 1998). Age date sources are 1-Page *et al.*1997; 2- Giles (2000); 3-Page & Sweet 1998; 4-Connors & Page (1995);5-Page(1983); 6-Page & Williams (1988); 7-Page (1998) ; 8-Pearson *et al.* (1992). All other ages are from Page & Sun (1998) or referenced in the text.

The closest matches to the *ca.*1790 Ma age peak come from mafic volcanics of the Argylla Formation dated at 1783±5 Ma (Fig.4.1 and 4.8 Page 1983), the Bottletree Formation in the Western Succession and felsic volcanics of unclassified "Soldiers Cap Group" from the Boomara Horst, with ages of 1775±4 & 1774±4 Ma (Page & Sun 1998). The presence of this peak within sample *WC-68* but absence in the other samples can be accounted for in several ways (1) a change in source area during the evolution of the Soldiers Cap Group; (2) changes in extrabasinal drainage patterns, *ie.* drainage stopped or was hindered from the Corella Formation/Mt Fort Constantine Volcanics and was increased from units of the Argylla Formation, influencing the presence/absence of the subtle secondary peak found in *BQ-012* and *PT-01* but absent in *WC-68*; (3) fluctuations in the dominance of at least two separate sediment distributaries. The exact mechanism responsible for this change is difficult to propose, based upon the available isotopic evidence. However, this stratigraphic level is also defined by a change from turbidity current dominated to storm current dominated sedimentation (Ch.3) and the presence of iron formations(Ch.7) suggesting that this provenance change may cryptically define a larger scale event.

Possible sources for the *ca.*1860 Ma age group in the Eastern Succession are poorly defined. The enigmatic Double Crossing Metamorphics with a maximum depositional age of 1840±20 Ma (Fig.4.1; Fig.4.8), (Beardsmore

1992; Page & Sun 1998) is geographically closest to the sample sites and is within the age overlaps. Within the greater Mt Isa Inlier there are also several units which have overlapping ages with this *ca.*1860 Ma population:- the Cover Sequence 1 1845-1870 Ma Leichardt Volcanics, and the *ca.*1860 Ma Kalkadoon Batholith (Page & Sun 1998; Fig.4.8). Both of these units are located presently west a considerable distance of the present distribution of the Soldiers Cap Group (Chapter 2, Figure 2.2). The *ca.*1970 Ma age peak has no obvious published precursors but is close to the age proposed for the earliest phase of rifting within the Mt Isa Inlier (1950-1900 Ma, Ch.2; Fig.4.8).

The oldest inherited ages are the population of Archaean to Palaeoproterozoic zircons present in all three samples. Similar inheritance ages have been noted in previous detrital zircon populations from the Mt Isa Inlier and the Eastern Succession (Belousova *et al.* 2001; Page & Sun 1998; Scott *et al.* 2000; Giles 2000). The distribtution of rocks of Archaean age in the Mt Isa Inlier is poorly constrained. McDonald *et al.* (1996;1997) reported an Archaean tonalite-trondjhemite granite in the Kurbayia Migmatite of the Kalkadoon-Leichardt Block. However, Page & Sun (1998) disputed this by dating a sample of Kurbayia Migmatite with SHRIMP methods at 1860-1840 Ma. Beardsmore *et al.* (1987; *cf.* Wyborn & Blake 1982) suggested, based upon poorly defined grain size indicators, the presence of an as yet unidentified older block of basement to the east of the Soldiers Cap Group. Alternately, as suggested by Scott *et al.* (2000) these inheritance ages may represent fragments of Archaean crust which they interpreted as originally underlying much of the Mt. Isa Inlier. The change in amount of Archaean zircons from *BQ-012*

(39%), taken from the base of the sequence, to *WC-68* (19%) and *PT-01* (12%) from the mid-upper sequence, may also be a function of the larger sample population analysed for BQ-012. However, the distinct change in sedimentology style and presence of hydrothermal activity at the base of the Mt Norna Quartzite (Ch.3 & 7) suggests that this change does represent a larger scale tectonic process. The presence of a small population of *ca.* 1680 Ma zircons (Fig.4.6) implies that deeper units of the Maronan Supergroup were exposed during the deposition of the Soldiers Cap Group. This confirms that intrabasinal recycling was occurring to some degree at Soldiers Cap Group time.

4.6 Summary

Based on the large numbers of 'magmatic' zircons (Groups 1&3) and age overlaps, possible Eastern Succession sources for the Soldiers Cap Group are (1) Corella Formation calcsilicates and equivalents; (2) Marraba Volcanics (*cf.* Ch.7); (3) felsic-intermediate units of the Mt Fort Constantine Volcanics; (4) the large mafic volcanic piles of the Argylla Formation located presently to the west; (5) unclassified "Soldiers Cap Group" felsic volcanics in the Boomara Horst; (6) granitoids of Wonga Extension age from the Jessie Granite; (7) inferred Cover Sequence 1 equivalents of the Double Crossing Metamorphics (Fig.4.1). Distal Cover Sequence 1 sources such as the Kalkadoon Batholith, Leichardt Volcanics and Kurbayia Migmatite may also have provided detritus to the Soldiers Cap Group. These mixed sources from the north, south and west when combined with sedimentological and reconstructed palaeoflow data (Ch.3), suggest that at Soldiers Cap Group time, the local sedimentary environment involved erosion and deposition in

small, localised basins with northeast-southwest long axes, with an active local environment and a moderate degree of erosion, transport and a lesser degree of intrabasinal recycling.

The presence of zircons of the same age as the earliest rift event in the Mt Isa Inlier, Cover Sequence 1 rocks (Leichardt Volcanics; Kalkadoon Granite) and later rifting events (Jessie Granite-Wonga Extension Event) suggests that units produced during the tectonic events recognized elsewhere in the Mt Isa Inlier were exposed at the time of Soldiers Cap Group deposition. It has been suggested that the Soldiers Cap Group formed distally to the Mt Isa Inlier and was transported as an allocthonous block from somewhere to the east of its present location (Laing 1998). The presence of zircons with distinct Eastern Succession and older basement affinities as well as Mt Isa Inlier rifting event signatures provide evidence that the Soldiers Cap Group likely lies close to its original position despite some degree of probable tectonic transport.

Giles & MacCready (1997) suggested that the Soldiers Cap Group was deposited to the east of the complex Cloncurry Fault – Cloncurry Overthrust, presently located at the Soldiers Cap Group/Doherty Formation contact. This was controlled by the erosion of older (Cover Sequence 1 & 2) from uplifted half-graben tilt blocks to the west of this complex fault zone. This provides an attractive hypothesis agreeing with data presented here. This will be discussed in the context of basin geometries and tectonostratigraphic links with the Mt Isa Inlier and other Northern Australian Proterozoic basins in Chapters 8 & 9.

Chapter Five- Volcanology of basaltic units of the upper Soldiers Cap Group

5.1 Introduction

Numerous basaltic bodies of varying thickness, petrography, alteration paragenesis and contact relationships are intercalated with metasediments of the upper Soldiers Cap Group (SCG). These have been previously interpreted as a series of syn-sedimentary sills, largely based upon their conformable nature with the SCG sediments (Derrick *et al.* 1976e; Blake and Stewart 1992; Davidson & Davis 1997; Williams 1997). A small andesite flow was identified by Davidson *et al.* (2002) and pillowed basalts noted by Ashley (1983) in the Monakoff area, Pumpkin Gully Syncline (PGS). However none of these previous studies went into any great detail on the volcanological features of the upper SCG.

As part of the broader study of the SCG several distinct volcanological facies were defined within the upper SCG through regional and prospect scale mapping and core logging. These facies were then used to define the genetic relationships between the basaltic units and host sediments and place the evolution of the mafic units of the SCG into the broader basin-scale context.

5.2 Nomenclature, distribution, petrography and alteration

5.2.1 Nomenclature and distribution

Detailed geological data was collected along regional sedimentological sections (see Chapter 3) and in prospect and regional scale mapping (1:25000 and 1:15000 scale Maps One and Two). In addition, diamond core from regional BHP Minerals

exploration drilling (KDD-03; AND-016; AND-029; App.7) and Great Australia

Minerals Monakoff resource definition/exploration drilling (MKD-01; MKD-3;

MKD-2; App.7) were logged in detail. Summary logs of drillholes MKD-01 and

AND-029 depicting representative volcanological lithofacies and their stratigraphic

relationships, are shown in Figure 5.1. Good stratigraphic and sedimentological

control was available in outcrop, allowing confident interpretation of the facing of

the sequence including the mafic units.

The basaltic units of the upper SCG have been referred to previously as ortho-

amphibolites, metadolerites, metabasalts, mafic volcanics, metavolcanics and high

Fe-metatholeiites (Arnold 1983; Ashley 1983; Blake & Stewart 1992; Derrick *et al.*

1976; Williams 1998). In this study, the terms basalt, dolerite and gabbro are

hereafter given the prefix *meta*. The terms basalt, dolerite and gabbro are used to

infer a pre-metamorphic grainsize and texture and as an identifying descriptive

scheme based upon grainsize, mineralogy and texture. The petrography of these units

is discussed in more detail below. The terms 'metatholeiite' and 'mafic' are also used

throughout this study as universal descriptors and for clarity in the geochemical

interpretation of these units (Ch.6).

Estimations by the author based on regional mapping, detailed section traverses and

prospect scale mapping show that the mafic units comprise 20-30% of the upper

SCG stratigraphic sequence. Stratigraphically, they occur within the entire upper

SCG from the basal Llewellyn Creek Formation (LCF), to the uppermost Toole

Creek Volcanics (TCV). Thick ($\geq$150m) metadolerites dominate the Mt Norna

Quartzite (MNQ) but are subordinate in the TCV across the study area.
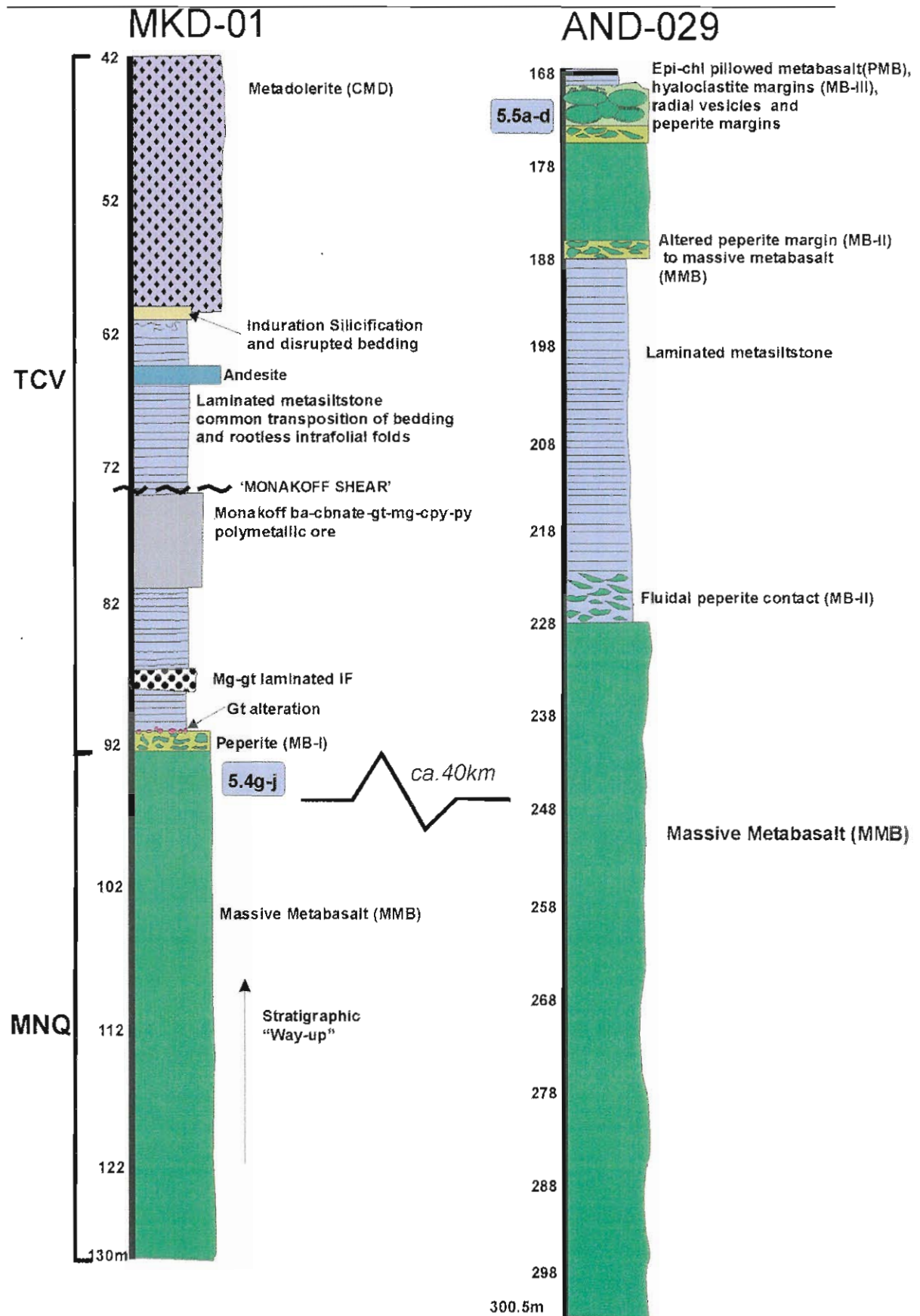
Figure 5.1: Representative logs of diamond drill holes intercepting extended intervals of metatholeiites AND-029 (BHP Minerals) and MKD-01 (Monakoff) depicting the major contact styles and their stratigraphic position. These drillholes are approximately 30km apart and are shown on Figure 5.3. Facing of AND-029 is uncertain and is not assigned a stratigraphic position but is inserted here to depict general relationships considered important in mafic volcanic units. MNQ= Mt Norna Quartzite; TCV= Toole Creek Volcanics. Location of figures depicting representative features on the drillhole logs are shown.

Similarly, basalts with clear extrusive features are present in parts of the Pumpkin

Gully Syncline (PGS) but are subordinate to absent in the Weatherly Creek Syncline

(WCS). Many of these mafic bodies in the MNQ/TCV are laterally extensive, and

interpretation of BHP Minerals detailed company airborne magnetics and drill core

suggests they continue for some 10's of kms under cover to the east (S.Konecny

pers. comm. 2000).

5.2.2 Microtextures

Thin sections of basaltic units and adjacent metasediments analysed by XRF

(Chapter 6) and other representative samples were examined to ascertain

metamorphic and relict textures, and alteration assemblages.

Few primary textures were preserved at the microscale due to persistent overprinting

by metamorphism, deformation and pervasive regional scale alteration events. On the

whole there is little variation both internally and regionally in the petrography of the

mafic units, allowing relatively small populations of type examples to be used to

outline the mineralogy of these units. All mineral identifications are based upon thin

section petrographic methods, *ie.* no microprobe work was undertaken as this was

beyond the scope of this project.

The distinction between metabasalt, metadolerite and metagabbros was defined

largely by features in outcrop, and to a lesser extent thin section features.

Metagabbros are defined by coarse to very coarse-grained units which have

preserved 1-2mm long pyroxene and plagioclase phenocrysts at outcrop and thin

section scale (Fig.5.2a). These units have previously been termed 'gabbro-textured'

amphibolites (Davidson 1998) and ortho-amphibolites (Blake 1987; Derrick *et al.*

1976e). Metadolerites are defined in this study by medium-coarse grained units, generally dark green to black, which have a commonly preserved porphyritic texture with pyroxene and feldspar phenocrysts in a fine grained groundmass of similar mineralogy and occasional sub-ophitic textures (Fig.5.2b). Metabasalts are defined here as fine-grained green-dark green units with no porphyritic textures observed at the outcrop scale (Figs.5.3-5.5). These have previously been described as 'metavolcanics' (Ashley 1983) and atypically as andesites (Ashley 1983; Davidson 1998).

The upper Soldiers Cap Group metabasalts, metadolerites and metagabbros have a mineralogy consistent with epidote-amphibolite facies metamorphism with pervasive retrogression to greenschist transition facies (Moody *et al.*1983). The rarely preserved peak metamorphic assemblage is:- green-brown amphibole-epidote±plagioclase±ilmenite and minor sphene (Fig.5.2c&d). This occurs as a groundmass of elongate-squat, green-brown amphiboles (under plane polarized light) varying in scale from 0.1-2mm length, commonly aligned to S_2 foliations, associated with sub-euhedral small epidotes. Ilmenite and rare sphenes occur as small >0.1mm grains associated with epidotes. This assemblage varies from very-fine grained in the metabasalts to very-coarse grained in the metagabbros.

The more common retrograde metamorphic assemblage is represented by actinolite±chlorite±albite±epidote(±clinozoisite)±talc (Fig.5.2b-d). Chlorite-actinolite likely formed by hydration of clinopyroxene, and clinozoisite has replaced original plagioclase. This assemblage is represented by elongate and commonly strained actinolites associated with chlorite, both of which are aligned to the

dominant foliation (Fig.5.2c-d), and small sub-euhedral andesines, very small euhedral clinozoisites with amorphous clots of talc.

Rare primary microscale textures preserved at the thin section scale include gabbroic textures comprising relict coarse-grained clinopyroxene and plagioclase laths incompletely overprinted by later alteration (Fig.5.2a). Ophitic textures are preserved in metadolerites and metagabbros with large, subhedral clinopyroxene and enclosed, altered plagioclase laths (Fig.5.2b). Within some metabasalts, vesicles up to 8mm across containing epi±qtz±cbnate are preserved, with the margins defined by elongate actinolite subparallel to foliations (Fig.5.2e). These vesicles are better preserved in many localities at the outcrop scale and are described in more detail below.

5.2.3 Regional alteration associated with metabasaltic units

Overprinting the metamorphic and primary fabrics of the basaltic units and adjacent metasediments are four distinct alteration events, some of which have previously been documented within the study area. These are described below, and include:- (1) pre-deformational epidote±quartz±carbonate alteration (*cf.* Williams 1997); previously documented post D_2 regional plagioclase-quartz±actinolite Na-metasomatism (Rubenach & Barker 1998; Williams & Blake 1993); (2) a post-peak metamorphic epidote-quartz alteration; (3) post D_3 K-feldspar±hematite±quartz, regional 'red-rock' alteration (Williams & Blake 1993); (4) scattered occurrences of garnet±magnetite alteration. There are also several distinct alteration styles associated with larger deposits in the study area. These include a pervasive Si-K-Fe-Mn predeformational footwall alteration at Monakoff (Davidson 1998) and a complex biotite-scapolite-plagioclase-sericite-siderite alteration zonation in the Mt

Freda deposit cluster (Davidson 1998). Observations of alteration styles and timing relationships at both outcrop and thin section scale broadly agree with these previously published alteration models for the Eastern Succession (Davis & Davidson 1997; Davidson *et al.* 2002; De Jong & Williams 1995; Rubenach & Barker 1998; Williams & Blake 1993; Williams 1998).

Epidote-quartz±carbonate(±garnet) alteration occurs as broadly symmetrical haloes 2-15m wide or discrete zones 1-6m wide and up to10m long at the contacts, both planar and brecciated, between metabasalts and metasediments. Within thin sections from metabasalts, this alteration varies from small (>1mm), subhedral epidote-quartz composite clumps overgrown by metamorphic amphibole/actinolite which define the dominant structural fabric (Fig.5.2d&g) and are overprinted by later feldspar alteration to large carbonate-quartz grains overgrown by later epidote (Fig.5.2d&g). Within the adjacent metasediments, it is represented by symmetrical haloes 2-15m wide of epidote-quartz±carbonate that are best observed in outcrop or core as distinctive pale-green to white 'bleached' or zones. At some metasediment-metabasalt contacts, more commonly those which are brecciated, numerous, large (up to 2cm in diameter), spongy, garnet crystals (Fig.5.4i-j) that decrease rapidly in size and number away from the contact are common (*cf.* Williams 1997; Davidson & Davis 1998; Davidson *et al.* 2002). Later garnet growth is associated elsewhere within the mafics with garnet-magnetite alteration controlled by later structural elements, discussed below. However the common association of this style of garnet associated with brecciated mafic-metasediment contacts discussed in detail below, and epidote-quartz±carbonate haloes, allows it to be interpreted as the product of an earlier, possibly synsedimentary, low-T alteration which has been a locus for renewed garnet growth during metamorphism and metasomatism. Epidote-

quartz±carbonate alteration is also commonly found as fill to vesicles in metabasalts (Fig.5.2e), which provides an important timing constraint. Where garnet and epidote are absent this alteration occurs as large zones of silicification in which sedimentary structures are commonly disrupted forming non-coaxial minor folds that are not congruent to any observed deformation event (Fig.5.4a&b). Based upon the overprinting relationships observed in outcrop, core and thin section this alteration style is interpreted as pre-deformational.

Regional Na-metasomatism is well documented and widespread within the region (Williams & Blake 1993; *cf.* DeJong & Williams 1995) and commonly occurs associated with both major structures and numerous mineral occurrences. Within the basaltic units of the SCG this alteration is not pervasive but where it does occur it is generally associated with large scale structural elements, or is spatially related to granitoids and is generally destructive of most primary textures. In the SCG mafics at the microscale, Na metasomatism occurs as either thin quartz-plagioclase veinlets or as a destructive replacement by 'flooding' of quartz-plagioclase through earlier textures (Fig.5.2g). At the macroscale Na metasomatism occurs as zones of *in-situ* brecciation hosted in structures within mafic units and in places can mimic volcanic breccias (Fig.5.2g).

Post-peak deformational epidote±quartz alteration occurs as sporadic patches of veinlets and spatially restricted ($10m^2$) zones of epidote-quartz flooding. Where observed in thin section and hand specimen this alteration consists of small, euhedral epidote±quartz crystals overprinting retrograde amphibole margins within metadolerites. This alteration is less common within the finer-grained metabasalts, where it occurs as veinlets of epidote±quartz.

K-feldspar±haematite±quartz regional 'red-rock' (Williams & Blake 1993) is widely recognized by workers in the Eastern Succession and occurs as either K-feldspar dominated veins or as destructive, replacive alteration of coarser grained mafic bodies by euhedral pink-red K-feldspar crystals and smaller, subhedral quartz crystals. Some examples are both texturally and mineralogically destructive. The best preserved large scale examples of this within the study area occur to the SE of the Pumpkin Gully Syncline were BHP drilling intersected a large zone associated with the confluence of several structures (E.Etchart *pers. comm.* 1998).

The latest alteration event, magnetite-garnet alteration, comprises subhedral magnetite-garnet (Fig.5.2h), which is commonly controlled by late (D_4) structural fabrics and is widespread across the study area, for example this alteration was observed in drillcore from Monakoff (MKD-01; Fig.5.1) and BHP exploration drilling some 30km SE (AND-029; Fig.5.1). This alteration differs from garnet associated with epidote-quartz±carbonate by the presence of subhedral magnetite and being found exclusively several metres or more away from mafic-metasediment contacts
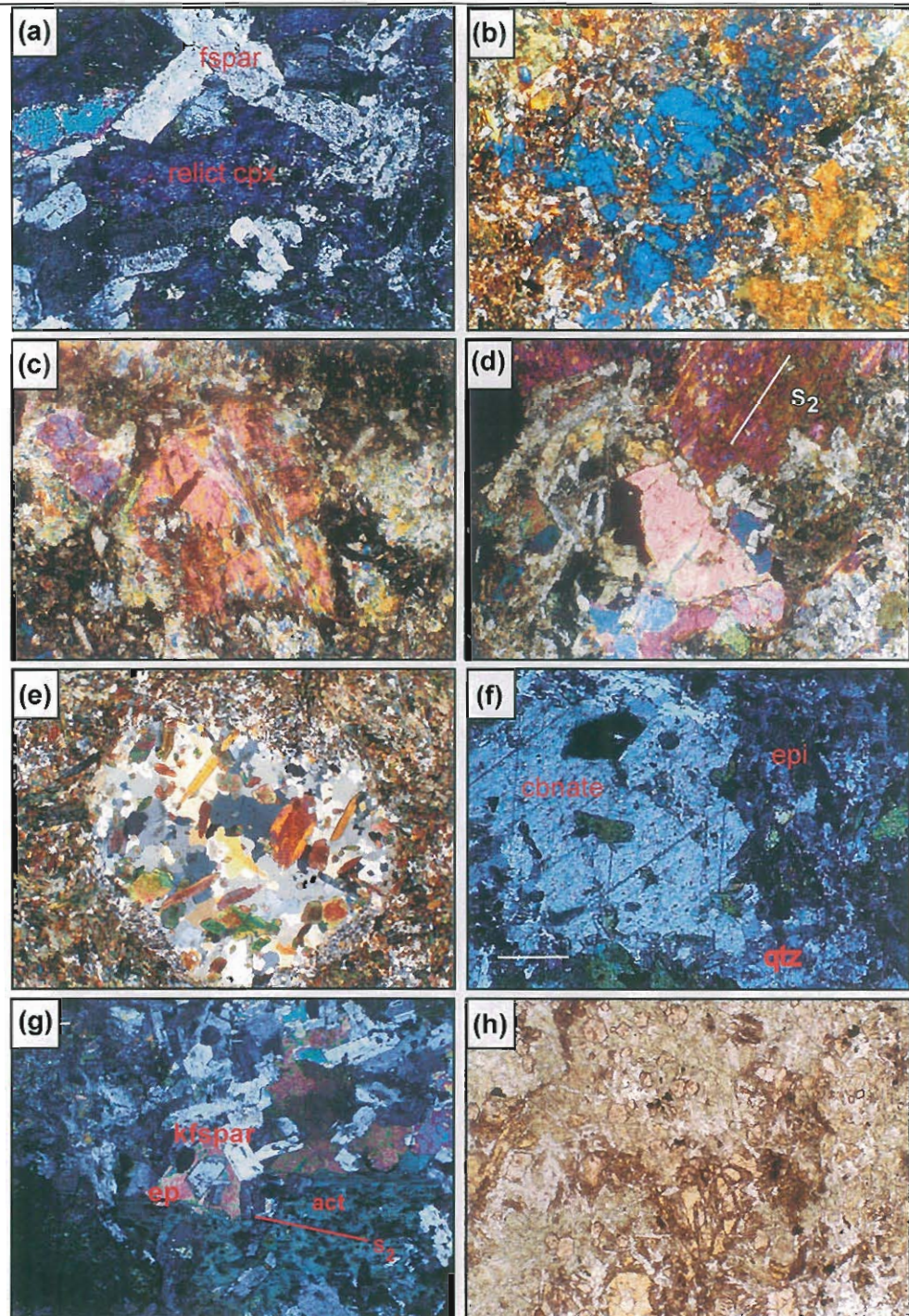
Figure 5.2: Examples of the preserved primary textures, alteration styles and metamorphic texturesof the metabasalts of the upper Soldiers Cap Group ;(a)relict cpx grain in metagabbro from the Pumpkin Gully Syncline (PG-105)photomicrograph (crossed polars) of epi-qtz-gt-cbnate alteration in metadolerite overprinting the retrograde assemblage, S_2 not well developed (PG-103);

(b)sub-ophitic texture in metagabbro (PG-105), mineral altering cpx is late qtz-albite (c) peak metamorphic amphibole retrogressed to biotite-chlorite on the rims (PG-105); (d) early epidote alteration overprinted by metamoprhic amphibole aligned to foliation, both overprinted by later feldspar alteration; (e) cbnate filled vesicle overprinted by late epi-qtz alteration (PG-79); (f) cbnate-qtz-epi filled amygdales within metabasalt from the Pumpkin Gully Syncline; alteration in metabasalt (PG-93) and overprinted by (ferro)actinolite and later regional metasomatic fspar alteration; (g) metamorphic actinolite, aligned to foliation, overprinting early epidote alteration (PG-79); (h) late garnet alteration overprinting metabasalt (PG-122). NB: Field of view of a-h is 5mm wide.
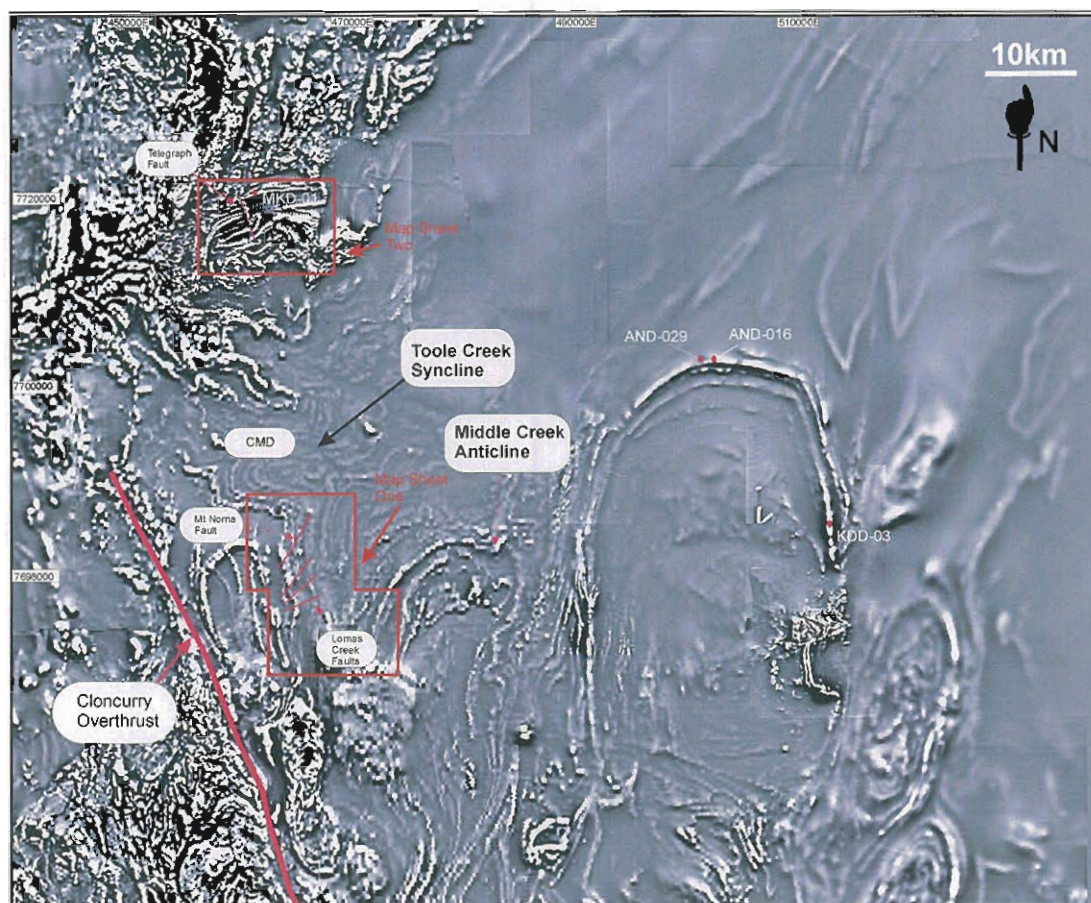
Figure 5.3: Regional aeromagnetic image (1st vertical derivative) depicting the distribution of the mafic bodies of the SCG, areas of outcrop mapped, exploration drill holes logged for this study and structures believed to be important in basin evolution. 'CMD' represents an example of a Coherent Metadolerite Sill

5.3 Geophysical distribution of mafic units

Detailed aeromagnetic surveys carried out by BHP Minerals as part of routine regional exploration, when tied with outcrop mapped and drillcore logged in this study provides a useful delineator of the SCG mafic units. In particular the large metadolerite bodies common in the upper MNQ and lower TCV in the WCS are clearly distinguishable in (Fig.5.3; *cf.* Map Sheet One & Map Sheet Two). These units are able to be traced from the WCS across several kilometers of strike in aeromagnetic and gravity images along the antiformal Kevin Downs structure (this study; S.Konecny *pers. comm.* 1999).

Additionally, exploration drill holes logged by the author (AND-019; AND-029; KDD-003; Fig.5.3) along this and associated structures intersected mafic units which were identified as SCG mafics through empirical geochemical fingerprinting (Ch.6;

Fig.6.7). Overall, this confirms the presence of the SCG mafic sequence across a larger area than previously believed by workers in the area and has important exploration implications which will be discussed in more detail in a later chapter.

5.4 Lithofacies descriptions and interpretations

Six volcanological lithofacies (*Monomict Breccia Type I; Monomict Breccia Type II; Monomict Breccia Type III; Massive Metabasalt; Pillowed Metabasalt; Coherent Metadolerite*) are defined here within the Soldiers Cap Group based upon lithology, internal structure and contact relationships with surrounding sedimentary units. The features of these lithofacies are summarised in Table 5.1, illustrated in Figs.5.1, 5.2, 5.3, 5.4 & 5.5, and are described below in more detail. The distribution of these lithofacies is discussed within each facies description, summarized in Table 6, and type example locations for each are noted on Map Sheet One and Map Sheet Two using the abbreviations given below. For descriptions of the petrography and structures within the associated metasedimentary rocks and iron formations (IF) see Chapter 3 and Chapter 7 respectively.

5.4.1 Monomict Breccia-I (MB-I)

Description

Lithofacies MB-I is a matrix supported breccia which consists of poorly-sorted, 0.5-20cm long 0.1-10cm wide, angular clasts of coarse grained metadolerite or metabasalt, with occasional 'jigsaw-fit' textures and chilled margins (Fig.5.4c-j) supported by a silicified metasiltstone matrix (Fig.5.4c-j). Remnant bedding is rarely preserved in adjacent sediments and the facies has an estimated average thickness from core and outcrop of up to 5m. The estimated lateral extent of this lithofacies is locally up to 25m and overall comprises ~<5% of the entire mafic sequence. This

breccia is often associated with upper CMD, basal and upper MMB contacts

(Fig.5.1;

Fig.5.4c-i) and ubiquitously with a 1-20m wide epidote-quartz-carbonate alteration

halo of the adjacent metasediments. Similar to MB-II there is a 5-20m wide

progression from MB-I to altered metasediments to unaltered metasediments. MB-I

was commonly locally constrained by facing indicators in adjacent sediments

including cross-laminae, cross-bedding and load structures (*cf.* Ch.3). This facies

occurs from the mid-LCF upwards to the upper-TCV within both the WCS and PGS.

(a)

(b)
metasiltstone
ep-qtz-cbnate(gt)
metabasalt
s
b
b
b
20cm

(c)

(d)
s
d
d
d
d
d
d
d
d
d
d

(e)

(f)
mb
metasiltstone
mb
mg-gt
mb
mb
10cm

(g)

(h)
gt
mb
mb
metasiltstone
5cm

(i)

(j)
metasiltstone
mb
gt
mb
gt
mg-gt
mb
5cm
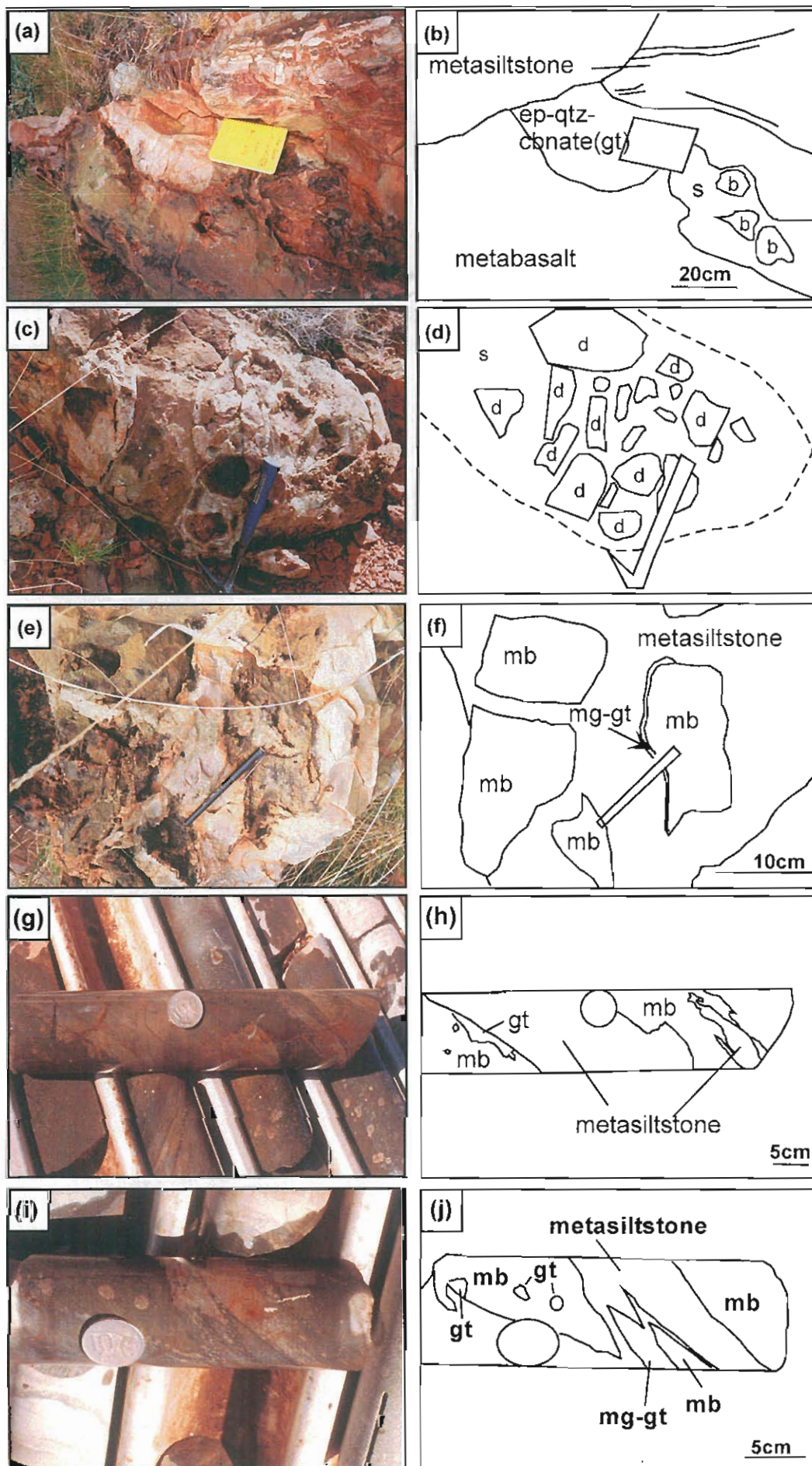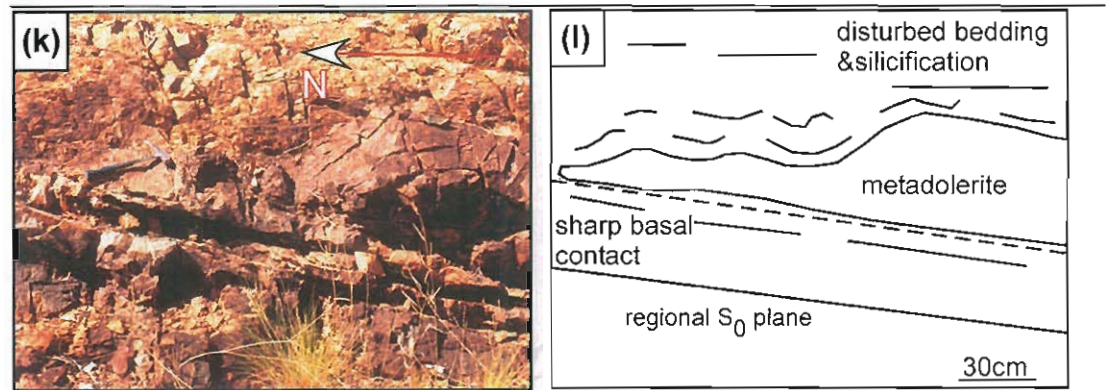
Figure 5.4: (a) epi-gt-qtz-cbnate altered contact between metabasalt and medium-fine grained metasediments Pumpkin Gully Syncline, contact is sharp in the upper left of the photograph and adjacent to this bedding is disturbed, at the bottom right it comprises a monomict breccia similar to that in (c); (b) line sketch depicting the major features of (a), s=metasediments; (c) monomict breccia comprised of metadolerite clasts within epidote-quartz-garnet-carbonate altered metasediments with destroyed bedding MNQ-TCV contact PGS; (d) line sketch depicting the major features of (c), d=metadolerite; (e) monomict breccia from contact between MMB and laminated metasediments clasts hosted by epidote-quartz-garnet-carbonate altered metasediments with no relict bedding; (f) line sketch depicting major features of (e); (g)monomict breccia with metabasalt clasts with garnet altered margins in silicified metasediments with rare preserved laminae (MKD-01-90m); (h) line sketch depicting the major features of (g); (i) blocky clast of metabasalt with magnetite-garnet altered margins within silicified metasiltsone with rare laminae preserved(MKD-01-92m; (j) line drawing of (i) depicting major features;(k) termination (left of photo) of a large metadolerite sill within laminated, silicified metasediments, note sharp base and disruption of laminae above within the zone of silification; (l) line sketch of (k) depicting major features.

Interpretation

Within complexly deformed volcanosedimentary sequences definitive interpretation

of coarse-grained brecciated volcanic-sediment contacts is often difficult. Particularly

in a sequence of coarse grained sedimentary units (*eg.* Squire & 2002).

The upper SCG, however is mostly composed of fine-medium grained

metasediments of fairly uniform composition and structure (*cf.* Ch.3). Preserved

examples of this facies also occur in drillcore from zones of significant structural

complexity where clasts have a pseudo-fluidal appearance (*eg.* Fig.5.4i-j) but overall

are generally angular.

The angular shapes ("polyhedral" of Squire & McPhie 2002), chilled margins and

metasediment-mafic mixing of MB-I is indicative of peperite, particularly blocky

peperite (Busby-Spera & White 1987). Blocky peperitic contacts are commonly

interpreted as the product of the intermixing of wet, unconsolidated host sediments

117

and coherent intrusions (Williams & McBirney 1979; McPhie 1993; McPhie & Houghton 1998; Dadd & van Wagoner 2002). The fragmentation of coherent igneous bodies to form peperite margins is dominated by steam explosions, dynamic stressing and quench fragmentation (Kokelaar 1986; Squire & McPhie 2002). Host sediment lithology, water content and rheological strength as well as intrusion temperature, magma viscosity and rate of magma supply are also important contributing factors in the style of peperite developed (Kokelaar 1986; Busby-Spera & White 1987; Squire & McPhie 2002; Wohletz 2002).

Blocky peperite is interpreted as the result of brittle behaviour by sills of relatively high viscosity intruding into wet sediments with a high local water content (Busby-Spera & White 1987; Squire & McPhie 2002). The spatial relationships of the magmatic clasts to each other and to the host sediment, is important in defining the local processes involved in peperite formation. For example the MB-I clasts which are angular, have chilled margins and no evidence of rotation (Fig.5.4c-h). The greater majority, would be interpreted on the criteria of Squire & McPhie (2002; *cf.* Kokelaar 1986) as representing in-situ quench fragmentation which requires a well defined sediment-magma contact and a brittle, high viscosity magma. Alternatively, MB-I clasts which do not have an obvious jigsaw-fit texture or chilled margins (*eg.* Fig.5.4g-h), would likely represent steam explosions at the sediment-magma interface which interacted violently and rapidly with adjacent sediments (Kokelaar 1986; Busby-Spera & White 1987; Squire & Mcphie 2002). The lack of evidence for clast rotation and the general high density of clasts precludes a component of dynamic stressing during peperite formation (*cf.* Kokelaar 1986; Squire & McPhie 2002). The presence of the distinctive alteration and disrupted/destroyed bedding adjacent to MB-I peperites is a feature commonly ascribed to fluidisation of the

sediment during blocky peperite formation (Kokelaar 1982; McPhie 1993; Brooks 1995; Squire & McPhie 2002).

The common association of MB-I with stratigraphically well constrained upper CMD/MMB contacts, associated epidote-quartz-carbonate alteration and induration/silicification, allow MB-I to be interpreted as peperite developing at the upper contacts of syn-sedimentary sills. No direct gradational relationships were observed in outcrop or core linking this facies with MB-II or MB-III. However, several outcrops in the Pumpkin Gully Syncline separated by 5-7m and containing MB-II suggests a tenuous temporal relationship.

5.4.2 Monomict Breccia Type-II (MB-II)
Description

This lithofacies is primarily distinguished from MB-I by clast shape and consists of zones 1-3m wide of poorly sorted, large (up to 50cm long axis), chaotically dispersed, irregularly shaped, lensoidal or bulbous ('amoeboid' Squire & McPhie 2002), subrounded mafic clasts with remnant glassy margins which are now magnetite-garnet altered, supported in a silicified metasiltstone matrix with either severely disrupted and chaotically folded or no remnant bedding (Fig.5.4a&b).

Overall, this facies represents ≤3% of the mafic sequence observed in outcrop and core and is restricted to the upper MNQ/lower TCV contact. Best examples are at this stratigraphic level in the western Pumpkin Gully Syncline. It is associated with upper and rarely lower, CMD & MMB (Fig.5.4a&b) contacts and in best preserved examples can be traced for 10-15m along strike. Similar to the MB-III facies there is

a marked progression over 5-20m from MB-II breccias to quartz-epidote-carbonate altered sediments to unaltered sediments.

Interpretation

Brecciated contacts between sediments and mafics which have clasts with rounded-subrounded or irregular shapes, a general "amoeboid" nature (Squire & Mcphie 2002), evidence of clast movement, or a chaotic distribution are commonly described as globular or fluidal peperites (Kokelaar 1982; Busby-Spera & White 1987; Squire & McPhie 2002). As with MB-I the uniform petrography of host sediments, clast style and distribution allows interpretation of this brecciated lithofacies as a fluidal peperite (Busby-Spera & White 1987; Squire & McPhie 2002). Fluidal peperites are commonly interpreted as the product of more ductile behaviour by magmas of a lower viscosity (Busby-Spera & White 1987; Squire & McPhie 2002), and with a concomitant insulating vapour film (*cf.* Kokelaar 1982), than those that produce blocky peperites. Formation of fluidal peperites is commonly discussed in terms of the ductile fragmentation of magmas requiring low viscosity and higher temperatures than other peperite styles (Kokelaar 1982; Busby-Spera & White 1987; Squire & McPhie 2002). To prevent direct contact between magma and pore water in sediments at an advancing magma front causing explosive results by more brittle behaviour, insulation by formation of vapour films at the magma-sediment interface is required (Kokelaar 1982; Squire & McPhie 2002). To produce and maintain these vapour films sufficient pore water must be present in the host sediments and steady temperature, most commonly through steady magma supply, must also be maintained (Kokelaar 1986; Squire & McPhie 2002). The environment which is most conducive to this environment is the advancing front of a magma intruding saturated, unconsolidated sediments. Given the relatively uniform nature of the sediments of the upper SCG there must be another influence apart from the host sediment

120

affecting the variation in peperite style between MB-I & MB-II. Importantly, the rate of magma supply during the formation of MB-II was sufficient to prefer ductile vs. brittle fragmentation and the production of brittle (blocky) peperites.

5.4.3 Monomict Breccia Type-III (MB-III)

Description

This brecciated lithofacies consists of unsorted, angular to curviplanar and elongate, 0.5-7cm long metabasalt clasts with a common and distinctive 'jigsaw-fit' in a massive, white-brown carbonate-quartz±epidote matrix (Fig.5.5a), and a clast-matrix ratio of 2.5:1. Thickness in outcrop and core is interpreted as a maximum of 2m thick. Very thin (>1mm), quenched edges, possibly originally glass but now altered to garnet±magnetite are common on smaller clasts (Fig.5.5a). This facies was observed in the PGS at the MNQ/TCV contact (Map Sheet Two) with the best example logged in regional exploration core to the southeast (AND-019; Appendix 7;

Fig.5.1; Fig.5.2; Fig.5.5a). This breccia, where observed, is part of a rarely exposed facies sequence, from massive or pillowed metabasalt (MMB or PMB), to MB-III, to monomict breccias interpreted as peperites (MB-II), to epidote-quartz±carbonate altered metasediments out to unaltered metasediments.

Interpretation

As with the other brecciated volcanic lithofacies in the SCG the interpretation of MB-III is largely dependent on sediment versus metabasalt relations. The monomict nature, jigsaw fit of clasts, alteration, inferred glassy clast margins, and the gradational association with lithofacies MMB and PMB suggest that this breccia represents an in-situ hyaloclastite. Where observed, the concordant nature and

progression from coherent mafic to breccia to sediment, and the presence of sedimentary matrix precludes the interpretation as an alteration breccia.

The term hyaloclastite is used here to infer the product of quenching and explosive brecciation (Kokelaar 1986) on the margins of a magma body at the contact with wet unconsolidated sediments or ambient water. The absence of any observed bedding and clast mixing discounts the possibility that this facies represents a resedimented hyaloclastite (McPhie & Houghton 1998). The association with pillows and pillow margin features (AND-029- Fig.5.1; Fig.5.5a) suggest that many of these breccias can be interpreted as subaqueous hyaloclastites (Yamagishi 1979; 1987). The rare gradational relationships observed with peperite (MB-II) and massive mafic bodies are a feature described as representative of intrusive syn-sedimentary sills (McPhie *et al.* 1993; McPhie & Houghton 1998; Squire & McPhie 2002).

Interpretation of MB-III is dependent upon the observations of the adjacent lithofacies. Based upon the association of some MB-III breccias with MMB and gradation to MB-II breccias, the interpreted origin for MB-III breccia in that instance is of an intrusive hyaloclastite at the upper contact of a syn-sedimentary sill. Where these breccias are noticeably thinner and associated with pillowed metabasalts (PMB) as observed in core (AND-029) MB-III is interpreted as in-situ hyaloclastites.

5.4.2 Pillowed Metabasalt (PMB)

Description

This lithofacies comprises fine-medium grained metabasalt bodies at least 5-10m thick, and up to 20m in mappable lateral extent. Both outcrop and core expose whole and fragmented pillows with lobate form up to 1.5m long and 1.0m wide (Fig.5.5b-

h), with aspect ratios of 0.6-1.3 (*cf.* Corsaro & Mazzoleni 2002), with chilled margins and marginal and/or radial pipe vesicles 1-5mm long, some of which are deformed and their long axes pointing generally E-W (Fig.5.5b-h). There is no evidence for reworking of pillows or interpillow sediment although some pillowed sequences in core (AND-029; Fig.5.1) have brecciated margins (MB-III) which are interpreted as in-situ hyaloclastites. This lithofacies was only observed in outcrop in the Pumpkin Gully Syncline at the contact between MNQ and TCV southeast of the Monakoff (*cf.* Ashley 1983; MKD-01-Fig.5.1), where they have previously been interpreted as 'autobreccias' and 'pseudobreccias' (Davidson & Davis 1995), and in core from BHP drilling to the east of the main study area (AND-019; AND-029; Fig.5.1). In outcrop this facies is stratigraphically above Coherent Metadolerite (CMD) and/or adjacent to outcrops of Massive Metabasalt (MMB) lithofacies (*cf.* Fig.5.1). Apart from MB-III breccias in core (discussed above), contacts were not observed for this facies. Pillow form and shape from examples near Monakoff provide way-up criteria indicating facing to the south, consistent with local and regional sedimentary facing. The presence of deformed marginal vesicles which have an E-W orientation suggests an original component of flow in this direction.

Interpretation

Pillowed basalts are generally accepted as the product of subaqueous volcanism following their observation of formation on the seafloor (Moore *et al.* 1973; Moore 1975). Their presence does not infer a particular water depth, as pillowed lavas have been observed in both abyssal (Moore 1975; Ballard & Moore 1977) and shallow marine sequences (Moore *et al.* 1973).

Pillow size and shape is a function of a host of interrelated factors including magma viscosity, temperature, composition, magma supply and palaeoslope (Moore *et al.*1973; Dimroth *et al.*1978; Dolozi & Ayres 1991; Walker 1992). Vesicularity in basalts is a function of many factors including volatile content, viscosity of the original magma, deformation during flow, interference and combination of adjacent vesicles and the confining pressure of the water column (McBirney, 1963; Williams and McBirney, 1979). As with pillow size and shape, vesicularity of pillows is not a reliable depth indicator, as 50% vesicular basalts have been observed at water depths greater than 4000m (Clague *et al.* 1990). Additionally, the general scarcity of outcrop of this facies does not allow any comparative estimates of vesicularity. The general lack of clear relations with adjacent facies does not allow for a confident interpretation of the role of this facies in the overall development of the SCG. However, it does suggest that constant supply of a relatively hot, viscous magma was occurring in a subaqueous environment of moderate paleaoslope. Any inference of proximity to a vent or magmatic centre would be largely spurious as pillowed lavas are observed forming underwater many km's from a vent (*eg.* Hawaii; Moore *et al.* 1973) and at vents at mid-oceanic ridges.

5.4.5 Massive Metabasalt (MMB)

Description

The Massive Metabasalt (MMB) lithofacies is composed of generally tabular basaltic bodies ranging in thickness from 5-75m, of variable lateral extent (20m-2km), which are subparallel to adjacent metasedimentary bedding (Fig.5.5e-h). The MMB lithofacies is found at various stratigraphic levels from upper Pon_2 upwards and represents at least 30% of the mafics of the SCG and commonly occurs stratigraphically above and/or adjacent to the PMB lithofacies in the PGS and CMD

lithofacies in the WCS where both are spatially associated with iron formations (Chapter 7). Lithologically they comprise massive to weakly vesicular, medium-fine grained metabasalts. Vesicles range from 1-8mm long and only occur at or near contacts. Other primary textures including phenocrysts, are only rarely preserved due to the multiple overprinting metamorphic and alteration events outlined above. MMB can be rarely associated with brecciated basal and upper contacts (MB-I; MB-II; MB-III; Fig.5.5a-b) and commonly have indurated, silicified and epidote-quartz±carbonate altered marginal sediments. A variation of this facies is found in the core of the Pumpkin Gully Syncline which comprises a ~1km thick sequence of undifferentiated, poorly outcropping, generally massive, metabasalts (Map Sheet Two).

Interpretation

Depending upon the associated lithofacies, MMB can be interpreted as the result of one of two processes. The presence of vesicles, and association with the PMB lithofacies suggests that in part, MMB may be the result of subaqueous basaltic lava flows. This interpretation is confirmed by the presence of basal brecciated contacts (MB-I; MB-II) and associated silicification which is a process commonly interpreted as representing the 'bulldozing' of subaqueous mafic flows into unconsolidated sediments (McPhie 1993; Beresford & Cas 2001; Dadd & van Wagoner 2002). Brecciated upper contacts combined with fluidisation of adjacent bedding (MB-II; MB-III) are indicative of MMB occurring as synsedimentary sills (Duffield *et al.* 1986; McPhie 1993; McPhie & Houghton 1998; Rawlings 1993). It is concluded that different parts of the MMB had subaqueous eruptive, and locally intrusive, histories.
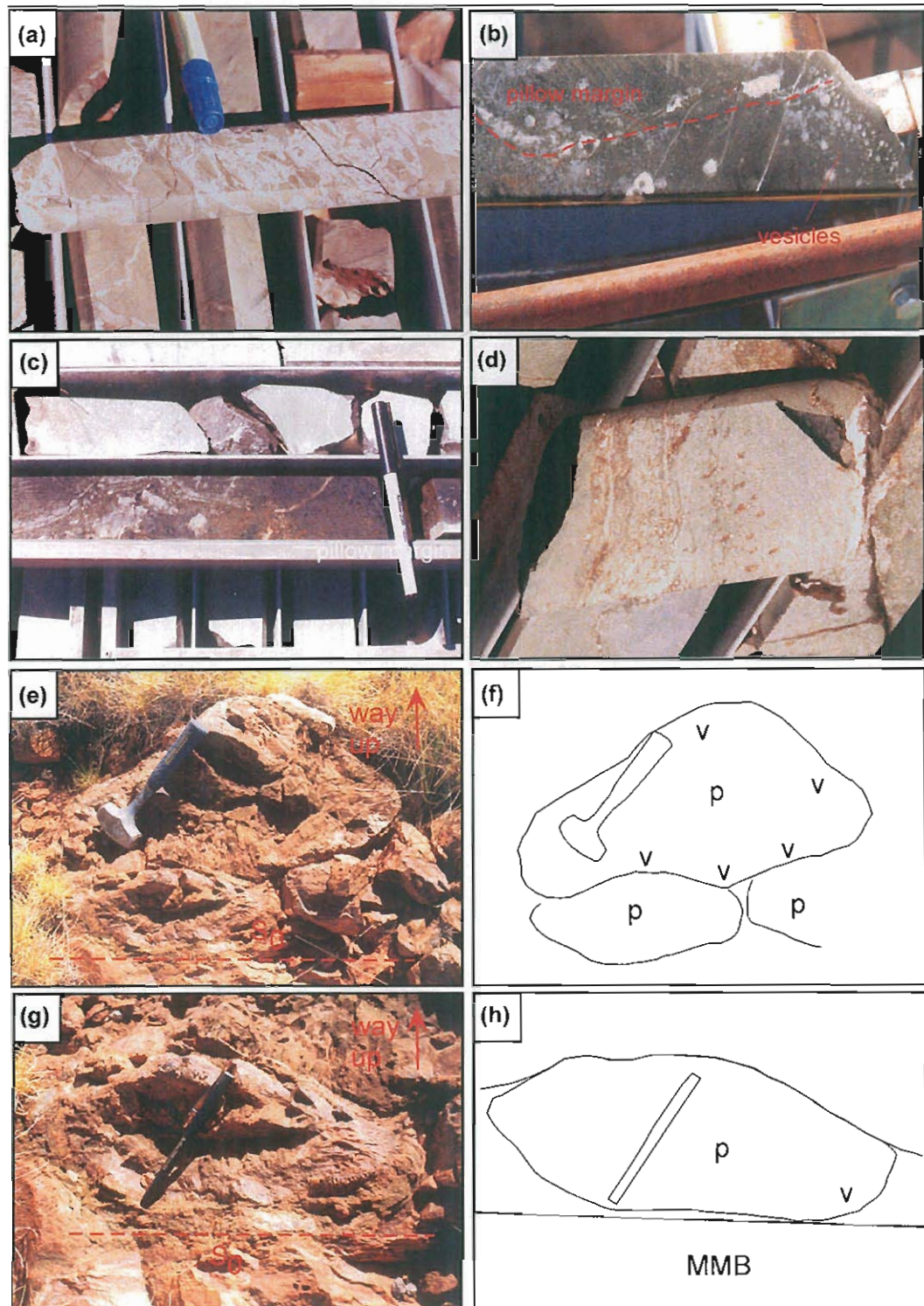
Figure 5.5: examples of extrusive features and synsedimentary contacts between metabasalts and metasediments in the upper Soldiers Cap Group; (a) monomict breccia MB-III in drill hole AND-029 (169m) interpreted as an in-situ hyaloclastite; (b) amygdaloidal pillow margin in metabasalt AND-029 (172-176m); (c) epi-qtz-cbnate altered pillow margin AND-029 (170m); (d)glassy pillowmargin with radiating pipe vesicles AND-029 (170m); (e-h) images and line sketches of lobate pillows in the PumpkinGully Syncline, north to the base of the figure regional bedding (S_0)depicted by the dashed red line in e&h, in (f)&(g) v= areas of increased vesicularity and p=pillow forms.

5.4.6 Coherent Metadolerite (CMD)

Description

This lithofacies comprises medium to very coarse-grained metadolerites and minor metagabbros that range from 2-200m thick and are laterally continuous for up to 1.7km (Map Sheet One). Where terminations of these sills are observed they either 'pinch-out' (Fig.5.4k-l) or are brecciated (MB-II, MB-I; Fig.5.1). These bodies are one of the few facies that can be mapped from their distinct aeromagnetic (Fig.5.2) and gravity highs, because they are normally enclosed by geophysically subdued sediment host units (Fig.5.3). This allows them to be traced for some distance under cover with a high degree of confidence. They are generally concordant with and subparallel to adjacent bedding both at the local and regional scales (Fig.5.4k-l). Internally, grainsize variations range from medium grained on the margins to coarse to very coarse-grained in central parts. Basal and upper contacts commonly have indurated and silicified haloes in which bedding is moderately

deformed or completely destroyed (Fig.5.4k-l). There is a common upper contact association with brecciated lithofacies (MB-I and MB-II). Generally, Coherent Metadolerite (CMD) units are located stratigraphically below intervals of PMB/MMB, this stratigraphy is best preserved in the western half of the PGS. This lithofacies is the dominant (50-60%) volcanic facies in the upper SCG and decreases in frequency from the MNQ to upper TCV.

Interpretation

Various authors (Kokelaar 1982; 1986; Duffield *et al.* 1986; Allen 1992; McPhie *et al.* 1993; McPhie & Houghton 1998) have interpreted the combination of disrupted host sediment bedding, induration and silicification, sub-parallelism with host sediments and brecciated upper contacts (MB-I & MB-II), here associated with CMD

127

units as indicative of syn-sedimentary sill sequences. Destruction of bedding and silicification around sill margins is commonly attributed to fluidisation of surrounding sediments related to the generation of water vapour generated by the intrusion of hot magma (Kokelaar 1982; Squire & McPhie 2002). Disruption and displacement of bedding can be related to the entrainment of sediment in pore fluid in restricted zones at the sediment-mafic contact (Squire & McPhie 2002). Given that sills are unlikely to produce fluidisation in host sediments at depths greater than ~1.6km (or 1km of sediments under a 1km deep water column; Kokelaar 1982) this prescribes the depth of intrusion for the CMD sills. No divergence of these sills was observed either on the local or regional scale suggesting that each sill represents a discrete magmatic event. With the exception of a local change in some palaeoflow markers (Ch.3), changes in sedimenatation patterns were not commonly observed stratigraphically above CMD sills. Additionally, the lack of localised breccias associated with CMD sills implies that these bodies did not inflate the sedimentary pile by any great degree. The CMD lithofacies is therefore interpreted here as the product of intrusion of massive dolerite and minor gabbro sills into a sequence of unconsolidated, wet sediments at or near the time of sedimentation.

5.5 Distribution and abundance of volcanic lithofacies

The facies described above were defined based upon genetic sedimentological and stratigraphic grounds and conform to, and form part of, the lithostratigraphy defined above (Ch.3). Similar to the distribution of sedimentological lithofacies, volcanic lithofacies distribution is controlled to some degree by the larger tectonostratigraphic elements in the study area and is discussed in this framework here. Two schematic stratigraphic sections from the WCS and PGS are presented in Figure 5.6, showing

the broad interpreted relationships between the mafic and sedimentary units of the SCG. The distribution of the volcanic lithofacies is also summarised in Table 5.1.

Type examples for the PMB and MMB lithofacies are located within the core of the Pumpkin Gully Syncline (Map Sheet Two; Fig.5.6). Only the basal portion of the MMB lithofacies shows definitive evidence for intrusion into wet sediments in the form of brecciated margins (MB-I; MB-II). The remainder outcrops poorly and is interpreted as a sequence of largely massive to weakly vesicular metabasalts.

The best evidence for extrusion within the PGS is the PMB lithofacies which is located near the stratigraphic base of the MMB sequence in the PGS. Within the PGS there are also 4 discrete CMD sills with distinctive alteration haloes and uncommon brecciated margins (MB-I; MB-II). These are laterally continuous for several kilometres and are located stratigraphically at the MNQ/TCV contact below the PMB and MMB lithofacies (Map Sheet Two; Fig.5.6). There appears to be some control exerted upon the distribution of these CMD sills within the PGS by the Telegraph Fault (Map Sheet Two). The stratigraphic distribution of volcanic lithofacies within the PGS is summarized in a representative stratigraphic column for the PGS (Fig.5.6).

As mentioned above (*cf.* Table 5.1), the synsedimentary breccias MB-I and MB-II were observed from the mid-MNQ to the uppermost exposed TCV in both the WCS and PGS (Fig.5.6). The best examples are preserved in outcrop at the MNQ-TCV contact in the PGS spatially associated with the PMB and MMB facies.
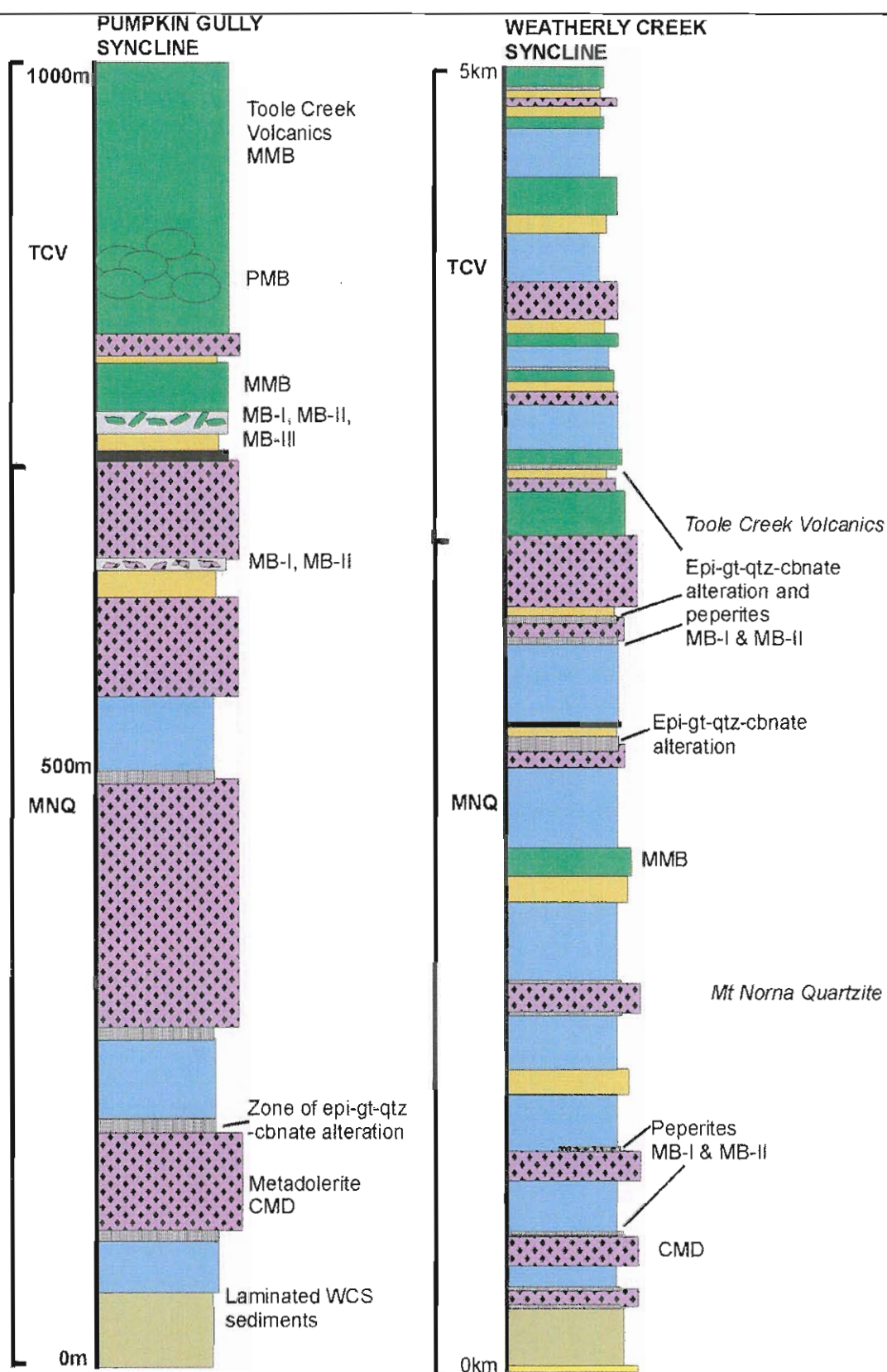
Figure 5.6: Schematic sections representing the distribution of volcanic lithofacies in the Pumpkin Gully Syncline and Weatherly Creek Syncline, volcanic facies outlined at the relative stratigraphic locations of type localities. These sections are schematic and so have no separation distance as shown in Figure 5.1. Abbreviations are the same as those used in the text.

Lithofacies	Textures	Thickness/Extent	Associated Facies	Stratigraphic Distribution	Interpretation
Monomict Breccia Type III (MB-III)	Angular-curviplanar, elongate 0.5-7cm long metabasalt clasts with jigsaw fit in a white-brown carbonate-quartz matrix.	Maximum thickness is 2m, uncertain lateral extent	CMD and MMB upper contacts and as marginal breccias to PMB in core.	Restricted to mid-TCV and core	Subaqueous in-situ hyaloclastite
Pillowed Metabasalt (PMB)	Pillowed fine-medium grained, massive to weakly vesicular metabasalts, vesicles marginal to radial. Pillows occur as whole 0.3-1.5m long and 0.4-1.0m wide pillows with chilled margins and fragments. No evidence of reworking or interpillow sediments.	5-10m thick, up to 20m lateral extent. Only observed in the PGS and some core.	Rarely associated with MB-III and spatially with MMB. No clear contact relationships were observed.	Restricted to the MNQ/TCV contact zone in the PGS and in core	Subaqueous basaltic lava flows
Monomict Breccia Type II (MB-II)	Zones of poorly sorted chaotically dispersed subrounded metabasalt clasts with rare magnetite-garnet altered margins, supported by a silicified metasiltstone matrix with chaotically folded or destroyed bedding.	1-3m wide, 15m mapped lateral extent. ~>3% of SCG mafics. Observed in the WCS and PGS.	Associated with upper CMD & MMB contacts.	From mid-MNQ to upper TCV	Fluidal peperite
Monomict Breccia Type I (MB-I)	Matrix supported breccia comprised of 0.5-20cm long, 0.1-10cm wide angular clasts of metadolerite or metabasalt, occasional jigsaw fit in a silicified metasiltstone matrix	Lateral extent ≤25m, thickness ranges from 1-5m. <5% of SCG mafics. Observed in the WCS and PGS	Clear contact relations between this facies and CMD, less commonly with MMB.	From mid-MNQ to upper TCV	Blocky peperite
Massive Metabasalt (MMB)	Tabular basaltic bodies subparallel to sedimentary bedding comprised of weakly vesicular (1-8mm) massive metabasalt.	5-75m thick, 20-2000m thick. Present from Pon₃ upwards, represent 20-30% of SCG mafics..	Occasional brecciated (MB-I; MB-II) upper and lower contacts and destroyed bedding and silicification.	Most common at the MNQ/TCV contact in the PGS, and less common within the TCV. Not seen in the MNQ.	Subaqueous synsedimentary flows and synsedimentary sills.

However, they do also commonly occur associated with CMD bodies in the mid-MNQ to lower TCV across the study area (Fig.5.6: Map Sheet One & Two). There is a broad change in the dominant peperite style from blocky (MB-I) associated with CMD in the mid-upper MNQ to fluidal peperite (MB-II) in the upper MNQ-TCV. MB-III is restricted to the MNQ-TCV contact in the PGS and also lithostratigraphically unconstrained drillcore from AND-019 to the east of the study area (Fig.5.1 and 5.2).

The Weatherly Creek Syncline hosts the best preserved examples of the CMD lithofacies in the study area. The type examples of CMD occur as at least 30 mappable sills varying from 5-200m thick within WCS (Map Sheet One) with several marking important stratigraphic changes, and as 4 mappable bodies in the PGS (Map Sheet One & Map Sheet Two). Based upon regional scale mapping and interpretation of aeromagnetics and gravity data, these sills are interpreted as comprising at least 30% of the volcanosedimentary sequence within the WCS and only 15-20% of the volcanosedimentary sequence in the PGS. Stratigraphically they occur from the basal LCF to the upper TCV (Map Sheet One). The stratigraphic locations of the major mafic units in the WCS are summarized schematically in Figure 5.6.

When a direct comparison is made between extrusive and intrusive events across the SCG it becomes evident that overall, intrusive events appear to have dominated representing ~30-50% of the entire sequence from the LCF to upper TCV and an estimated $\geq$70% of the mafic sequence. However, the exception to this is the Pumpkin Gully Syncline, where greater than half the sequence is comprised of what is probable extrusive basalts. This suggests, similar to other geological evidence

(Ch.3;Ch.6) that the geological environment of the PGS differed in subtle but important ways to the rest of the SCG basin.

5.6 Discussion

Although there is little continuity of outcrop and available drill core does not intercept large intervals of volcanic lithofacies, the geographically widespread, and in places, stratigraphically well constrained volcanic lithofacies described above allow a confident genetic interpretation of the basaltic units of the upper SCG.

The presence of peperite (lithofacies MB-I & II) and hyaloclastite (MB-III) upper margins to basaltic units, associated disruption of bedding at basal and upper contacts, internal grain size variations and pre-deformational epidote-quartz±carbonate alteration, are all features indicative of sills intruding wet, unconsolidated sediments (McPhie & Houghton 1998; McPhie *et al.* 1993). On the basis of these contact and alteration relationships, the coherent, bedding subparallel basaltic units (CMD & MMB) of the upper SCG are interpreted here as a sequence of sills intruding wet, unconsolidated sediments at or very soon after deposition. Blocky peperite on sill margins indicates explosive reactions at a well defined sediment-mafic contact between a brittle, higher viscosity sill and saturated local sediments (Busby-Spera & White 1987; McPhie 1993; McPhie & Houghton 1998; Dadd & van Wagoner 2002). Fluidal peperite (MB-II) on sill margins shows that lower viscosity sills with entrainment and possible transport of clasts via vapour films subparallel to sill margins was the dominant process (Busby- Spera & White 1987).

Globally, where well exposed sequences of peperite have been studied and peperite facies sequences mapped, variations in peperite style have been variously attributed to variations in host sediment grain size, variations in intrusive viscosity and temperature, and sequential intrusions (Goto & McPhie 1996; *cf.* Dadd & van Wagoner 2002). The variation present in peperites in the SCG (MB-I & MB-II) cannot be related to the host sediments due to the overall constant mean grain size and petrography across the SCG (Ch.3). A rapid decrease in local temperature allowing a decline in the stability of vapour films necessary for the production of fluidal peperites is one method of producing variations in peperite textures. However, the lack of preservation of common in-situ cooling textures such as a jigsaw-fit fracture (not peperite) network and common in-situ hyaloclastites (Squire & McPhie 2002), make confirmation of this mechanism difficult.
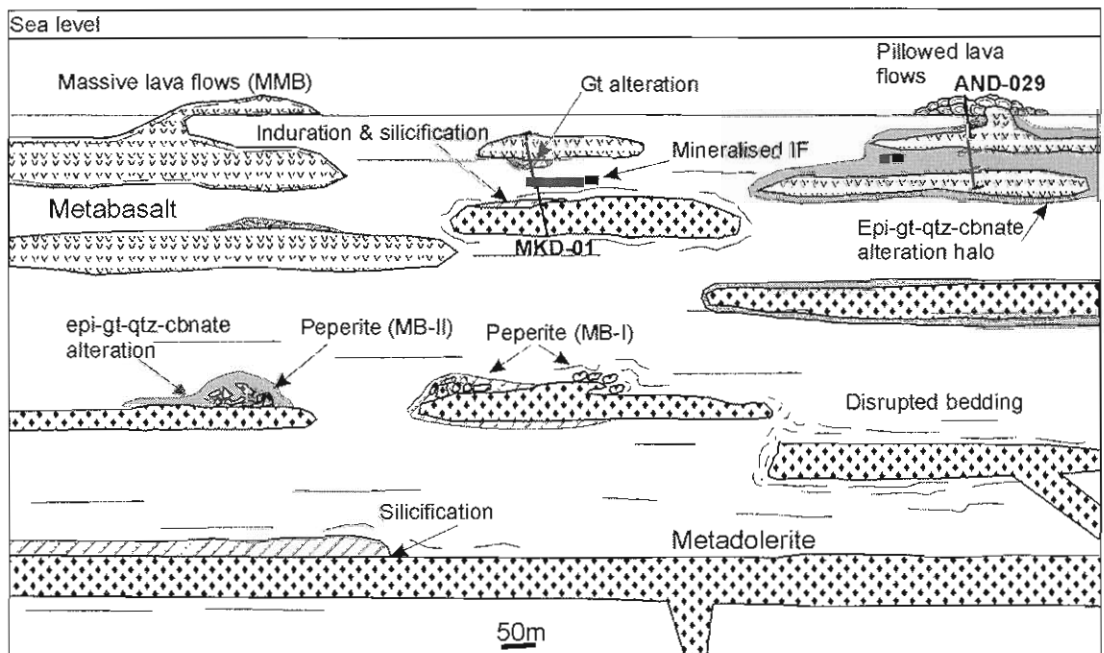
Figure 5.7: Diagrammatic representation of the interpreted lateral and vertical relationships between the various volcanological lithofacies, as well as the interpreted spatial relationship between sills and many SCG iron formations lateral and vertical scales are somewhat arbitrary.

The sequential intrusion of sills of various viscosities in the SCG is the most likely method of producing the variations of peperites observed (Goto & McPhie 1994). An advancing front of a mafic intrusion or protruding lobes of magma if they maintain a

higher temperature, and lower viscosity, will produce the fluidal peperites more common on metabasalt margins than metadolerite margins in the upper half of the sequence (Squire & McPhie 2002). Disruption of early formed blocky peperite by later intrusions is a process which can produce isolated blocky clasts of mafic material within sediment explaining the lack of common jigsaw-fit textures in the blocky peperite in MB-I (Kokelaar 1986; *cf.* Goto & McPhie 1994).

An alteration/silicification halo, in this case epidote-quartz±carbonate, and bedding destructive haloes surrounding SCG mafic bodies is a feature of synsedimentary sills commonly described by workers in volcanosedimentary sequences (*eg.* McPhie 1993; McPhie & Houghton 1998; Rawlings 1998). Most workers in volcanosedimentary terranes have focused on the effects of intrusion on the relict textures of the host sediments and peperite generation and not focused on element mobility at the sediment-mafic contact at the time of intrusion. However, several important major elements (Si, Fe, Mn, Mg, Ca, Na, K) are well known to be mobile at the time of deposition of basaltic bodies in ancient seafloor hydrothermal systems (MacGeehan & MacLean 1980; Mottl 1983). Based upon this knowledge of element mobility, the epidote-quartz±carbonate alteration is likely a product of alteration of primary minerals by a vapour phase related to peperite formation, of extant mineral phases in the sediments (*eg.* biotite-phlogopite, quartz), by fluids expelled from the Fe-Si rich minerals (amphibole, pyroxenes, epidote) within the mafics. Additionally, the epidote-quartz±carbonate alteration may also be a metamorphic upgrading or overprinting of hydrothermal seafloor alteration (*eg.*saussaritisation). One important feature to note is that both mafic sills associated with some of the iron formations studied in Chapter 7 have a similar epidote-dominant alteration halo suggesting similar fluid-rock interaction histories. Significant scope therefore exists for a

detailed isotopic study of these geologically important alteration haloes to determine the nature of the fluids related to both mafic intrusion and iron formation genesis.

Based upon textural features and relationships outlined here, the sills of the Soldiers Cap Group are interpreted as intruding at relatively shallow depths as fluidization, peperites and destruction of bedding, is unlikely to occur at depths greater than 1.6km in a sedimentary column (Kokelaar 1982). The formation of sills as opposed to extrusive flows is largely a function of the movement of magma through the host basin. Most magma bodies will be attempting to move to an environment of least lithostatic pressure *ie.* surface. These bodies will stop in the subsurface and form sills if the density of the magma is greater than the density of the host rocks. The density for basalt is ~2.6 g/cm^3 and unconsolidated seafloor sediments ~1.5-2.0 g/cm^3 (Beresford & Cas 2001) so in a sequence such as the SCG, sills should be and are common. Similarly, any magma propagating into unconsolidated, wet sediments will only rise to the level of neutral buoyancy for that body (Lister & Kerr 1990). When a sill is intruded into unconsolidated sediments, the local specific gravity is increased through compaction, silicification and fluidisation of the sediments requiring the next sill to be intruded higher in the sequence to overcome this local increase in density and gravity (Anderson & Goodfellow 2000). Basin sedimentation also exerts important controls on the style of magmatism, *ie.* if magmatic rates are high then extrusive events will take place in preference to intrusive events. The lack of tight dating control on the sills and metasediments does not allow for any precise determination of timing, however, following the processes suggested by Anderson & Goodfellow (2000; *cf.* Lister & Kerr 1990), stratigraphically deeper sills would be emplaced first, followed by shallower sills and then seafloor extrusives. If the magma bodies which formed underlying sills reached the surface they would have a

significantly higher density than the underlying unconsolidated sediments and may produce invasive flows (Beresford & Cas 2001) with distinctive basal peperites. However, the relatively poor spatial distribution of definitive extrusive facies makes confident interpretation of this process difficult.

Pillowed and vesicular metabasalt (PMB & MMB), with minor associated hyaloclastite (MB-III) are features indicative of subaqueous lava flows. Given their volumetric restriction within the sequence and stratigraphic level above CMD and MMB sills (Fig.5.6; Table 5.1), these units are interpreted as the end product of a feeder system represented by the more voluminous underlying sills. Interpreted spatial and genetic links between sills, flows, peperite or hyaloclastite margins and alteration are displayed in Figure 5.7.

Whilst the sill sequence of the upper SCG can be differentiated on stratigraphic, geochemical and textural grounds and there is good evidence that the basaltic units discussed here represent the expression of a differentiating underlying magma chamber (Chapter 6), no large feeder system or dyke has yet been found in this study or anecdotally.

Similar to the metasedimentary units, significant fault control (20-30 % thickness variations) is exerted by interpreted syn-depositional faults (Chapter 8) such as the Telegraph Fault, on several basaltic sills (Map Sheet One). Additionally, several large faults terminate otherwise continuous sills (Mt Norna Fault, Telegraph Fault, Map Sheet Two). The possibility that these faults represent primary magma conduits cannot be discounted. However, given the polydeformational and complex alteration history of the area, defining any remnants that may lie within these faults is

Chapter Six- Geochemistry of ferrobasalts of the upper Soldiers Cap Group

6.1 Introduction

The mafic units of the Soldiers Cap Group (SCG) are syn-depositional metabasalts and metadolerites (Ch.5), with a distinct Fe-rich chemistry (>12% FeO_t) defining them as ferrobasalts (McBirney 1993; *cf.* Williams 1998). Within the Eastern Succession, and elsewhere in the Australian Proterozoic (*eg.* Broken Hill Block and Georgetown Inlier), similar units are commonly associated with economically important base and precious metals mineralisation, that are in turn spatially associated with iron formations and ironstones. These ferrobasalts and similar units in the region have been previously interpreted as the product of large degrees of partial melting in extensional environments (Glikson & Derrick 1970; Withnall *et al.*1985; James *et al.*1987; Davidson 1998; Williams 1998; *cf.*Ch.7). This makes the understanding of the timing and genesis of these units potentially important to the knowledge of the evolution of their host sequences.

This chapter aimed to (1) document the geochemical character of, and spatial variations within the SCG ferrobasalts; (2) define the nature of Fe-enrichment within the SCG ferrobasalts and delineate, if any, the relationship this may have had with hydrothermal activity in the sequence; (3) determine the nature and scale of magma chamber(s) that sourced the voluminous sill sequence of the upper SCG; and (4) define a geochemical 'fingerprint' to distinguish the ferrobasalts of the upper SCG from other mafic units within the Eastern Succession and the Mt Isa Inlier .

Across the study area there are several examples of post-D_1 mafic sills (*eg.* Ryburn *et al.* 1987 1:100 000 map sheet). This chapter does not deal with these, only with mafic bodies identified by mapping as pre-deformational. Therefore, to complete the aims of this chapter, wholerock geochemical and corresponding petrographic samples for use in this study were taken from ferrobasalts which based upon consistent contact relationships and stratigraphic locations, are interpreted as synsedimentary sills and flows (*ie.* pre-D_1; *cf.*Ch.5).

Multiple regional scale sodic-calcic alteration and high-grade metamorphic events, outlined previously in Chapter 5, are likely to have affected the primary concentrations of major elements such as Na, Ca, Fe, P and K to varying degrees. To avoid any related element mobility and contamination problems, discussed in more detail below, trace elements generally considered immobile, Ti, Zr, Nb, Y (Floyd & Winchester 1978), were used as the main tools in the geochemical analysis and interpretations. These trace elements were also combined with other elements known to behave uniformly during fractionation and differentiation to define original chemical and petrogenetic characteristics of the ferrobasalts.

6.2 Analytical Methods and Previous Studies

6.2.1 Analytical Methods

For this study 79 samples representative of ferrobasalts of the upper Soldiers Cap Group were taken during detailed mapping from the sequence of sills and flows on the western limb of the Weatherly Creek Syncline (WCS; *n*=42; Fig.6.1b), across the exposed extent of the Pumpkin Gully Syncline (PGS; *n*= 31; Map Sheet Two) and a small number from the Toole Creek Syncline (TCS; *n*=6; Fig.6.1a).
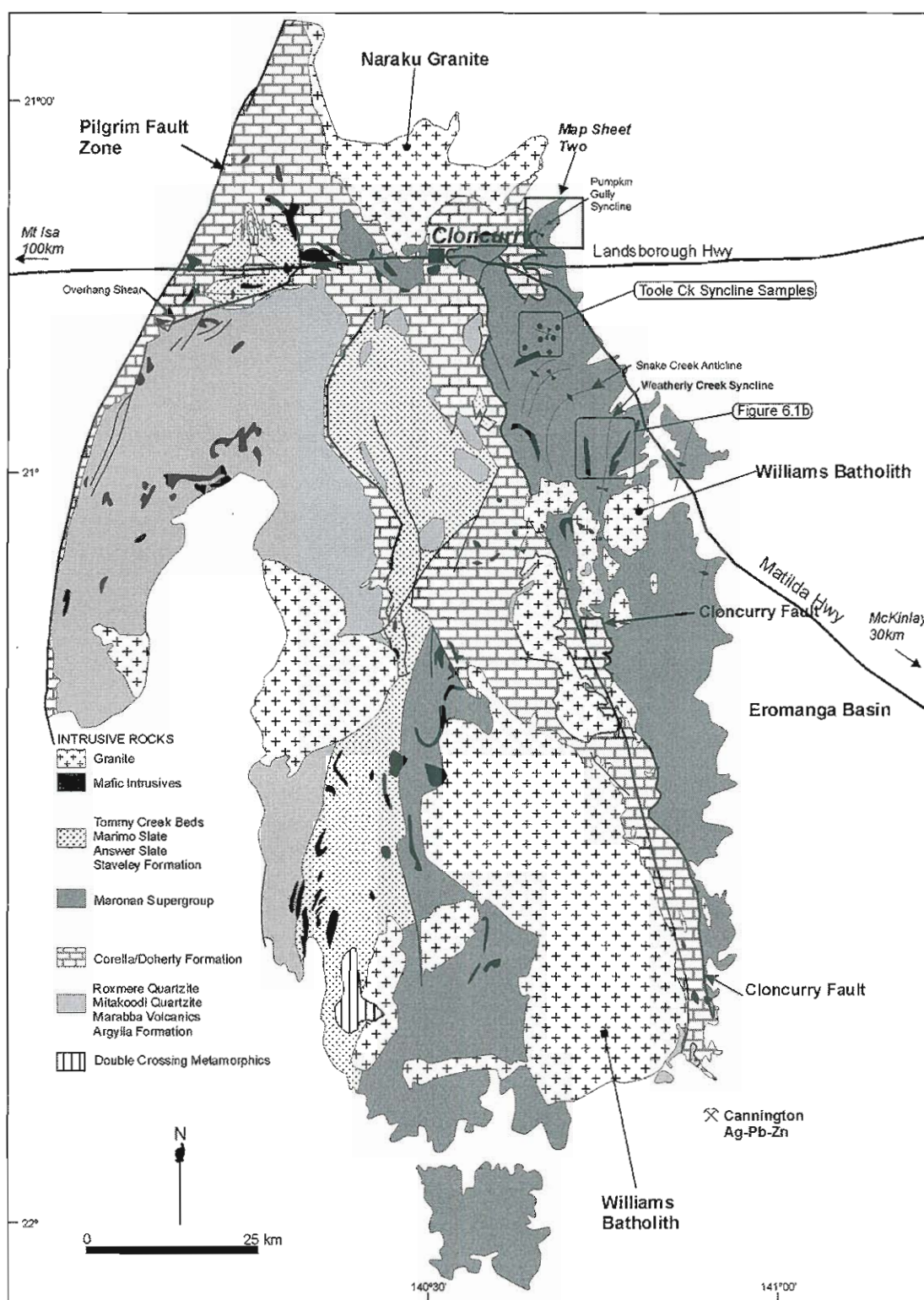
Figure 6.1a: Regional geological diagram depicting the location of the 6 samples taken from the Toole Creek Syncline area relative to the Weatherly Creek Syncline and Pumpkin Gully Syncline.

141
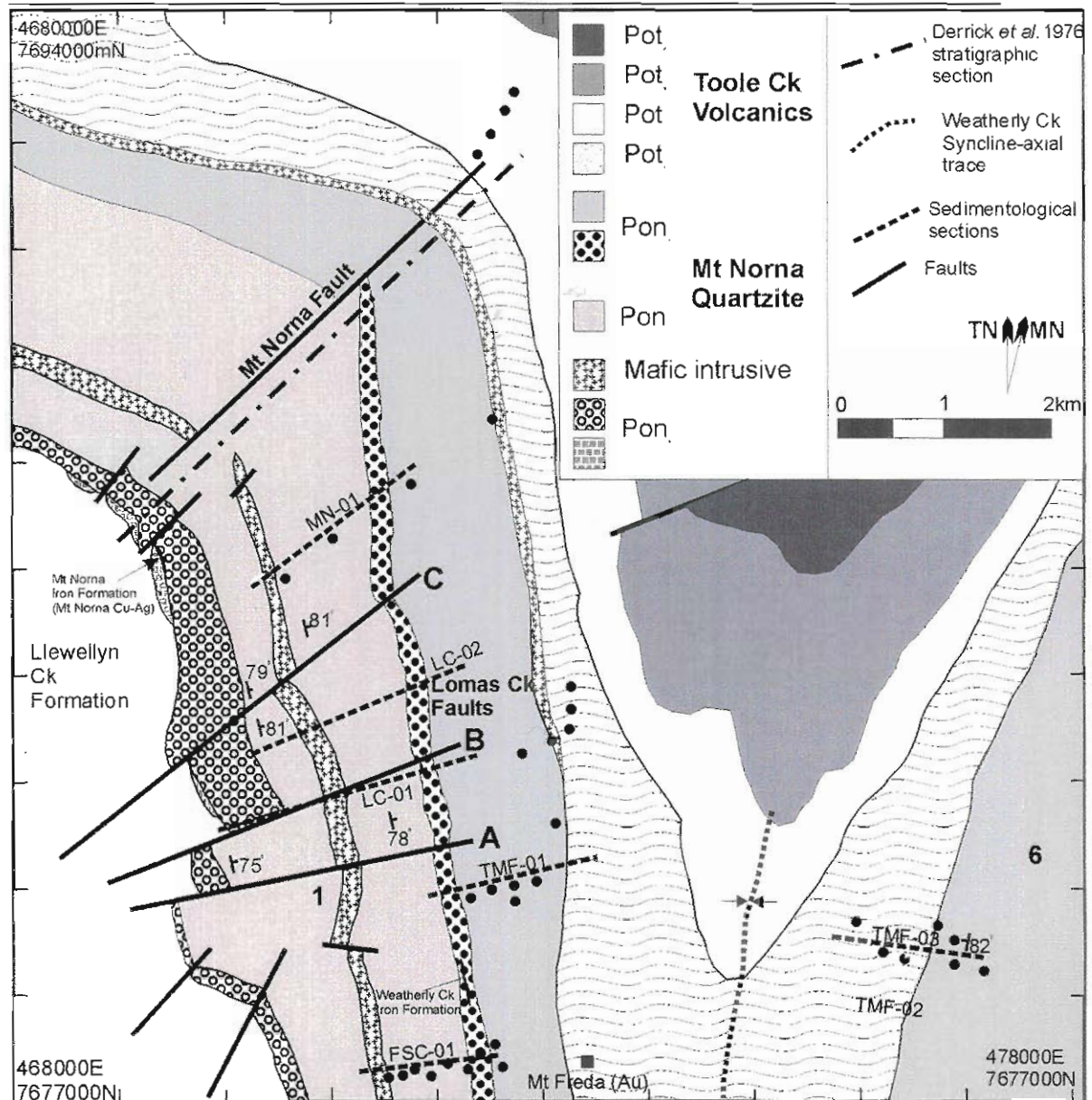
Figure 6.1b: Simplified geological interepretation of the Weatherly Creek Syncline area depicting the locations of samples of mafic units analysed in this study. Note individual points may represent more than one sample. Sample locations and numbers for samples from the PGS and TCS are compiled in Appendix Three.

These samples were analysed for major, trace and rare-earth elements by a combination of XRF and solution ICP MS at both the University of Tasmania and Australian Laboratory Services in Cloncurry.

All samples were crushed with a steel-plate hydraulic crusher until the sample consisted of ~0.5cm^3 chips. These were sorted to remove any remnant weathered

fragments and then milled in a tungsten-carbide mill with a fine-quartz sand wash between samples. A total of 40-50g of sample was milled to obtain a representative assay, larger samples (80-100g) were taken for coarser-grained samples and split where necessary. Major elements were determined on fused discs and trace elements from pressed pills at the University of Tasmania on a Phillips PW 1480 XRF Spectrometer using the methods of Norrish & Hutton (1969). Loss on ignition was determined by heating samples to 1000°C for 16 hours and measuring the mass change by weight. These results were standardised to both internal and international standards (Appendix Three) with standards and blanks run after every 10 samples. Representative analyses are presented below in Table 6.1.

Trace elements and REE compositions of a subset of 4 samples were determined by ICP MS solution analysis using a HP 4500 ICP MS at Australian Laboratory Services, Cloncurry after tungsten-carbide milling, again with quartz washes between samples, and HF/HS_2O_4 digestion. These analyses were standardised to internal reference standards, and digested and analysed with two separate calibration solutions and two randomly selected duplicates. Analyses of duplicates were within 5-10% of values obtained by XRF at the University of Tasmania. Possible incomplete dissolution of refractory phases was monitored by comparison of ICP MS results with values obtained for Zr, Y and Nb by XRF. These values agreed throughout the sample set to within ±5%, suggesting that refractory phases were either absent or more likely completely dissolved during digestion.

Analyses for trace and rare earth element diagrams were normalised to MORB values given by Pearce (1983), with La from Bevins *et al.* (1984) and chondrite values from Boynton (1984).

	PG-120	PG-121	PG-93	PG-106	PG-126	PG127	WC39	WC76	WC11	WC56
SiO_2	48.26	47.99	47.49	47.28	42.59	53.94	50.45	46.62	50.46	49.47
TiO_2	0.95	0.96	0.89	.0.88	1.23	1.25	1.86	1.55	2.24	1.29
Al_2O_3	14.20	14.31	13.40	14.14	15.81	9.85	12.67	13.54	14.31	13.67
Fe_2O_{3tot}	12.25	12.12	11.40	12.46	14.73	11.91	16.43	16.08	17.15	14.25
Fe_2O_3	1.23	1.21	1.14	1.25	1.47	1.19	1.64	1.61	1.72	1.43
FeO_t	11.02	10.91	10.26	11.21	13.26	10.72	14.79	14.47	15.44	12.83
MnO	0.21	0.22	0.18	0.17	0.21	0.22	0.28	0.23	0.3	0.2
MgO	7.94	8.13	9.11	8.13	3.00	3.66	6.05	7.1	3.52	6.48
CaO	12.47	12.2	12.15	10.52	17.95	14.06	8.96	10.05	8.49	8.66
Na_2O	1.58	1.95	2.09	2.23	1.13	1.05	2.03	2.1	2.18	3.54
K_2O	0.09	0.12	0.83	1.54	0.11	0.11	0.31	0.31	0.27	0.18
P2O5	0.06	0.06	0.06	0.05	0.09	0.1	0.17	0.14	0.2	0.12
Total	100.17	99.95	99.65	100.02	99.65	99.62	100.03	99.7	100.1	99.79
LOI	2.16	1.90	2.05	2.63	2.8	3.48	0.82	1.98	0.98	1.93
Sc	43.00	39.80	42.00	43.10	45.20	42.20	44.80	44.70	48.70	47.40
V	310.90	309.10	295.10	317.80	476.80	361.80	463.30	557.90	521.30	355.40
Cr	227.90	225.80	369.70	229.20	74.40	76.40	96.10	97.00	32.90	86.40
Ni	115.60	110.10	149.40	109.30	18.30	21.10	54.00	58.70	34.80	63.40
Rb	<1	1.50	41.40	77.20	1.10	1.30	9.40	284.40	2.30	3.20
Sr	140.53	113.39	126.81	154.45	123.48	92.22	88.00	27.80	98.20	175.70
Y	17.20	16.80	15.70	14.60	28.10	21.30	31.50	35.50	33.90	23.70
Zr	52.77	53.26	46.83	39.50	75.14	82.47	107.10	137.90	129.60	86.00
Nb	3.14	2.94	2.84	2.55	4.31	4.12	6.30	7.40	8.40	5.60
La	n.d.	n.d.	14.8	16.8	4.4	3.8	5.7	16.0	11.0	3.3
Ce	n.d.	n.d.	29.80	39.90	13.10	4.70	12.90	24.60	19.70	16.70
Nd	115.60	110.10	21.50	16.00	9.60	3.10	11.10	16.20	12.50	10.00
U	<1.5	<1.5	<1.5	<1.5	<1.5	<1.5	1.60	<1.5	<1.5	<1.5
Th	<1.5	<1.5	<1.5	<1.5	<1.5	<1.5	<1.5	<1.5	<1.5	<1.5

Table 6.1: representative analyses from the upper Soldiers Cap Group, PG sample prefix denotes Pumpkin Gully Syncline and WC all other areas, including the Toole Ck Syncline(WC-76). n.d.= not analysed for in this suite; <1.5 below detection

6.2.2 Previous Geochemical Studies

Despite many years of focused geological study on the Eastern Succession and the existence of substantial government and company geochemical databases, there is little published specifically on the geochemistry of the SCG. Limited whole-rock geochemical data on SCG mafics led Glikson *et al.* (1976; *cf.* Bultitude & Wyborn 1982) to propose that the basalts of the Eastern Fold Belt with geochemical ocean floor tholeiite affinities were produced at a continental margin. Wilson (1987) agreed with this interpretation and noted strong iron enrichment, low potassium values and generally low abundances of incompatible and siderophile elements, particularly in samples he took from the SCG. Adshead (1995) described ultramafics ('amphibole peridotite') at Osborne but defined them as genetically unrelated to other continental tholeiites in the region. Davidson (1998) provided data from samples of interpreted SCG amphibolites from the Mt Freda locale, which showed that the 'unaltered' samples had a distinct fractionation trend defined by changes in TiO_2. Williams (1998; *cf.* Smith 1999) provided one of the most detailed geochemical studies of mafic rocks of the Maronan Supergroup available to date by analysing numerous samples from the Maramungee, Fairmile and Cannington deposits. He proposed that the amphibolites from these localities were Fe-metatholeiites with intracontinental tholeiite signatures which were produced by fO_2 controlled differentiation of Ti-V bearing magnetite and apatite from primitive magmatic compositions in high-level magma chambers in an extensional setting.

6.3 Geochemical characteristics of the upper Soldiers Cap Group ferrobasalts

A range of representative samples are provided above in Table 6.1 to outline the basic chemistry of the sample set. The petrography and field relationships of these units are outlined in Chapter 5. The mafic units of the Soldiers Cap Group are

metabasalts and metadolerites with a distinct Fe-rich chemistry (12-18wt% FeO_t)

relative to other mafic units in the greater Mt Isa Inlier, low to moderate TiO_2 (0.5-

2.24 wt%), high SiO_2 46.6-53.9 wt%, low to moderate Ni (20-150 ppm) and Cr (75-

370ppm) defining them as ferrobasalts with continental tholeiite characteristics

(*ferrobasalt* $\geq$12wt% FeO_t; McBirney 1993). Henceforth, based upon this relatively

distinct lithogeochemistry the mafic units of the SCG sampled for this study will be

referred to as ferrobasalts.
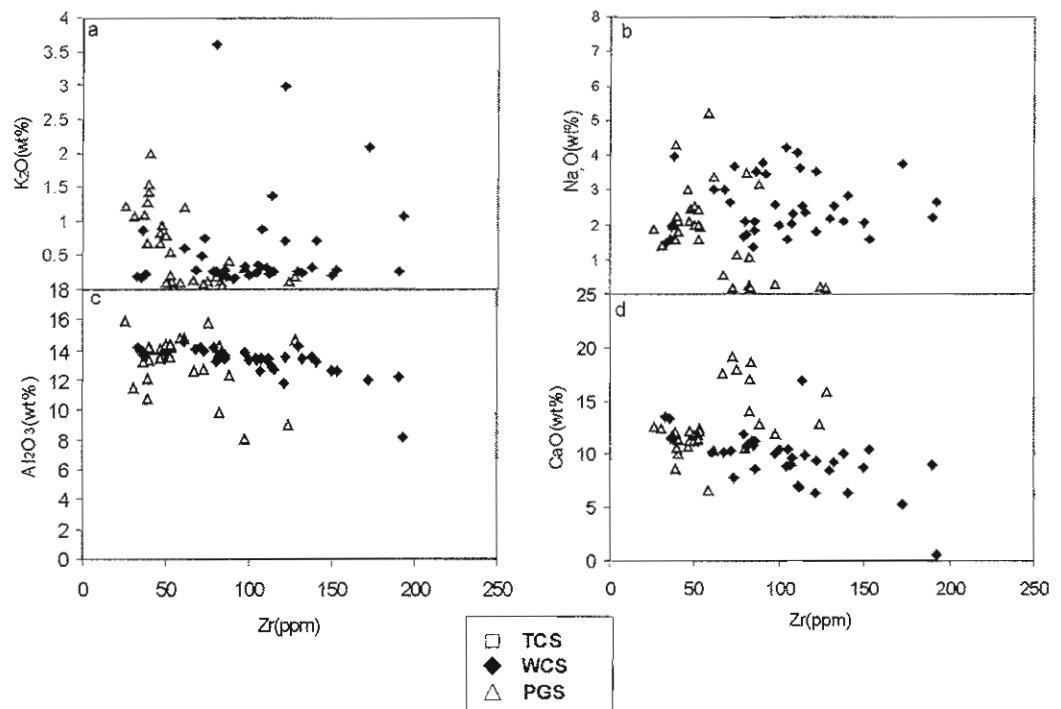
Figure 6.2(a-d): Bivariate plots of Zr versus those elements believed to be mobile during alteration and metamorphism of the Soldiers Cap Group ferrobasalts. Filled diamonds represent samples from the WCS; open triangles those from the PGS; open squares TCS.

Element mobility is a major issue in the geochemical interpretation of polydeformed,

high metamorphic grade sequences. Therefore, those elements commonly considered

immobile during metamorphism and alteration were first tested for immobility and

those found to behave as such, subsequently used to define the primary geochemical

characteristics of the SCG ferrobasalts.
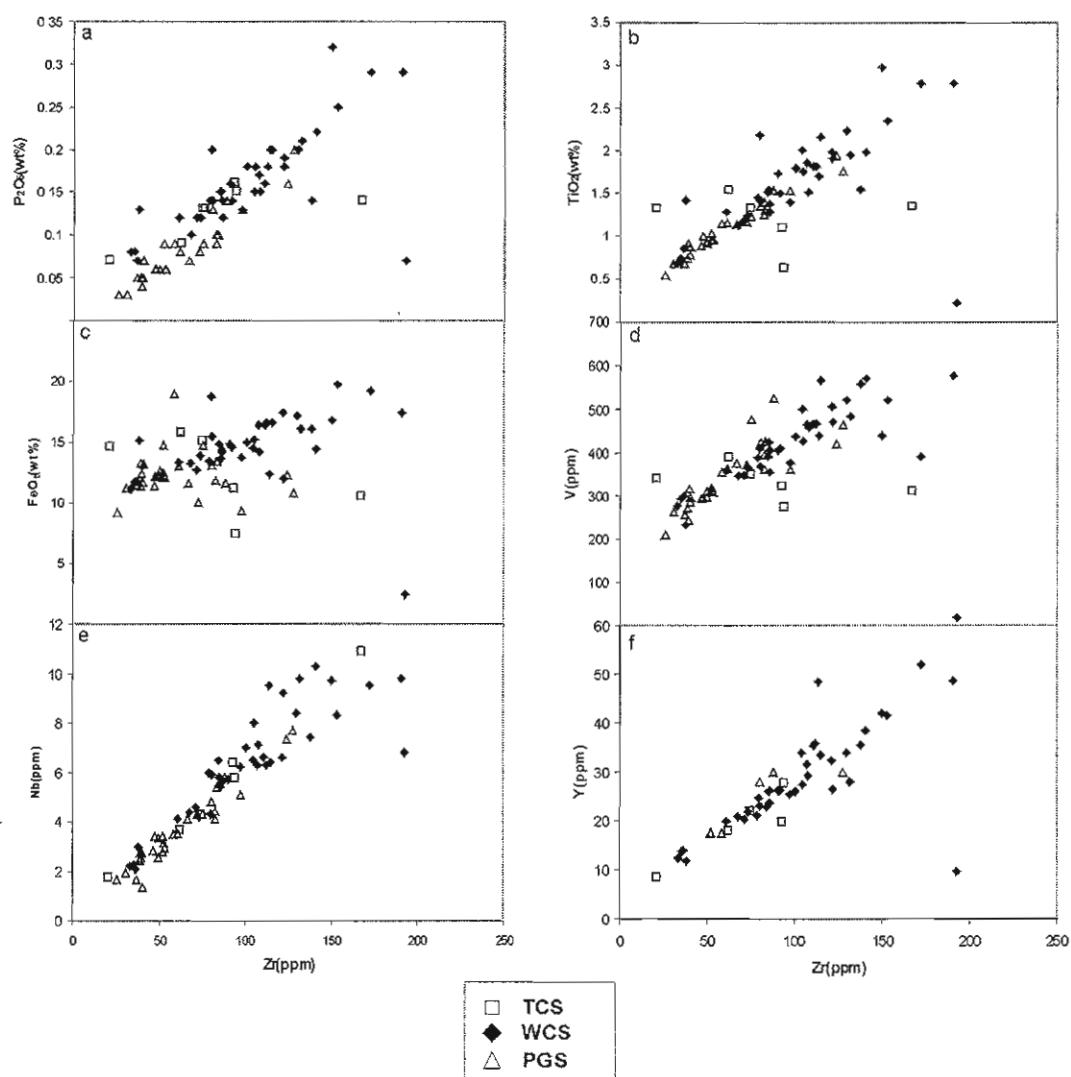
Figure 6.3: Trace and major elements plotted against Zr showing those elements believed to behave uniformly during fractionation. Legend as for Figure 6.2. Note Y was not analysed for all PGS samples.

Using the plots suggested by Barrett & MacLean (1994; *cf.* Finlow-Bates & Stumpfl 1981) to test element mobility shows that that many of the major elements involved in regional metasomatism, such as Na, Ca and Al were mobile to varying degrees (Fig.6.2a-d; Fig.6.3d) and those elements commonly considered immobile (Zr, Nb, Y, Ti, V) behaved as such (Fig.6.3). Scatter of samples from the TCS and PGS in Figure 6.3c represents minor Fe mobility which is likely related to later magnetite and/or hematite rich alteration events (Ch.5 and Ch.7).

The tholeiitic nature of the ferrobasalts mentioned above is also defined by bivariate plots using Zr as an immobile indicator element showing that these units have relatively low ratios of Zr/Y ~3-3.2 and Zr/Nb ~14-15 (Fig.6.3; Saunders *et al.* 1992; Sivell 1988). The tholeiite geochemical character of the Soldiers Cap Group mafics is further reinforced by a strong Fe-enrichment trend (*cf.* Williams 1998), with samples throughout the Soldiers Cap Group suite consistently showing extreme values of up to 18wt% FeO_t with increasing FeO_t / $[FeO_t+MgO]$ and Zr (Fig. 6.3c; Fig.6.4).
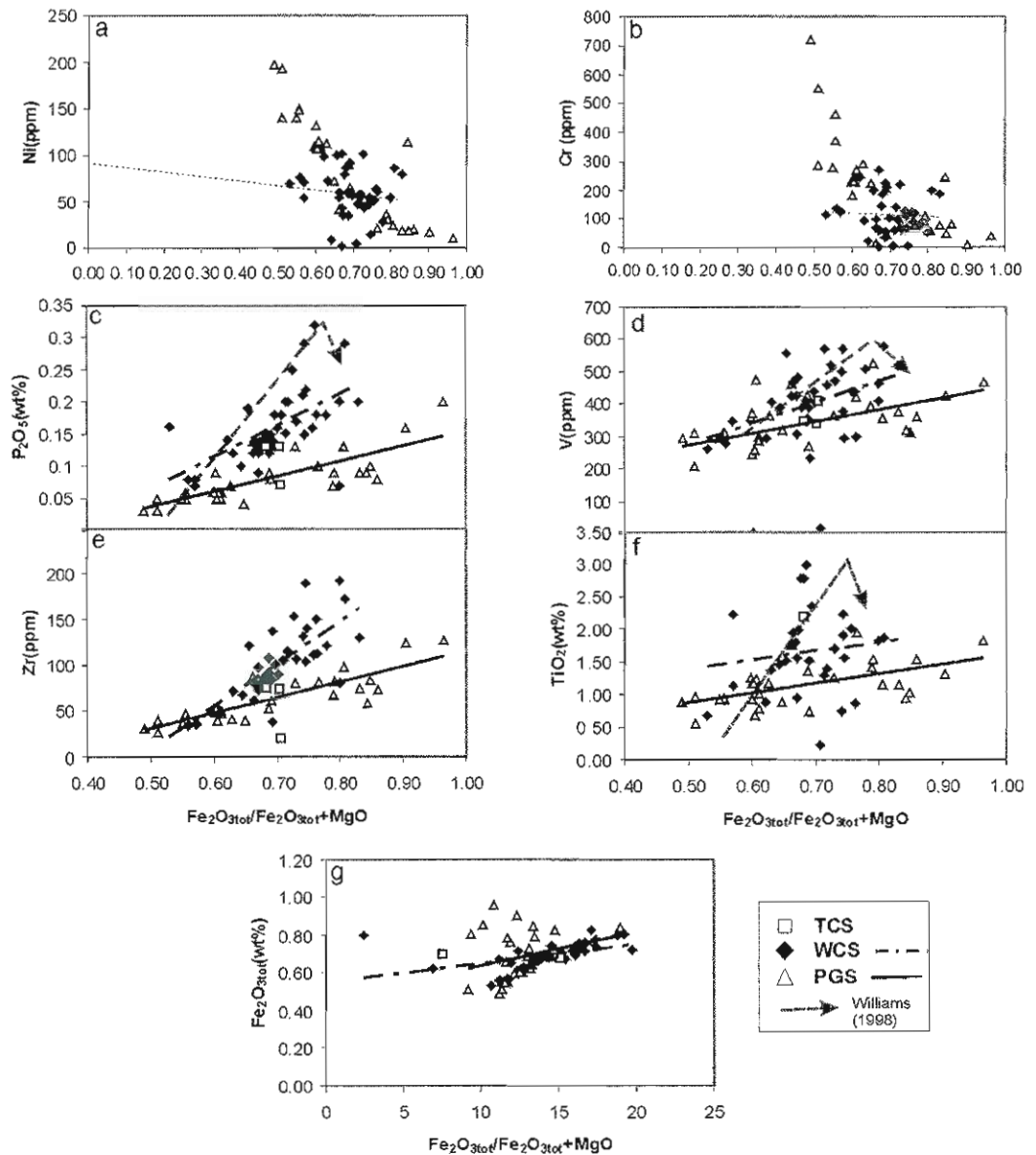
Figure 6.4 (previous page):Variation of selected major and trace elements with Fe₂O₃ₜₒₜ/Fe₂O₃ₜₒₜ+MgO calculated from weight percentages depicting interpreted fractionation/differentiation trends. Dashed magenta arrows represent trends defined by Williams (1998); other trend lines (see legend) represent linear retrogression trend lines, calculated by Excel, for the WCS, PGS & TCS sequences.

If as suggested earlier (Ch.5), the Soldiers Cap Group metatholeiites represent a sequence of upwardly prograding sills and lesser flows, then stratigraphically controlled geochemical variations could reasonably be expected to be evident in the sample population on the scale of the study area and also within individual stratigraphic units. There are significant internal geochemical variations evident within the samples taken from both the WCS and PGS. When those elements known to behave consistently during fractionation (Ti, V, P and Fe) are plotted against an immobile indicator element, in this case Zr, the SCG samples define linear trends, suggesting a broadly co-genetic history and similar parent magmas (Fig.6.3).

The interpreted lack of mobility of these elements during metamorphism and alteration, discussed above, precludes the interpretation of these trends as pseudo-fractionation (*cf.* Barrett & MacLean 1994). Plots of these fractionation indicator elements vs. $FeO_t/[FeO_t+MgO]$ also define two distinct trends (Fig.6.4a-e). These plots show samples from the WCS population to have strongly increasing Ti, V, P and Fe with increasing $FeO_t / [FeO_t+MgO]$, along pathways broadly similar to those presented by Williams (1998; *cf.* James *et al.* 1987) for Maronan Supergroup metatholeiites.

The trends of Williams (1998) are represented by dashed magenta arrows on Figure 6.4 a,b,d. Samples from the PGS do not follow the trend of these other regional and local metatholeiites. Instead they lie along a less P, Ti and V enriched trend with tight groupings except for FeO_t (Fig.6.4e) which, as mentioned above was likely affected by Fe mobility during alteration. Some few samples which are less altered

(Fig, 6.3c) show that overall the PGS is less Fe-enriched than the WCS sequence. The few samples taken from the Toole Creek Volcanics are distributed relatively evenly across the two other sample suites on these plots with the exception of Zr versus Fe_2O_{3tot} where there is an outlying population (Fig.6.4c). This is probably the product of Fe mobility during alteration of the Pumpkin Gully Syncline.

This consistent increase of Fe_2O_{3tot}, P_2O_5, TiO_2 and V with increasing fractionation, indicated by increasing Zr and FeO_t / $[FeO_t + MgO]$ abundances (Fig.6.3a-d and 6.4), indicates that fractional crystallisation of Ti-magnetite and apatite were suppressed until late in the sequence, a characteristic feature of tholeiitic magmas in intracontinental rift sequences and also noted in those elsewhere in the Northern Australian Proterozoic (James *et al.* 1987; Williams 1998). The geochemical variations in the Soldiers Cap Group evidenced by the strongly fractionated WCS and less fractionated PGS suggests that these processes were not homogeneous across the Soldiers Cap Group and that this may also represent a larger scale geochemical provinciality in the Maronan Supergroup.

Determination of an in-situ versus larger scale differentiation is difficult given the relatively large sampling intervals. However, with the exception of minor internal grain size variations (Ch.5), the metatholeiites are petrographically uniform with no observed evidence for layering, suggesting that in-situ differentiation (*eg.* Skaergaard) did not occur (*cf.* Williams 1998).

Chondrite normalised rare earth element patterns from a limited subset of four samples from the WCS, are near flat with overall enrichment compared to chondrite and have a slight enrichment in LREE ($La_N/Lu_N \sim 1.7$ Fig.6.5a). Additionally, there is a weak negative Ce anomaly in the sample suite (Fig.26a) which has been noted in

other basaltic units in the region (Stavely Formation-Davidson 1991). Negative Ce

anomalism in volcanosedimentary systems is generally considered indicative of the

interaction between seawater and geological units through processes such as the low

temperature circulation of seawater through basaltic units on the seafloor (Elderfield

& Greaves 1981; Elderfield & Greaves 1982; Maynard 1983; Rollinson 1993;

*cf.*Ch.7).
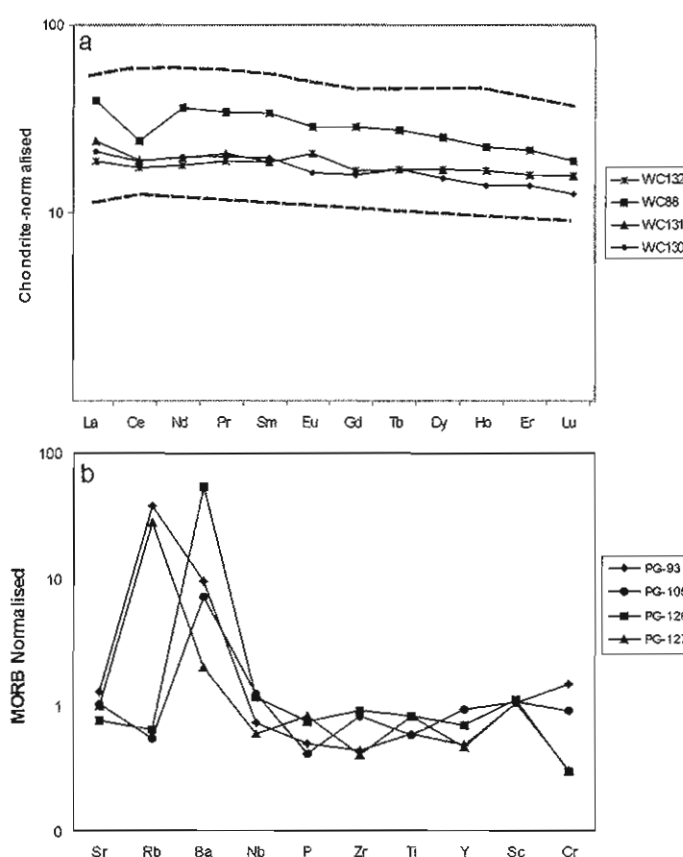
Figure 6.5: (a) chondrite normalized REE pattern for selected Soldiers Cap Group samples, normalizing values from Boynton (1984); dashed line depicts the extent of the samples presented by Williams (1998) and also encompasses the samples of James *et al.* (1987); (b) MORB normalized (Pearce *et al.* 1982) trace element pattern for selected least fractionated Soldiers Cap Group metatholeiites from the PGS.

The flat REE patterns presented here in Figure 6.5a are broadly similar to those

obtained from amphibolites at Cannington (S.Bodon *pers.comm.* 2001), other

Maronan Supergroup samples (Wilson 1987), and from crustally contaminated Fe-

metatholeiites in the similarly aged Broken Hill Block (James *et al.* 1987). REE

patterns differ from those of Williams (1998) in having a lesser degree of LREE

enrichment-HREE depletion and lacking a distinctive positive Eu anomaly.

The distribution of Ba, Rb and K in MORB normalised patterns from ferrobasalts

(Fig.6.5b) is highly likely to be due to the effects of regional sodic-calcic alteration

and is interpreted as not representing a primary geochemical signature. However this

plot was retained as it was useful in depicting the lack of an apparent Nb anomaly.

Slightly elevated values of compatible LILE and LREE (Fig.6.5) suggest that the

ferrobasalts of the Soldiers Cap Group were derived by partial melting from a

moderately enriched MORB source followed by extensive high-level fractionation.

Negative Nb anomalism in continental tholeiites is commonly interpreted as the

result of crustal contamination of magmas which have risen to high crustal levels

(Cox & Hawkesworth 1985). The lack of a distinct negative Nb anomaly in

normalised trace element data precludes any large degree of crustal contamination

being involved in the magmatic history of the SCG ferrobasalts.
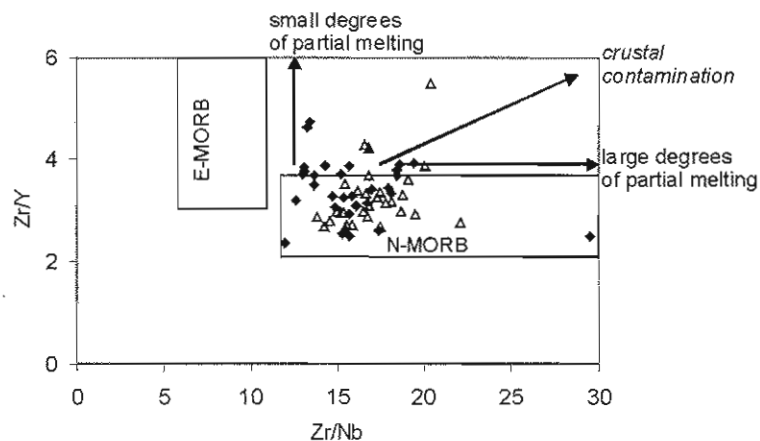
Figure 6.6: Zr, Y and Nb ratios used to qualitatively estimate the degree of partial melting and crustal contamination responsible for the geochemical signature of the Soldiers Cap Group ferrobasalts (after Le Roex 1987; *cf.* Anderson & Goodfellow 1995). Symbol legend as for Figure 6.4.

A qualitative estimation of the degree of crustal contamination and/or partial melting

involved in the genesis of the Soldiers Cap Group metatholeiites is depicted in a plot

of Zr/Y versus Zr/Nb (Fig.6.6-after le Roex 1987; *cf.* Anderson & Goodfellow 2000).

In this diagram, which is applied assuming that modern plate tectonic concepts and

compositions are applicable to the Proterozoic, high Zr/Nb-low Zr/Y ratios represent

high degrees of partial melting and the low Zr/Nb-high Zr/Y ratios low degrees of

partial melting and crustal contamination which is depicted by a spread of data along

the line shown on Figure 6.6. Bivariate plots of all data using Zr as an immobile

indicator element shows that the metabasaltic units have distinctively tholeiitic,

relatively low ratios of Zr/Y ~3-3.2 and Zr/Nb ~14-15 (Fig.6.3; Saunders *et al.*

1992 ; Sivell 1988. When plotted on Figure 6.6 there is a distinct difference in the

Zr,Nb and Y ratios of the WCS and PGS samples. Samples from the WCS define a

trend along the line of inferred crustal contamination and a lesser but definitive trend

along the line of small degrees of partial melting (Fig.6.6). Samples from the PGS

define a coherent trend along the line of crustal contamination (Fig.6.6). Analysis of

samples from the TCS, physically between the two zones of differing melt

characteristics of the PGS and WCS, has geochemical features of both (Fig.6.4 and

6.5). This supports a mechanism of interfingering of mafic bodies derived from the

two sources (WCS and PGS) producing the TCS mafic sequence.

Using this diagram the processes involved in the genesis of the SCG ferrobasalts can

be qualitatively assessed. Overall, the relatively tight spread around low Zr, Y and

Nb ratios of the data suggests a large degree of partial melting of a MORB source (*cf.*

Anderson & Goodfellow 2000; le Roex 1987), major element compositions of the

SCG ferrobasalts infers at least 10% partial melting (*cf.* McKenzie & Bickle 1988).

Spread of the data from the WCS towards high Zr,Y and Nb ratios (Fig.6.6),

particularly towards higher Nb, suggest a component of crustal contamination

combined with partial melting. Data for the PGS ferrobasalts plots on Figure 6.6

largely along the line interpreted as representing crustal contamination and partial melting with little significant scatter.

6.4 Geochemical Discriminators

As outlined in the introduction of this chapter, one aim of the present geochemical study was to define distinctive geochemical "fingerprints" of the SCG mafic rocks overall that could be employed in polydeformed and complexly altered sequences to assist future exploration under cover in the region. Assessment for this "fingerprint" was done by comparing SCG ferrobasalt trace element data to that available from other mafic units in the Mt Isa Inlier (Toole Creek Volcanics, Eastern Creek Volcanics, Magna Lynn Metabasalt, Fiery Creek Volcanics, Marraba Volcanics). This data is compiled on a CD and attached as Appendix Three.

This data was obtained from the AGSO Rockchem database, published (Smith 1999; Williams 1998; Wilson 1982;1987) and unpublished data (S.Bodon *pers. comm.* 2000) whole-rock geochemistry, all presented as part of the geochemical database used in this study as Appendix Three. Parts of the AGSO database were not incorporated, where the wet chemistry methods used were not comparable to the detection limits used for the current samples. Combining the results obtained in the present study with those from these other sources, a total of some 250 results were available for characterisation.

The first part of the process was the determination of the means and standard deviations of trace elements and culling of outliers, defined as analyses 2σ from the calculated mean. Various combinations of selected single elements, element ratios, natural log (*ln*) of single elements and natural log of inter-element ratios were then

154

plotted on binary scatterplots in an attempt to discern any clear separations in the combined dataset.
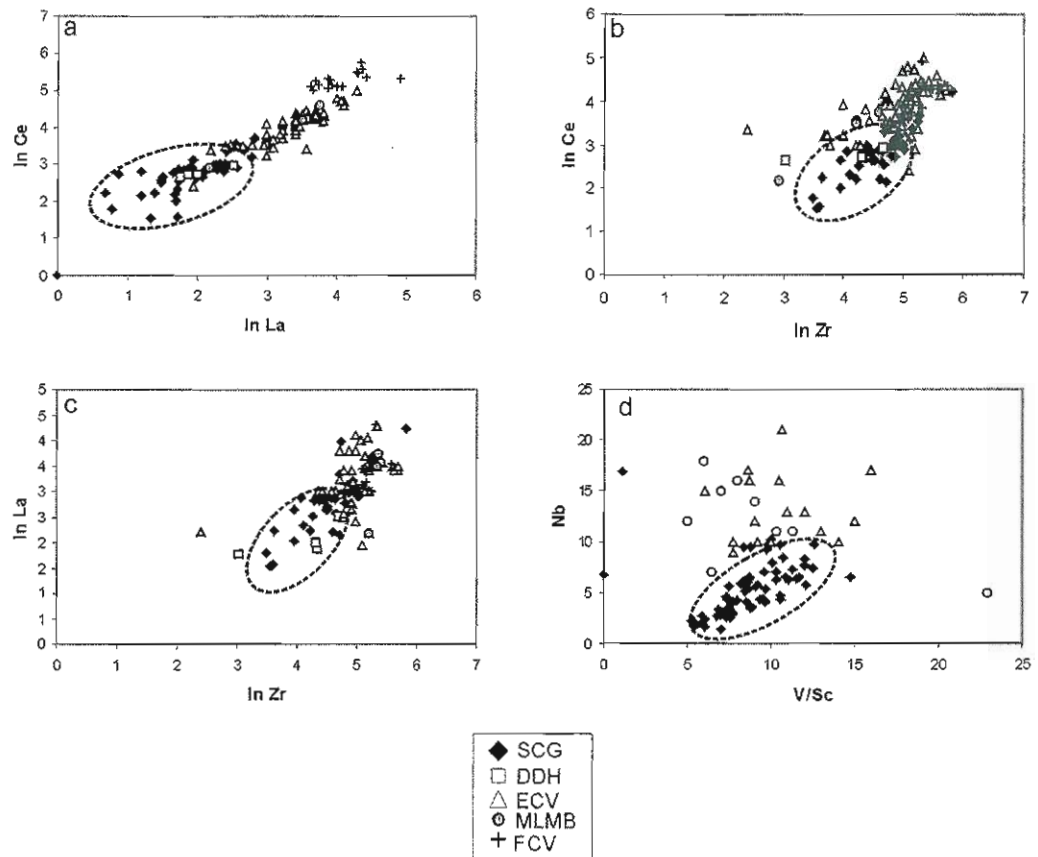
Figure 6.7: Discrimination diagrams used for the geochemical 'fingerprint' constructed for the Soldiers Cap Group metatholeiites, all axes are shown as ppm or *ln* ppm. Arbitrary fields which may be useful for discrimination are shown. SCG= Soldiers Cap Group; DDH= samples taken from AND-019 & AND-029; ECV=Eastern Creek Volcanics; MLMB= Magna Lynn Metabasalt; FCV= Fiery Creek Volcanics.

Overall, there were not many plots that provided clear separation of the data. The best of these used immobile elements Zr and Nb, REE, as well as transition elements La,V, Sc. Ratios and/or natural logs of these elements were also employed and provided the best separation of the data (Fig.6.7) and allowed a preliminary "fingerprint" to be outlined for the SCG. La seems to provide the best discriminator for the SCG with plots involving either La or *ln* La versus the other elements mentioned above providing the best discrimination. Ce should be used carefully due to its possible mobility in some samples (*e.g.* Fig.6.7a). However, the coherence of La-Ce trends in Figure 6.7a provides evidence that this is not a common feature. One

important feature is that samples taken from outcrop within the Weatherly Creek Syncline and those taken from core 20-30km east plot within the same broad discriminatory field, indicating that this discriminatory technique is applicable over large distances. The immobile elements V, Sc and Nb are also useful in discriminating SCG volcanics with generally lower values than other Eastern Succession mafic units (Fig.6.7d).

The advantage of this fingerprinting is that these elements are easily and relatively cheaply analysed by commercially available XRF or ICP-MS methods during routine exploration. Combined with the alteration halo discussed in Chapter 5 and the geochemical halo around iron formations discussed in Chapter 7, these empirical discriminators may provide a useful tool for identifying Soldiers Cap Group mafic units under cover in drillcore or in rock chip samples during future exploration.

6.4.1 Maronan Supergoup Geochemical Variations

Plots of immobile trace elements Zr, Nb, Ti and Y provided a good separation of SCG (WCS, PGS and TCS) amphibolites and other amphibolites within the Maronan Supergroup (Cannington, Maramungee, Pegmont, Fairmile; Fig.6.8a-b). Data was obtained from several sources including the present study, Cannington (Bodon 2002), published data-Maramungee, Fairmile and Pegmont (G.J. Davidson *unpub. data;* Williams 1998) and the AGSO Rockchem database. Results were from various mineralised, unmineralised, and syn-pre D_1, D_2 amphibolites. Figure 2.1b (Ch.2) outlines the relative tectonostratigraphic locations of the samples taken by the abovementioned authors and used in this study. Figure 6.8a-b shows an example of the best plots, on which several distinct patterns emerge from the regional data.
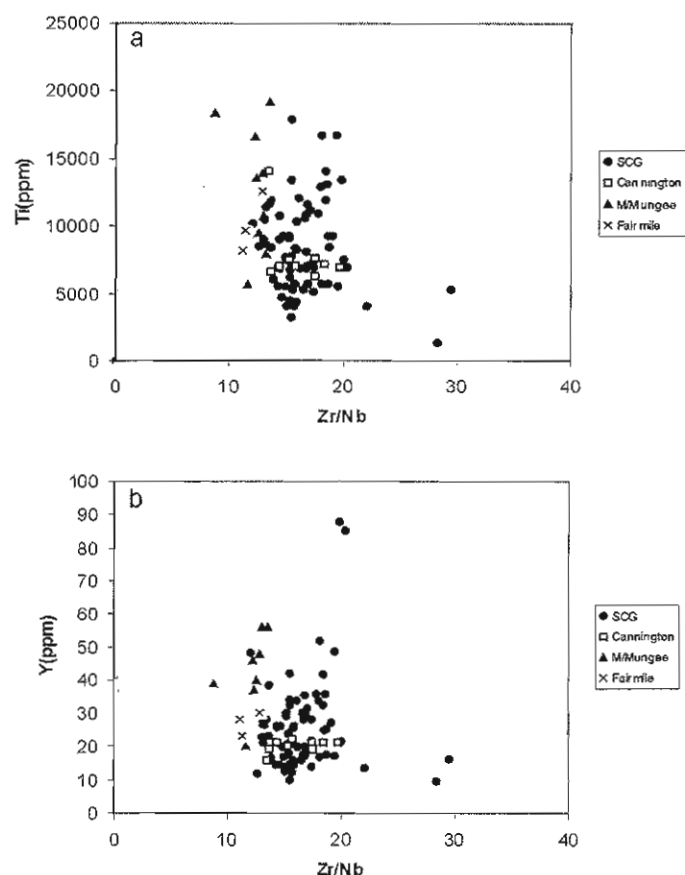
Figure 6.8: Plots of immobile elements used as regional discriminators for Maronan Super group mafic units. SCG=Soldiers Cap Group (this study); Cannington from Bodon (2003); M/Mungee= Maramungee from Williams (1998); Fairmile also from Williams (1999).

There is a relatively clear separation of the stratigraphically higher SCG mafics from those lower within the Maronan Supergroup (Fig.6.8; Maramungee/Pegmont) with the exception of those from Cannington. The samples from Maramungee appear more differentiated than any from the northern SCG sample set suggesting possible longer residence times in the parent magma chambers or discrete separate parental melts, all pointing to a regional scale change in the geochemical evolution of the Maronan Supergroup before or during SCG time. This, combined with evidence provided here for geochemical differences between the WCS, PGS and TCS areas of the SCG suggests that there is also a distinct chemical provinciality within other parts of the Maronan Supergroup.

6.5 Discussion

6.5.1 Ferrobasalt genesis

It is generally thought that ferrobasalts which commonly have high densities (Brooks *et al.*1991), are produced in discrete, high level magma chambers separated from the main magma source in restricted tectonic environments such as continental margins (East Greenland-Brooks *et al.* 1991) or propagating tips of active oceanic rifts (Speiss Ridge- le Roex *et al.* 1982; Galapagos Rift- Fornari *et al.* 1983; Juan de Fuca Ridge- Sinton *et al.* 1983). The degree of fractionation in these ferrobasalts is controlled by localised physical and chemical factors such as magma chamber size, the rate of magma resupply and redox controls on fractionating phases such as magnetite (Brooks *et al.* 1991; le Roex *et al.*1982; Robson & Cann 1982; Sinton *et al.*1983).

The geochemical differences between the WCS and PGS sequences evident in their differing P-Fe evolutionary trends *etc.*, shows they underwent differing fractionation histories or possible differing degrees of crustal contamination and/or partial melting (Figs.6.3, 6.4 and 6.5). Good control on stratigraphy and widely mappable volcanological features (Ch.5) shows that the development of sills and flows was broadly contemporaneous in both areas. Additionally, the convergence of chemical evolutionary trends (Figs.6.3 and 6.4) show that the two groups likely were generated from a comparable parent magma. This precludes the interpretation that the two sequences may be the product of discrete magma pulses and suggests the involvement of more than one higher level magma chamber, following separation of melts from a main parent magma chamber.

Differentiation of a ferrobasalt along an extreme iron enrichment trend, such as that observed for the WCS, requires a relatively large (>5km^3 Hogg *et al.*1988; 1989), closed magma chamber with low magma resupply, a slow cooling rate and low fO_2 to suppress magnetite fractionation until late in the crystallization sequence (Brooks *et al.* 1991; le Roex *et al.* 1982; Robson & Cann 1982; Sinton *et al.* 1983; *cf.* Williams 1998). Mobility during alteration of Fe makes the relative level of Fe-enrichment in the PGS difficult to determine. However, as mentioned above several samples that are less altered plot on a lower Fe-enrichment trend than the WCS. These less Fe-enriched metatholeiites of the PGS could have been produced in a smaller (*ca.*≥ 5km^3; Hogg *et al.*1988; 1989) open system magma chamber compared to that related to the WCS sequence, one which had a faster resupply rate and higher oxidation state. The latter is more likely to develop distal from the main axis of rifting (Sinton *et al.* 1983).

Degree of crustal contamination could also have been an important controlling factor on the geochemical differences between the PGS and WCS. Figure 27 whilst useful in qualitatively assessing the process involved in the genesis of the SCG ferrobasalts, does not quantitatively define WCS versus PGS crustal contamination. Conceivably, based on the fractionation trends outlined in Figures 24 &25 the PGS trends may have been influenced by a higher degree of crustal contamination and the concomitant assimilation of crustal material, hence the less Fe-enriched nature. Significant scope therefore exists for a detailed isotopic and trace element study focused on determining the degree and nature of crustal contamination internally within he SCG. Alternately, Figure 6.3g, assuming this is not an alteration effect, shows that magnetite crystallization was promoted instead of suppressed early in the

history of the PGS and TCS. This provides significant scope for further petrographical studies which could conceivably have implications for global ferrobasalt genesis models.

6.5.2. Regional implications

Eruption of ferrobasalt lavas as seen predominantly in the PGS ferrobasalts, is relatively rare in the global rock record as a result of their high density, and is interpreted as the result of renewed rifting and/or replenishment of an open magma chamber (Brooks *et al.* 1991), both implying an increase in tectonothermal activity. The Soldiers Cap Group has been interpreted by most authors as a product of a relatively quiescent 'sag-phase' of intracontinental rifting (Beardsmore *et al.* 1987; Blake & Stewart 1992) and hence is unlikely to be located at an actively extending classical 'oceanic rift', the common environment for modern ferrobasalts (Fornari *et al.* 1983; le Roex *et al.* 1982; Sinton *et al.* 1983). However, the emplacement of at least two relatively large magma bodies in the base of the northern Clocnurry Basin (*cf.*Ch.2 & Ch.8) implies regional heat flow at SCG time may have been considerably higher than has been previously thought. The prolonged fractionation and crystallisation history of the SCG ferrobasalts suggests that a significant amount of heat would have been transferred to the basin. This concurs with and reinforces the evidence from the basin evolution studies (Ch.8) and interpretations of the genesis of iron formations (Ch.7) both of which suggest that the host basin to the SCG was tectonothermally active and may have involved a noteworthy component of extension relatively late in the basin history. This also has important implications for the possible production of metal rich fluids discussed in more detail in subsequent chapters (*cf.*Ch.7 & 9).

6.6 Summary

Interpretation of altered and brecciated contacts between metabasalt, metadolerite and metasediments as intrusive contacts, combined with pillows and vesicular margins, (Ch.5) allows the SCG ferrobasalts to be defined as a sequence of synsedimentary sills and lesser, stratigraphically higher flows. Geochemical signatures define these units as crustally contaminated continental tholeiites (ferrobasalts) derived from partial melting of a largely N-MORB-like source. Fractionation of Ti-magnetite and apatite along divergent Fe-enrichment trends in discrete magma chambers at the base of the SCG sequence, controlled the distribution of major and trace elements. The evolution of these trends was controlled by magma conditions (resupply, fO_2, cooling rate and crustal contamination) in at least two discrete high level magma chambers that were contemporaneous but spatially separated. The presence of these discrete chambers imparted an as yet spatially unconstrained geochemical provinciality within the Soldiers Cap Group. This is reflected in the larger scale variability of the mafic units so that the western limb of the Weatherly Creek Syncline can be distinguished geochemically from the Pumpkin Gully Syncline.

These magma chambers have a close relationship with renewed rifting within the Soldiers Cap Group represented by increased hydrothermal activity at the base of the Mt Norna Quartzite (Ch.7) and changes in sedimentation style within the sequence (Ch.3). Whilst there is no direct evidence of hydrothermal activity as a result of intrusion these mafic bodies could have acted as a driving force for circulation of hydrothermal fluids within the basin.

The spatial extent of the two major chambers 'sphere of influence' also remains undefined. These two sources individually provided interfingering sills within the Toole Creek Syncline area, represented by the 'intermediate' chemistry between the lower-Fe suite in the north (Pumpkin Gully Syncline) and a higher Fe-suite in the south (Weatherly Creek Syncline).

Chapter Seven- Soldiers Cap Group iron formations as windows into the hydrothermal evolution of a base-metal bearing, Proterozoic, rift basin[1].

7.1 Introduction

The metasediments of the Maronan Supergroup and Soldiers Cap Group (SCG) are host to numerous barren and mineralised iron-oxide rich metasediments, commonly referred to as 'iron formations' and 'ironstones'. The main aim of this study was to determine the geological nature and genesis of the problematic iron formations and determine their relationships to the host SCG. This is important, as iron formations of SCG age are generally rare in the rock record (Solomon and Sun 1997). They are also commonly base or precious metals-mineralised and so may have significant vector potential for mineral exploration. Lastly, if it can be shown that these iron formations formed locally through hydrothermal activity, then they provide a window into the early hydrothermal history of the host basin. The approach taken here was to study typical relationships where they could be best understood, and place the results in the context of wider regional and global studies.

In this study, description and nomenclature follows that of Gross (1965) in defining an iron formation as a banded-laminated ferruginous unit, containing 15 wt% or more iron, and broadly conformable with the surrounding rocks. Ironstones are defined as massive, ferruginous units that can be both concordant and discordant with the surrounding units. SCG iron formations have many features in common geologically and geochemically with 'exhalites' of the Broken Hill Block and Olary Domain, Australia (Bierlein 1995; Lottermoser 1989; Lottermoser *et al.* 1994; Parr

---

[1] This chapter was accepted to the Australian Journal of Earth Sciences and is attached as a reprint in Appendix 6

1992), and the apatite rich iron ore deposits of Kainuu, Finland (Laajoki 1986) or

Avnik, Turkey (Helvaci 1984). They do not resemble 'Hamersley-style' BIF's, so the

commonly invoked models of ancient 'BIF' formation (Holland 1973; 1984; Laberge

1973; Morris 1985; 1993) are not strictly applicable here. The numerous,

stratigraphically widespread, ironstones both barren and copper-gold mineralized,

within the SCG are generally interpreted as the product of late structurally controlled

metasomatism (Davidson 1996) and fall outside the scope of this study. Other

geologically similar 'stratabound' iron formations depicted on the Cloncury 1:100

000 sheet (Ryburn *et al.* 1987; *eg.* Mt Norna South, on the southern limb of the

Pumpkin Gully Syncline, and notably 'garnet sandstones' at Hot Rocks), were

excluded from this detailed study. The reasons for this are firstly, that the WCIF and

MNIF are located within the area of most detailed mapping undertaken in this study,

and secondly budget and time constraints did not allow extensive sampling of these

other iron formations.

The basis of this study was detailed geological and whole-rock geochemical data

collected from the well exposed, laterally extensive and weakly mineralised

Weatherly Creek Iron Formation (WCIF), with more limited data collected from the

Cu-Ag mineralised Mt Norna Iron Formation (MNIF) and local weakly mineralised

to barren, iron formations in the Pumpkin Gully Syncline (Map Sheet One; Fig.7.1;

Fig.7.2 a,b). These stratigraphic iron formation names (WCIF and MNIF) are

informal, but are used here to facilitate discussion and define the individual iron

formation lenses used in this study.

7.2 Sampling and Analytical Techniques

Detailed mapping at 1:10000 scale and focused rock-chip sampling of the WCIF and

MNIF and several iron formation lenses in the Pumpkin Gully Syncline (Fig.7.1;

Fig.7.2a,b) was undertaken during regional scale mapping. Company aeromagnetics tied to detailed logging of exploration drill core also was used to determine the extent of iron formations under cover. These three iron formation lenses were selected due to their relative lack of complex regional alteration overprint, moderate deformation, lateral continuity, well-defined stratigraphic position and well defined local geological environment.

Representative samples from the WCIF (*n*=16) and MNIF (*n*=6) were thin sectioned, slabbed, and their petrography examined in detail, these were then used to define basic textural terms for use in the description of chemical sediments in the study area. The lenses were sampled as uniformly as possible with individual hand samples ranging in size from 1.5-8kg, taken from laterally equivalent segments of the iron formations defined by mapping. Samples from the WCIF were analysed for major and selected trace elements (*n*=16; Table 7.1) and REE (*n*=10; Table 7.3), whilst only REE and selected trace elements were determined from the MNIF (Table 7.2). Major element data used to compare SCG iron formations studied here with regional equivalents was taken from collations of all available relevant whole rock data in an unpublished report written by G.J. Davidson (University of Tasmania) for BHP Minerals in 1994 (data collated in Appendix Three).

Sample preparation and analysis was identical to that outlined in Chapter 5 for the characterization of the basaltic units of the SCG. Major elements were determined on fused discs; Zr, Nb, Sr, Y & Mo were determined from pressed pills at the University of Tasmania. Other trace elements and REE compositions were determined by ICP MS solution analysis after HF/H_2SO_4 digestion. Analyses of randomly selected duplicates were within 5-10% of each other. Similar to the analyses of mafic units ICP MS Zr values were validated by cross-checking with XRF results.

REE values were normalised to the values of chondrite recommended by Boynton (1984). The Eu anomaly (Eu/Eu*) was calculated using the formula of McLennan (1989). Ce anomalies (Ce/Ce*) were calculated using the formula of Toyoda & Masuda (1991), and anomalies that were not <0.9 were considered geologically insignificant (*cf.* Davidson *et al.* 2001).

7.3 Detailed Geology of the Soldiers Cap Group iron formations

7.3.1 Weatherly Creek iron formation (WCIF)

The WCIF (Fig.7.2a), the main focus of this study, is a discrete concordant lens, 2-5m wide, approximately 1900m in lateral extent, that is sub parallel with adjacent lithologies (Fig.7.2a). These include psammopelites of the Rippled Facies, metadolerite sills and minor, discontinuous and thin (≤0.5m) garnetiferous schists. The mapped contacts show that the WCIF is broadly conformable and hosted in, a generally northward thickening psammopelite lens, and is in gradational contact at the southern end with a medium-grained, thinly laminated-cross bedded psammite (Rippled Facies-Ch.3; Fig.7.2a). Although the northern end of the WCIF outcrops poorly, a sharp contact with strongly foliated pelitic schist was observed. The nature of the host pelite and psammites suggest that the WCIF was deposited during more quiescent sedimentation compared to the under- and overlying massive quartzites, which are the products of high-density turbidity currents related to tempestites. High-Fe metatholeiite (*cf.* Williams 1998) conformably underlies the WCIF for much of the length (Fig.7.2a). Several small scrapes containing Mt Freda-style supergene Cu-oxides (malachite-azurite; Arnold 1983; Davidson 1998), ankerite veins and minor sulphides (pyrite-arsenopyrite) occur at the southern end of the WCIF and postdate the pervasive fabrics.
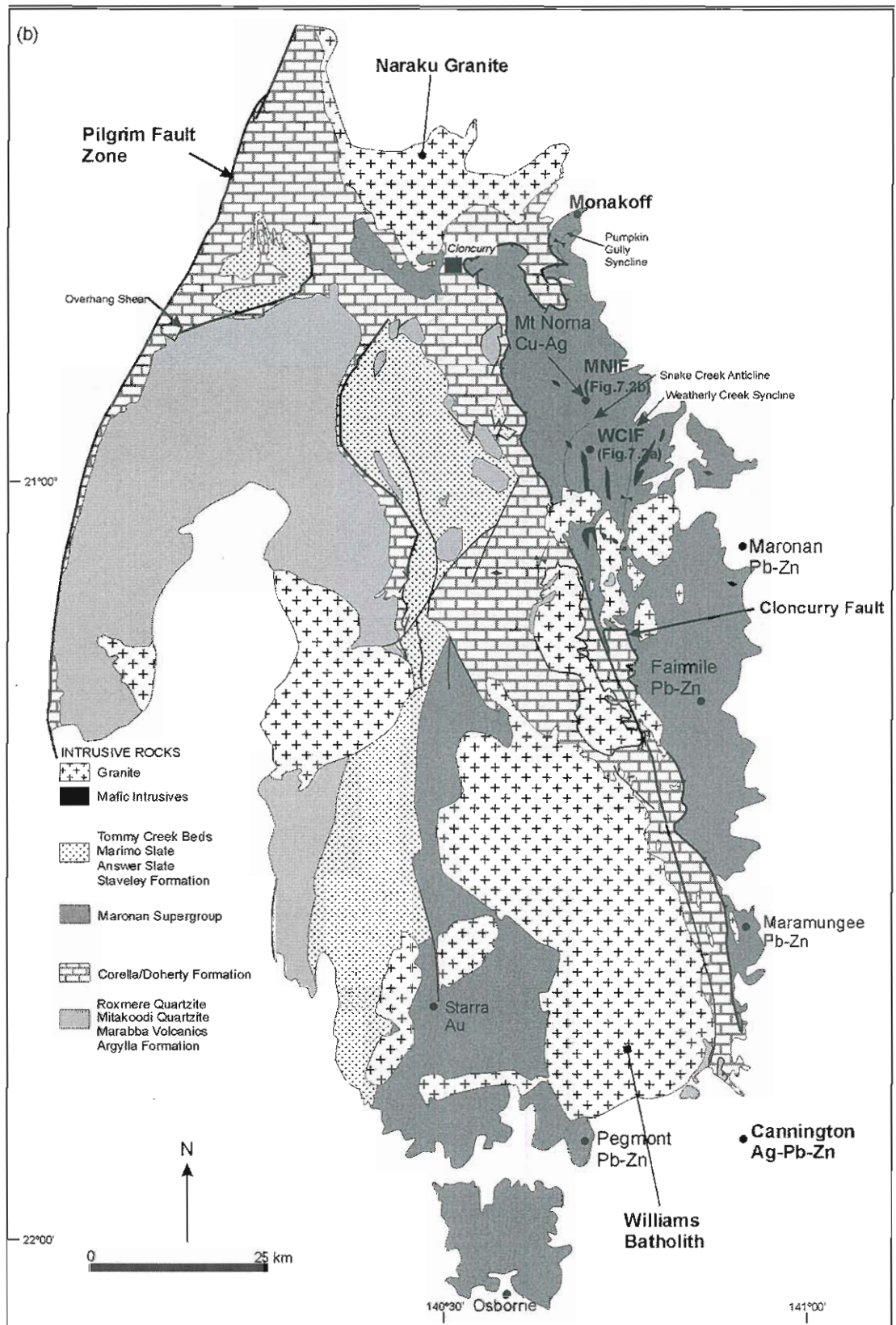
Figure 7.1: Simplified regional geology depicting location of the Soldiers Cap Group iron formations and other important Maronan Supergroup examples. Areas of Figures 7.2 a and b also shown.

Structure within the WCIF is locally quite variable, however, early Fe-Mn-P rich laminae, which are sub parallel to S_0 in the adjacent metasediments, are preserved throughout the deformational history. Fabrics, including S_2, are easily traceable across iron formation metasediment/metabasalt contacts within the study area. At the localities of samples WC-78 & WC-95 (Fig.7.3g) the WCIF has undergone a high degree of structural deformation with rare tight-isoclinal D_1 folds which have folded original laminae and are overprinted by D_2 and later fabrics. However, these structures are anomalous and not the norm for the WCIF. No cataclastic textures indicative of D_1 mylonites as suggested by Laing (1990; 1998) were observed at the hand specimen or thin section scale elsewhere in the WCIF or other iron formations in the SCG.

Commonly associated with the chemical sediments are conformable, epidote-quartz±carbonate(±garnet) alteration zones within adjacent metabasaltic and metasedimentary units (*cf.*Ch.5). Zones of massive, very fine grained epidote-quartz studded with subhedral garnets 1-2mm in diameter, form asymmetrical 2-15m wide haloes, which are commonly developed on the stratigraphically lower side, subparallel to, chemical sediments. In metadolerites adjacent to iron formations this alteration assemblage is characterized by small (>1mm), subhedral epidote-garnet and rare siderite grains overgrown by peak metamorphic (ferro)amphiboles, which define the dominant peak metamorphic structural fabric-S_2 (Ch.5). A similar pre-D_1 alteration assemblage was noted by Williams (1997) associated with iron formations in the Pumpkin Gully Syncline. Similar alteration was also noted by Davidson *et al.* (2002) associated with the polymetallic Monakoff deposit, and was ascribed a pre-deformational timing.

In detail the WCIF consists of banded garnet-dominated *'garnet quartzites'* which comprise fine- to very-fine (>0.5-3mm) garnet (calcic almandine)-quartz-apatite±quartz±stilpnomelane laminae interleaved with monotonous magnetite-hematite-quartz±grunerite laminae (Fig.7.3a,c-e). These garnet quartzites are defined by their high modal percentages of garnet (60%) and apatite (10-15%).

Relationships between the alternating laminae in garnet quartzites are complex at microscale. Internally, the garnetiferous layers have sharp contacts with magnetite-hematite-quartz±grunerite layers (Fig.7.3a,c-e). Primary sedimentary laminations may be preserved as 'dirty' inclusion trails of quartz-magnetite (Fig.7.3c-e). These laminae are commonly overgrown by later, coarse apatite (Fig.7.3d). Overgrowing this is a garnet-grunerite-stilpnomelane metamorphic assemblage indicative of amphibolite-upper greenschist metamorphism of iron formations (Fig.7.4j; Klein 1973; Maynard 1983, Deer *et al.*1992). Later (D$_2$-D$_3$) magnetite-hematite regional alteration occurs preferentially within S$_2$ foliations as coarse and occasionally acicular magnetite which overprints earlier magnetite-apatite (Fig.7.3f). Dennisonite (6CaOAl$_2$O$_3$.2P$_2$O$_5$.5H$_2$O), is present as rare (<1%), very small (<0.5mm), acicular randomly oriented crystals throughout the garnetiferous laminae, commonly overgrown by subhedral garnets. Alignment of quartz-rich laminae defines a mineral lineation within S$_2$ which fans into the adjacent garnetiferous and iron-oxide rich laminae and can also be traced into adjacent host rocks (Fig.7.3f).
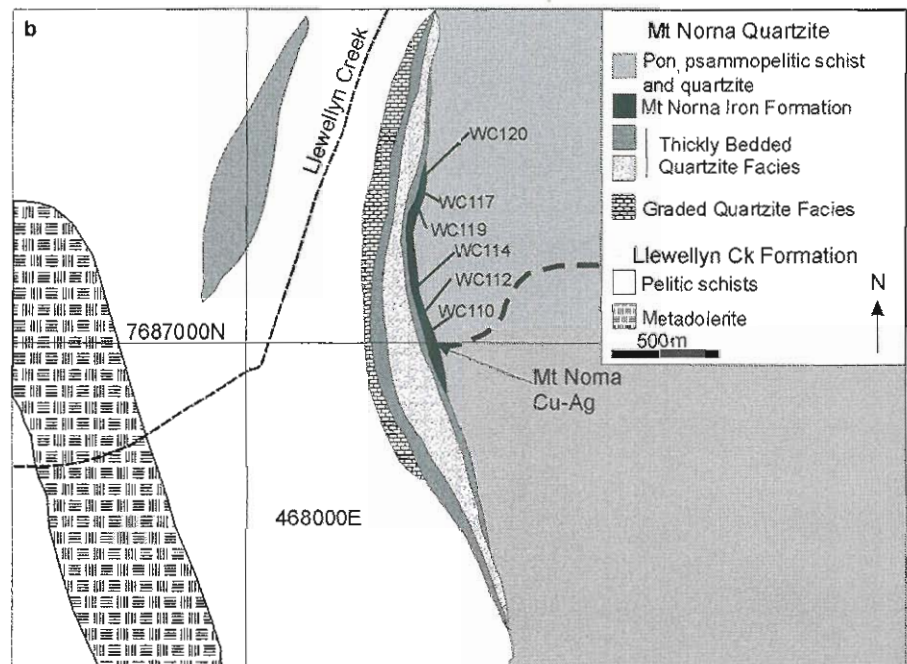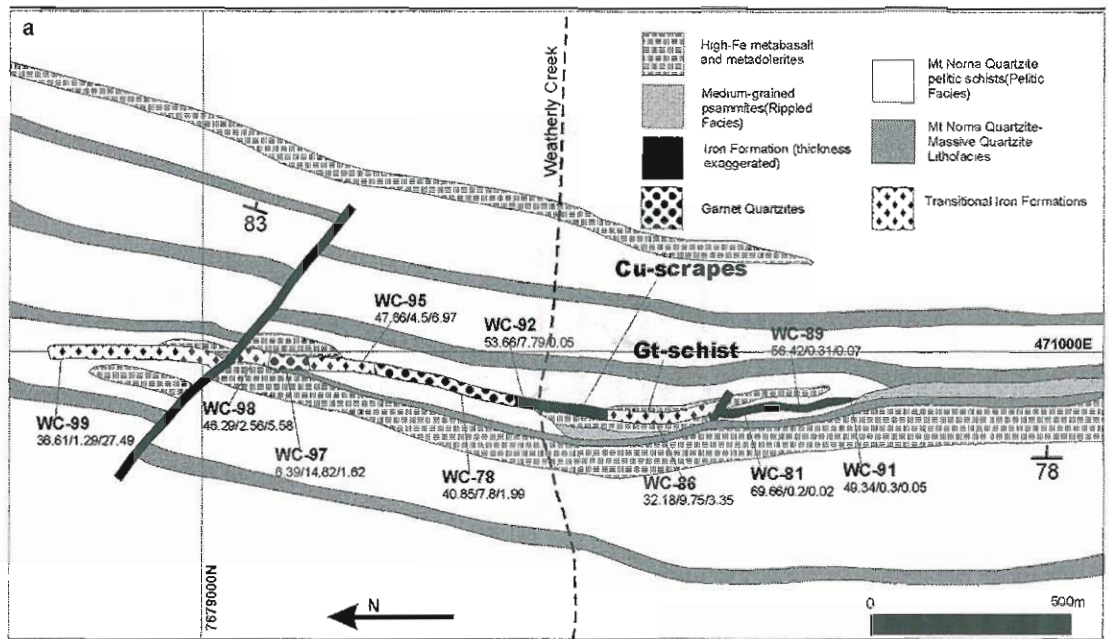
Figure 7.2 (previous page) : (a) Simplified 1:10 000 scale geological fact map of the Weatherly Creek iron-formation and surrounding units. Locations of samples used in the present study (e.g. WC-99) are displayed below which are $Fe_2O_3/P_2O_5/MnO$ values in wt%; (b) Simplified 1:10 000 scale geological fact map of the Mt Norna iron-formation and adjacent units; samples analysed in the present study are depicted. The datum used for grid references is AGD 94.

Small selvedges of garnetiferous pelitic schist less than 0.5m thick, which extend for a lateral distance of 5-7m are commonly associated with garnet quarztites. These comprise muscovite-plagioclase-quartz schists with S_2 foliations wrapping around the garnets indicating a pre-D_2 timing.

Garnet quartzites have diffuse contacts with *transitional iron formations*, (Fig.7.3b and m), which have greater amounts of magnetite-hematite-quartz-grunerite laminae and lower garnet-apatite contents (20-30% gt; ~5% ap). These transitional iron formations have diffuse contacts with iron oxide-silicate *banded-laminated iron formations (IF)* (Fig.7.3i), which have interlaminated monotonous hematite-magnetite±quartz±garnet and magnetite-hematite-grunerite layers with apatite largely absent and garnet a minor component (~10%).

Klein (1973) noted that original iron oxide and silicate laminae are present in similar iron formations up to and including amphibolite facies metamorphism, with the only effect being an increase in the original grain size of the constituent quartz and magnetite grains present in laminae. The absence of martitisation in the SCG suggests that during regional metamorphism little to no mobilisation of oxygen occurred in iron formations (Klein 1973; Morris 1985; Powell *et al.* 1999). No stromatolitic (*cf.* Ryburn *et al.* 1988) or other structures indicative of biogenic activity were observed in the iron formations or adjacent units during this study.
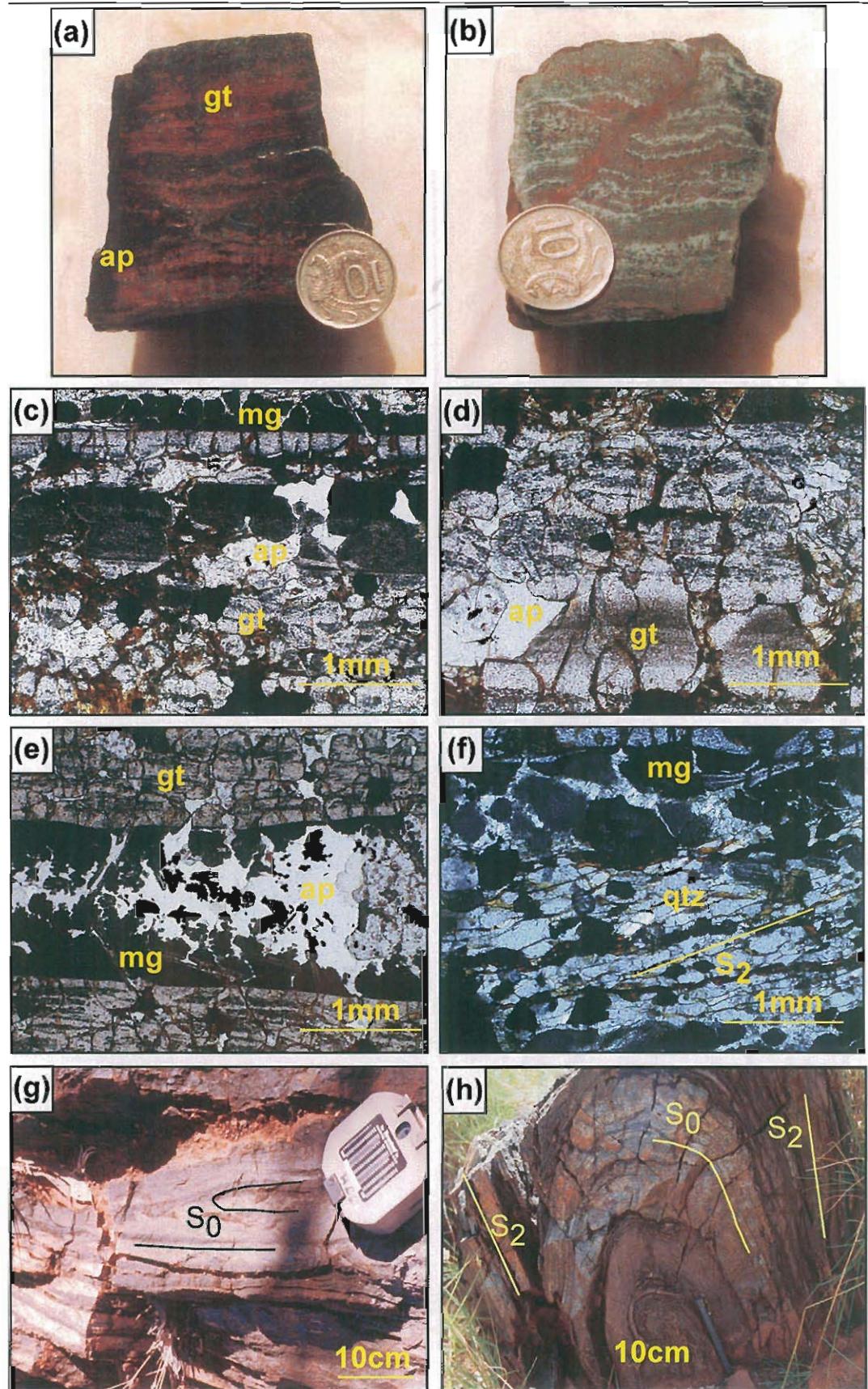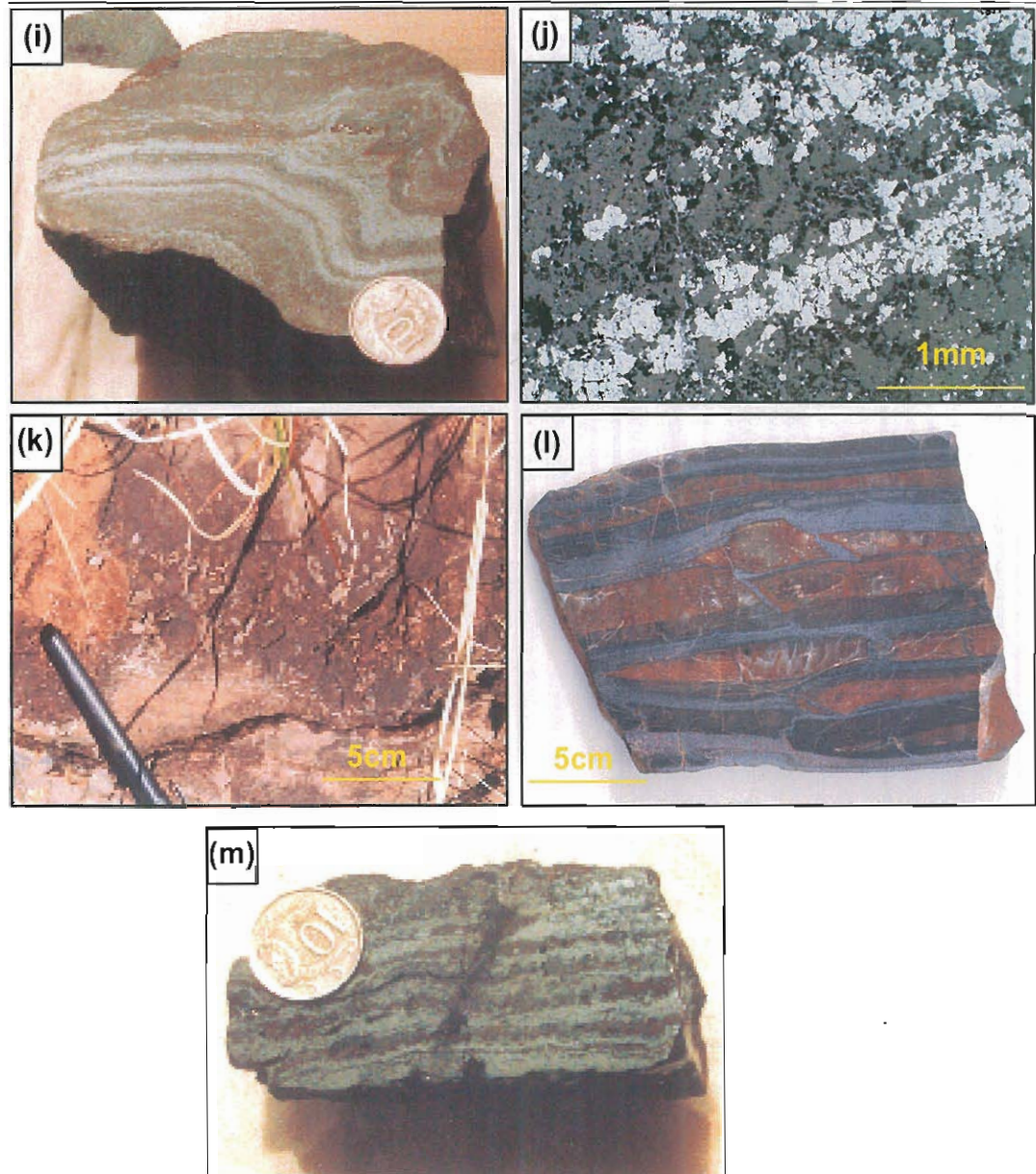
Figure 7.3: (a) garnet quartzite, Weatherly Creek Iron Formation, sample WC-78. Dominantly garnet layers defined by *gt,* dominantly apatite layers by *ap*; (b) transitional iron formation, Weatherly Creek Iron Formation sample WC-86; (c) photomicrograph (uncrossed polars) of garnet quartzite showing sharp contacts between garnetiferous and iron-oxide rich laminae as well as the later overgrowth of apatite and garnet sample WC-78; (d) photomicrograph (uncrossed polars) garnet quartzite (WC-78) depicting relict sedimentary laminae overgrown by garnet and later apatite; (e) photomicrograph (uncrossed polars) of garnet quartzite (WC-78) showing the sharp contacts between garnetiferous and iron oxide rich laminae and associated apatite; (f) photomicrograph (crossed polars) depicting the regrowth of early quartz in silicate laminae in iron formation Weatherly Creek Iron Formation, alignéd parallel to regional $D_2(S_2)$; (g) tight isoclinal D_1

folds in WCIF; (h) S_0 refolded by subsequent deformations including S_2 Pumpkin Gully Syncline

(i) crenulated folds in iron formation, (WC-66) Weatherly Creek Iron Formation;
(j) photomicrograph,reflected light, uncrossed polars, of iron formation Mt Norna Iron Formation depicting the mg and hm laminaeand the upgrading effect of regional metamorphism; (k) sharp contact between iron formation and a medium grained, rippled and cross-laminated psammite, GR (466100E 7717900mN), Pumpkin Gully Syncline, upper Mt Norna Quartzite (Pon_3);

(l) Pumpkin Gully Syncline from the contact between theToole Creek Volcanics and Mt Norna Quartzite; (m) transitional iron formation WCIF sample WC-95.

7.3.2 Mt Norna Iron Formation (MNIF)

The Cu-Ag mineralised MNIF (Fig.7.2b; Arnold 1983) is approximately 800m in lateral extent, outcrops on the eastern slopes of Mt Norna itself (Fig.7.2b), and comprises a 1-7m thick IF with very minor garnet quartzites. It occurs near the base of the Mt Norna Quartzite and is in conformable contact with underlying Thickly Bedded Quartzite Facies, Graded Quartzite Facies and Polymict Breccia Facies with no evidence for erosional contact. Several smaller lateral equivalents are evident on regional aeromagnetics and aerial photographs (*eg.* Mt Norna South-Arnold 1983; Map Sheet One). These are hosted along strike to the south of Mt Norna in geologically similar and stratigraphically equivalent pods of Basal Quartzite Facies Association lithologies.

The MNIF is thickest in the centre and tapers out at both ends (Fig.7.2b) and comprises a hematite-magnetite±quartz±garnet and magnetite-hematite, thinly-laminated to massive iron formation. A small pit and several deep shafts are located at the thickest part of the outcrop concurrent with the occurrence of rare garnetiferous 1-10m x 0.5-7m 'pods' in the MNIF. These garnetiferous bodies are controlled by localised shear fabrics running sub parallel to the surfaces of the MNIF and their contacts overprint earlier D_1-D_4 fabrics. These 'pods' contain disseminated chalcopyrite-arsenopyrite-malachite-azurite and are interpreted as the host to the Mt Norna Cu-Ag mineralisation.

Pre-mineralisation structure at the workings is the most complex observed during this study. The fabrics here include tight isoclinal-rootless intrafolial folds of primary laminae overprinted by later deformations. To the north of the workings stratigraphically above and below outcropping massive-laminated iron formation, several small pods, 1-3m thick and of uncertain lateral extent, of Polymictic Breccia

Facies (Ch.3) occur. Contacts between this breccia and the MNIF, where mappable, appear to be sharp and conformable. The limited lateral and stratigraphic extent combined with poor outcrop and steep local topography makes confident interpretation of this unit difficult. Overprinting relations outlined here show that the breccia predated D_2, and the conformable contacts with the MNIF suggest a possible earlier timing. Elsewhere along the MNIF structural overprints are largely similar to that in the WCIF with D_2 fabrics dominating which are traceable into adjacent metasediments. As with the WCIF, early laminae, equivalent and sub parallel to S_0 in adjacent units, are preserved and overprinted by later crenulations and cleavages ranging from D_1-D_4.

7.3.3 Pumpkin Gully Iron Formations

Polymetallic, metasomatised iron formations and structurally controlled ironstones at Monakoff, related prospects and unmineralised occurrences, in the Pumpkin Gully Syncline (Fig.7.1) have been well studied (Ashley 1983; Davidson 1997; Davidson and Davis 1997; Davidson *et al.* 2002; Williams 1997). The main iron formation at Monakoff has some features in common with the MNIF and WCIF, but is complexly overprinted by syn-$D_{2.5}$ metasomatic products (biotite), currently dated using Ar-Ar at 1508±10 Ma (Perkins 1997; *cf.* Davidson & Davis 1997). Mineralisation is not hosted directly in the iron formation but is focused in an adjacent shear zone (Davidson & Davis 1997). The Monakoff iron formations are banded, quartz-magnetite-hematite±(barite-garnet) horizons associated with laminated fine-medium grained metasediments, and syn-sedimentary basalt-andesite sills (Davidson and Davis 1997). The paragenesis and relations of complex carbonate-barite and garnet alteration assemblages associated with polymetallic mineralisation and minor

localised predeformational Mn-Al-K-Fe metasomatism at Monakoff, are described in detail by Davidson *et al.* (2002).

Away from the Monakoff horizon there are several other outcropping iron formations, which were the focus of this study. Aeromagnetics show these horizons to be very extensive (1-5km along strike), forming a geophysical marker horizon above and/or close to the Mt Norna Quartzite-Toole Creek Volcanics contact. However, these horizons only have sporadic outcrop expression. Well-exposed examples are cited below, in which two differing styles of contacts allow determination of the relationships to surrounding units.

To the west of the Monakoff pit (GR 466100E 7717900N) a 1-2m thick magnetite-hematite-quartz laminated (1mm-2cm) iron formation is in direct contact with metasediments of the uppermost Mt Norna Quartzite, approximately 800m down stratigraphy from the mapped contact with Toole Creek Volcanics. Here, a 1-3m thick psammitic bed 1-3m thick has an erosional base, which contains clasts of the underlying iron formation (Fig.7.3k). These clasts are angular and elongate (1-2cm), chaotically arranged and have distinctive relict magnetite-garnet-quartz laminae. The adjacent psammite is medium bedded and the underlying iron formation retains magnetite-garnet-quartz laminae on a similar scale to the clasts. Along strike the outcrop is poor, rendering the extent of this type of contact difficult to determine.

Approximately 350m southeast of this occurrence, close to the mapped Mt Norna Quartzite-Toole Creek Volcanics contact (GR 469500E 7718150N) a thin (1-3m), laterally restricted (10-20m), laminated (1-20mm) IF occurs. This horizon is interleaved with adjacent metabasalt flows and metadolerite sills and in hand specimen comprises bands of magnetite-hematite±garnet (Fig.7.3l) hosted by

176

laminated pelite overprinted by the distinctive epidote-quartz±carbonate(±garnet) alteration halo. This pre-deformational alteration halo was first noted in the Pumpkin Gully Syncline by Williams (1997) and has been mapped by the author elsewhere associated with other local iron formations as large, conformable, broadly symmetric haloes up to 20m wide in host mafics and metasediments.

7.4 Geochemistry of Soldiers Cap Group Iron Formations

7.4.1 Major and trace element geochemistry

Geochemical data collected during this study was used to define geochemical signatures of the chemical sediments and compare these to others within the Maronan Supergroup (*eg.* Newbery 1991), and with published major element data from similarly aged iron formations in the Broken Hill Block (Stanton 1976a,b). Tables 7.1 and 7.3 present analyses of garnet quartzite, transitional iron formation and IF from the WCIF and Table 7.2 presents the results of ICP-MS analyses of the REE content of the MNIF.

Other well-studied iron formations within the Maronan Supergroup (Pegmont, Monakoff) fall into several distinctive compositional groupings (Fig.7.4a-c). Si, Fe, Mn, P and Ca are the major components of the WCIF, and Ba and V are present as minor but important components (Table 7.1). Compared to other iron formations in the Maronan Supergroup (Pegmont and Monakoff-Pumpkin Gully Syncline examples), WCIF major elements such as Fe, Mn, Ca and P oxides are more variable (Fig.7.4a-c); Ca/(Ca+Mg) in particular extends to lower values than in the other IF (Fig.7.4c). Compared to iron formations from the similarly aged Broken Hill Block the WCIF is generally higher in Fe_2O_3 and SiO_2 (Fig.7.4a,c), and broadly equivalent in P_2O_5 (Fig.7.4a) and MnO (Fig.7.4b).
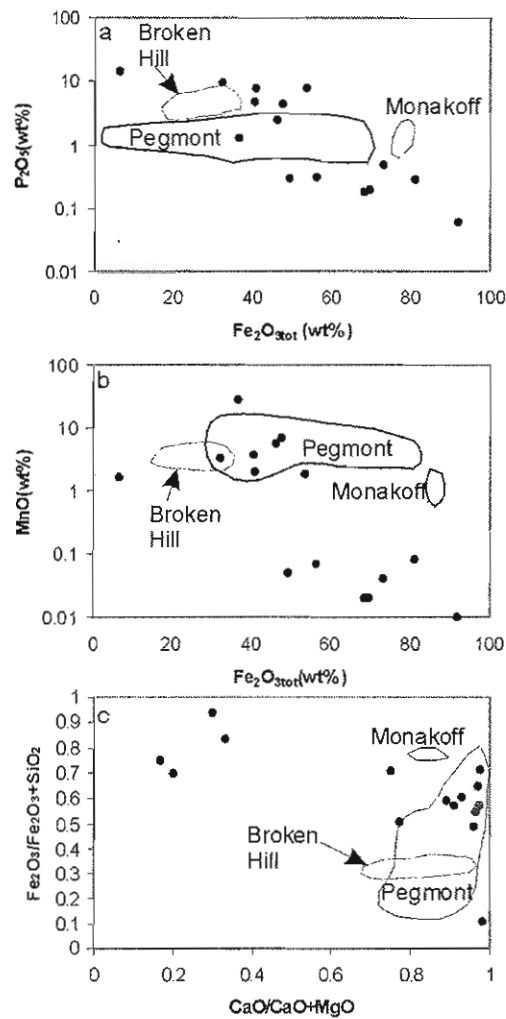
Figure 7.4: Selected major element fields for Maronan Supergroup iron formations, Pegmont and Broken Hill iron formation compositions taken from Newbery (1991), Stanton (1976a) and unpublished data of the authors.

Spatially, P_2O_5 is elevated at the centre of the WCIF, directly associated with garnet quartzites and decreases sharply at the edges (Fig.7.2a; Fig.7.5c). MnO & CaO behave similarly and vary widely across the WCIF with the highest values being associated with transitional iron formations and garnet quartzites (Fig.7.2a; Fig.7.5c). Elevated Al_2O_3 occurs at the northern end of the WCIF adjacent to the fault and is associated with garnet quartzites, transitional iron formations and elevated MnO values.
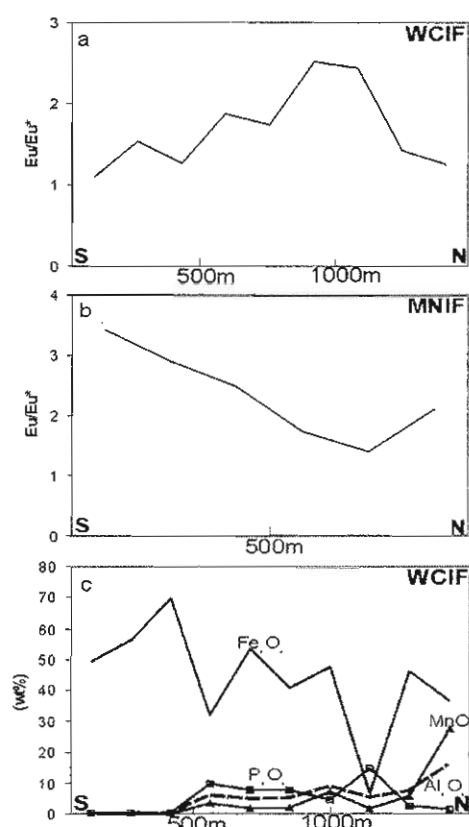
Figure 7.5: Along strike chemical variations (a) Eu/Eu* WCIF (b) Eu/Eu* MNIF (c) P, Fe, Mn, Al variation along strike in the WCIF.

Combined with other local and regional iron formation data (unpublished, this study; Arnold 1983; Newbery 1991), trace elements in the WCIF were found to have distinctive values when compared to iron formations from Pegmont. These include elevated Ni, Co, Cr and Sc (Table 7.1) which are particularly associated with Mn-rich garnet quartzites and transitional iron formations, and high values of other trace elements including Sc, Y, La, Ce, Pb, Cu and Zn (Table 7.1). When compared to local and regional values, the MNIF is enriched in Cu, Ag, As and Zn, but depleted in Pb and V.

Inter-element relationships in iron formations are complex, commonly reflecting the contributions of several sources, including clastic, hydrogenous, and evolving hydrothermal fluid sources (Parr, 1992; Peter & Goodfellow, 1996; Davidson et al., 2001). For the WCIF, principal component analysis (well detailed in Le Maitre

1982), and binary scatter plots of major elements, has proved most useful for defining graphical interelement relationships in the data set. For the purposes of analysis, the major element data in Table 7.1 was converted to centre log ratios using the software package MVSP version 2.2j, with those values below detection being assigned a value of one third of the detection limit (trace element data were not used in the analysis because some elements were not analysed for all samples). These ratios were used to construct an Aitchison covariance matrix. This approach was taken to determine inter-element correlations in a way that address the effects of closure, which are likely to be profound in these Fe-dominated rocks. The software was used to calculate principal component coordinates. Two eigenvectors, *ie.* the coefficients of the discriminant functions, were sufficient to account for 84.5% of the variance in the major element data. The scaled principal component scores are shown in Table 7.4a and b, and plotted in Figure 7.6. Figure 7.6 indicates that the iron formations consist of two main chemical components: (1) a high Ca-P-Mn-Na-Mg inter-correlated group; and (2) a Si-Fe inter-correlated group. These groupings indicate that there is no clear positive correlation between Fe and Mn or Fe and P. Concentration of these elements apparently occurred by separate processes or from different sources.

Eigenvectors	Component loading	Component loading
	axis 1	*axis 2*
SiO_2	0.227	-0.135
TiO_2	0.102	-0.075
Al_2O_3	0.054	-0.088
$Fe_2O_{3\,(T)}$	0.436	-0.119
MNO	-0.424	0.596
MGO	-0.054	-0.211
CAO	-0.604	-0.151
NA_2O	0.19	-0.167
K_2O	0.318	0.645
P_2O_5	-0.245	-0.295

Table 7.4a: Eigenvectors (component loadings) for the major elements in the WCIF.

Sample	axis 1	axis 2
WC78	-0.99	-0.336
WC81	1.05	0.102
WC86	-0.912	0.056
WC89	0.546	0.141
WC91	0.528	0.05
WC92	-0.882	-0.347
WC97	-1.234	-0.434
WC98	-0.589	0.304
WC99	-0.436	1.131
WC02	0.982	-0.081
WC10	-0.812	0.001
WC27	1.033	-0.292
WC28	0.707	-0.058
WC29	1.009	-0.236

Table 7.4b: Principal component scores for the major elements in the WCIF, represented graphically in Figure 7.6
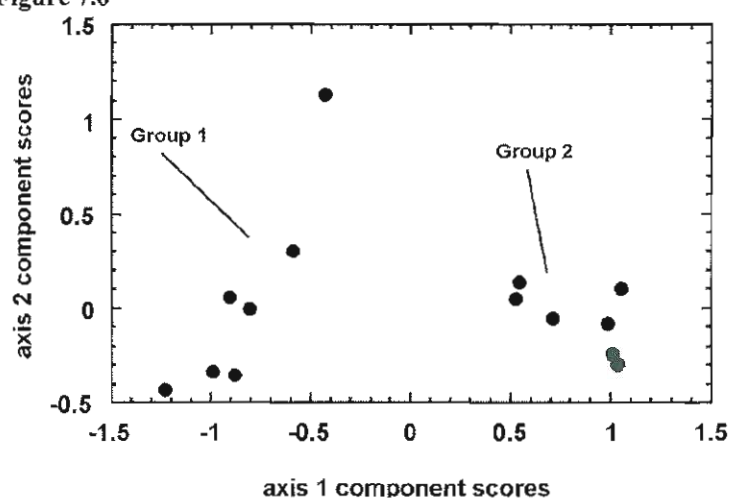
Figure 7.6: Component scores developed using Aitchison principal component analysis in the software package SMVP version 2.2j. Axis values are presented in Table 7.4.

The element groupings were further refined using bivariate plots, which were useful for addressing a greater level of detail than was possible through the multivariate analysis. The resulting plots, combined with the principal component analysis, show that two main groups of elements have graphical and statistical inter-element correlations:-

(1) Mn, P, Al, Ti, Zr, Mg, Ca, Na, K, As, Pb, Ni, ΣREE, Eu, Eu/Eu*, (Figs.7.7 and 7.8)

(2) Fe, Si, Ce/Ce° (Figs.7.7 and 7.8)
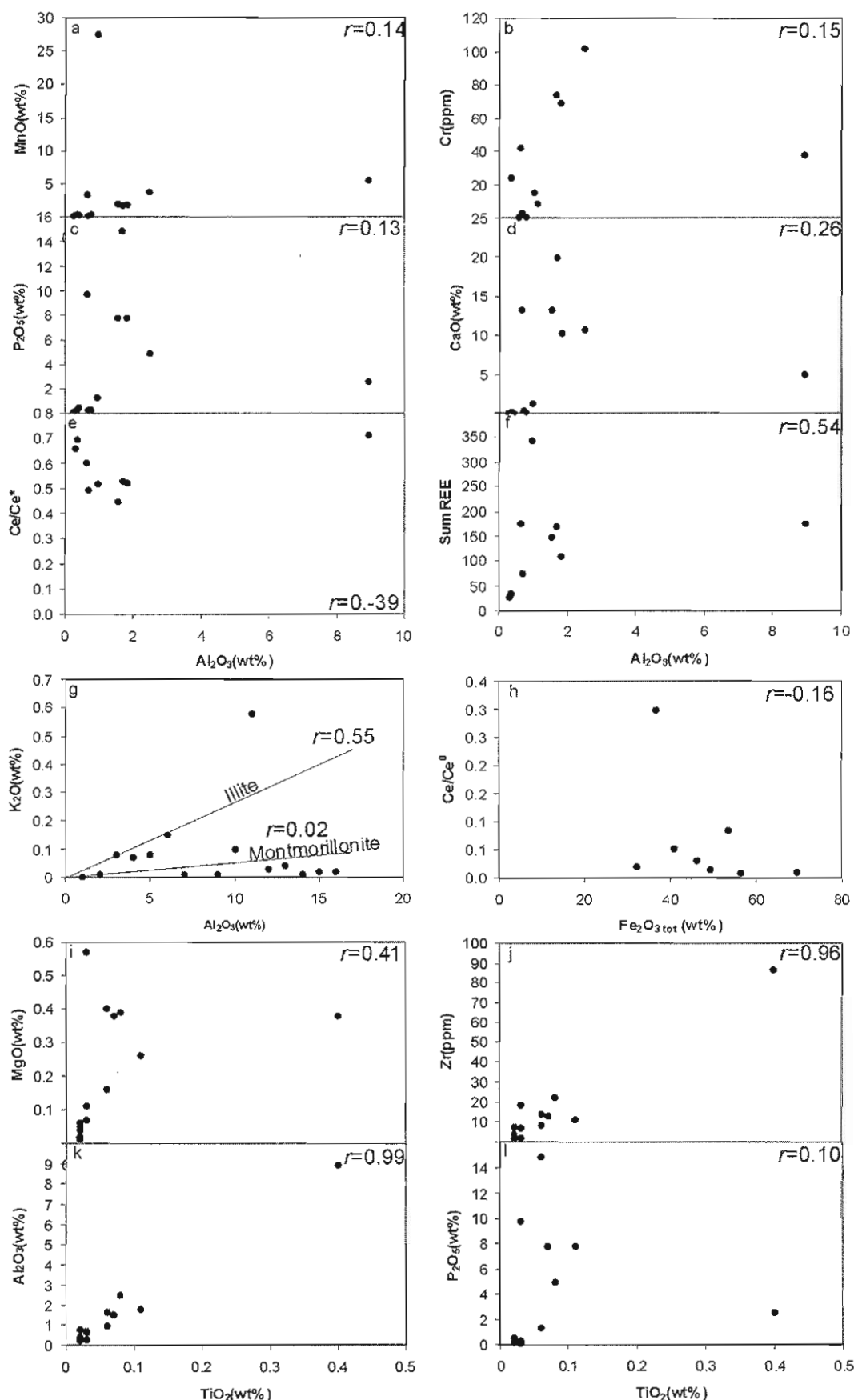
Figure 7.7: Various bivariate scatter plots of major indicator elements from the Weatherly Creek Iron Formation used to define detrital components. Correlation coefficients are quoted at the 95% confidence level.
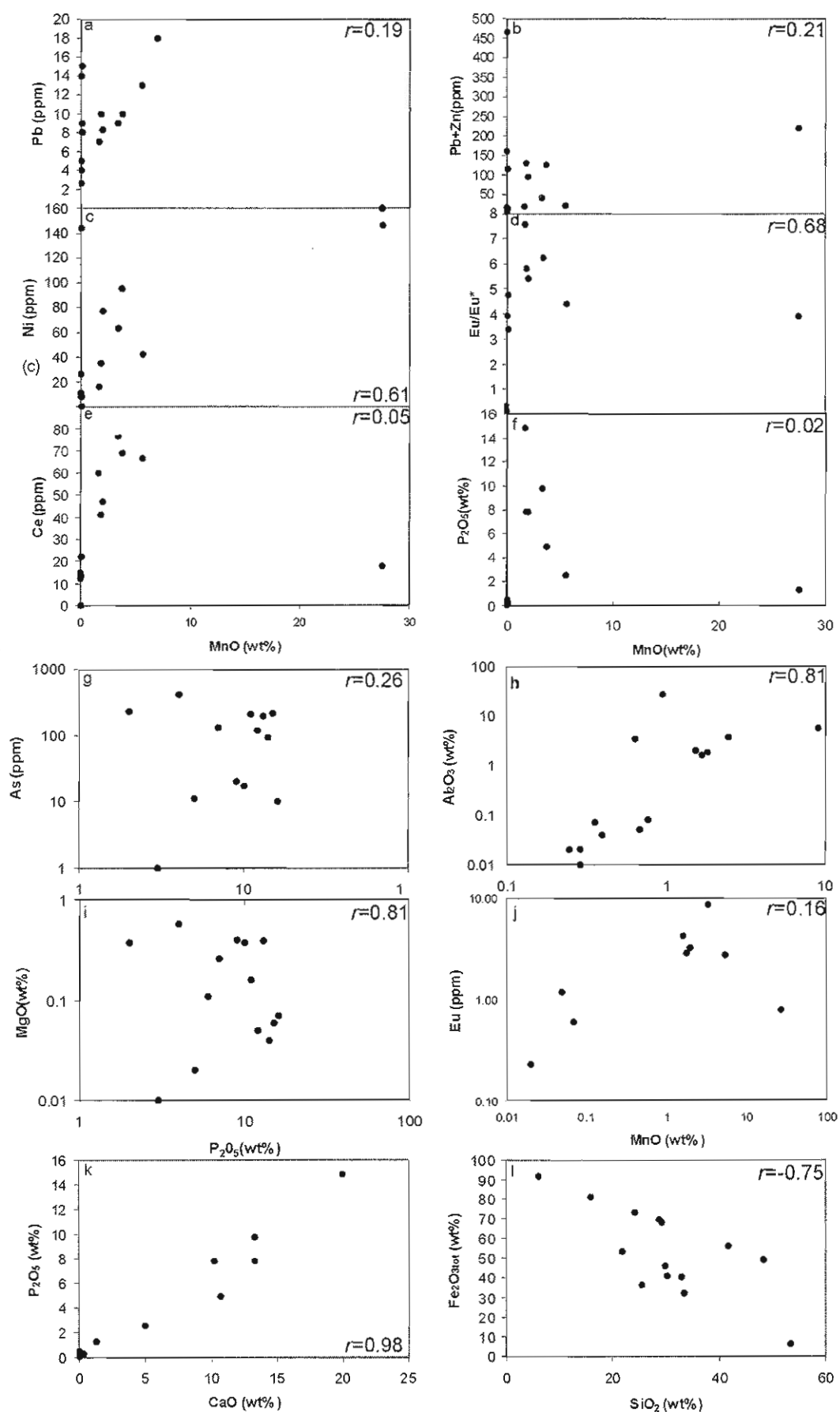
Figure 7.8: Bivariate scatter plots of major elements from the Weatherly Creek Iron Formation used to define hydrothermal and hydrogeneous components. Correlation coefficients are quoted at the 95% confidence level.

7.4.2 Rare Earth Element Geochemistry

REE/chondrite normalised plots such as those presented here (Fig.7.9) are commonly used in geochemical studies of chemical sediments (*eg.* Lottermoser 1989; Parr 1992; Peter and Goodfellow 1996). REE are generally considered immobile through low fluid-rock interaction metamorphic and alteration events (Bau 1991; Bingen *et al.* 1996; Rollinson 1993; Michard and Alberade 1986; Michard 1989). There is no clear evidence in outcrop, hand specimen, petrography or major element geochemistry that the late sodic-calcic metasomatism prevalent in parts of the SCG (de Jong & Williams 1995) affected the WCIF and MNIF or local host rocks. However, the MNIF, like the Monakoff IF, likely experienced epigenetic metal addition. REE data was collected from the MNIF to assess the effects on iron formation chemistry of an overprinting Cu-Ag mineralising event.

Normalised REE data for the WCIF are atypical for similar aged iron formations (*eg.* Broken Hill) with LREE enriched-HREE depleted patterns (Fig.7.9a; Table 7.2) and positive Eu and weak to moderate negative Ce anomalies (Fig.7.9a). Eu/Eu* is relatively consistent across the WCIF, with elevated anomalies associated with apatite-rich garnet quartzites, transitional iron formations and elevated Fe, Mn and P values (Fig.7.9a). The LREE are particularly elevated (Table 7.3) in samples of garnet quartzite and transitional iron formation. Overall, LREE in the WCIF are generally elevated compared to the MNIF (Table 7.2 & 7.3; Fig.7.9).
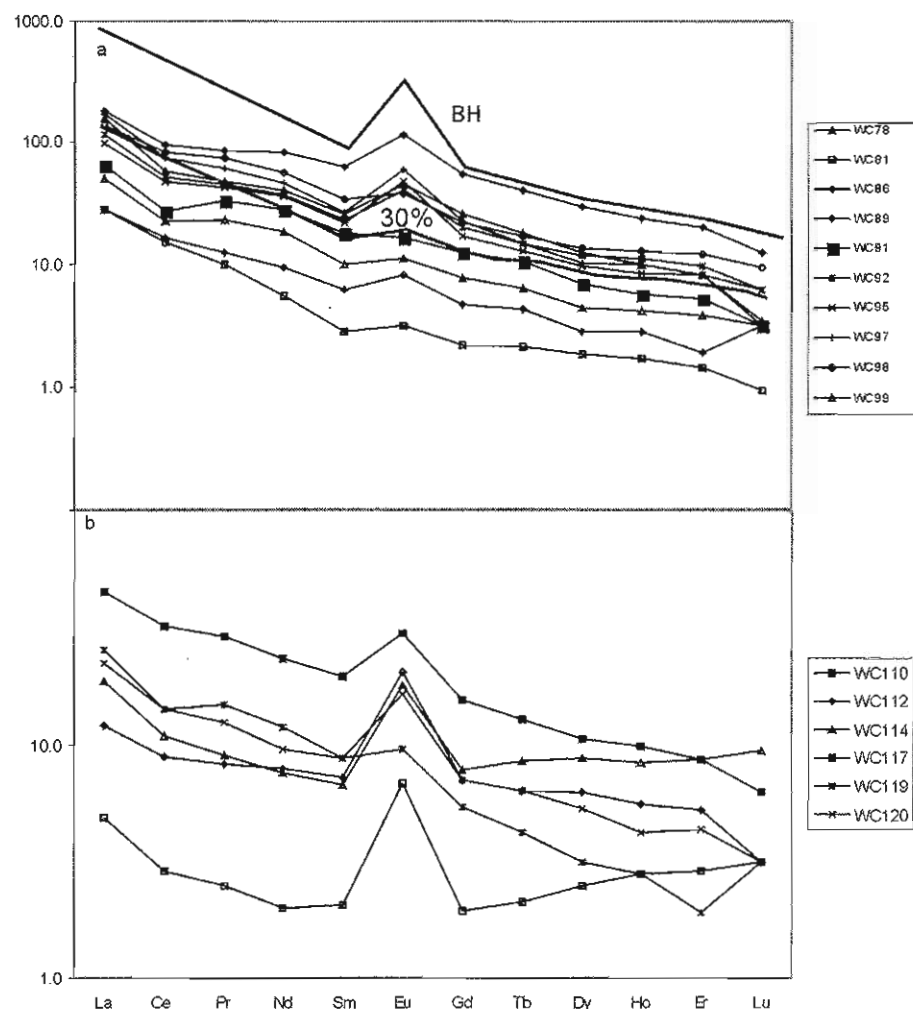
Figure 7.9: Chondrite normalised REE plots for (a) WCIF, BH= Broken Hill exhalites proximal to ore from Lottermoser (1989); 30%= > 30% detrital component (b) MNIF detrital component not plotted as major elements not analysed. Refer to Figure 7.2 for location of samples.

Although normalised data for the MNIF have overall lower values (ΣREE=8-74ppm) than the WCIF (ΣREE=27.7-244.7) and are less LREE enriched, the MNIF has a similar chondrite normalised pattern, with consistent positive Eu (Fig.7.9b, 7.5b) and weak negative Ce (Fig.7.9b) anomalies.

The REE patterns documented here are similar to those in unmineralised iron formations within the SCG (Davidson 1996), and in base metals mineralisation from the Cannington Pb-Zn deposit (Bodon 1996), and also in iron formations from the Broken Hill Block and Olary Domain associated with base-metals mineralisation (Fig.7.9; *cf.* Parr 1992; Bierlein 1995). The broad similarity of REE patterns in the

detailed sampling of a single SCG iron formation (WCIF), provides evidence that only a small number of samples are necessary within a long strike length (*ca.*2km) for adequate geochemical characterisation.

7.5 Discussion

7.5.1 Previous Models for Soldiers Cap Group and other geologically similar iron formations

Newbery (1991)(*cf.* Stanton & Vaughan 1979; Vaughan & Stanton 1984) studied in detail the petrography, host relationships and textures of the base-metal mineralised Maramungee and Pegmont iron formations in the lower Maronan Supergroup, the latter he interpreted as laterally equivalent to the MNIF. The Pegmont iron formation is a stratiform body, hosted by metasediments adjacent to the Llewellyn Creek Formation-Mt Norna Quartzite contact. According to Newbery (1991), the Pegmont iron formation grades laterally from a P-Fe-Mn centre to an Al-Si rich margin and has a close spatial and genetic relationship with nearby quartz-gahnites and tourmalinites, which are absent from the SCG chemical sediments studied here. Newbery (1991) proposed that, based on textural and geochemical characteristics including the presence of a significant detrital component and the lack of an alteration halo, Pegmont represented precipitation from mixing of exhalative brines and descending oxic waters in restricted basins associated with medial-distal turbidite fans distal from any volcanic or hydrothermal activity. The WCIF, MNIF and Pumpkin Gully iron formations, whilst broadly similar to Pegmont, differ in being deposited in a storm influenced shelf sequence (Ch.3), are proximal to volcanic activity, and have common and well defined syn-depositional alteration haloes. Geologically similar iron formations in the Broken Hill Block and Olary Domain have been defined by previous authors (Bierlein 1995; Lottermoser 1989; Lottermoser *et al.* 1994; Parr 1992; Stanton 1976a,b; Stanton & Vaughan 1979) as

the product of hydrothermal exhalation and mixing with seawater and rapid covering by incoming detritus.

Laing (1990;1998) proposed that some "quartz+iron-oxide(magnetite dominant)-massive to laminated" 'ironstones' in the SCG (Pumpkin Gully-Monakoff; Hot Rocks; Dairy Bore) are syntectonic D_1 or D_2 overprinted mylonites, and also that many of the banded iron formations found in the Maronan Supergroup may have been the result of alteration of existing calcsilicate sediments. Clastic reworking (Fig.7.3k), synsedimentary alteration haloes, relationships with synsedimentary mafic sills, detrital and hydrothermal geochemical signatures (Figs. 7.8, 7.9 and 7.10) provide strong evidence that the MNIF, WCIF and at least two Pumpkin Gully Syncline iron formations, are the product of synsedimentary and not syntectonic processes.

7.5.2 Origin of major and trace element variations in Soldiers Cap Group iron formations

The use of certain suites of indicator elements is common in studies of iron formations to determine the various sources (clastic, hydrothermal, hydrogeneous) for major, trace and rare-earth elements. The dataset from the WCIF defined at least three distinct sources, discussed in detail below.

Data for the WCIF, Mt Norna Quartzite & Toole Creek Volcanics (Appendix Three) and Fe-metatholeiites was plotted with several other relevant lithologies on an Fe/Ti versus Al/(Al+Fe+Mn) diagram (Fig.7.10). On this plot, hydrothermal components are represented by elevated Fe and Mn, clastic input by Al and Ti (Peter & Goodfellow 1996.

188
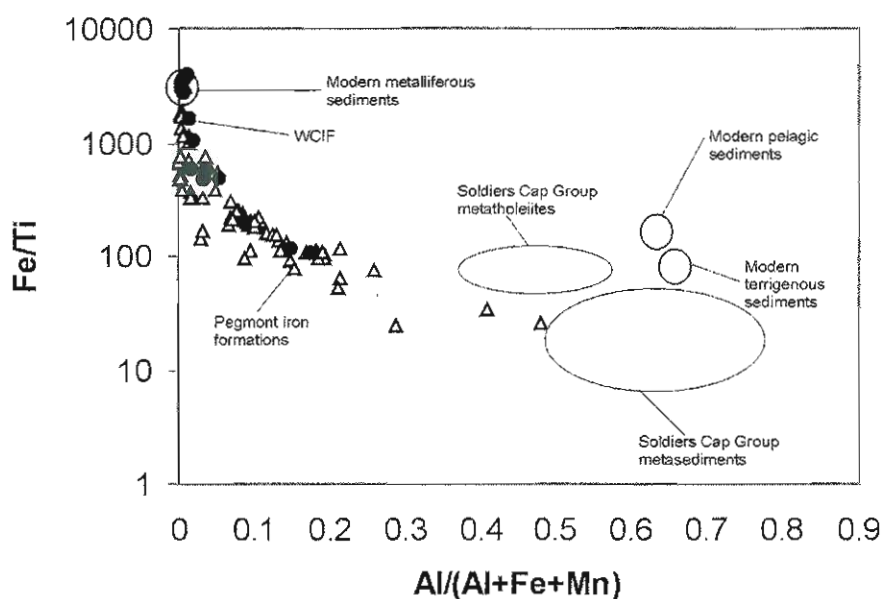
Figure 7.10: Diagram after Peter & Goodfellow (1996) used to determine the detrital versus hydrothermal component based upon Al/Ti and Fe-Mn content, WCIF (filled circles) and Pegmont (open triangles) plotted. Values for metasediments taken from authors unpublished data, metatholeiites from authors unpublished data (Appendix Three), fields for metalliferous, clastic and terrigenous sediments from Peter and Goodfellow (1996)

The limited data from the WCIF plots on a mixing line, with the Pegmont IF, between a modern metalliferous seafloor hydrothermal sediment component and a terrigenous sediment component. Although this terrigenous component does not match SCG Fe-metatholeiites or SCG metasediments, the WCIF have a clear trend towards the SCG metasediments suggesting that SCG metasediments may have had a significant clastic input into the chemical makeup of the WCIF. However, none of these values derive from host units to the WCIF and so SCG metasediments and metatholeiites cannot be discounted as a detrital source. Percentages of detrital and hydrothermal components can be qualitatively assessed using arbitrary end-members on Figure 7.10 with Fe/Ti >7000 representing hydrothermal processes and Al/(Al+Fe+Mn) >0.6 representing detrital end-members *(cf.* Peter & Goodfellow 1996). Using this quantitative calculation for the WCIF, detrital components range from 0.5-29 vol% and hydrothermal from 1.6-53 vol%.

189

The elements Al, Ti, Zr, Si, Mg, Ca, Ni, Cr and K are accepted as commonly present in detrital sediments. They dominate the inter-correlated group identified by multivariate analysis and bivariate plots above (Mn, P, Al, Ti, Zr, Mg, Ca, Na, K, As, Pb, Ni, ΣREE, Eu, Eu/Eu*; Fig.7.7). Relatively low detrital mineral abundances may still significantly influence iron formation geochemistry, as shown in the above analysis. Therefore, more focused graphical analysis using bivariate diagrams can help determine the nature and provenance of the detrital component. Trends on Figure 7.7g favour a mixture of montmorillonite (K_2O/Al_2O_3 ~0.016) and muscovite (K_2O/Al_2O_3 ~0.22) for the original K-rich detrital phase in the WCIF. A remnant mafic signature is evidenced by a positive Al–Cr correlation (Fig.7.7b). The correlation of REE with other detrital elements (Fig.7.7e-f) provides evidence that much of the REE were also detrital (*cf.* Peter & Goodfellow 1996). Uniform TiO_2/Zr (~0.008; r=0.96) and TiO_2/Al_2O_3 (Fig.7.7c &g; r=0.98) ratios imply a relatively constant detrital zircon source for the WCIF. Assuming that Ti and Zr were not significantly fractionated from one another during transport and deposition (a proposition most favoured in shale and silt fractions), possible Mt Isa Inlier sources based upon TiO_2/Zr ratios from the AGSO Rockchem geochemical database include volcanics of the Magna Lynn Metabasalt (TiO_2/Zr~0.009) and the Marraba Volcanics (TiO_2/Zr~0.006) both of which are located within the adjacent Eastern Succession and Kalkadoon Leichardt Block. In contrast, the associated mafic rocks of the SCG have average TiO_2/Zr ratios of 0.026. This concurs with detrital zircon studies (Ch.4) which show that the dominant detrital source for the SCG was from these and other units at a similar tectonostratigraphic level (Ch.4; Fig.4.8).

The elements Fe, Mn, P, Pb, Sr and Eu are generally elevated in silicate minerals, Fe-Mn oxides, sulphides and carbonates precipitated by active seafloor hydrothermal systems (Gross 1993; Peter & Goodfellow 1996). They are a group of elements not

normally found to be detrital, with the exception of immature magnetite heavy mineral concentrations. The multivariate analysis indicates that Fe was coprecipitated with Si in the WCIF (Fig.7.8l), whereas Mn and P showed an unusual positive correlation with detritally sourced elements such as Al (Fig.7.7a,c). In general the very high abundances of these four elements are unlikely to be accounted for detritally. By analogy with other chemical sediment systems, it is likely that these elements in general reflect the precipitation of Fe-Mn oxides and silicates from hydrothermal solutions (Gross 1993; Peter & Goodfellow 1996), with iron oxides and cherts being physically separated in time from the deposition of Mn and P-bearing phases. The deposition of the latter is likely to have required nucleation upon, or reaction with, detrital phases, or even have occurred in the sub-surface porosity provided by clastic interbeds, to account for the Mn-P-Al-Ti intercorrelations.

Strong Ca-P correlations (Fig.7.8k; $r=0.89$) favour apatite as the main Ca phase. The strong graphical and statistical correlation between Eu, Eu/Eu*, Mn and P (Fig.7.8d,j) can be accounted for by Eu preferentially entering apatite during hydrothermal precipitation.

The trace elements Ni, Th, U, V, Co, Fe, Ag, As, Pb, Zn, Mn and Ce are some of the range of elements commonly adsorbed onto Fe-Mn coatings on the surface of detrital particles and hydrothermal precipitates and are an indicator of hydrogeneous processes (Dymond *et al.* 1973; German *et al.* 1991). Input from such sources in iron formations is defined by correlations of these trace elements internally and with Fe and Mn (Peter & Goodfellow 1996; Davidson et al. 2001). Except for Ni and Pb these correlations are absent in the WCIF (Fig.7.8a-b). The strong positive Pb-Mn correlation (Fig.7.8a-b), moderate correlation between and relatively high ratio of

MnO/Pb+Zn (~0.03; Fig.7.8b) is consistent with hydrogeneous Pb uptake (*cf.*

Davidson *et al.* 2001).

7.5.3 Origin of Soldiers Cap Group iron formation REE patterns

A pattern of positive Eu anomalies and LREE enrichment-HREE depletion (Fig.7.9a,

b) in chondrite normalised Proterozoic iron formations, which is similar to modern

ocean floor metalliferous sediments (Courtois & Treuill 1977; Michard 1989;

Michard & Alberade 1986; Michard *et al.*1983; Barrett *et al.* 1990;) and seafloor

hydrothermal fluids (Klinkhammer *et al.*1994; Mills and Elderfield 1995), has in

ancient examples (*eg.* Broken Hill), commonly been interpreted as the product of

exhalation proximal to a seafloor hydrothermal centre (Lottermoser 1989; Parr 1992;

Bierlein 1995; Peter and Goodfellow 1996).

Europium generally occurs in solution as Eu^{2+} and Eu^{3+} complexed with various

anions (Rollinson 1993; Michard *et al.*1983). Production of a positive Eu anomaly

occurs where Eu^{2+} is transported in solution preferential to Eu^{3+}. Transport and

precipitation of Eu complexes is strongly dependent upon physicochemical

conditions, namely temperature and to a lesser extent fO_2 and pH (Sverjensky 1984).

Divalent Eu is stable in reduced hydrothermal fluids at temperatures $\geq 250°C$ and is

commonly scavenged from the breakdown of feldspar (albite) in sediments and

volcanics, so the feldspar content of source rocks has a significant control on the

scale of Eu anomalies. No analyses were available for metasedimentary units directly

associated with the SCG iron formations. Regional data collated by the authors from

unpublished reports and company databases shows SCG metasediments to generally

have values too low in REE to be a possible source. However, the units directly

underlying the SCG iron formations, including the lower SCG and upper Fullarton

River Group, are mostly quartzofeldspathic quartzites, with up to 35% plagioclase feldspar (*cf.* Ch.3). The weaker Eu anomaly present in the WCIF compared to the MNIF may be a factor of dilution by a sedimentary component similar to that evident in the major element data for the WCIF. Spry *et al.* (2000; *cf.* Peter & Goodfellow 1996) proposed that a >~30% detrital component is sufficient to mask REE anomalies. Samples plotted on REE normalized diagrams with a calculated ≥30% detrital component (based upon the rationale behind Fig.7.10) still retained positive Eu anomalies (Fig.7.9a, b) suggesting that detritus did not have a significant diluting affect on SCG iron formation REE patterns. However, as outlined below other dilution factors are also likely, including mixing with seawater and there still remains at least 20 vol% in the 'element budget' unaccounted for. In summation, the positive Eu anomalies presented here for SCG iron formations provide evidence that the WCIF and MNIF were the product of reduced fluids with reservoir temperatures ≥250°C.

The most likely cause of the physicochemical change necessary for the precipitation of Eu and the associated silicates and oxides in the system studied here is the presence of cold, oxic seawater. Some evidence for this exists in the weak negative Ce anomaly present in all samples from both the WCIF and MNIF (Fig.7.9a,b); this appears to have been strongest during Fe precipitation, based upon the increasing strength of Ce depletion at higher Fe contents (Fig.7.7h). Strong negative Ce anomalism in volcanosedimentary systems is generally considered indicative of seawater (Elderfield & Greaves 1981; Elderfield & Greaves 1982; Maynard 1983; Rollinson 1993). In other studies of Proterozoic iron formations in the Mt Isa Inlier and worldwide this anomaly has been interpreted as the result of mixing of seawater and hydrothermal fluids (Davidson 1996; Large *et al.*1996; Peter and Goodfellow

1996). Additionally, the strong negative correlation between Al_2O_3 and Ce/Ce°

(Fig.7.7e; $r=-0.39$) indicates the presence in the system of detritus lacking a Ce

anomaly (*cf.* Peter & Goodfellow 1996). Hydrogeneous scavenging of seawater Ce^{4+}

by Mn was minimal at this site, since this produces strong positive Ce anomalies in

modern manganiferous precipitates.
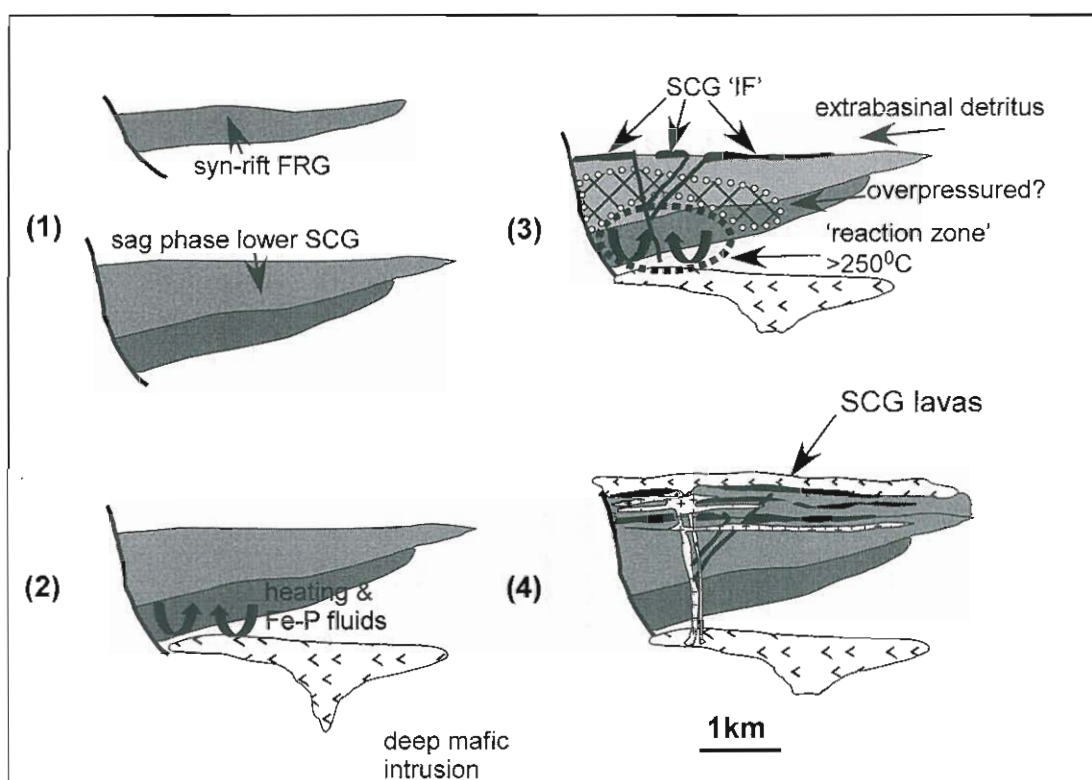
Figure 7.11: Schematic diagram of the evolution of the SCG iron formations (1) deposition of the underlying Fullarton River Group (FRG) and deposition of the lower Soldiers Cap Group; (2) intrusion of deep-seated mafic body which causes heating in the lower basin levels and expulsion of Fe-P rich fluids; (3) set-up of convection cells and breaching by extensional faults resulting in expulsion of hydrothermal fluids which combine with extrabasinal detritus to produce the SCG iron formations; (4) continued rifting and volcanism/magmatism and deposition of base metals enriched iron formations

7.5.4 Mafic magmatism and Soldiers Cap Group iron formations

The metatholeiites of the upper SCG are largely synsedimentary intrusive sills and

flows (Ch.5) which have a common spatial association with iron formations. The

voluminous synsedimentary sills of the SCG represent a significant increase in local

and regional heat flow and these may have been linked to the genesis of the iron

formations either through either local heating around sills or larger scale basinal convection processes.

Einsele *et al.* (1980) proposed the temperature adjacent to dolerite sills intruded into saturated sediments as shallow as 100m, to be as high as 400°C in the immediate vicinity of the sill-sediment contact. Conceivably, the temperatures inferred above of ≥250° necessary for the production of Eu anomalies and precipitation of Fe, Mn and P phases could have been attained by the intrusion of sills into the wet, unconsolidated sediments of the SCG, setting up local convection cells, operating close to the time of iron formation deposition. The scale of these cells based upon the lateral extent of the iron formations could have been in the order of 10-1000m wide and of indeterminate depth. However, two important factors preclude the interpretation of the SCG iron formations as the product of local heating around sills. These are the lack of observed metal (Pb-Zn) sulphide assemblages expected through the exhalation of >250°C fluids, and most importantly the fact that if local convection was occurring related to intrusion, then iron formations similar to the WCIF would be found throughout the SCG at the level of all sills and not at the limited stratigraphic levels outlined in this study.

As mentioned above the emplacement of the voluminous mafic sills and related underlying magma chambers into the sedimentary pile of the SCG would have elevated basin temperatures (Fig.7.11). This could conceivably have produced deep-seated basin scale convection cells in appropriate aquifers of the required temperatures of ≥250°C (Fig.7.11 [3]). Breaching of one of these systems by a major extensional fault system and expulsion at or near the surface through leakage up faults into either a stratified brine-pool style system or restricted sub-basin provides a

more likely alternative to local convection (Fig.7.11[3]). A definitive assessment of the shallow versus deep nature of the source of SCG iron formation fluids would best be undertaken by radiogenic isotopic studies. This provides significant scope for further studies and would also be important in future basin prospectivity evaluations.

7.5.5 Sources of anomalous phosphorus

Compared to iron formations elsewhere in the rock record, P_2O_5 up to 15wt% is an anomalous feature of the WCIF (Fig.7.4a) which has few, if any analogues in the extant literature. Iron formations similar in age and geological setting from the Broken Hill Block and Olary Domain have been studied in detail by numerous previous authors (Stanton 1976a,b; Stanton & Vaughan 1979; Bierlein 1995; Lottermoser 1989; Lottermoser *et al.* 1994; Parr 1992). However, there is little information published on these iron formations pertaining directly to P-enrichment in what are interpreted as primary units. Additionally, there were no readily available published analyses of primary iron formations which contained values of P presented here for the SCG. Similarly, studies of broadly similar iron formations in the Abitibi Belt in Canada (*eg.* Peter & Goodfellow 1996) did not present levels of P comparable to the SCG iron formations.

Therefore the source of such anomalously high primary P in SCG iron formations remains without any clear precedent in the literature. Possible methods in which phosphorus, as fine-grained apatite, could have been introduced into the WCIF system, are discussed here. Additionally, consideration of the genetic models of the closest analogues to the SCG iron formations (Kiruna, Sweden & Avnik, Turkey) will be undertaken here.

Biogenic processes are a common cause of the concentration of P on the seafloor, but can be discounted here, based on a lack of evidence of any remnant biological activity in the SCG apart from sporadic and poorly understood black shales in the Toole Creek Volcanics not associated with iron formations. Adsorption of P (orthophosphates) onto Fe-oxides related to biogenic activity and chemical precipitation from the water column (Bjerrum & Canfield 2002) is a possibility, however, the lack of Fe-P correlation within the WCIF precludes such a mechanism (*cf.* Davidson *et al.* 2001).

An extrabasinal or local detrital SCG source of P (*cf.* Bjerrum & Canfield 2002) derived from temporally equivalent, felsic volcanics or sedimentary units is unlikely as the sedimentary conditions at the time of deposition were not appropriate for placer formation. Additionally, there is no evidence in the whole rock data, for a component of detrital P. Adjacent metasediments of the SCG generally have low modal apatite (<0.5%) and P_2O_5 of 0.01-0.21 wt% (Appendix Three). Mechanical reworking and 'winnowing' of components lighter than apatite by active sedimentary currents as suggested by Yang & Zeng (1993) is also discounted, as except for one of the Pumpkin Gully iron formations, sedimentary reworking of SCG iron formations was not observed.

Enrichment through metamorphic P-metasomatism of early apatite is a possibility. However, no P-metasomatic textures were observed at any scale during this study. Similarly, post depositional epigenetic enrichment of phosphate as suggested by Robertson (1982) is also unlikely given the lack of phosphatic lithologies nearby.

A strictly primary magmatic source derived from an intermediate-felsic rock as suggested by Frietsch & Perdahl (1995) for the apatite rich iron formations of

Kiruna, Sweden, and a similar source for the comparable Avnik ores in Turkey (Helvaci 1984), is not feasible given the lack of felsic-intermediate volcanic rocks in the SCG. Additionally, the WCIF and MNIF do not have the chondrite normalised negative Eu anomaly characteristic of Kiruna-style deposits (Frietsch & Perdahl 1995).

The correlation of elements such as Ca, P, Eu and Pb (Fig.7.7, Fig.7.8) in the WCIF combined with a positive Eu anomaly (Fig.7.9a), are features indicative of seafloor hydrothermal processes (Sverjensky 1984; Gross 1993). Hence a major component of the elevated P values in the WCIF are interpreted here to have resulted from hydrothermal precipitation of apatite. Also, the highest P values are concurrent with garnet quartzites and transitional iron formations with high Fe-Mn and Eu/Eu* values, which are generally interpreted as indicators of hydrothermal activity.

Elevated P (+/-Fe-Mn-Ca) values are a common feature of Broken Hill-type deposits and associated chemical sediments (Stanton 1972; 1976a; 1976b; Lottermoser 1989; Lottermoser *et al.*1994; Lottermoser & Ashley 1995; Walters 1996) and have been noted at Cannington (Bodon 1998). This distinctive geochemical signature provides a potential direct link between the SCG iron formations and Broken Hill-type mineralisation.

Treloar & Colley (1996) studied massive, magnetite-apatite ores hosted by a sequence of calc-alkaline andesites and basalts, associated with iron-enriched felsic magmas in northern Chile. They proposed, based upon detailed mineral chemistry and paragenetic studies, that these deposits were the result of the release of hot, acidic and reduced Fe-P enriched fluids from fractionated Fe-rich magmas in which magnetite-apatite crystallization was suppressed until late in the magmatic history

(*cf.* Brooks *et al.*1991). These fluids mixed with meteoric fluids in the host rocks, providing the physicochemical changes necessary to deposit high concentrations of Fe-oxides and apatite. Similar to the SCG iron formations, these deposits have an epidote dominant alteration halo.

Whilst the overall tectonic environments and magma geochemistry are different and the deposits studied by Treloar & Colley (1996) are epigenetic and deposited in structural conduits, the method of fluid genesis and precipitation may provide a close analogue for the genesis of the SCG iron formations. Williams (1998) interpreted metatholeiites of the SCG as ferrobasalts produced in high-level magma chambers in which magnetite crystallization along a distinct Fe-enrichment trend was suppressed until late in the sequence. Similarly, evidence presented above in Chapter 6 suggests that P was also an important primary phase fractionating during the evolution of the SCG mafic sills and lavas. Whilst the absolute values of P_2O_5 in SCG mafics are low (<1wt%) the possibility that the deep-seated magma chambers postulated above provided Fe-P rich fluids to a basin scale aquifer is plausible and provides a solution to the problem of anomalous P in SCG iron formations. Figure 7.11 depicts an interpreted method of genesis for the Fe-P rich fluids which were likely the source of the SCG iron formations.

7.6 Conclusions

Despite the high metamorphic grade and polydeformational history, primary depositional features and geochemical signatures are preserved in the iron formations studied in detail here. They are composed of petrographically and chemically distinct, garnet quartzites, transitional iron formations and banded iron formations. Contact relations with surrounding lithologies show these, and other stratigraphically

equivalent lenses, to be broadly contemporaneous to host sediments and

metatholeiite intrusions.

Fe, and Si precipitated from lower temperature hydrothermal fluids, Mn, P, Eu and

perhaps As were co-precipitated from higher temperature solutions, and shared an

undefined relationship with detrital phases. Al, Ti, Zr, Mg, Ca and K were mainly

contributed as mafic sedimentary detritus, the source of which is likely mixed Cover

Sequence 1 and 2 units to the west and north (*cf.* Ch.4). Hydrogenous processes were

responsible for deposition of Pb and Zn through adsorption on to Mn phases.

Normalised REE patterns are remarkably similar to those of modern metalliferous

seafloor sediments and display anomalies controlled by hydrothermal activity (Eu)

and influences of seawater (Ce).

Evidence presented here suggests that the iron formations of the upper Soldiers Cap

Group are products of the mixing and evolution of hydrothermal fluids and seawater

at the sediment-water interface. Relevant genetic models for iron formations

commonly refer to processes involving seafloor mounds/sinters in VMS systems (*eg.*

Davidson *et al.* 2001), or precipitation from hydrothermal vents or vent fields on the

seafloor into stratified basins (*eg.* Peter & Goodfellow 1996; *cf.* Newbery 1991). The

banded nature, lack of metal sulphides and the spatial restriction of Soldiers Cap

Group iron formations to more quiescent sedimentary environments, favours

deposition via the latter method. This would have involved localised exhalation of

hydrothermal plumes resultant from the tapping of deeper reservoirs, which mixed

with cold, reduced seawater in localised depressions with a less active sedimentary

environment than much of the rest of the Soldiers Cap Group (Fig.7.11; *cf.* Newbery

1991; Peter & Goodfellow 1996). This lateral restriction and lack of metal sulphides

has important implications for exploration in the region. The lack of sulphide

assemblages implies that metal carrying fluids were transported elsewhere in the basin and so, similar iron formations in the Maronan Supergroup may host Pb-Zn mineralisation (*eg.*Pegmont).

Following emplacement of Fe-tholeiite magma chambers into the base of the thick sedimentary pile of the Soldiers Cap Group, hot, acidic Fe-P rich fluids, possibly released from fractionated magma chambers, circulated in a regional aquifer, possibly with an overlying overpressured zone, which stripped REE from underlying units (Fig.7.11). Reaction of this fluid with feldspar at temperatures $\geq 250°C$ in the lower Soldiers Cap Group and underlying Fullarton River Group (FRG) released Eu and potentially, base metals (Fig.7.11). The fluids ascended to surface along extensional faults to pond and mix with cold, oxic seawater in relatively quiescent segments of a storm-dominated shelf, precipitating Fe, P and Mn rich minerals on the seafloor (Fig.7.11). Extrabasinal sources provided detritus deposited at the same time as the hydrothermal precipitates, which in places influenced the primary geochemical signature of the iron formations (Fig.7.11). Tholeiite magmas began to form the most voluminous sill complexes after the deposition of the Soldiers Cap Group iron formations in the upper Mt Norna Quartzite and Toole Creek Volcanics providing evidence that large-scale Fe-P rich fluid release and exhaustion of the deep aquifer occurred prior to the peak of magmatic activity (Fig.7.11).

The presence of the distinctive 'Broken Hill-type' Ca-Fe-Mn-P and REE geochemical 'exhalite' signature and the presence of numerous iron formations, which are considered in some cases to be lateral markers but not direct vectors to ore (Walters 1996), suggests that the Soldiers Cap Group may host as yet unidentified base metal mineralisation of this style. Further work is required to determine if lateral chemical zonation exists at >1km scales within each of the 3 main iron

formations of the Soldiers Cap Group. For instance, a regional study of the isotopic

characteristics of each horizon may provide vectors to hotter and/or more

hydrothermally active areas with greater base-metal forming potential. Significantly,

in targeting basins with two major rift stages, the Soldiers Cap Group provides

evidence that metalliferous fluids may be released prior to rather than during or after,

the second main tectonomagmatic event.

Chapter Eight- Basin evolution during upper Soldiers Cap Group time

8.1 Introduction

A major component of this study was an attempt to reconstruct the initial geometry
and define the evolution of a well preserved and continuously outcropping section of
the Soldiers Cap Group (SCG), the western limb of the Weatherly Creek Syncline,
and lateral equivalents. This was completed by combining palaeoflow indicators with
the detailed sedimentological (Ch.3) and volcanological (Ch.5) facies patterns as
well as whole rock geochemistry (Ch.6), provenance dating (Ch.4) and the geology
and geochemistry of iron formations (Ch.7). An attempt was also made to determine
the nature of several faults which appear to have had an effect on adjacent lithologies
in the mid-Mt Norna Quartzite (MNQ) to lower-Toole Creek Volcanics (TCV).
Although ideally isopachs, or length balancing methods (*eg.*Betts *et al.* 1999) would
have been used to reconstruct the basin or part thereof, this was not attempted due to
the generally steep dip of bedding and complexity of folding. No attempt has been
made to include the stratigraphy south of the Williams Batholith that Beardsmore *et
al.* (1988) correlate to the SCG, because of a lack of defined stratigraphic sections in
the latter.

8.2 Previous interpretations and basin extent

Previous palaeogeographic interpretations (Beardsmore *et al.* 1987; Newbery 1990)
in the region were based mainly on larger scale studies and interpretations of regional
map patterns. Newbery (1990) defined the Cloncurry Basin which comprises the
greater outcropping area of the Maronan Supergroup, bounded by the Cloncurry

Fault in the west and open to the east (Fig.8.1). This Cloncurry Basin is thought to

have been deposited in a steadily westward deepening basin up to 150km wide

(Loosveld 1988) and of uncertain length.
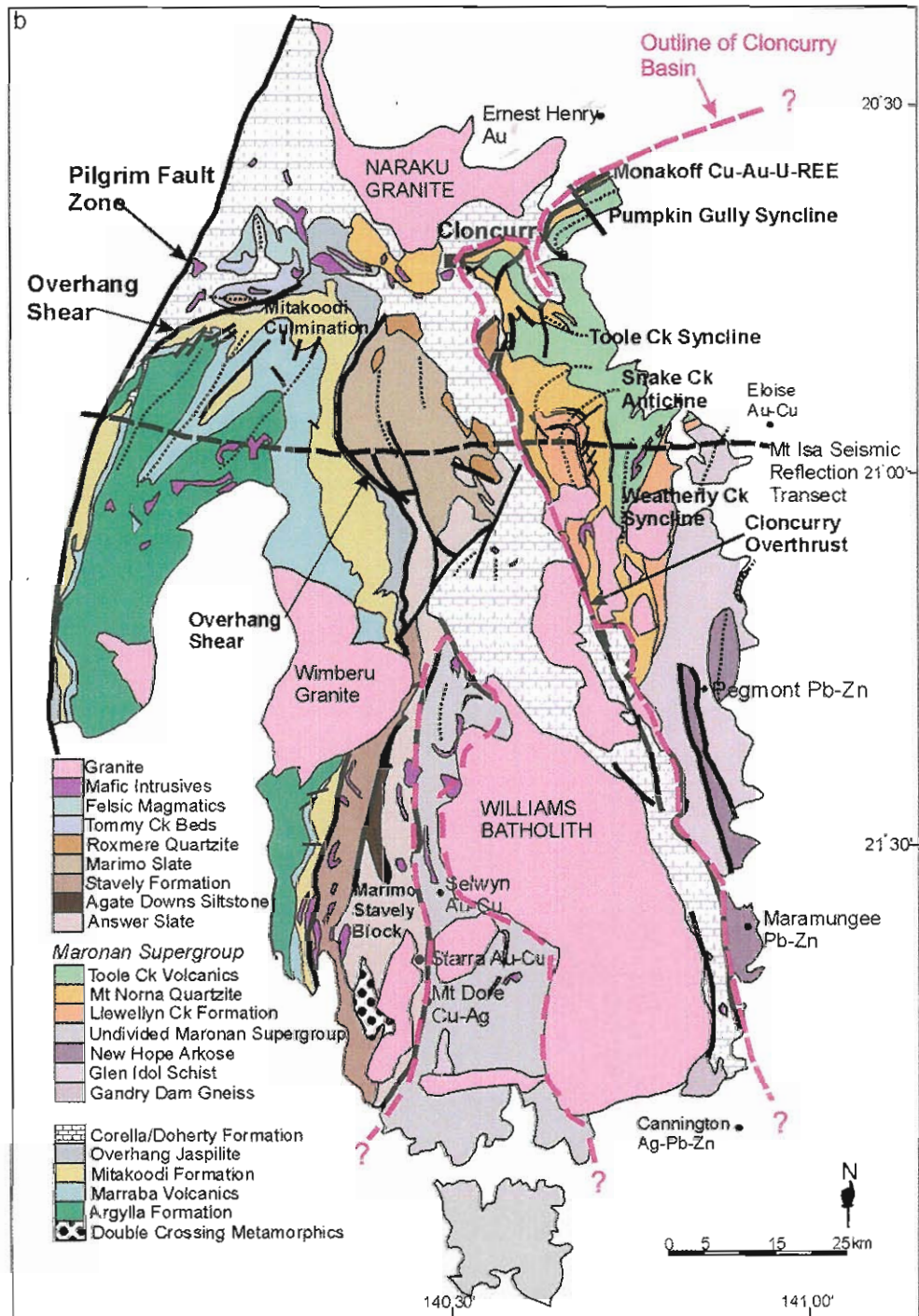
Figure 8.1: Simplified geology, stratigraphy and tectonic elements of the Eastern Succession modified from Betts *et al.* (1999).

Based on aeromagnetic image interpretations, regional exploration drill core logging,

and discussions with BHP Minerals geoscientists during the course of this research,

the SCG is thought by the author to extend for at least several 10's of kilometres

under younger cover to the east (Fig.5.3; Ch.5). The exact of the easterly margin remains undefined. In the west, the SCG terminates against the complex and multiphase Cloncurry Overthrust (Fig.8.1). In places the mapped outcrop expression of the SCG (Cloncurry 1:100 000 sheet of Ryburn *et al.* 1987) gives it the impression that it is thickened significantly near the termination at the Cloncurry Overthrust, but no structural/stratigraphic studies were undertaken here to determine if this is the case. To the north, the nature of boundaries, excluding tectonic contacts in the Pumpkin Gully Syncline (Williams 1997; Map Sheet Two), are ambiguous (Fig.8.1; *cf.*Ch.2). To the south the Maronan Supergroup is intruded by the Williams Batholith, in structural contact with units of the Mary Kathleen Group and abuts the Cloncurry Overthrust (Ch.2; Fig.8.1).

The main sediment source for the Cloncurry Basin was previously thought to have been to the east, inferred from an unqualified decrease in grainsize and feldspar content in Soldiers Cap Group units towards the west (Blake 1987; Beardsmore *et al.*1987; Beardsmore 1992; Newbery 1990; Loosveld 1989). This remains largely unproven and in the light of detrital zircon data presented in Chapter Four, suggesting a source to the west, north and south, is likely incorrect. Giles & MacCready (1997) proposed the Cloncurry Overthrust (Fig.8.1) to have originally been a major extensional structure at the time of deposition of the SCG (*cf.* Giles 2000; Ch.4). They based this interpretation largely upon outcrop patterns which they interpreted as wedges of sediment thickening towards a growth fault

8.3 Review of Soldiers Cap Group Volcano-Sedimentary Relationships

The well constrained lithostratigraphy, sedimentary lithofacies (Ch.3), detrital provenance studies (Ch.4), mafic volcanological lithofacies and whole rock

geochemistry (Ch.5&6) and genesis of iron formations (Ch.7) were invaluable in defining the geological evolution, including evidence for renewed extension, of the upper SCG. Prior to any detailed discussion on basin evolution these will be briefly revisited here.

8.3.1 Sedimentology

Using the features of the sedimentological facies defined in Chapter 3, the upper SCG (MNQ-TCV) is now defined as the product of storm current generated 'tempestites' on a narrow and relatively shallow shelf environment. Reconstructions of palaeoflow indicators show that there are components of alongshore (oscillatory storm currents) and shore oblique-normal (tempestite turbidity currents) sediment movement. Broadly there is a sharp change from 'turbidite' dominated sedimentation in the LCF, to the debris flow and hydrothermal activity of the lower MNQ, to a sequence dominated by oscillatory current overprints in the mid-upper MNQ and TCV (Ch.3). This change may represent renewed extension occurring in at least two stages in the Soldiers Cap Group history. Further evidence for this exists in the control on sedimentation exerted by the Lomas Creek Faults and Mt Norna Faults (Fig.8.2) and the presence of the Weatherly Creek iron formation at the change from turbidity dominated to tempestite dominated in the mid-MNQ. The combination of change in sedimentary environment, control by faults on sedimentation and palaeoflow, and the stratigraphic location of iron formations at the base and mid-MNQ is interpreted as evidence for renewed localised extension.

8.3.2 Mafic Volcanology and Geochemistry

Based upon brecciated contacts interpreted as peperites and hyaloclastites, the mafic units of the upper SCG are believed to be a sequence of synsedimentary sills and

minor flows. In detail, the mafic sequence mirrors the upward change in sedimentation by a change from dominantly Coherent Metadolerite facies sills with blocky peperite margins to Coherent Metadolerite and minor Massive Metabasalt facies bodies with fluidal and blocky peperite margins and local subaqueous flows up sequence (Ch.5). This is interpreted as the result of sequential intrusion of mafic bodies of differing viscosities implying overall continued extension throughout the basin. The lack of mapped localised breccias and onlapping contacts in the Weatherly Creek Syncline precludes the interpretation of any inflation of the sedimentary pile by mafic intrusions. Overall the emplacement of this sequence of mafic bodies is one of the best lines of evidence for renewed extension during MNQ and TCV deposition.

The Pumpkin Gully Syncline and Weatherly Creek Syncline mafic sequences are geochemically distinct from one another in their degree of Fe-Ti enrichment (Ch.6). This is interpreted to be the product of at least two different magma chambers derived from a single parent chamber producing contemporaneous sills and lesser flows which interfingered at intermediate spatial locations outside each chambers zone of influence. This interpreted interfingering is based upon the 'intermediate' composition of a limited sample set from the Toole Creek Syncline, geographically located between the PGS and WCS (Fig.8.1).

The mafic magmatic history below the basal-MNQ was not examined during this study. However, mapping by Ryburn *et al.* (1987; *cf.* Loosveld 1988; Lewthwaite 2000) defined large amphibolite bodies which appear to have been deformed during D_1-D_2 and so are likely syndepositional. The closest of these amphibolite bodies are ~800-900m stratigraphically below the Mt Norna iron formation (Fig.8.2).

8.3.3 Iron Formations

Two iron formation horizons at the lower-MNQ (Mt Norna Iron Formation) and mid-MNQ (Weatherly Creek Iron Formation) and smaller lateral equivalents are now interpreted as the product of seafloor exhalation of Fe-P rich hydrothermal fluids with seawater mixed with Si-Al-Mg rich detrital input probably from mafic volcanics of Cover Sequence 2. The iron formations appear to predate the major phase of mafic magmatism in the TCV and were likely the product of heating of basinal brines in by deep-seated mafic magma chambers, and expulsion to the surface along faults reactivated by renewed extension. The local environment at the Mt Norna iron formation and smaller lateral equivalents (*eg.* Mt Norna South- Map Sheet One) is defined by a subtle change from lower energy turbidity currents of the LCF to quasi-steady high energy turbidity currents of the basal MNQ (Ch.3) and an input of Cover Sequence 1 and 2 and Archaean aged zircons (Ch.4). Thickening of the Mt Norna iron formation is closely associated with a series of northeast striking faults, the Mt Norna Faults (Fig.8.2). At the stratigraphic level of the Weatherly Creek iron formation, there is a sedimentary transition from turbidite-dominated sedimentation to an environment in which storm generated currents were dominant. Faulting associated with the thickening of the Weatherly Creek iron formation is restricted to the local scale (Fig.8.2). In the Pumpkin Gully Syncline the position of iron formations is broadly related to the change from syn-sedimentary sill intrusion in the upper-MNQ to subaqueous lavas of the lower-TCV.
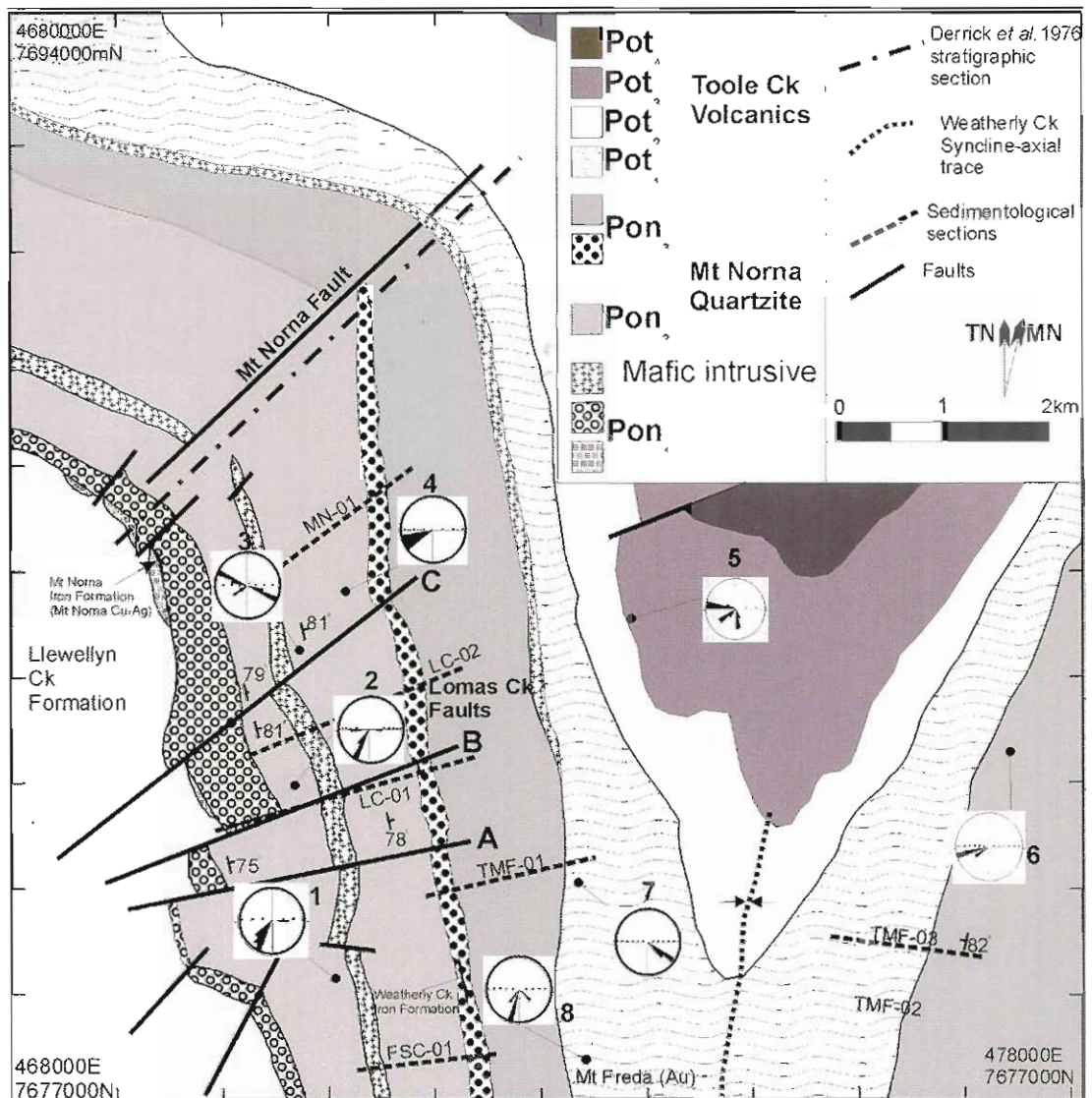
Figure 8.2: Simplified fact geology of the Weatherly Creek Syncline depicting the major sedimentological units, reconstructed palaeocurrents and sample locations, major faults discussed in this chapter and sedimentological sections used in this study. A,B,C define the three Lomas Creek Faults.

8.4 Nature of faults in the study area

8.4.1 Weatherly Creek Syncline

Within the study area there are several large, north-northeasterly striking faults that

define mappable thickness changes in the volcanosedimentary sequence of the lower

MNQ-lower TCV. The two major areas of disruption in the Weatherly Creek area are

the Mt Norna Faults (named here) consisting of a cluster of one large and two

smaller parallel faults (Map Sheet One), and the Lomas Creek Fault (*cf.* Arnold

1983), and two smaller adjacent faults, all three here named the Lomas Creek Faults, designated from north to south A,B &C (Fig.8.2; Fig.8.3 & Map Sheet One).

The Mt Norna Fault strikes northeastly and has an approximate length of 5km (Fig.8.2; Fig.8.3 & Map Sheet One), is apparent on airphotos and aeromagnetic images as a sharp lineament that disrupts bedding form lines and follows the line of a local creek (Mountain Home Creek). Distinct aeromagnetic units, generally mafics, traceable north and south along strike, are cut by the trace of the Mt Norna Fault (Fig.8.2; Fig.8.3 Map Sheet One). Mapping also shows that locally the Swaley facies association and Quartzo-pelite facies association, which are laterally continuous for several kilometres to the south of the fault, are attenuated across the Mt Norna Fault (Fig.8.2). Within the basal MNQ, the Mt Norna Fault presently dissects the Basal Quartzite Facies Association into elongate pods separated by pelitic schists of the lower MNQ-upper LCF (Fig.8.2; Map Sheet One). Where observed in mapping, the surface expression of this fault is represented by increased foliation intensity in the adjacent pelites and some stretching within the foliation of centimetre scale quartz clasts.

The Lomas Creek Faults (Fig.8.2) disrupt the Basal Quartzite, Quartzo-pelite and Quartzo-psammite facies associations within the lower-MNQ. These faults have a subtle to nondescript outcrop expression. They are best observed at the map scale where using field mapping, aeromagnetics and airphotos, they appear as discrete lineaments which disrupt regional bedding and lithological units and appear to control marked thickness changes in well constrained sedimentary units (Fig.8.2; Fig.8.3 & Map Sheet One). The apparent thickness of Pon_1 decreases from ~900m to 700m to 250m thick across the faults from north to south, with the thickest segments

always being on the northern side (Fig.8.2; Map Sheet One). Concurrently, in the mid-MNQ (*Pon₂*) there is a mappable apparent thickness change that is the inverse of the *Pon₁* situation. *Pon₂* thins from ~2500m to 1900m to 1200m northwards across the Lomas Creek Faults (Fig.8.2; Map Sheet One). The generally steep-subvertical nature of bedding in the Weatherly Creek Syncline implies that these apparent thicknesses are close to true thickness. Measured dips of bedding are consistent across the area discounting the possibility of these apparent thickness changes being related to orientation changes within individual fault blocks (Fig.8.2; Map Sheet One). Concurrent with the thickness change there are changes in the sedimentary environment across the Lomas Creek Faults. To the north of fault 'C' there are small, 10-50m long pods of lateral equivalents to the Mt Norna Iron Formation which are not present further up sequence or to the south of fault 'B'. A subtle increase in the thickness of Pelite Facies beds from 3m to a maximum of 5-6m to the south of fault 'C' implies a slightly deeper, quieter environment in the southward thickened fault block. The upper part of the thickened *Pon₂* wedge to the south of fault 'A' is host to the Weatherly Creek Iron Formation (Fig.8.2). Reconstructed palaeoflow markers (Ch.3) are also controlled to some degree by the Lomas Creek Faults. Tempestite generated palaeocurrents to the north of fault 'B' (Fig.8.2) indicate an east-west local shoreline and shore-oblique transport to the southwest. To the south of fault 'A' (Fig.8.2) slump fronts and HCS palaeocurrents suggest a northwest-southeast shoreline and sediment transport offshore to the southwest. The lack of palaeoflow markers in *Pon₁* makes interpretation of fault control in the basal part of the sequence difficult.
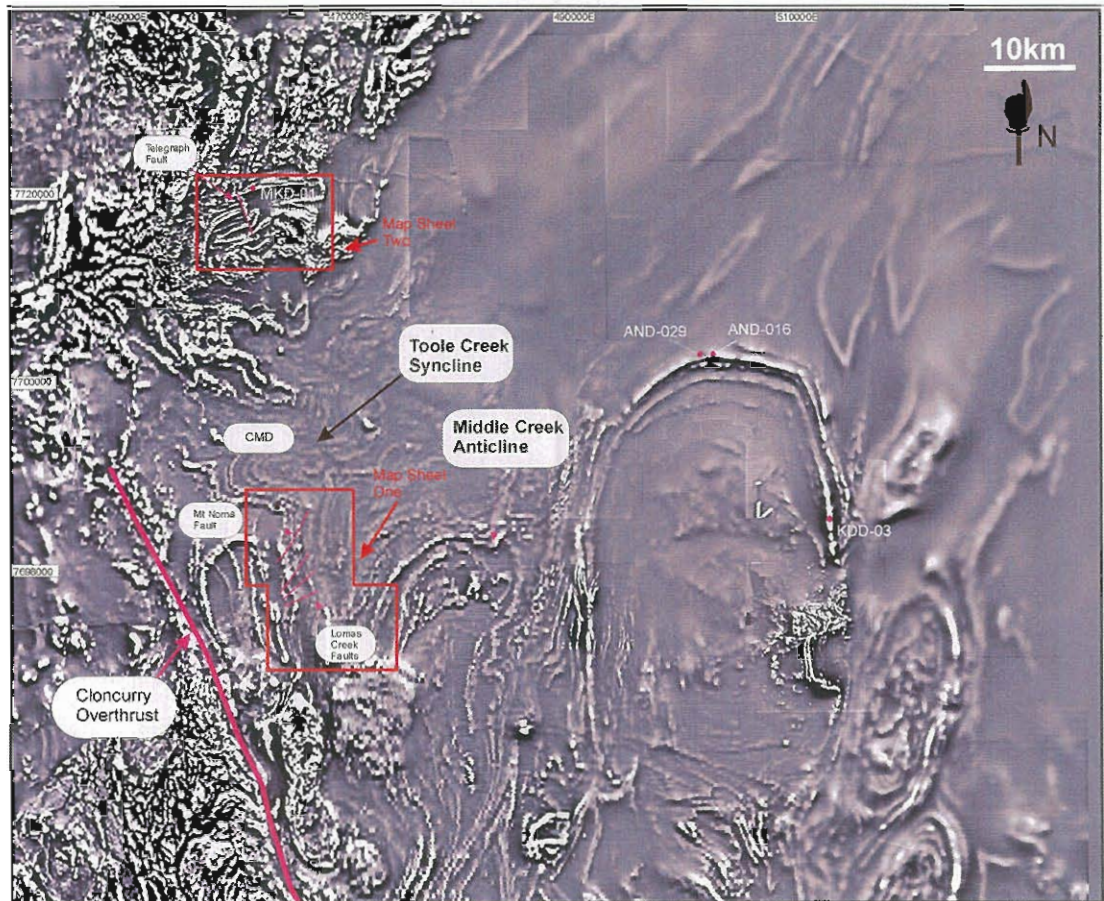
Figure 8.3: Regional aeromagnetic image (1st vertical derivative) depicting the distribution of the mafic bodies of the SCG, areas of outcrop mapped, exploration drill holes logged for this study and structures believed to be important in basin evolution. 'CMD' represents an example of a Coherent Metadolerite Sill

8.4.2 Pumpkin Gully Syncline

Within the Pumpkin Gully Syncline the north striking Telegraph Fault disrupts and influences the distribution of the Psammo-pelite facies association, as well as the associated, but volumetrically lesser, Quartzo-pelite facies association, and mafic sills and flows of the lower TCV (Fig.8.4; Ch.5). Assuming correlations based upon occurrences below the MNQ-TCV contact, thickness changes of up to 40% in all units occur across the Telegraph Fault from east to west (Fig.8.4). Outcropping to the west of this fault is the distinctive breccia of the Disrupted Facies (Ch.3) which is interbedded with Quartzo-pelite facies association lithologies, sporadic iron formations, metadolerite and metabasalt sills (Map Sheet Two).
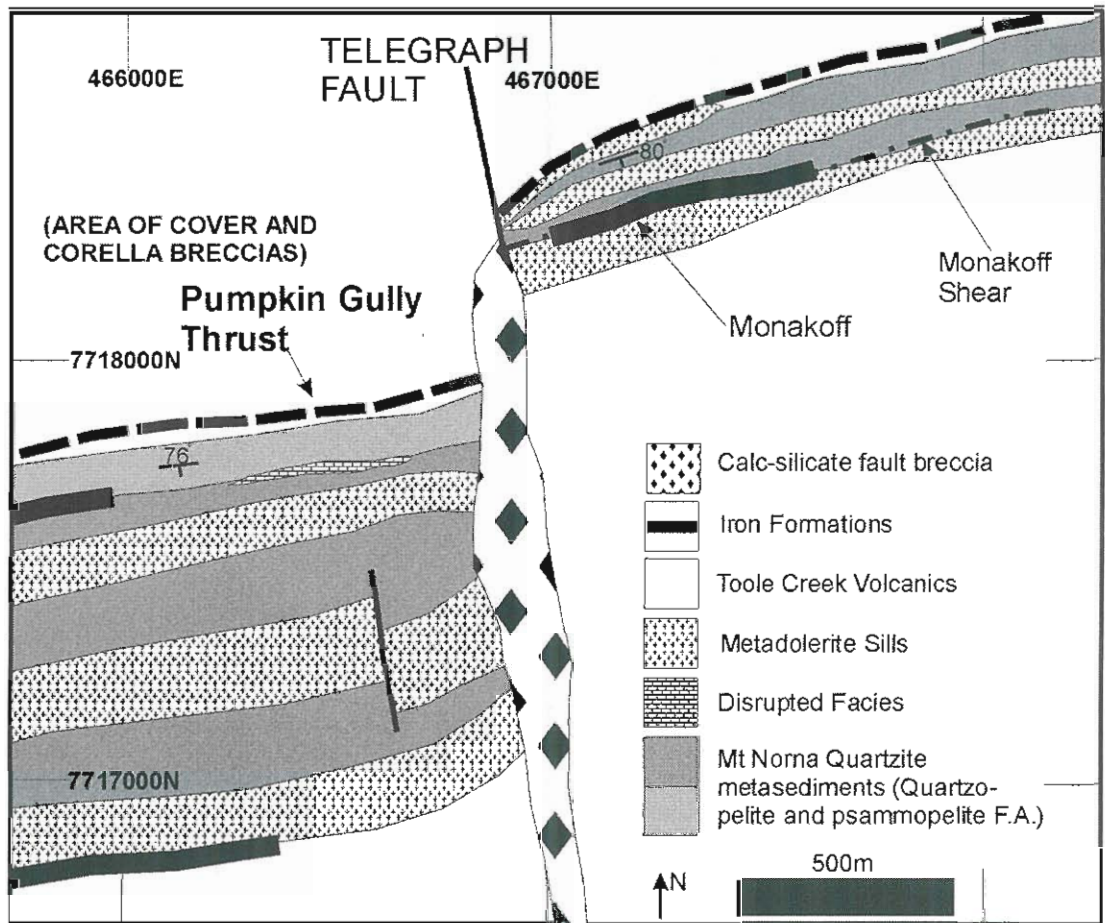
Figure 8.4: Simplified geology of the central Pumpkin Gully Syncline focused on the Telegraph Fault and adjacent thickness changes in upper SCG mafics and metasediments.

The Telegraph Fault has undergone extensive reactivation during regional deformation and even forms the focal point for D_3 and post-D_3 metasomatic alteration. Strong tectonic overprints are present in the area of the Telegraph Fault complicating interpretations of initial features.

These include the Pumpkin Gully Thrust, (Fig.8.4; Williams 1997), which is interpreted as a D_1 structure locally controlling the SCG/Corella Formation breccias contact, as well as the Monakoff Shear ~30m north of the main ore hosting iron formation (Davidson *et al.* 2002). Pods of tectonically disrupted Gilded Rose Breccia/Corella Breccias and rare SCG blocks, are emplaced along the Telegraph Fault. It is very unlikely given the tectonic and alteration overprint that primary fault

213

features are preserved within the plane of the Telegraph Fault itself. However, the mapped thickness and lithology changes across this structure imply a component of synsedimentary movement with the western block likely having been the footwall. Alternately, the presence of the breccias of the Disrupted Facies associated with syndepositional mafic sills suggests localized inflation of the sedimentary pile.

There is also a marked difference in the volcanosedimentary history of the Pumpkin Gully Syncline when compared with the Weatherly Creek Syncline (Ch.3). The MNQ-TCV transition in the Pumpkin Gully Syncline is marked by a change from the largely unidirectional currents of the Psammopelite Facies Association to the oscillatory current generated beds of the Quartzo-pelite Facies Association up sequence to the MNQ/TCV contact. This sedimentological change is succeeded abruptly by a change from dominantly Coherent Metadolerite/Massive Metabasalt syn-sedimentary sills to Massive Metabasalt with definitive extrusive features. Additionally, there are several iron formations at the MNQ/TCV contact associated with synsedimentary metadolerite and metabasalt sills.

8.5 Discussion

8.5.1 Review of palaeoflow markers

Confident reconstruction of palaeocurrent data in structurally complex terranes such as the Eastern Succession is hampered by the ambiguity present as a result of tectonic overprints (Ch.3). However, when integrated with the rest of the available geological data, palaeoflow data collected in this study was useful for determining broad sediment dispersion patterns at the time of deposition. Leeder & Jackson (1993) suggest that palaeocurrents should only be interpreted when 'observations are made on a scale comparable to that of the largest fault segments'. In the case of the SCG this is uncertain as the exact dimensions of fault segments are ill-defined.

Therefore the interpretation of palaeoflow relative to faulting has been limited to the area of data collection along the western limb of the Weatherly Creek Syncline.

As discussed in Chapter 3, palaeocurrents in tempestite sequences can have a wide range of orientations largely due to the nature of the processes of combined flow (Myrow & Southard 1996). Semi-qualitative assessment of palaeoflow through palinspastic reconstruction (Ch.3), shows that the dominant palaeoflow direction during deposition of *Pon₂* was south-southwest flowing from an east-west or northwest-southeast oriented local shoreline. This agrees with a broadly southerly deepening depocentre developing at *Pon₂* time.

Examples from active, intracontinental rift systems show that the dominant palaeocurrent orientation is commonly at a low angle or subparallel to fault scarps which mark local basin margins (Allen & Densmore 2000; Gawthorpe & Leeder 2000; Sharp *et al.* 2000). This is at odds with the evidence presented here which implies largely basin margin normal transport. However, it should be noted that most studies of modern rifts represent subaerial (*ie.* fluvial and alluvial fans) environments, not shallow marine like the SCG and are undertaken on generally larger scales (10-100's of kilometres).

8.5.2 Lomas Creek Fault Evolution

Despite complex Isan Orogeny overprints, inverted extensional faults have been recognised in sequences in the Mt. Isa Inlier through recognition of preserved stratigraphic 'wedges' and distinctive intensified folding adjacent to the fault plane (Betts 2001; Betts *et al.* 2002; *cf.* Gawthorpe & Leeder 2000; Sharp *et al.* 2000). The recognition of thickness changes in bedded metasediments outlined here, detrital

215

zircon signatures (Ch.4), volcanological processes (Ch.5) and the presence of iron

formations (Ch.7) at differing stratigraphic levels, presents sufficient evidence

for the Lomas Ck Faults, and perhaps the Telegraph Fault in the Pumpkin Gully

Syncline, as representing previously unrecognised extension events in the upper

SCG.

To produce the observed variations in thickness and map patterns, a change in the

movement on the Lomas Creek Faults between the deposition of *Pon*$_1$ & *Pon*$_2$ is

necessary. Two possible models (Fig.8.5a&b), one involving compression and the

other extension, are proposed here for this event. The first ("Scenario A") involves:-

1-deposition of *Pon*$_1$ in a northerly deepening local basin controlled by the Lomas

Creek Faults during extension, and formation of the Mt Norna Iron Formation and

smaller lateral equivalents; *2*- mid-basin inversion which reverses the movement

sense on the Lomas Creek Faults; *3*-creation of a new local depocentre to the south in

which *Pon*$_2$ was deposited; *4*- intrusion of a large metadolerite sill at the top of *Pon*$_2$ i

showing little to no effect from the Lomas Creek Faults; *5*- units of the Quartzo-

pelite facies association and Swaley Psammite facies association are deposited over

the top of this sequence.
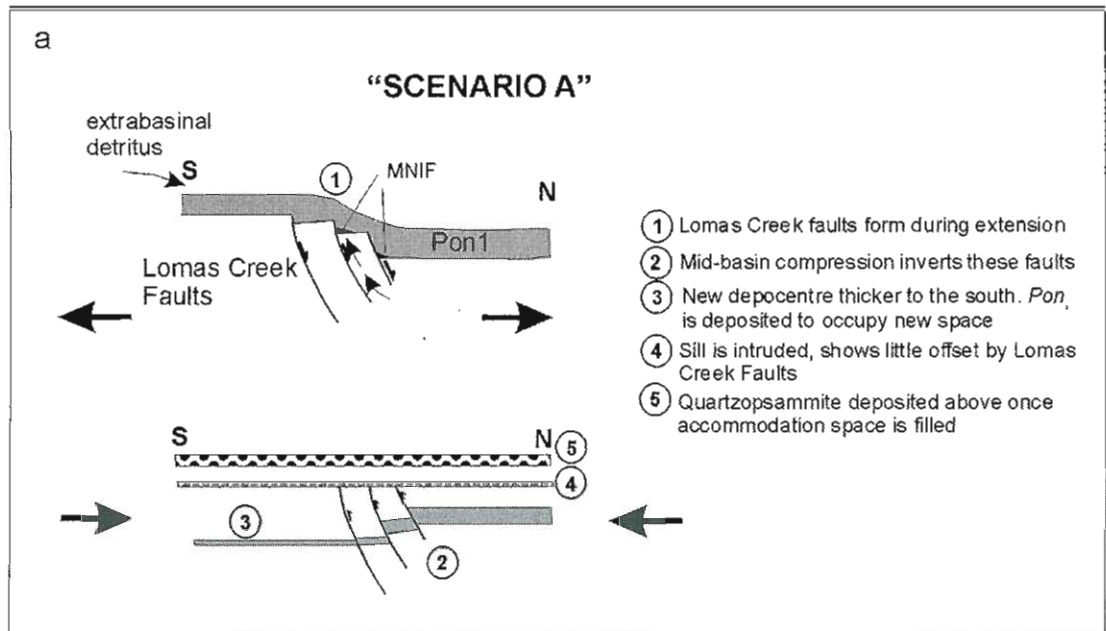
Figure 8.5a: Schematic depiction of the interpreted options for the mid-basin inversion responsible for thickness changes mapped across the Lomas Creek Faults.

The second model (Fig.8.5b-"Scenario B") involves:- *1*- deposition of *Pon₁* during a rifting phase where there are numerous closely spaced faults defining graben and half-graben, outlined in more detail below; *2*- larger scale rotation of the faults about a horizontal axis by domino-block rotation related to the transfer of faulting to a larger basin bounding fault (Barr 1987; Gawthorpe & Leeder 2000; Sharp *et al.* 2000), again discussed below. *Pon₂* is then deposited in the newly developed space to the south. The Weatherly Creek iron formation is formed through the passage of still permeable Lomas Creek Faults and the large metadolerite sill at the top of *Pon₂* intruded.
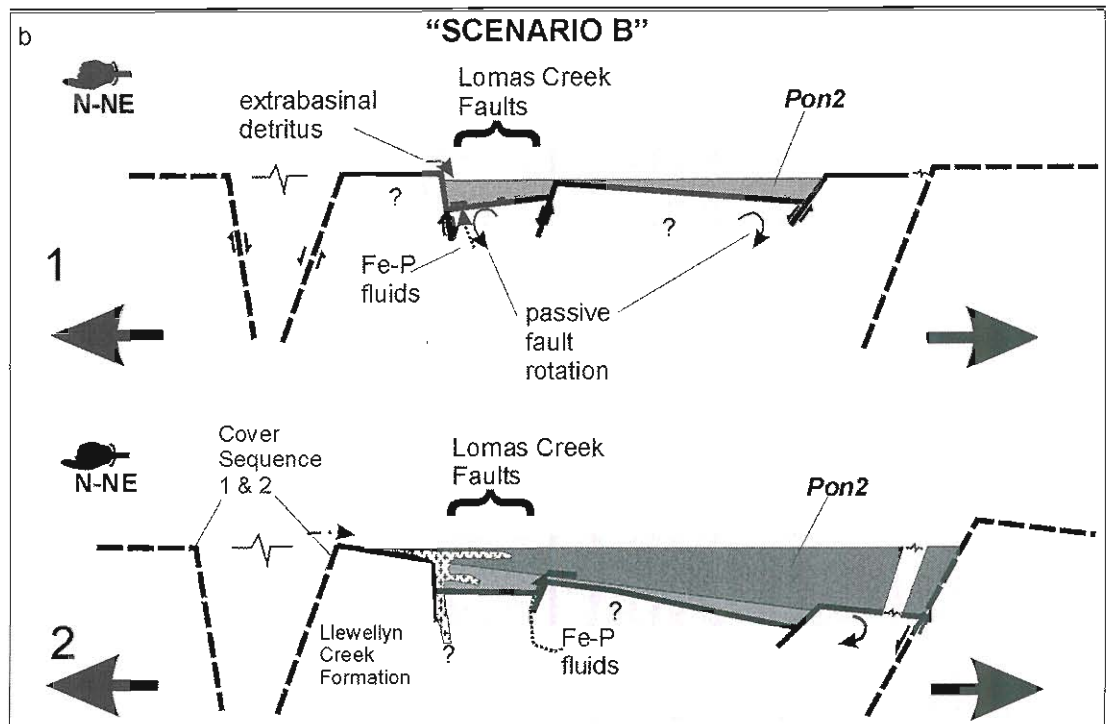
Figure 8.5b: Cartoon depicting the larger scale processes involved in the evolution of the Lomas Creek Faults during continued extension in the upper Soldiers Cap Group, modified from Sharp *et al.* (2000). Large solid arrows represent inferred extension directions. "Basement" is the extent of the Llewellyn Creek Formation limited to the interpreted area of Map Sheet One.

Scenario A requires a significant component of compression at mid-MNQ time. This is uncommon, as generally faults will be reactivated based upon the principle of 'least-work'. Extension requires considerably less energy than that required for overcoming friction necessary to invert these faults. Introducing a component of strike-slip movement along the Lomas Creek Faults could conceivably change the transpression-transtension regime by producing compression at a jog or jink in the fault. The lack of available kinematic indicators and subvertical present orientation of the Lomas Creek Faults prevents any determination of potential strike-slip processes. The passage of hydrothermal fluids (iron formations-Ch.7) and perhaps mafic bodies along the Lomas Creek Faults during MNQ time implies that the faults were not 'closed' by a compressive regime.

Models of rifting in modern basins generally invoke several distinct phases of normal fault development (*eg.* Gawthorpe & Leeder 2000; Sharp *et al.* 2000). Gawthorpe & Leeder (2000) suggested that the early phases, their 'initiation phase', is dominated by numerous, close spaced, normal faults which control local half-graben depocentres. Following this initiation phase, larger faults within the system can become inactive and cease extending ('fault death'-Gawthorpe & Leeder 2000). Generally, at this stage movement can transfer from the close spaced faults of the initiation phase, through the interaction and linkage of numerous faults, to movement on larger scale faults (Gawthorpe & Leeder 2000; Sharp *et al.* 2000). These larger scale faults commonly define the local graben or basin margin.

Using the fault evolution models of Gawthorpe & Leeder (2000) and models of passive rotation of normal faults applied to younger rifts (Barr 1987; Sharp *et al.* 2000), a generalised evolution of the Lomas Creek Faults from the time of deposition of the basal MNQ-lower TCV is presented here in cartoon form as 'Scenario B' (Fig.8.5b; Table 8.1). Sediments of *Pon$_1$* and possibly the Llewellyn Creek Formation, were deposited as a northward thickening wedge in a half-graben bounded by the Lomas Creek Faults (Fig. 8.5b; *cf.* Sharp *et al.* 2000). The relationship of these faults to the Llewellyn Creek Formation at this stage is unclear, but their development/rejuvenation coincides with the abrupt increase in sand supply represented by the basal MNQ. Hydrothermal activity at this stage was high with expulsion of Fe-P rich fluids along faults such as the Mt Norna Fault, to produce the Mt Norna iron formation and lateral equivalents (Fig.8.5b).

During transfer of deformation from the Lomas Creek Faults to an as yet unidentified boundary fault located to the south, syndepositional passive rotation of the faults about a horizontal axis and localised flexure of the footwall (Barr 1987; Sharp *et al.* 2000) resulted in renewed extension, and the creation of new accommodation space. This resulted in a local depocentre to the south in which *Pon₂* sediments were deposited (Fig.8.5b). Concurrent uplift/exposure of the adjacent hangingwall sequence (Fig.8.5b) may have exposed significant expanses of older sediments. The low numbers of Maronan Supergroup aged zircons within the samples studied in Chapter 4 discounts significant exposure of the Maronan Supergroup at this stage.

Models and examples from modern and ancient rift basins often cite increased strain in the local hanging wall of normal faults which results in folding represented by monoclines and/or hanging wall synclines (Gawthorpe *et al.*1997; Gawthorpe & Leeder 2000; Betts, Lister & Giles 2002). There is no evidence for complex folding adjacent to the Lomas Creek Faults (Fig.8.2; Fig.8.3) suggesting that such processes did not occur here.

Giles & MacCready (1997) suggested that the modern Cloncurry Overthrust may have originally been a basin bounding fault providing a possible location for the transfer of movement to the postulated southerly fault. This study focussed mainly upon the area of the western limb of the Weatherly Creek Syncline and so the direct relationship between the Cloncurry Overthrust and the Soldiers Cap Group was not studied. However, whilst this provides a model with which evidence collected in this study broadly agrees, the presence of Maronan Supergroup units to the west of the the Cloncurry Overthrust (Fig.8.1) suggests that it may represent a younger boundary related to tectonic transport (*eg.* Laing 1998) not a primary basin bounding fault.

8.4 The Cloncurry Basin Revisited-Evidence for Continued Extension

The area of SCG studied here represents a segment on the western margin of the ancient Cloncurry Basin of Newbery (1990; *cf.* Beardsmore *et al.* 1988). Based on sedimentary facies analysis, limited reconstruction of palaeoflow patterns (Ch.3), relationships of lithofacies to large faults (Ch.8), detrital zircon provenance (Ch.4), volcanology and geochemistry of mafic units (Ch.5&6), and the genesis of iron formations (Ch.7), several interpretations are made about the nature, orientation and development of the northern Cloncurry Basin at the time of deposition of the upper SCG. The interpreted environment of the SCG at upper-MNQ time (*Pon$_2$*) is depicted in Figure 8.5 and outlined at six 'time-slices' through the SCG (Table 8.1). Discussions of comparisons of the SCG to two analogous Proterozoic basins (Georgetown Inlier & Belt-Purcell Basin) are provided in Chapter 9.

Firstly, the local palaeoenvironment is different to that interpreted by previous researchers in the area (Ch.3). The upper SCG is defined here as the product of tempestites on a shallow, proximal-medial shelf. Components of both alongshore and offshore flow to an interpreted southerly depocentre are evident in reconstructed palaeoflow markers.

Locally in the Weatherly Creek Syncline, mapped sediment thickness patterns, zircon provenance dating (Ch.4) and palaeoflow markers suggest a south-southeasterly deepening local depocentre controlled locally by extensional structures (Lomas Creek Faults; Fig.8.5). Detrital zircon age data (Ch.4; *cf.*Ch.7) shows that extrabasinal transport (Fig.8.5; Fig.8.6) and erosion were active and that the source for basin fill was likely from Cover Sequence 2 rocks or as yet unidentified Cover Sequence 1 and Archaean units.
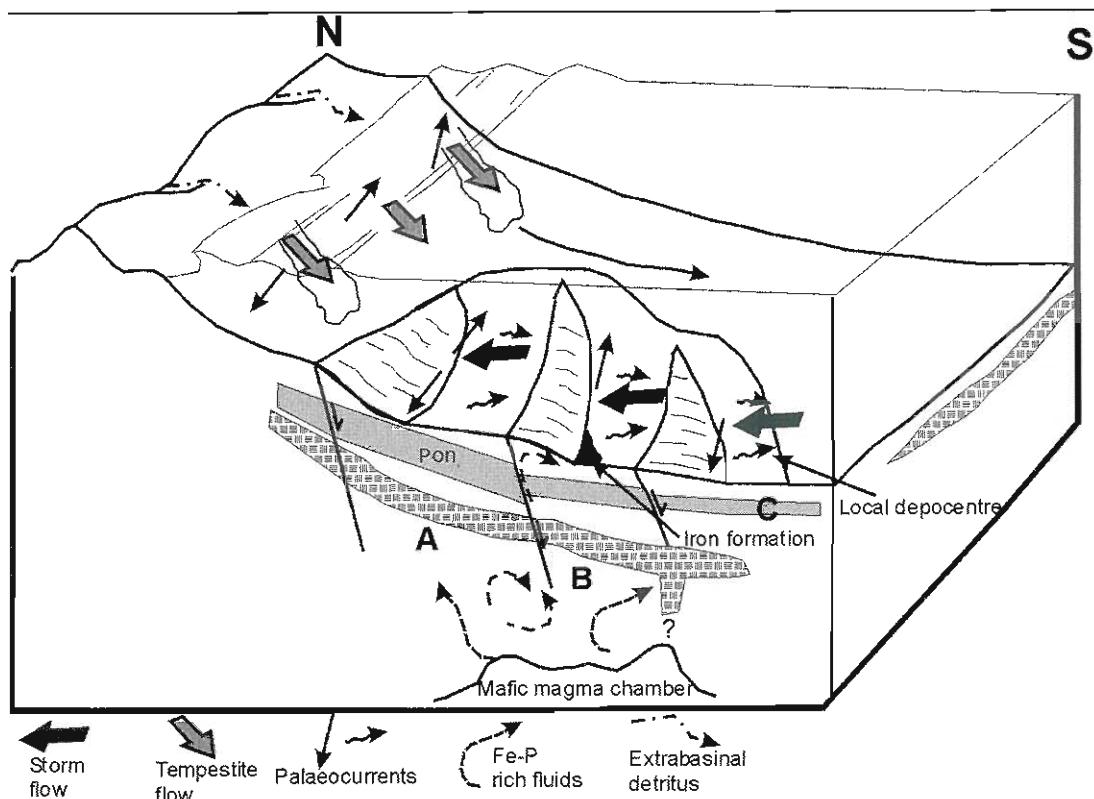
Figure 8.6: Schematic representation of the sources of basin fill and orientations of faults following rotation about a horizontal axis for the Soldiers Cap Group, at *Pon₂* time, based upon sedimentological, provenance and palaeflow data, lateral and vertical scales are arbitrary. A,B & C represent inferred fault bound blocks. Processes occurring range from storm induced current flow, "reflected" across-slope movement of sediments and exhalation of iron formations underlain by the intrusion of a large inferred mafic (ferrobasalt) magma chamber (outlined at the base of the figure).

The clusters of large, dominantly northeast oriented faults that dissect the mid-upper Mt Norna Quartzite (Mt Norna Fault and Lomas Creek Faults) are interpreted here as syn-sedimentary normal faults reactivated\rotated during deposition of the Mt Norna Quartzite and later inverted during the Isan orogeny. These faults bound broadly southerly dipping, tilted fault blocks that had a localised affect on basin topography, palaeoflow and sediment thickness (Fig.8.5; Fig.8.6). These faults also provided pathways for rising hydrothermal fluids that produced local iron formations (Fig.8.5; Fig.8.6). The more regional extent of iron formations (Ch.7) suggests that many similar localised extensional structures existed across the basin.

Stratigraphic Level	Local Tectonics	Sedimentation	Magmatism	Hydrothermal Acitivity
Toole Creek Volcanics	Continued steady extension	Deeper water facies including sporadic black shales	Syn-sedimentary dolerite/gabbro sills and extrusive ferrobasalts	Sporadic small iron formations
Upper Mt Norna Quartzite (*Pon₃*)	Continued steady extension	Continuing tempestite-turbidite deposition	Syn-sedimentary dolerite/gabbro sills	Weatherly Creek iron formation at base
Mid Mt Norna Quartzite (*Pon₂*)	Extension on Lomas Creek Faults combined with rotation to produce a southward deepening local basin. Transfer of movement to a southern boundary fault	Change from turbidity to tempestite sequence. Continued extrabasinal input.	Syn-sedimentary dolerite/gabbro sills	Weatherly Creek iron formation at top
Lower Mt Norna Quartzite (*Pon₁*)	Extension on Cloncurry Fault, Lomas Creek Faults and Mt Norna Fault, n-ward deepening	Energetic, high density turbidity currents, high extrabasinal input	Syn-sedimentary dolerite/gabbro sills	Mt Norna iron formation at base
Llewellyn Creek Formation	Undefined.	Turbidite sequence	Large dolerite/gabbro sills	Undefined

Table 8.1: Interpreted chronology of tectonism, sedimentation, volcanism and hydrothermal activity during the formation of the upper Soldiers Cap Group, north of the Williams Batholith.

Mafic magmatism and volcanism also appears to have had an important influence on basin development. However, there is no evidence that it fundamentally influenced basin topography. For instance, there is no evidence for inflation of the sedimentary pile by the intrusion of mafic units (*eg.* no onlapping sediment/mafic contacts or localised brecciation, Fig.8.1). The intrusion of mafics appears to be a driving force behind the circulation of hydrothermal fluids responsible for the deposition of the Weatherly Creek and Mt Norna iron formations. This is similar to models of hydrothermal evolution associated with the Moyie Sills in the Proterozoic Aldridge Formation in Canada, host to the massive Pb-Zn Sullivan deposit. Comparisons between mafic magmatism and hydrothermal history in the SCG and global analogues are explored further in Chapter 10.

Deposition of the Toole Creek Volcanics represented continued extension and deepening of the Cloncurry Basin, with an increase in mafic volcanism represented by the thicker pile of mafic volcanics above the MNQ. Hydrothermal activity, in the form of iron formations, appears to have been limited to the earlier parts of the sequence and is relatively rare in the TCV.

The possibility that the variations between mafic geochemistry, magmatic history and sedimentation mechanisms between the Weatherly Creek Syncline and Pumpkin Gully Syncline represent several smaller fault controlled sub-basins, perhaps related to at least two separate underlying mafic magma chambers, cannot be discounted. Unfortunately, the structurally dismembered nature of the sequence makes this difficult to resolve. Further work focused along similar lines to the study here of the Lomas Creek Faults in the Pumpkin Gully Syncline and Toole Creek Syncline areas would greatly assist the resolution of this question.

It is worth noting that this new analysis of the upper SCG defines a change in geological environment from the 'sag-phase' rift fill of the Llewellyn Creek Formation and upper Fullarton River Group to renewed extension and mafic magmatism. There is limited evidence for syndepositional extension and magmatism in the latter units (Blake *et al.* 1987; Beardsmore *et al.* 1988; Newbery 1990). Beardsmore *et al.* (1988; *cf.* Newbery 1990) did suggest that the immature sediments of the basal Fullarton River Group were derived from exposed syndepositional felsic volcanics and that bimodal volcanism was related to high heat flow and high extension rates. The detailed history of extension in the lower Maronan Supergroup is not known, providing a need to evaluate this using the detailed sedimentological, geochemical and volcanological methods of this study. Given the metal endowment

of the Maronan Supergroup (*eg.* Cannington) this would be extremely useful in confining the basin conditions present during formation of Broken Hill-type deposits.

8.4 The Soldiers Cap Group in an Australian Proterozoic context

8.5.1 Mt Isa Inlier Tectonostratigraphic Context

The published age overlaps between the Western Succession Mt Isa Group and Soldiers Cap Group has been used to suggest that both are products of a single tectonic event, the 1710-1655 Ma Mt Isa Rift Event (Ch.2; Fig.2.2; Betts 1997; O'Dea *et al.* 1997; Page & Sun 1998; Betts & Lister 2001). Renewed northwest-southeast directed rifting of Mt Isa Rifting Event age has been noted in the Western Succession (Betts *et al.* 1999). North-south directed extension has also been recognised in the older *ca.*1740Ma Wonga Extension Event of the Eastern Succession (Passchier 1986; Betts & Lister 2001; Betts *et al.* 1999). Although complex Isan Orogeny overprints make exact reconstructions difficult, the overall southward deepening of the Soldiers Cap Group outlined in this study broadly agrees with these regional extension events and implies that the larger scale connection between the Eastern Succession and the remainder of the Mt Isa Inlier suggested by previous authors may be applicable (O'Dea *et al.* 1997; Betts & Lister 2001).

The lack of large sequences of carbonates evident in similarly aged units of the Western Succession does imply that the broad geological environment of the Maronan Supergroup was significantly different to that occurring in the rest of the Mt Isa Inlier. One way to interpret this is that the Maronan Supergroup represents an 'exotic' extrabasinal crustal block tectonically transported from the east during the Isan Orogeny (*cf.* Laing 1998). However, the likelihood of an Eastern Succession/ Mt Isa Inlier detrital source evidenced in detrital zircon spectra, points to the Maronan

Supergroup as being close to 'in-place', in contradiction to the models requiring

extensive westward tectonic transport (*eg.* Laing 1998).

There is significant scope for future provenance-driven research defining where the

Maronan Supergroup falls within the larger scale tectonic evolution of the Mt Isa

Inlier and Proterozoic Northern Australia and testing this against recent plate tectonic

driven reconstruction models (Giles & Betts 2002 a,b).

8.5.2 Australian Proterozoic tectonostratigraphic links

The close temporal and geological links between the Maronan Supergroup, Broken

Hill Block and Georgetown Inlier and base-metals mineralisation in the former two

terranes, have resulted in two differing tectonic models for their genesis, the Hiltaba

Event of Lister *et al.* (1997) and the Diamantina Orogeny of Laing (1996).

The Diamantina Orogen of Laing (1996) was interpreted as affecting a large part of

the Proterozoic Australian crust including the Broken Hill Block, Mt Isa Inlier and

the Georgetown Inlier. This tectonic event is interpreted as coeval with the

neighbouring Carpentaria Orogeny, overlying a Barramundi Orogeny substrate, and

involving the 'classical' Proterozoic rift sequence of ensialic extension and

subsequent compressional closure (*cf.* Kroner 1983; Etheridge *et al.* 1987; O'Dea *et*

al. 1987). The Diamantina Orogen is described by Laing (1996) as differing from the

surrounding orogens in having a greater volume of mafic magmatism, pelitic

metasediments and higher Fe-oxidation state.

The 'Hiltaba Event' was proposed by Lister *et al.* (1997) as having an influence over

the continental crust of Australia at ~1590 Ma and being linked to a major

metallogenic event responsible for the Cu-Au deposits in the Gawler Craton, and base metals mineralization in the Broken Hill Block and western Mt Isa Inlier. The tectonic model proposed by Lister *et al.* (1997) involved the subduction of the 'Hiltaba Slab', mafic underplating and magmatism in the overlying plate at an active tectonic margin which stretched from South Australia (Gawler Craton) to Proterozoic Northern Australia (Mt Isa Inlier), including the Broken Hill Block and Georgetown Inlier. The ~1590 Ma Hiltaba Event would be represented in the Eastern Succession by peak metamorphism (1584±4 Ma Page & Sun 1998; Giles 2000). This idea of far-field tectonics influencing the geology of the Mt Isa Inlier has been more fully explored recently by Giles *et al.* 2002 (*cf.* Giles & Betts 2000a,b; Betts *et al.* 2002) who suggested that *ca.* 1.8-1.6 Ga aged convergent margin tectonics were largely responsible for the evolution of the Mt Isa Inlier. According to this model the Mt Isa Inlier is the product of extension within a backarc basin in the interior of the Proterozoic Australian continent related to subduction at a convergent margin to the south.

A detailed discussion of the relative merits of these models is beyond the aims of the present study and will not be undertaken here. However, it should be noted that detrital zircon dating, and detrital geochemical signatures in iron formations provided by this study suggests that the Soldiers Cap Group could have been derived largely from local (Eastern Succession) sources, and mafic sills in the Soldiers Cap Group do have distinctive intracontinental tholeiite chemistry and a lack of any subduction signatures (*cf.* Wyborn & Blake 1982; Williams 1998).

Chapter Nine- Comparison of the Soldiers Cap Group to the Aldridge Formation, B.C. Canada, and the Etheridge Group, Georgetown Inlier northeast Queensland and implications for base-metal exploration

9.1 Introduction

Numerous previous authors have discussed the similarities between the Maronan Supergroup and the Willyama Supergroup in the Broken Hill Block (*eg.* Laing 1990;1996) using them as the basis of direct correlation. Despite a recent compilation of age data and definition of tectonomagmatic events by Raetz *et al.* (2002), definition of discrete extension structures or remnant basin architecture is problematic due to the severe deformation and metamorphic history of the Broken Hill Block. Therefore, the Broken Hill Block was considered inappropriate for a direct comparative study with the Soldiers Cap Group, but will still be discussed below in context with tectonostratigraphic links between several Australian Proterozoic terranes.

Two other Mesoproterozoic rift terranes, the Georgetown Inlier (Etheridge Group, northeast Queensland) and the well-studied Belt Purcell Basin (Aldridge Formation, British Columbia, Canada) which both contain late stage mafic magmatism within siliciclastic upper sediment packages, were considered ideal comparator basins. The purpose of such comparison is to evaluate mineralisation potential in the Soldiers Cap Group and provide possible directions for future exploration. Specifically, this section aims to provide criteria for the recognition of renewed rifting in intracontinental basins by determining the geological variability amongst rift basins with histories of renewed rifting.

The recent publication of a comprehensive volume on the Sullivan Pb-Zn deposit and surrounding units by the Mineral Deposits Division of the Geological Association of Canada (Lydon *et al.* 2000) greatly assisted the proposed comparison. The author also attended a field visit and an international conference focused on the geology of the region in May 2000. A literature search and discussions with University of Tasmania academics and postgraduates was the main basis of the comparative study of the Etheridge Group in the Georgetown Inlier.

9.2 Etheridge Group, Georgetown Inlier, northeast Queensland, Australia

This comparison was based largely upon a literature search which produced a relatively limited but useful dataset. Much of this data predates and is included in a detailed synthesis of the Georgetown Inlier by Withnall *et al.* (1988; *cf.* Bain *et al.*1985a; 1985b, Withnall 1983;1985a;1985b; Withnall *et al.* 1976). Only limited geochemical data is available in Withnall (1985a). U-Pb SHRIMP dating of mafic intrusives is available in Black *et al.* (1998).

9.2.1 Geological Setting

The Georgetown Inlier (Fig.9.1) represents the largest expanse of Proterozoic rocks exposed in northeastern Queensland, covering some 25-30 000 km^2 bounded to the east by the northern end of the Palaeozoic Tasman Orogeny and separated from other Proterozic units in the region (Coen and Yambo Inliers) by the Mesozoic sediments of the Carpentaria Basin. The Georgetown Inlier has been divided into three Subprovinces from west to east:- the Croydon, Forsayth (central and oldest) and Greenvale respectively (Henderson 1980; Withnall *et al.* 1980).
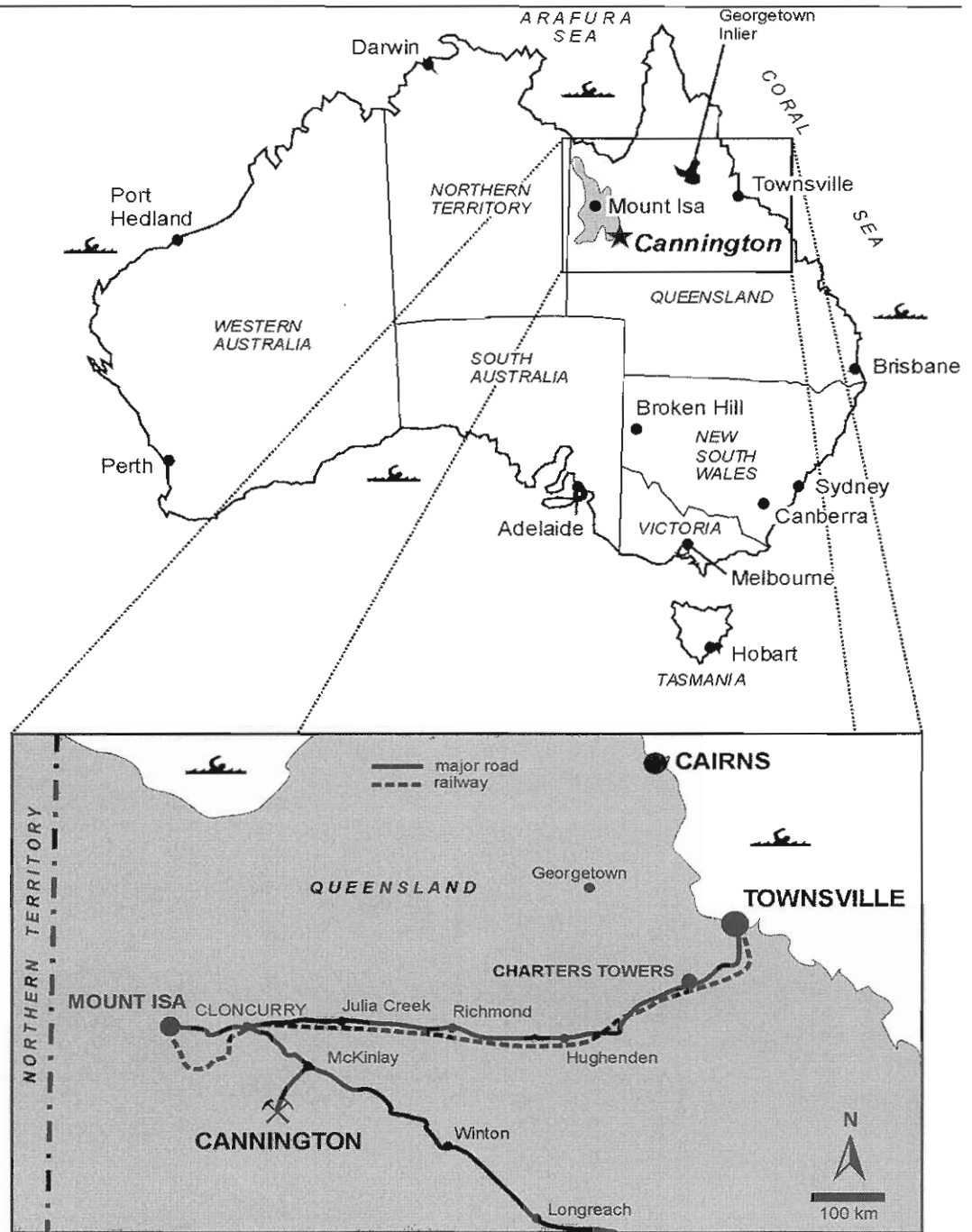
Figure 9.1: Location of the Georgetown Inlier relative to other Australian Proterozoic elements

The Etheridge Group comprises over half of the outcrop area of the Forsayth

Subprovince (Withnall *et al.* 1988). The base of the Etheridge Group itself is not

exposed but the overall sequence is interpreted as having a minimum thickness of

13km (Withnall *et al.* 1988). The Etheridge Group has been subdivided by Withnall

& Mackenzie (1980; *cf.* Withnall *et al.* 1988) into the basal shallow water sediments

of the Bernecker Creek Formation which are interpreted as stratigraphically equivalent to the gneisses, mica schists and quartzites of the Einasleigh Metamorphics. This is overlain by the various shallow water sedimentary units of the Robertson River Subgroup (Fig.9.2; Fig.9.3) and the aphyric metabasalts of the Dead Horse Metabasalt. Overlying this basaltic sequence are the subtidal sediments of the Corbett Formation and Lane Creek Formation. Possible chemical sediments and "tourmaline rich rocks" are present in the Tin Hill Quartzite Member which are located stratigraphically in the mid-Corbett Formation (Fig.9.2; Withnall *et al.* 1988). Overlying the Etheridge Group are the fluvio-marine metasediments of the Langlovale Group, subaerial felsic volcanics of the Croydon Volcanic Group and fluvial sandstones-silstones of the Inorunie Group (Withnall *et al.* 1988; Black *et al.* 1998). Intruding the Etheridge Group from the basal units to the Lane Creek Formation are the metadolerite, metagabbro and amphibolite sills of the Cobbold Metadolerite (Fig.9.2).

The tectonostratigraphic history of the Etheridge Group is relatively poorly constrained due to the lack of exposed basement and until recently, a lack of reliable U-Pb geochronology. Following recent U-Pb SHRIMP dating on zircons (Black *et al.* 1998) from intrusive units in the Etheridge Group, it was inferred that deposition of the sedimentary pile on a broad stable shelf in an epicontinental sea (Withnall *et al.* 1988) began at ~1700 Ma and continued for at least 100 Ma. Subsidence within the basin appears to have been relatively uniform until after the extrusion of the Dead Horse Metabasalt, when there is a marked change from shallow- to deep-water facies. Granitoid intrusion occurred synchronous with the main deformation events.

Deformation within the region is defined by two major Proterozoic events, the 1570±20 Ma (Black *et al.* 1979) Ewamin Orogeny and the recently U-Pb dated ~ 1550 Ma Jana Orogeny (Black *et al.* 1998). The Ewamin Orogeny (D_1) formed upright to overturned, tight folds with 1-10km wavelengths and a concurrent axial planar schistosity-gneissosity. The Jana Orogeny (D_2) is represented by N-S oriented upright folds with 1-2km wavelengths which vary from very tight-isoclinal in the eastern part of the Inlier to more open in the west (Withnall *et al.* 1988).

Metamorphism within the Inlier ranges from lower greenschist facies in the southeast to a granulite facies core in the northeast, and is interpreted as being largely confined to the Etheridge Group (Black *et al.* 1998). Metamorphic events dated by Rb-Sr isochrons (Black *et al.* 1979), are closely linked to the two major orogenic events D_1 (M_1), occurring at 1570±20 Ma, which reached amphibolite facies conditions and D_2 (M_2), occurring at 1470±20 Ma, which in places reached granulite facies conditions (Withnall *et al.* 1988; Black *et al.* 1998). In the higher grade portion of the Inlier the early metamorphic events linked to D_1 are difficult to define due to the strong overprint of D_2. Several later metamorphic events tied to later orogenic events have been associated with retrogression and have been suggested as being largely Palaeozoic events.

Granitic intrusions occurred throughout the Inlier over a period from 1540-1560 Ma largely concurrent with orogenic events and include granites in the Croydon Volcanic Group (Esmerelda Granite 1558±4 Ma; Black & McCulloch 1990) and other granitoids in the Forsayth Subprovince (Forsayth Granite 1550±6 Ma & Mistletoe Granite 1544±7 Ma; Black & McCulloch 1990).

Langdon River Mudstone		
Candlow Formation		
Heliman Formation		
Townley Formation		

Robertson River Subgroup	Lane Creek Formation	Cobbold Metadolerite	Juntala Metamorphics
	Tin Hill Quartzite		
	Corbett Formation		
	Dead Horse Metabasalt		
	Daniel Creek Fomation		Einasleigh Metamorphics
	Bernecker Creek Formation		

Figure 9.2: Stratigraphy of the Etheridge Group. After Withnall *et al.*(1988).

9.3.2 Sedimentology

Sedimentary structures have been obliterated in the higher grade sections of the
Etheridge Group, however in many places primary sedimentary features are
preserved. These have been outlined in Withnall *et al.* (1988) but will also be
summarized here for a later comparison with the detailed sedimentology of the
Soldiers Cap Group outlined in Ch.3.

The Bernecker Creek Formation (Fig.9.2; Fig.9.3) is comprised of dolomitic-
calcareous fine-grained sandstones with a wide variety of sedimentary structures
including wave ripples, wrinkle marks, aeolian microridges, swash marks, all
features indicative of periodic exposure (Withnall *et al.* 1988). Tidal influences are
defined by flaser- and wavy-bedding but an absence of bipolar cross bedding. Scour
and fill features, lag gravels and planar- and trough-cross laminations are all features
interpreted by Withnall *et al.* (1988) as indicative of channelisation.
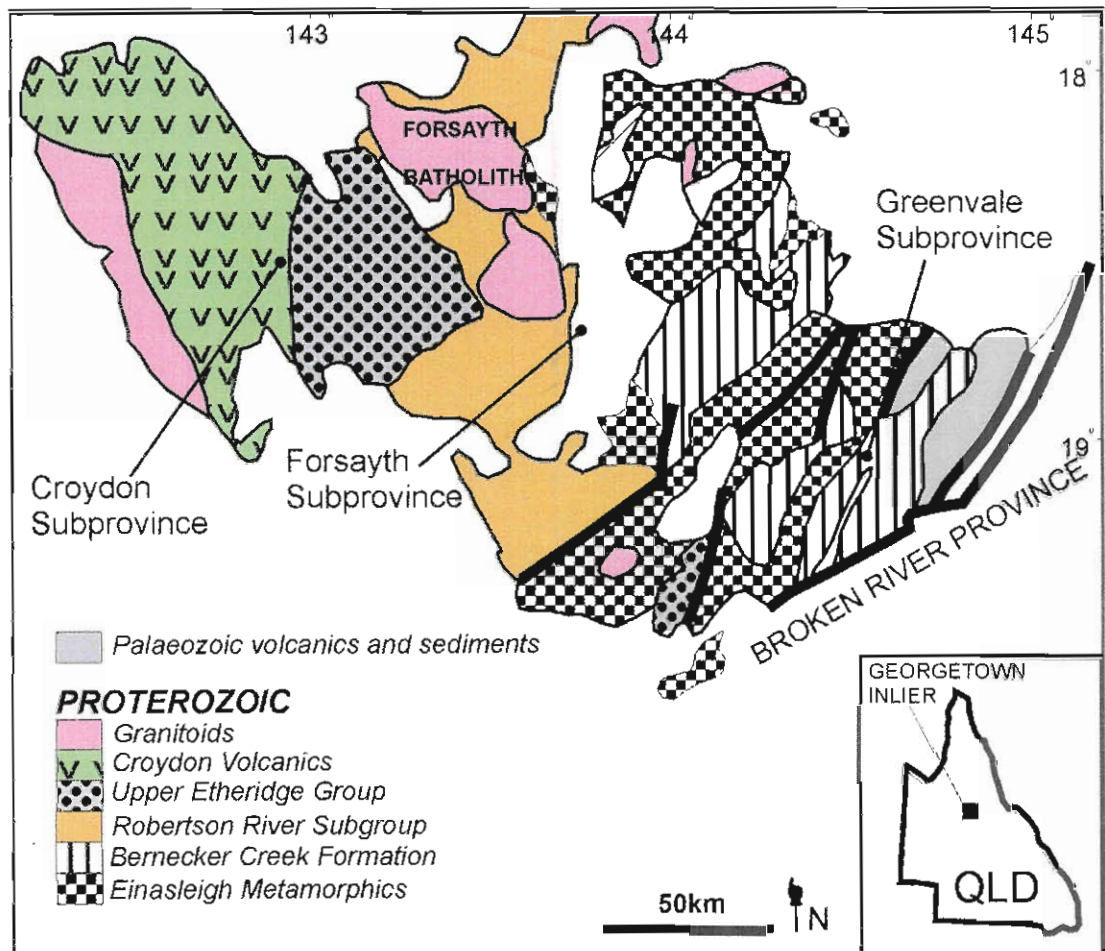
Figure 9.3: Simplified regional geological interpretation of the Georgetown region, modified from Withnall *et al.* (1988).

Horizontally laminated bedding, sand shadows and streaming lineations are all features suggested as indicative of a beach or shoal environment. All of these various lines of sedimentological evidence were combined by Withnall *et al.* (1988) to infer that the Bernecker Creek Formation was deposited in an active, wave dominated shore line or tidal flat.

The overlying Daniel Creek Formation (Robertson River Subgroup-Fig.9.2) is generally more pelitic and less calcareous and has more evidence of scouring and less of periodic exposure which lead Withnall *et al.* (1988) to suggest a deltaic as opposed to near-shore environment. Overlying the southern half of the Daniel Creek Formation are the metabasalts of the Dead Horse Metabasalt (Fig.9.2) which comprise mainly aphyric metabasalts with some pillow lava and hyaloclastites

intercalated with minor mudstone and chert. A change in environment from the shallow-water facies underlying the Dead Horse Metabasalt is represented by the Corbett Formation which is comprised of deep water mudstones and minor chemical sediments and tourmaline rich rocks of the Tin Hill Quartzite Member (Fig.9.2). The Lane Creek Formation is largely interpreted as a deeper water unit similar to the Corbett Formation (Withnall *et al.* 1988). However, the presence in the upper part of small-scale trough cross bedding and marly limestone and calcareous beds may indicate the return of shallower water conditions (Withnall *et al.* 1988).

Numerous metadolerite sills collectively termed the Cobbold Metadolerite, from 3-500m thick, and traceable for up to 10km along strike and intrude sediments from the lower Etheridge Group up to and including the Lane Creek Formation (Fig.9.2). Contact relationships between the mafics and sediments are poorly defined although Withnall *et al.* (1988; *cf.* Black *et al.* 1998) described them as sills and rare dykes. Primary textures were rarely preserved within these units and include preserved plagioclase laths and blastophytic amphiboles (Black *et al.* 1998).

The units of the upper Etheridge Group are composed of differing amounts of carbonaceous mudstone, siltstones, fine-grained sandstones and rare thin limestones. Sedimentary structures include slumping, distorted bedding, disrupted laminae, sandstone dykes, flame structures and load casts with a lack of channeling and scouring (Withnall *et al.* 1988). Rare gypsum pseudomorphs and stromatolites have been noted and in combination with the features described above led Withnall *et al.* (1988) to propose a tidal-flat environment for the upper Etheridge Group.

9.3.3 Mafic Magmatism

As mentioned above there are two main mafic units contained within the sedimentary

sequence of the Etheridge Group, the Dead Horse Metabasalt and the Cobbold

Metadolerite (Fig.9.2). Withnall (1985a) analysed some 54 samples from these units

and used major element ratios to define differences between the units and attempt a

petrochemical classification to compare these units to modern volcanics and attempt

to provide a tectonic setting for them. As discussed in Chapter 5, the use of major

element ratios in the classification of metamorphosed and altered mafic rocks is

fraught with numerous pitfalls. The most important effect being the degree of

mobility of those elements commonly used in petrogenetic classifications such as Fe,

Mg, Al, Na and K. Evidence from the Soldiers Cap Group presented in Ch.6 shows

that many of these elements were mobile during metamorphism and alteration and

would therefore provide spurious results on commonly used petrogenetic

classifications. However, Withnall (1985a) attempted to address element mobility

using log molecular proportion ratios, after Beswick & Soucie (1978), which

theoretically delimits unaltered 'greenstones' to a narrow range. Using this

discriminator they defined Fe and Mg as relatively immobile and that K, Na and Rb

were mobile. The likely mobility of elements used by Withnall (1985a) in the

Soldiers Cap Group prevents a direct graphical comparison between the two

sequences.

Using 'Mg-number' and 'immobile elements' (Ti, Fe, Mn, P, Zr, Y & Nb) Withnall

(1985a) defined the two mafic units as being from a chemically similar parent

magma but the result of at least two separate magma 'pulses'. Withnall (1985a) also

showed that samples of the Cobbold Metadolerite from throughout the sequence

were less fractionated on the whole than the metabasalts of the Dead Horse

Metabasalt. Differing trends in Ni & Cr were interpreted as being the product of different fractionation histories. Ratios of immobiles (Zr/Nb) were used to define the Cobbold Metadolerite and Dead Horse Metabasalt as a comagmatic tholeiitic suite with an interpreted clinopyroxene fractionation trend.

Using the database available at that time Withnall (1985a) directly compared the Etheridge Group mafics with other Australian Proterozoic mafic units including the Soldiers Cap Group. In this comparison Withnall (1985a) noted that "the mafic rocks from the Etheridge Group show the most similarities to those from the Soldiers Cap Group" and were also comparable to other 'first-cycle' mafic units in the Australian Proterozoic.

Overall, the interpreted evolution of Withnall (1985a) was of at least two discrete pulses of magmatism within a shallow-water (shelf) sedimentary sequence represented by the Cobbold Metadolerite and an overlying phase of extrusion represented by the Dead Horse Metabasalt. Tectonically, they were inferred as the product of convective mantle upwelling producing extension in the overlying sialic crust.

9.3.4 Summary and Comparison to the Soldiers Cap Group

The Georgetown Inlier is interpreted by Withnall *et al.* (1988) as the product of 'sag-phase' Proterozoic intracontinental rifting. The concurrent underlying 'rift-phase' is either not exposed or under younger cover to the east (Withnall *et al.* 1988). The Etheridge Group was deposited on a broad continental shelf in a shallow water environment. Fractionated Fe-rich mafic rocks of the Cobbold Metadolerite were intruded into the lower Etheridge Group in at least two discrete pulses. Extrusion of

the Dead Horse Metabasalt accompanied a change from shallow water facies of the lower Etheridge Group to the deeper water and minor chemical sediments of the upper Etheridge Group. Granitic magmatism occurred largely at the same time as major deformation events.

There are a number of striking similarities between the Etheridge Group and the Soldiers Cap Group, outlined in Table 9.1, including (1) similar aged environments of deposition in the 'sag-phase' of an intracontinental rift, on a shallow shelf, broadly deepening up-sequence (2) geochemically (and temporally) similar voluminous continental tholeiite volcanism/magmatism (Withnall 1985a) with a similar Fe-rich evolutionary trend (3) similar ages of mafic magmatism (sills and flows) associated with late stage tectonothermal activity at *ca.* 1690-1670 Ma (Toole Creek Volcanics versus Cobbold Metadolerite) and a change in sedimentation styles (4) 'chemical sediments' present in both sequences (Tin Hill Quartzite-metachert) located stratigraphically above and/or equivalent to large volumes of mafics (5) the presence of BHT style mineralisation (*eg.* Railway Flat, Mt Misery; *cf.* Willis 1996) with similar Pb isotope signatures to Eastern Succession mineralisation (Carr & Sun 1996).

The differences between the two terranes are subtle but include (1) discrete pulses of mafic magmatism in the Georgetown Inlier opposed to relatively constant sequential intrusion in the Soldiers Cap Group (2) lack of distinctive iron formations in the Georgetown Inlier, the Tin Hill Quartzite may be analogous but this is unequivocal (3) lack of evidence for renewed extension along faults within the basin.

Combined with the previously published temporal and geological links (Laing 1990; 1996; Black *et al.*1995; Black *et al.* 1998; Page & Sun 1998) and the inferred tectonic links (Laing 1996; Lister *et al.* 1997) the geological similarities expressed here show that the Etheridge Group and the Soldiers Cap Group are close geological analogues. However, as mentioned above there is no direct evidence they were ever in spatial contact and the larger scale tectonic implications of this remain a topic of some debate (*eg.* Laing 1996-Diamantina Orogeny vs. Lister *et al.* 1996 Hiltaba Event) and an intriguing area for further study.

9.4 Aldridge Formation, British Columbia, Canada

The comparison of the Soldiers Cap Group to the Aldridge Formation, host to the world-class Sullivan Pb-Zn-Ag deposit, was one of the motivations of the present study. Based upon the excellent work presented in Lydon *et al.* (2000) and a field visit to the district, comparisons of the tectonomagmatic setting (Höy *et al.* 2000); sedimentary basin development (Price & Sears 2000; Turner *et al.* 2000a; Turner *et al.* 2000b); magmatic history (Anderson & Goodfellow 2000; Gorton *et al.* 2000); chemical sediment geology and geochemistry (Jiang *et al.* 2000; Slack *et al.* 2000) and the hydrothermal evolution and overall setting of the Sullivan orebody (Lydon & Paakki 2000; Turner *et al.*1996; Turner *et al.* 2000b), with the Soldiers Cap Group were possible. Table 9.1 provides a summary of the various geological parameters used in the comparative study.

9.4.1 Belt-Purcell Basin Regional Setting

The Belt-Purcell Basin is a major Proterozoic tectonostratigraphic element which stretches from southwest British Columbia across the United States border (Fig.9.4). The Aldridge Formation (Prichard Formation in U.S.) makes up the majority of the

sedimentary sequence of the Belt-Purcell Basin. Four successive tectonic events have been recognised in the Aldridge Formation (Höy *et al.* 2000) each directly linked to changes in sedimentation, and increased hydrothermal and magmatic activity.

The Aldridge Formation is divided into the informal but widely accepted, Lower, Middle and Upper sequences (Fig.9.5; Höy *et al.* 1993). The massive Sullivan deposit lies at the Lower-Middle Aldridge transition. Voluminous mafic sills intrude at least half of the Lower Aldridge Formation and a lesser amount are present in the Middle Aldridge (Turner *et al.* 1995). These sills are spatially and temporally linked to Sullivan Pb-Zn mineralisation and associated alteration (Turner *et al.* 1995). Significant syn-rift faulting imposed important controls on sedimentation and is also closely linked to base-metals mineralization (Lydon 2000).

Structure within the region is dominated by the north-plunging Purcell Anticlinorium (Price 1981). Locally, the Aldridge Formation is deformed into broad and open folds with a northerly trend cut by north-trending zones of tighter folding and intensified cleavage. The ~1340 Ma East Kootenay Orogeny (Anderson & Davis 1995) produced lower greenschist-amphibolite assemblages across the region. During the late Jurassic to mid-Cretaceous, the rocks of the Belt-Purcell were thrust eastward along the structures of the Rocky Mountain thrust and fold belt, with some of these structures reactivating Proterozoic extensional faults (Höy *et al.* 2000).
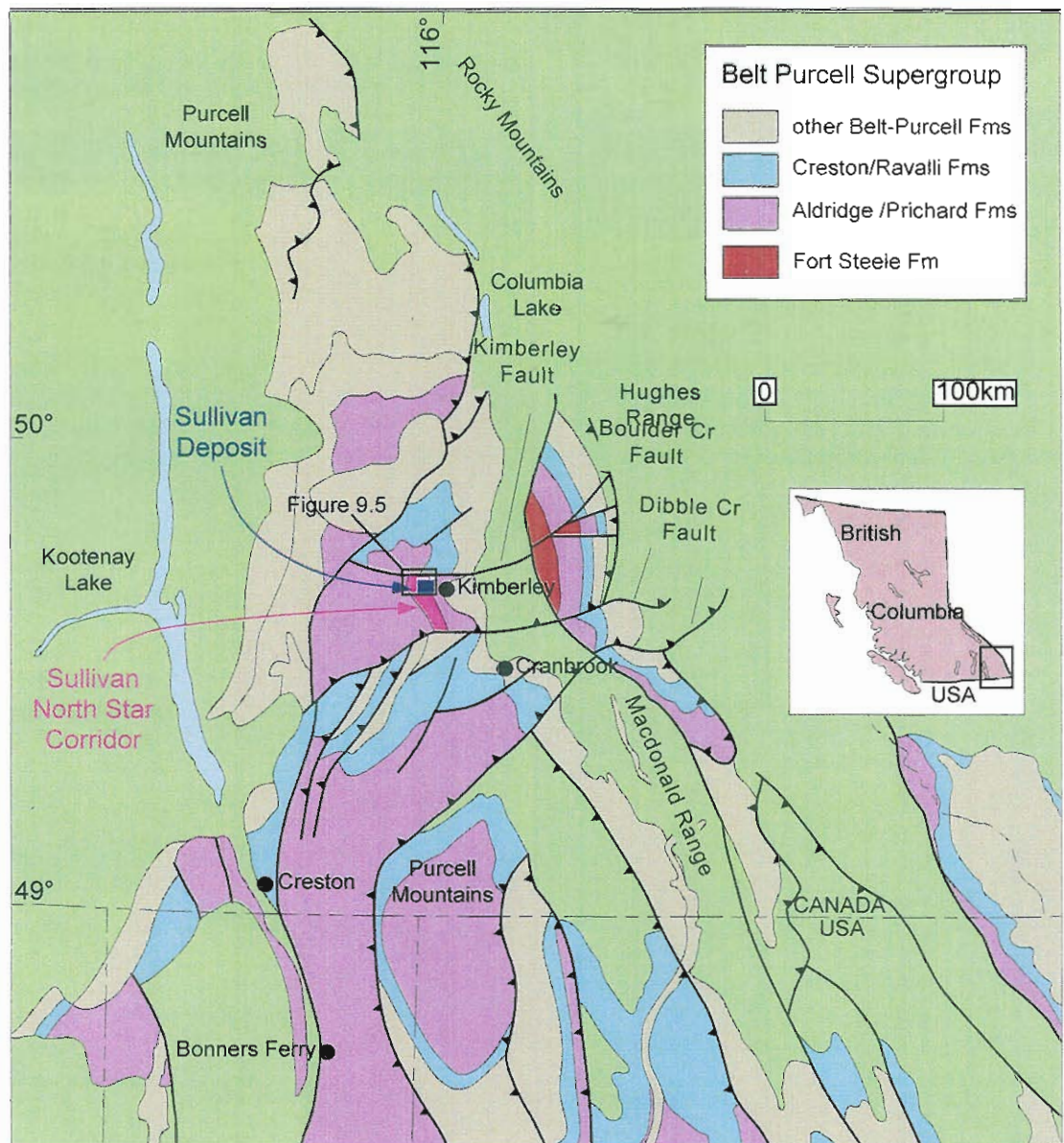
Figure 9.4: Regional geological setting and extent of the Belt-Purcell Basin in British Columbia modified from Turner *et al.* (2000a). Area of Figure 9.5 highlighted.

Workers in the region have defined the Sullivan-North Star Corridor (Turner *et al.* 1995; *cf.* "Sullivan-North Star Graben" and "Sullivan North Star-Rift") a north-trending 1-2km wide, 7km long belt of mineralised and altered Aldridge Formation and Moyie Sills (Fig.9.5). Turner *et al.* (1995) defined the Sullivan-North Star Corridor as a north-trending graben terminated at its northernmost end by the Kimberley Fault and having significant control on the distribution of sedimentation, mineralisation and sill emplacement (*cf.* Turner *et al.* 2000a,b).
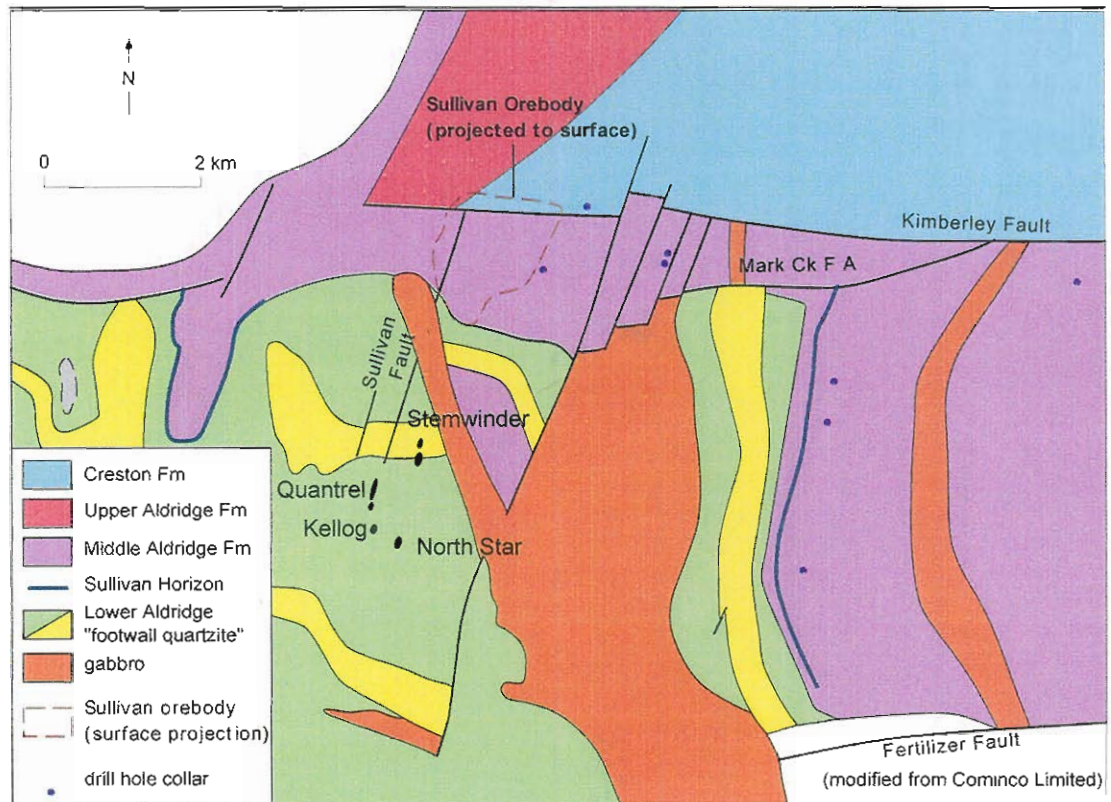
Figure 9.5: Simplified local geological interpretation of the Aldridge Formation in the Sullivan region. Modified from Goodfellow 2000.

The Sullivan deposit is situated at the juncture of the Sullivan North Star Corridor and the Kimberley Fault (Fig.9.4 & 9.5). The remainder of this discussion will mainly focus on the well studied geology of the Sullivan-North Star Corridor and the immediate surrounds to the Sullivan deposit.

9.4.2 Aldridge Formation

The Aldridge Formation is represented by at least 12km of 'syn-rift' siliciclastic sediments the base of which is not exposed, deposited in a north-northwest deepening basin (Höy *et al.* 2000). The presence of synrift faulting within the basin is generally accepted by most workers in the region and has been tied to at least four extensional events (Höy *et al.* 2000). Basin bounding faults active during sedimentation have been defined by facies and sediment thickness changes. Smaller scale syn-rift faults interpreted to have been active during ore deposition are defined

by zones of increased hydrothermal activity, distinctive fragmental units and

sulphide veins (Höy *et al.* 2000; Turner *et al.* 2000a,b). These growth faults had a

significant control on the location of base-metals mineralisation and the local

distribution of sedimentation and hydrothermal flow (Höy *et al.* 2000; Turner *et al.*

2000a,b).

The Aldridge Formation is subdivided into three informal, but widely accepted

subdivisions; Lower, Middle and Upper (Höy *et al.* 2000). The Lower Aldridge is

comprised of a sequence of siltstones and sandstones taken to represent turbidites

(Turner *et al.* 1995; Höy *et al.* 2000), and concordant and discordant bodies of

conglomerates, breccias and pebbly sandstone, collectively termed 'fragmentals'

(Turner *et al.* 1995). The Middle Aldridge overlies the massive sulphides of the

Sullivan deposit and is composed of 2400m of quartzites and siltstones again thought

to represent a turbidite sequence (Höy *et al.* 2000). The Upper Aldridge conformably

overlies the middle Aldridge and consists of ~300m of laminated siltstones and

argillites interpreted as the result of deposition in a shallowing basin.

The exposed Lower Aldridge amounts to up to 2000m of siltstones, sandstones and

argillites interpreted as distal turbidites that grade northeasterly into the fluvio-

deltaic wackes and arenites of the Fort Steele Formation (Turner *et al.* 2000a). The

upper parts of the Lower Aldridge are defined by an upward increase in grain size

and the presence of coarse-grained 'fragmentals' up to and including the

stratigraphic level of the Sullivan deposit – the 'Sullivan Horizon' (Turner *et al.*

2000a). The Footwall Quartzite (Fig.9.5) marks the first input of coarser sediment

into the sequence and is also concurrent with increased hydrothermal activity (Höy *et*

al. 2000; Turner *et al.* 2000a). The Middle Aldridge, is defined by northward

prograding turbidite sequences which in the upper part of the unit are defined by fining upward quartzite-argillite units.

Fragmental units within the Aldridge Formation generally consist of breccias with locally derived clasts and a massive sand-siltstone matrix. Anderson & Höy (2000; *cf.* Höy *et al.* 2000) subdivided them into four styles based upon relationships to surrounding units; (1) 'Proximal' facies which are crudely layered and variably altered, interpreted as being proximal to vents and to mud-volcanoes; (2) 'Discordant' fragmentals with clear cross-cutting relationships to surrounding sediments, generally at a high-angle, and located within or associated with syndepositional faults; (3) large stratabound sheets ('debris flow facies') interpreted as the product of either debris flows or similar mud-volcano activity to the proximal fragmentals; (4) 'sill concordant' facies which are laterally extensive sheets spatially associated with the Moyie Sills. Overall, these 'fragmentals' are interpreted as the product of fluidisation of the sediments through the fault release of 'geopressured' fluids (Turner *et al.* 1996; 2000a; Anderson & Höy 2000). Many of these 'fragmentals' are overprinted by later hydrothermal alteration events, a key piece of evidence indicating the use of the same channels by fluidised sediments and hydrothermal fluids.

9.4.3 Moyie Sills

The tholeiitic-alkalic Moyie Sills comprise up to 30% of the Lower Aldridge Formation (Höy 1982; Anderson & Goodfellow 2000). They are comprise predominantly gabbro, and are geochemically and mineralogically differentiated up-sequence (Anderson & Goodfellow 2000; Gorton *et al.* 2000). Isolith maps of Moyie Sills shows that the greatest thickness of sills is concurrent with the interpreted rift

axis (Höy *et al.* 2000). Geochemically they are defined as tholeiitic gabbros and diorites with continental affinities, have incompatible element concentrations similar to E-MORB, are LREE enriched-HREE depleted, and have been separated into two stratigraphically separate geochemical groups (Anderson & Goodfellow 2000). Anderson & Goodfellow (2000), based upon the contact relationships between Moyie Sills and adjacent Aldridge Formation sediments, proposed them to be the products of intrusion into unconsolidated, wet sediments (*cf.* Holm *et al.* 1998). Interpreted volcanic units in the Aldridge Formation are restricted to rare lapilli-tuffs (Höy *et al.* 2000). No lava flows have been described from the Aldridge Formation, although Ethier *et al.* (1976) quote the presence of the 'Purcell Lavas' some 7000m stratigraphically above the Sullivan horizon.

Based upon element fractionation trends, Anderson & Goodfellow (2000) interpreted the Moyie Sills as the result of at least two separate intrusive pulses, an 'upper' and 'lower' sill sequence (Fig.9.6). The Sullivan deposit overlies their lower sill sequence. Fractionation and enrichment in the Moyie Sills is similar to that in the Soldiers Cap Group with variations in Ti, Fe, P, Ni and Cr interpreted as mineral fractionation patterns (Fig.9.6; Anderson & Goodfellow 2000; Gorton *et al.* 2000). Anderson & Goodfellow (2000), based on a detailed whole rock and Nd-Sr isotope study, proposed that the Moyie Sills were a sequence of fractionated, crustally contaminated magmas produced in an aulacogen by partial melting of lithospheric mantle or a decaying plume below rifted continental crust.
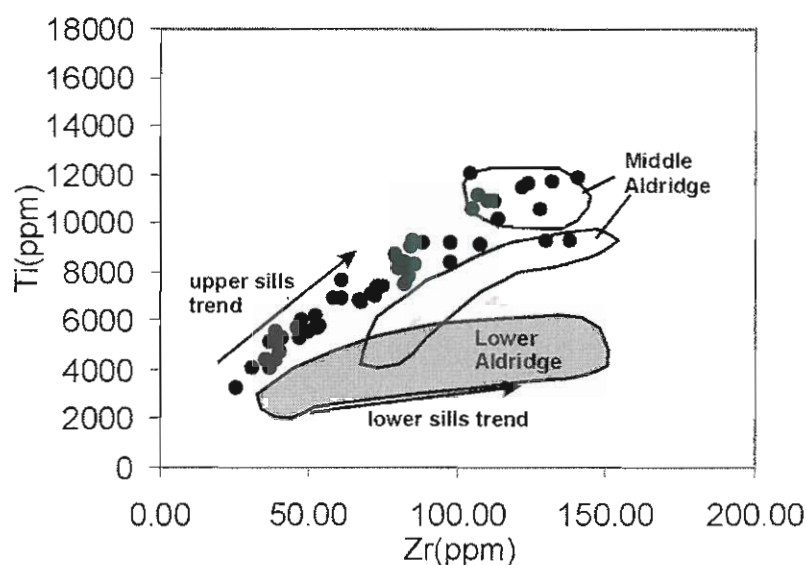
Figure 9.6: Plot showing Ti vs. Zr in ppm, for *all* Soldiers Cap Group mafic units analysed in this study overlain by the outlines of the fields of Moyie Sills within the Lower and Middle Aldridge and the fractionation trends defined by Anderson & Goodfellow (2000).

Based upon the contemporaneity of an increase in the volume of the Moyie Sills and the presence of the Sullivan deposit, previous authors have suggested the sills had a primary control on the formation of the Sullivan deposit (*eg.* Hamilton 1984). However, Anderson & Goodfellow (2000) dispute this based upon a lack of a Moyie Sill Pb isotopic signature in the Sullivan deposit. Instead they suggest that the sills are the result of a major deep-seated thermal event in the basin and may have been the catalyst required to initiate hydrothermal fluid flow and renewed extension on existing faults. Later post-ore Moyie Sill intrusions have been linked to the generation of distinct post-ore albite-sericite alteration along existing faults (Turner *et al.* 2000b).
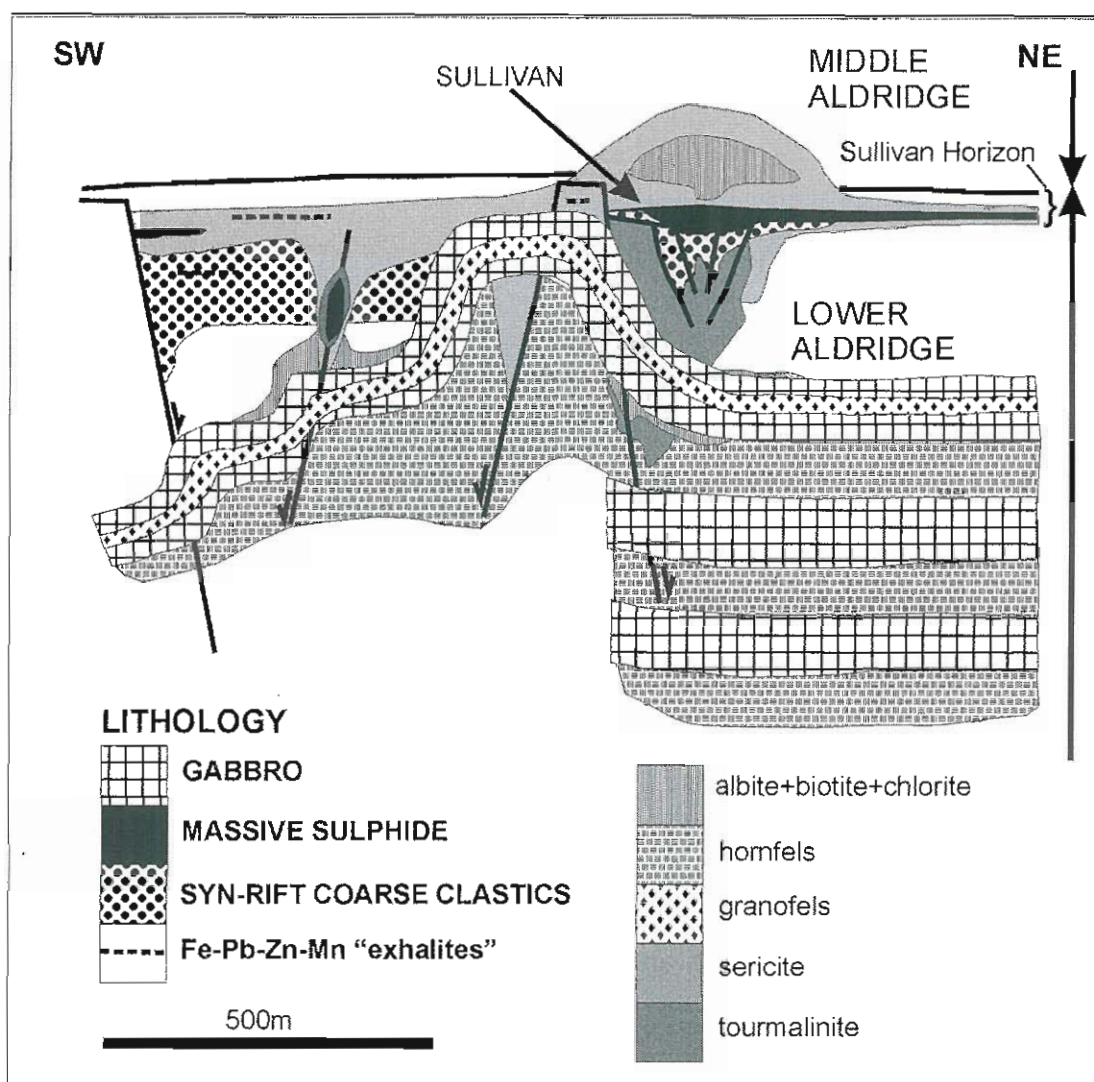
Figure 9.7: Schematic section of the Sullivan Graben modified from Turner *et al.* (2000b) depicting the range of alteration styles and their relationships to major lithological boundaries and faults. Disseminated garnet and chlorite alteration not shown.

9.4.4 Hydrothermal History

The complex evolution of the hydrothermal field represented by the Sullivan-North Star Corridor has been well studied and within Lydon *et al.* (2000) numerous authors present alteration sequences. Turner *et al.* (2000b) provide a detailed summary of this, divided broadly into events related to ore formation and to mafic intrusion, and this is followed here.

Fe-Mn and occasionally base metals mineralised, 'exhalites', occur at various stratigraphic levels within the Aldridge Formation, 1-300m below and up to and

including the Middle Aldridge contact above the Sullivan horizon (Slack *et al.* 2000;

Turner *et al.* 2000b). These units are generally associated with renewed rifting and

hydrothermal activity associated with an influx of coarser grained conglomerates in

the Lower Aldridge (Turner *et al.* 2000b). Mud-volcanism and related clastic feeder

dykes represented by the numerous fragmentals outlined above and some of the

numerous tourmalinites present throughout the Aldridge Formation defines one of

the earliest hydrothermal events of Turner *et al.* (2000b) related to ore formation.

These tourmalinites occur regionally as semi-conformable bodies controlled by faults

and envelopes to mineralized veins, and the largest occurs below the Sullivan deposit

as a pipe overprinting some earlier fragmental textures (Fig.9.7). Turner *et al.*

(2000b) based upon the superposition of tourmalinite on fragmentals in the Sullivan

footwall feeder zone, interpreted this style of alteration as being closely related to ore

forming events and fluids. Geochemically, these units are defined by an increase of

up to 50% in B-Mn-Mg-Cu-Pb-Zn-As relative to 'unaltered' Aldridge sediments,

negative Eu anomalism in the 'shallow footwall', and positive Eu anomalism in the

Sullivan hanging wall (Jiang *et al.* 2000; Slack *et al.* 2000; Turner *et al.* 2000a). Mn-

rich garnet 'coticules' are expressed in the immediate area around Sullivan as either

disseminated garnet, or as garnet rich beds in the immediate and deep footwall to the

Sullivan deposit (Slack *et al.* 2000; Jiang *et al.* 2000). Geochemically these units are

defined by having up to 50% increases in B, Fe, Mn, Mg, Ca, F, Li, Y, Eu, Zn, Pb,

Sn & As relative to 'unaltered' Aldridge metasediments (Slack *et al.* 2000).

Tourmalinites and coticules are interpreted as forming through subseafloor

replacement or interaction of exhalative fluids at the sediment-water interface related

to extension events and increased hydrothermal flow both pre- and syn-

mineralisation (Jiang *et al.* 2000; Slack *et al.* 2000;Turner *et al.* 2000b). Compared to

the Soldiers Cap Group iron formations, the tourmalinites and coticules overall are lower in P and Fe, have greater metal endowment represented by common base metal sulphides, and represent the movement of B-rich fluids derived from evaporate borates in the sedimentary pile (Slack *et al.* 2000). Geochemically and petrographically, the garnet rich coticules are closer to the Soldiers Cap Group chemical sediments than are the tourmalinites.

Following Mn-rich garnet alteration, Turner *et al.* (2000b) defined chlorite-pyrrhotite alteration directly associated with the large pyrrhotite body in the lower part of the Sullivan deposit. This alteration style they defined as the product of seafloor metasomatism replacing seafloor sulphides during hydrothermal upflow from the main vent (*cf.* Taylor *et al.* 2000).

Intrusion of the Moyie Sills into the buried Sullivan Graben resulted in the formation of distinctive granofels (quartz-plagioclase) alteration at sill margins through recrystallisation of sediments and also the remobilisation of fluids within the basin and movement of albitising fluids along reactivated syn-rift faults (Fig.9.7; Turner *et al.* 2000b). This also resulted in the replacement of existing sediments along and above earlier active structures by albite-sericite alteration (Fig.9.7). Overprinting the albite alteration in some places is a sericite alteration event which deeper within the Aldridge occurs as zones controlled by the location of coarse-grained clastic rocks and clastic dykes. This overprints some tourmalinites, and occurs above Sullivan higher as more laterally extensive zones, including (at Sullivan) an envelope around the hangingwall albitic alteration. Turner *et al.* (2000b) interpreted the overprinting of sericite on albite as the product of mixing of albite rich fluids with cooler ambient basin water.

9.5 The Soldiers Cap Group, Aldridge Formation and Etheridge Group -variations on a theme?

When the Soldiers Cap Group and Aldridge Formation are compared directly there are a number of striking similarities: (1) they are both interpreted as the product of Proterozoic rifting in intracratonic basins; (2) both contain voluminous sequences of synsedimentary sills, with continental tholeiite affinities, distinct iron enrichment trends produced by partial melting of MORB sources, some crustal contamination, and a close spatial and temporal association with hydrothermal fluid movement; (3) syndepositional alteration on the margins of synsedimentary sills; (4) Fe-Mn-(Pb-Zn) "exhalites" related to renewed rifting and the influx of coarser sediment; (5) garnet-rich hydrothermal chemical sediments with elevated Mn, LREE enriched-HREE depleted REE profiles at various stratigraphic levels associated with extensional structures and base-metals mineralisation; (6) synsedimentary faulting linked to basin configuration and internally divides local graben structures into fault bound, discrete sub-basins that have local controls on sedimentation and hydrothermal fluid movement; (7) both are associated with world-class base-metal deposits, the massive Sullivan (Fe)-Pb-Zn (Aldridge) and Cannington Ag-Pb-Zn deposits (Maronan Supergroup). However, the SCG overlies the host sequence to Cannington (Fullarton River Group), whereas the Aldridge Formation is the actual host to the Sullivan deposit. These two deposits have previously been considered as geological analogues (Turner *et al.* 1996; Willis 1996; *cf.* Sangster 1993). However, importantly, Cannington is a classic Broken Hill-type (BHT) deposit (Beeson 1990), formed early in the rifting phase of the Maronan Supergroup, whereas Sullivan is an unusual SEDEX-style deposit with BHT features (*eg.*tourmalinites, K alteration, Fe-Mn rich exhalite chemistry).

While the large number of geological similarities between the Soldiers Cap Group and the Aldridge Formation outlined above suggest that they may be close analogues several important features are absent from the Soldiers Cap Group including: (1) a clear definition of the renewed rift architecture *ie.* a lack of distinctive large scale 'syn-rift' features; (2) the lack of definitive feeder zones for fluid flow related to hydrothermal events and mafic sills; (3) shallow water tempestite setting instead of a deeper water 'turbidite' setting; (4) 'fragmentals' sedimentary breccias and clastic dykes or mud volcanoes; (5) postdepositional alteration related to mafic intrusion and overprinting products of hydrothermal events; (6) B-Pb-Zn enrichment in hydrothermal sediments and negative Eu anomalism.

Timing of magmatism relative to hydrothermal and fault extension activity is also an important factor in the comparison of these two basins. Emplacement of large mafic bodies deep in the sedimentary pile which heat basinal fluids is interpreted as occurring in both instances. Synsedimentary faulting is interpreted as breaching these basinal fluid cells and allowing the egress of hydrothermal fluids. In the Aldridge Formation, early extension is associated with varying hydrothermal events, later activity is associated with mafic sill emplacement which does not produce extrusive volcanism. Peak hydrothermal events are represented by the confluence of exhalation, fluidisation of sediments and synsedimentary faulting. Importantly, the SCG differs from this by having an early phase of extension, hydrothermal activity and magmatism followed by further extension and importantly, extrusive volcanism.

The range of similar features outlined in Table 9.1 for the Soldiers Cap Group, Aldridge Formation and the Etheridge Group suggests that they also shared a close geological history. This shared evolution involved continued or renewed extension,

magmatism and hydrothermal activity within the shallow upper parts of intracontinental rift basins generally thought to be devoid of active extension and hydrothermal activity. These similarities between the two Proterozoic Australian examples and the Aldridge Formation suggests the possibility of an identifiable variant on the sag-phase of classical intracontinental rifting (Kröner 1983; Etheridge *et al.* 1987).

The features within the Soldiers Cap Group and Etheridge Group that define this variation are :- (1) a large volume of mafics both intrusive and extrusive representing sequential intrusive events; (2) shallow water associated with the middle parts of the sequence; (3) importantly, shallow water hydrothermal activity not yet proven to contain base metal mineralisation related to renewed extension.

Compared to this the Aldridge Formation represents a deeper basin in which the mafic magmatic history is represented by sills with no volcanism suggesting that deeper examples may only ever contain intrusion. Therefore, do the two Australian examples represent an end-member of an as yet unclassified variation on intracontinental rifts. Importantly, in the Soldiers Cap Group and Aldridge Formation hydrothermal activity is directly linked to mafic magmatism and this is generally though to only occur within the rift phase of intracontinental basins. The relationship between faulting, mafic magmatism and hydrothermal flow also appears to be important in both sequences, for example in the model for genesis of iron formations presented in Chapter 7.

From an exploration viewpoint what is important in the Soldiers Cap Group is defining whether the iron formations represent a basin event similar to that which

formed the Fe-Mn exhalites below Sullivan, or are related to a later 'post-ore' movement of fluids and mafic intrusions. Goodfellow (2000) proposed that the Sullivan deposit was the product of rupturing of a geopressured (*cf.* Turner *et al.* 2000b) subseafloor fluid system by renewed extensional faulting resulting in expulsion of hydrothermal fluids along these faults to the surface. Similar processes were occurring in the Soldiers Cap Group in the rupture of a subsurface aquifer to produce the iron formations within the Mt Norna Quartzite. The question remains were these equivalent to the hydrothermal sediments in the Sullivan footwall, ore horizon or hangingwall.

Generally, it would appear that the former is the case for the Soldiers Cap Group and therefore any future search should be focussed at or above the lower-mid Mt Norna Quartzite.

Water depth appears to be a critical feature in the formation of the Soldiers Cap Group iron formations. Even though the environment at Soldiers Cap Group time is considerably more active than previously thought it was still conducive to deposition of hydrothermal sediments within small localised seafloor depressions. This active, storm dominated environment of the Soldiers Cap Group would not have been conducive to the more quiescent stratified brine pool required by Goodfellow (2000) for formation of the Sullivan deposit, suggesting also that this style of mineralisation is therefore more likely higher up in the Toole Creek Volcanics. In an environment lacking well defined, stratified brine pools or local basins, such as the upper Soldiers Cap Group, syndiagenetic replacement forming 'Century-style' deposits at structural traps (Broadbent *et al.* 1998), may also be a viable option for the deposition of base metals mineralisation.

9.6 Recommendations for future exploration

The well publicised geological links of the Soldiers Cap Group to the Broken Hill Block and the discovery of the world-class Cannington Ag-Pb-Zn deposit have resulted in considerable interest in the Maronan Supergroup in the last 10 years or more from both academic and industry geoscientists. The outcropping area of the Soldiers Cap Group and some of that under shallow cover has been extensively explored for Broken Hill-type and also Cu-Au-Fe oxide mineralisation by numerous companies utilising modern exploration techniques and models for a number of years. Therefore it is fair to say that the likelihood of the discovery of a new deposit on the scale of Cannington in this area of outcrop is either low or not visible to current technology. Current exploration models for sediment hosted base metals deposits are divided into either epigenetic or syngenetic and empirical or model specific (*cf.* Walters 1996; Willis 1996) and along with the genesis of BHT's are still a cause for considerable scientific debate. Discussion of the merits of the current exploration and genetic models is beyond the scope of this project and will not be entered into here.

The evidence presented here of similarities to known hydrothermal events and the host terranes (Aldridge Formation-Sullivan) is convincing evidence that the Maronan Supergroup and in particular the upper Soldiers Cap Group may as yet host undiscovered Sullivan-style base metals mineralisation under cover to the east. The tracing of the upper Soldiers Cap Group through BHP aeromagnetics shows that it is laterally extensive for several 10's kms to the east, possibly further, and is possibly structurally repeated for a considerable distance. Particularly the iron formations which are vital to identifying any hydrothermal activity, are traceable by

Regional Tectonostratigraphy	Proterozoic 1690-1670 Ma (max. depositional ages) Late stage of an intracontinental rift,increased tectonothermal activity	Proterozoic 1690-1670 Ma Mafic and felsic magmatism- intracontinental rift environment	Proterozoic minimum age of 1445-1468 Ma. Deepening intracratonic basin- Aldridge represents late stage extension
Deformation & Metamorphism	4 discrete deformation events of the Isan Orogeny (peak=1584±2 Ma) metamorphism=amphibolite facies	Two syn-metamorphic deformation events with metamorphic grade increasing from amphibolite to granulite eastwards	Mid-Proterozoic East Kootenay Orogeny Amphibolite facies metamorphism
Lithostratigraphy	*ca.*5km of interbedded quartzites, psammites, psammopelites, pelites and metadolerite, metabasalt and chemical sediments (iron formations)	*ca.* 12km of subtidal sandstones, quartzites and chemical sediments underlain by turbidites, overlain by wave-dominated shoreline sediments, intruded by voluminous metadolerite sills	Three informal subunits made up of dominantly turbidites >2700m thick,and thick synsedimentary sills, ≥30% of sequence, base not exposed
Depositional environment	Storm dominated shelf with density currents generated by oscillatory storm currents in localised basins controlled by synsedimentary faults, intruded by synsedimentary Fe-metatholeiite sills	Subtidal wave influenced, broad, shelf-shoreline evidenced by wavy bedding, intraclasts and evaporite molds	Interpreted as a deep-marine turbidite sequence, intruded by the Moyie Sills. Local growth faulting controls sedimentation and hydrothermal flow...
Geochemistry	Mafic geochemistry- continental tholeiite sills with strong evidence for fractionation in high level magma chambers ; Iron formations have distinctive hydrothermal REE signatures; U-Pb detrital zircons define REE signatures and detrital provenance changes in the SCG	Cobbold Metadolerite, Dead Horse Metabasalt and Einasleigh Metamorphics (amphibolites) defined as low-K continental tholeiites, incompatible depleted and MORB-like	Tholeiitic gabbros and diorites of the Moyie Sills with continental affinities, which can be separated into two distinct stratigraphically separated groups, interpreted as the product of two magma chambers. Show degrees of crustal contamination and evolution along an iron enrichment trend
Extension Events	Two likely lower-MNQ & mid-MNQ	At least two	Four discrete events
Hydrothermal events	Iron Formations associated with voluminous syn-sed. mafic intrusions-+ve Eu anomalies, Proterozoic "exhalite" REE pattern, remnant hydrothermal and detrital signature	Uncertain, suggested cherts in the lower Etheridge Group may be chemical sediments	Exhalatives (tourmalinites, coticules) associated with Pb-Zn mineralisation and 'fragmentals" at various stratigraphic levels-+ve Eu anomalies

Table 9.1: Outlines of the major geological and tectonic characteristics of the three Proterozoic sequences used for the comparative study and evaluation.

aeromagnetics to a similar extent and have been logged in exploration core to the east of the study area. With the exception of detailed aeromagnetic and gravity surveys and several exploratory holes drilled by BHP Minerals the Soldiers Cap Group under cover remains relatively under-explored. The presence of the largely barren Weatherly Creek and Mt Norna Iron Formations which are interpreted as the product of cycling hydrothermal fluids from reservoir temperatures of >250°C (Ch.7), also implies that elsewhere within the basin these fluids were carrying metals and may be attractive targets in their own right. Combined with the presence of iron formations, voluminous mafic magmatism and synsedimentary faulting all point to the Soldiers Cap Group being considerably more tectonothermally active than previously thought and hence an attractive exploration target.

The Sullivan deposit has been considered a less metamorphosed and deformed equivalent of BHT deposits (Turner *et al.* 1996; Willis 1996; Large *et al.*1996; *cf.* Sangster1993), essentially a SEDEX member of a BHT-SEDEX continuum, the other end represented by deposits such as Cannington. Combining this with the similarity of the Soldiers Cap Group to the host sequence for Sullivan suggests that using exploration models based purely on one BHT or SEDEX 'end-member' may be unsuitable. Instead, an empirical targeting sequence approach considering the criteria relevant to locating centres of likely hydrothermal activity (mineralised and barren) will be used here. This targeting sequence assumes that belt selection has already occurred and that there is a reasonable level of geological knowledge in the region.

Ideally, this is the sequence although it can easily be adapted in polydeformed terranes such as the Eastern Succession to only use those elements clearly visible to the user.

The sequence is as follows:-

(1) identification of faults which based upon mappable thickness, sedimentological or volcanological features can be interpreted as syndepositional extension faults

(2) definition of broad lithostratigraphic changes in sediment grain size or type, and volume of mafic intrusives which may indicate renewed extension, presence of a unit which could act as a 'cap' to keep underlying hydrothermal cells under pressure

(2) intersections of extensional faults although not discounting individual examples which could host mineralised subvertical host sequence discordant massive sulphide veins or potential 'oil-trap' replacement style targets

(3) identification of zones of fluid outflow through the presence of Fe-Mn-P alteration or Fe-P-Mn-Pb-Zn-Ag rich hydrothermal sediments or clastic dykes/mud volcanoes

In the Eastern Succession, these target areas could be best identified initially by detailed geophysics to define the extent and geometry of the sequence under cover and any possible basin controlling structures (*cf.* Betts *et al.* 2002). This could be followed up by detailed mapping and sampling of prospective areas (where possible) followed by geochemical analysis of drill core utilising the preliminary geochemical/alteration markers and fingerprints defined in this study for mafic volcanics and iron formations.

The similarities outlined above between the Etheridge Group and Soldiers Cap Group indicate that it has a geological signature which could be prospective for Sullivan-style mineralisation. Hence the Etheridge Group and lateral equivalents

would be another area in which this methodology could be applied in first-pass

regional exploration, also providing a useful test of the ideas presented here.

Chapter 10- Conclusions and Recommendations for future work

10.1 Sedimentology (Chapter 3)

Evidence gathered from regional mapping, and the definition of 4 sedimentary facies

associations and 10 sedimentary lithofacies allowed a new interpretation of the

sedimentological environment of deposition of the upper Soldiers Cap Group (Mt

Norna Quartzite and Toole Creek Volcanics) in the northern part of the Cloncurry

Basin:-

- a revised lithostratigraphy for the Soldiers Cap Group arose from this study, with the Mt Norna Quartzite now subdivided into 3 major subunits with 5 minor subunits defining lithostratigraphic units considered important to the understanding of basin evolution

- swaley- and hummocky- bedforms combined with hummocky cross stratification (HCS) and rippled bedforms in quartzites, psammites and psammopelites point to a continuous influence of storm currents on the sequence

- the sedimentology changes up sequence from a turbidity current-dominated, with minor sandy debris flow, regime at the basal-MNQ, to storm current-dominated in the mid- to upper-MNQ, which when combined with the evolution of the mafic volcanics and iron formations is an important indicator of renewed rifting within the basin

- the currently proposed sedimentological model is one of storm loading of a narrow shelf producing currents which above storm wave-base were overprinted by oscillatory current activity, and generated below storm wave-base turbidity currents (tempestites)

- reconstructed palaeocurrents taken from turbidity and storm-generated currents agree with detrital U-Pb data *ie.* a broadly south-southeasterly deepening basin

10.2 Detrital U-Pb dating studies (Chapter 4)

Using the recently developed Laser Ablation Inductively Coupled Plasma Mass

Spectrometry (LA ICPMS) method, U-Pb ages were determined from detrital zircons

in samples of quartzites taken from across the stratigraphy of the upper Soldiers Cap

Group. This defined several detrital age populations, provenance changes and

possible source areas for the quartzites of the upper Soldiers Cap Group. These

include:-

- a *ca.*1750 Ma inheritance dominant in the upper part of the sequence consistent with derivation from volcanic units of Cover Sequence 2 in the Eastern Succession (Argylla Formation, Mary Kathleen Group, Mt Fort Constantine Volcanics, Marraba Volcanics, Magna Lynn Metabasal, Jessie Granite)

- a *ca.*1790 Ma peak for which the closest aged source rocks are parts of the Argylla Formation or the Bottletree Formation in the Western Succession

- an enigmatic *ca.*1860 Ma age dominant in the lower sequence which is only matched in the Eastern Succession by the poorly understood Double Crossing Metamorphics, currently located to the southwest of the Maronan Supergroup, or Cover Sequence 1 units in the Western Succession (Leichardt Volcanics, Kalkadoon Granite)

- other minor populations include:- a *ca.*1970 Ma age early rift phase age; a *ca.* 1680 Ma Soldiers Cap Group/Maronan Supergroup age; a *ca.*1580 Ma metamorphic overgrowth age

- Archaean aged zircons, representing an ill-defined extrabasinal source and/or high degree of recycling, were present in all samples

- provenance changes evidenced by the absence of subtle peaks on probability graphs representing a combined *ca.*1860 Ma and *ca.*1970 Ma population suggest changes in extrabasinal drainage patterns

- overall, this new provenance data is consistent, with but does not unequivocally prove, that the Soldiers Cap Group was formed locally and was deposited in a broadly southerly deepening basin adjacent to the exposed Mt Isa Inlier

10.3 Mafic Volcanology (Chapter 5)

Identification of 6 volcanological lithofacies during mapping and logging of

exploration and mine core allowed the confident interpretation of the style and

timing of emplacement of the voluminous mafic bodies in the upper Soldiers Cap

Group: -

- sill margin textures including fluidal and blocky peperites, in-situ hyaloclastites, disrupted bedding, and distinctive pre-deformational alteration now expressed as quartz-epidote±carbonate(±garnet) haloes at the margins of large mafic bodies, are consistent with emplacement as a sequence of synsedimentary sills

- pillow forms and localised breccias interpreted as pillow margin breccias, allowed parts of the upper Soldiers Cap Group to be interpreted as the product of subaqueous extrusion of basalts

- broad changes in peperite style up-sequence suggest that the SCG mafic units represent a sequence of sills prograding through a wet, unconsolidated sedimentary pile

10.4 Mafic Geochemistry (Chapter 6)

Whole-rock geochemistry (XRF and ICP MS) investigations of the mafic units in the

upper Soldiers Cap Group allowed an interpretation of their primary chemistry and

petrogenetic development. This included: -

- definition as high Fe-metatholeiites (ferrobasalts >12 wt% FeO_t) with distinctive intracontinental rift signatures produced by partial melting of an N-MORB source, similar to other Australian Proterozoic mafic sequences such as those of the Willyama Supergroup and Georgetown Inlier

- these ferrobasalts were developed in at least 2 discrete magma chambers, in one of which early fractionation of Ti-magnetite and apatite was suppressed and in the other, near continuous Fe-Ti-P fractionation occurred

- the degree of fractionation and the overall ferrobasalt chemistry was controlled by internal processes in these magma chambers including chamber size, amount of re-supply of new magma batches, fO_2, crustal contamination and the rate of rifting

- the emplacement of these magma chambers reinforces the idea of a renewed phase of tectonothermal activity at upper Soldiers Cap Group time

- immobile and rare earth elements (Zr, Nb, Y, La) define an empirical geochemical 'fingerprint' for the Soldiers Cap Group mafic rocks which could assist their identification in future exploration

10.5 Iron Formations (Chapter 7)

Geological and geochemical studies of several previously problematic barren and weakly Cu-Ag-Pb-Zn mineralised iron formations in the upper Soldiers Cap Group, allowed confident interpretation of the origin of their distinctive mineralogy and chemistry:-

- contact relationships, conformable quartz-epidote±carbonate(±garnet) alteration haloes within host metasediments and metatholeiites, and preserved geochemical signatures, allowed many of these iron formations to be interpreted as primary chemical sediments, instead of products of epigenetic metasomatism as proposed by earlier authors

- multivariate statistics applied to major element values of the Weatherly Creek Iron Formation defined genetic groupings of elements: (1) a high Ca-P-Mn-Eu-Na-Mg inter-correlated group; (2) a Si-Fe inter-correlated group; (3) Fe-Mn and Fe-P had no clear correlation

- these groupings provide evidence that the geochemical composition of the Weatherly Creek Iron Formation developed in two chemically different stages or was derived from two major competing element sources

- bivariate plots were then used to further define groupings with strong interelement correlations, these include: (1) Mn, P, Al, Ti, Zr, Mg, Ca, Na, K, As, Pb, Ni, ΣREE, Eu, Eu/Eu*; (2) Fe, Si, Ce/Ce°

- distinct geochemical sources defined for the iron formations through bivariate plots are: (1) a detrital component with element ratios largely consistent with a mafic extrabasinal source; (2) a hydrothermal P-Mn-(Eu) rich, sulphide poor component; (3) a hydrothermal Fe-Si source; (4) a minor hydrogeneous input of (Pb+Zn)-Mn

- a consistent positive Eu anomaly that remains even with a high detrital component, suggests that the hydrothermal component (calculated as up to 80 vol% for some samples), was derived from a source containing hot, reduced and acidic fluids with temperatures $\geq 250°C$

- these fluids were generated in basin-scale aquifers in which convection was driven by the transfer of heat from the intrusion of large Fe-metatholeiite magma chambers into the base of the sequence

- negative Ce anomalism, local interpreted paleaosedimentary environments, combined with petrography, major element geochemistry patterns, contact

263

and alteration relationships, all suggest exhalation of Fe-P-Mn rich fluids from these aquifers onto the seafloor at the sediment-water interface in localised, relatively quiescent depressions

- expulsion of fluids occurred when the underlying reservoirs were tapped by extensional faults associated with renewed tectonothermal activity in the basin which occurred prior to the main phase of sill emplacement and extrusive volcanism

- these iron formations have important economic implications as the noteworthy lack of metal sulphides but evidence of fluid conditions conducive to base-metal transport, and relationship between fluids and extension suggests that base-metal sulphides may have precipitated elsewhere in the basin, providing an attractive future exploration target

10.6 Basin-scale Reconstructions (Chapter 8)

Limited palaeocurrent data was combined with sedimentology to define flow regimes in the ancient Cloncurry Basin. Utilising published extensional faulting models applied to modern active rifts, the nature and possible evolution of one major fault system in the study area was determined. Assumptions made in the unfolding the deformation in the area mean that reconstructed palaeoflow markers are less reliable than in other less deformed terranes. Overall, this reconstruction defined several important features:

- sedimentation patterns and palaeoflow markers in the Weatherly Creek Syncline were controlled by several large faults (Lomas Creek Faults, Mt Norna Fault) which had a synsedimentary extensional history and originally separated several half-graben tilt blocks

- by using models of rifting in modern systems a model was proposed for the generation of the Lomas Creek Faults as early close-spaced normal faulting controlled by an easterly margin fault, then during passive rotation, fault movement shifted to an as yet unidentified southerly basin bounding fault

- the broad spatial and temporal associations between mafic magmatism, provenance changes, synsedimentary faulting and circulation and exhalation of fluids resulting in deposition of iron formations, leads to the interpretation that the upper Soldiers Cap Group represents a much more tectonothermally active system than previously thought

10.7 Analogous Basins and Exploration Potential (Chapter Nine)

The Soldiers Cap Group was compared to the Aldridge Formation (Belt Purcell Basin, B.C. Canada), and the Etheridge Group (Georgetown Inlier, NE Queensland), in an attempt to evaluate potential analogues and the key features related to tectonothermal activity in these basins and the relationship of this to hydrothermal activity:-

- vital similarities between the upper Soldiers Cap Group, Etheridge Group and the Aldridge Formation include thick siliciclastic sediment piles; voluminous synsedimentary sills with intracontinental tholeiite geochemical signatures; chemical sediments at various stratigraphic levels; and synsedimentary faulting

- key features which vary between the two sequences are: interpreted water depth and sedimentary processes; extrusive volcanism; mud-volcanoes and/or 'fragmentals'; B-Pb-Zn enrichment in hydrothermal sediments; well constrained rift architecture; confidently identified hydrothermal pathways

- the Etheridge Group also has large tholeiite mafic complexes (*eg.* Cobbold Metadolerite, Dead Horse Metabasalt), chemical sediments, and a generally shallowing upwards sedimentary pile, and is considered by the author to be analogous to both the Soldiers Cap Group and Aldridge Formation making it an extremely attractive target for future exploration

- additionally, the occurrence of BHT style mineralization and chemical sediments higher in the Etheridge Group is compelling evidence that, similar to the Soldiers Cap Group, renewed rifting occurred in this terrane

- these analogies were used to construct an empirical exploration model, which was based on an incorporation of parts of published SEDEX and Broken Hill-type genetic models, to be applied to the Soldiers Cap Group and/or Etheridge Group in future

10.8 Recommendations for Future Work

Mainly due to monetary, time, equipment and software availability restrictions,

several promising areas of research which arose during the course of this study were

not able to be investigated fully and warrant further work by researchers in the

region. These include: -

- utilising mixing models similar to those used by Raetz *et al.* (2002; *cf.* Sambridge & Compston 1994), or applied multivariate statistics to unravel the mixed provenances in the Soldiers Cap Group

- REE and/or isotopic study by LA ICPMS of Soldiers Cap Group detrital zircons, and zircons from the proposed source units, to test the provenance hypotheses advanced here

- a microscale geochemical study of Soldiers Cap Group iron formations with the main aim of furthering the interpretations presented in this study of the chemistry and timing relationships of the unusual garnet-apatite laminae

- a more detailed isotopic study of the various iron formations and their immediate host rocks would be invaluable to the understanding of fluid evolution, particularly Pb isotopes, which are very useful in BHT systems *eg.* mineralisation at Cannington has a distinctive mantle or lower crustal signature, which on the basis of the model advanced here should differ significantly from Soldiers Cap Group iron formations.

- Sampling and analyses of the Hot Rocks iron formation occurrence to test for (dis)similarities with the Mt Norna and Weatherly Creek Iron Formations and to tie this in with the overall understanding of Maronan Supergroup geological evolution

- focused geochemical sampling and whole-rock analyses, possibly combined with microscale geochemistry, to determine whether the sequence of the Soldiers Cap Group metatholeiites underwent in-situ differentiation (*eg.* Williams 1998), combined with isotopic studies to define the degree of crustal contamination

- further detailed whole-rock geochemistry focusing on HFSE elemental analyses to constrain the size and geometry of the underlying magma chambers, and by extrapolation, their relationship to the overlying iron formations and their parent fluids *ie.* can a better understanding of these relationships lead to predictions of hydrothermal activity?

REFERENCES

ADSHEAD N.D. 1995; Geology, Alteration and Geochemistry of the Osborne Cu-Au
Deposit, Cloncurry District, NW Queensland, Australia

AIGNER T. 1985: Storm depositional systems. Springer-Verlag, New York, 174pp.

ALLEN C.M., BALLARD J.R., CAMPBELL I.H., PALIN J.M., ROHRLACH B.D.
& SETIABUDI B.T. 2001; U-Th-Pb dating of zircon with a focus on Post-
Palaeozoic rocks: Advantages of the Eximer Laser Ablation ICP-MS method; In:-
2001-A hydrothermal odyssey: Townsville May 17-19 2001, James Cook
University, EGRU Contribution No. 59, pp 1-2

ALLEN J.R.L 1968; *Current Ripples*. North Holland Publishing Company,
Amsterdam, pp.433

ALLEN J.R.L. 1985; *Principles of Physical Sedimentology*. Allen & Unwin
Publishing, pp.272

ALLEN P.A. & DENSMORE A.L 2000; Sediment flux from an uplifting block.
Basin Research, **12,** 367-380

ALLEN R.L. 1992; Reconstruction of the tectonic, volcanic and sedimentary setting
of the strongly deformed Zn-Cu massive sulphide deposits at Benambra, Victoria.
Economic Geology, **87,** 825-854

ANDERSON H.E. & DAVIS D.W. 1995; U-Pb geochronology of the Moyie Sills,
Purcell Supergroup, southeastern British Columbia: implications for the
Mesoproterozoic geological history of the Purcell (Belt) basin. *Canadian Journal
of Earth Sciences,* **v.32,** pp.1180-1193.

ANDERSON H.E. & GOODFELLOW W.D., 1995; Petrogenesis of the Moyie Sills,
southeastern British Columbia: implications for the early tectonic setting of the
Middle Proterozoic Purcell Basin. *Geological Association of
Canada/Mineralogical Association of Canada Annual Meeting, Final Program
and Abstracts,* **20,** A-2

ANDERSON H.E. & GOODFELLOW W.D. 2000; Geochemistry and isotope
chemistry of the Moyie Sills: Implications for the tectonic setting of the
Mesoproterozoic Purcell Basin. In:- The Geological Environment of the Sullivan
Deposit , British Columbia, (eds) J.W. Lydon, J.F. Slack, T H¬y and M.E.
Knapp; *Geological Association of Canada, Mineral Deposits Division,* **MDD
Special Publication No.1,** pp.225-244

ARNOLD G, 1983; The Cloncurry Authorities to Prospect:- Miscellaneous Report
No. 1117, April 1983

ASHLEY P.M. 1983; Recent exploration results from the Monakoff Prospect, near Cloncurry, northwest Queensland. Minerals Department Esso Australia Ltd.

van ACHTERBERGH E., RYAN C.G., JACKSON S.E. & GRIFFIN W.L. 2001; Appendix III. Data reduction software for LA-ICP-MS. In- P.Sylvester (ed). Laser Ablation-ICPMS in the Earth Sciences- Principles and applications. *Mineralogical Association of Canada, Short Course Series,* **no.29,** pp.239-243

BAIN J.H.C. & WITHNALL I.W. 1980; Mineral Deposits of the Georgetown Region, northeast Queensland. *In:-* The Geology and Geophysics of Northeastern Australia. R.A. Henderson and P.J. Stephenson *(eds.). Geological Society of Australia, Queensland Division.*

BAIN J.H.C., WITHNALL I.W., OVERSBY B.S. & MacKENZIE D.E. 1985a; Geology of the Georgetown region, Queensland. 1:250 000 scale map. *Australian Bureau of Mineral Resources.*

BAIN J.H.C., BLACK L.P., MacKENZIE D.E., OVERSBY B.S., WITHNALL I.W. & HOLMES R.D. 1985b; Tectonic evolution of the Georgetown Inlier, Queensland. In:- Tectonics and Geochemistry of Early to Middle Proterozoic Fold belts, Programme and Abstracts, Combined IGCP Meeting on the Proterozoic fold belts (215) and Proterozoic Geochemistry (217), Darwin 7-14 August 1985. *Australian Bureau of Mineral Resources, Record* **1985/28,** unpubl., pp.5-7

BALLARD R.D. & MOORE J.G. 1977; Photographic atlas of the Mid-Atlantic Ridge Rift Valley. Springer-Verlag New York 1286pp.

BARNES R.G. 1988; Metallogenic studies of the Broken Hill and Euriowie Blocks, New South Wales, 1, Styles of mineralisation in the Broken Hill Block. *Bulletin-New South Wales Geological Survey,* p.115

BARR D., 1987; Structural/stratigraphic models for extensional basins of half-graben type. Journal of Structural Geology, **9,** 491-500

BARRETT T.J., JARVIS I. & JARVIS K.E.1990; Rare earth element geochemistry of massive sulphides-sulphates and gossans on the Southern Explorer Ridge. *Geology,* **18,** 583-586

BARRETT T.J. & MacLEAN W.H. 1994; Chemostratigraphy and hydrothermal alteration in exploration for VHMS deposits in greenstones and younger rocks. *In:-* Lentz D.R. ed, Alteration and alteration processes associated with ore forming systems, *Geological Association of Canada Short Course Notes,* **no.11,** pp.433-467

BAU M. 1991; Rare-earth element mobility during hydrothermal and metamorphic fluid-rock interaction and the significance of the oxidation state or europium. *Chemical Geology,* **93,** 219-230

BEARDSMORE T.J., NEWBERY S.P. & LAING W.P. 1988; The Maronan Supergroup: An inferred early volcanosedimentary rift sequence in the Mount Isa Inlier, and it's implications for ensialic rifting in the middle Proterozoic of northwest Queensland. *Precambrian Research*, **40/41,** 487-507

BEARDSMORE T.J. 1992; Petrogenesis of the Mt Dore-style breccia-hosted copper-gold mineralisation in the Kuridala-Selwyn region of northwestern Queensland. Unpublished PhD thesis, James Cook University of Queensland.

BEESON R. 1990; Broken Hill-type lead-zinc deposits: an overview of their occurrence and geological setting. *Institute of Mining and Metallurgy Transactions,* **99,** B163-175.

BELL T.H. & HICKEY K.A. 1996; Multiple deformations with successive subvertical and subhorizontal axial planes: their impact on geometric development and significance for mineralisation and exploration in the Mt Isa region. *James Cook University Economic Geology Research Unit Contribution,* **55**, p.14

BELOUSOVA E.A., GRIFFIN W.L., WALTERS S.G. & O'REILLY S.Y.O, 2001; Crustal evolution and crust-mantle interaction in the Mount Isa Eastern Succession: Terrane Chron analysis of detrital zircons, In:- 2001-A hydrothermal odyssey: Townsville May 17-19 2001, James Cook University. *Economic Geology Research Unit Contribution No. 59*, pp.18-19

BERESFORD S.W. & CAS R.A.F. 2001; Komatiitic invasive lava flows, Kambalda, Western Australia. *The Canadian Mineralogist,* **39**, 525-535

BERRY R.F., JENNER G.A., MEFFRE S. TUBRETT M.N. 2001; A North American provenance for Neoproterozoic to Cambrian sandstones in Tasmania. *Earth and Planetary Science Letters,* **192 (2),** 207-222

BESWICK A.E. & SOUCIE G. 1978; A correction procedure for metasomatism in an Archean greenstone belt. *Precambrian Research,* **6,** 235-248

BETTS P.G. 1997; The Mount Isa Rift Event: An example of Middle Proterozoic intracontinental extension. PhD Thesis, Melbourne, Monash University (unpublished).

BETTS P.G., AILLERES L. & LISTER G.S. 1997; Geological Overview of the Mount Isa Terrane. In:- L. Ailleres & P.G. Betts (eds) Structural Elements of the Eastern Successions, p.17-36. *Australian Crustal Research Centre, Technical Publication 63*, pp.175.

BETTS P.G., AILLERES L., GILES D. & HOUGH M. 2000; Deformation history of the Hampden Synform in the Eastern Fold Belt of the Mt Isa terrane. *Australian Journal of Earth Sciences,* **47(6),** 1113-1126

BETTS P.G. & LISTER G.S 2001; Comparison of the 'strike-slip' versus 'episodic rift-sag' models for the origin of the Isa Superbasin. *Australian Journal of Earth Sciences,* **48,** 265-280

BETTS, P. G., GILES, D., LISTER, G. S. & FRICK, L. R. 2002a; Evolution of the Australian lithosphere. *Australian Journal of Earth Sciences* **49**, 661-695

BETTS P.G., LISTER G.S. & GILES D. 2002b; Ancient normal faults, basin inversion, tectonics and exploration for SHMS Pb-Zn deposits. *In:*- Applied Structural Geology for Mineral Exploration and Mining-International Symposium, Kalgoorlie 2002, Abstracts Volume. S. Vearncombe (*ed.*), pp.11-14

BETTS P.G., LISTER G.S. & POUND K.S. 1999; Architecture of a Palaeoproterozoic rift system: evidence from the Fiery Ck Dome region, Mt Isa Terrane. *Australian Journal of Earth Sciences,* **46,** 533-564

BEVINS R.E, KOKELAAR B.P. & DUNKLEY P.N. 1984; Petrology and geochemistry of lower- to middle-Ordovician igneous rocks in Wales: a volcanic arc to marginal basin transition. *Proceedings of the Geological Association,* **no.95,** p.337-347

BIERLEIN F.P. 1995; Rare-earth element geochemistry of clastic and chemical metasedimentary rocks associated with hydrothermal sulphide mineralisation in the Olary Block, South Australia. *Chemical Geology,* **122,** 77-98

BINGEN B, DEMAIFFE D. & HERGOTEN 1996; Redistribution of rare earth elements, thorium, and uranium over accessory minerals in the course of amphibolite to granulite facies metamorphism: the role of apatite and monazite in orthogneisses from southeastern Norway. *Geochimica Cosmochima et Acta,* **60,** 1341-1354

BLACK L.P. & McCULLOCH M.T 1990; Isotopic evidence for the dependence of of recurrent felsic magmatism on new crust formation: an example from the Georgetown Inlier of northeastern Australia. *Geochimica Cosmochima et Acta,* **54,** 183-196

BLACK L.P., BELL T.H., RUBENACH M.J. & WITHNALL I.W. 1979; Geochronology of discrete structural-metamorphic events in a multiply deformed Precambrian terrane. *Tectonophysics,* **92,** 171-194

BLACK L.P., GREGORY P., WITHNALL I.W. & BAIN J.H.C. 1998; U-Pb zircon age for the Etheridge Group, Georgetown region, north Queensland: implications for relationship with the Broken Hill and Mt Isa sequences. *Australian Journal of Earth Sciences,* **45(6),** 925-936

BLAKE D.H. 1987; Geology of the Mt Isa Inlier and environs, Queensland and Northern Territory. *Bureau of Mineral Resources, Australia, Bulletin,* **no. 225,**83pp

BLAKE D.H., JAQUES A.L. and DONCHAK P.J.T. 1983; Selwyn region, Queensland. Bureau of Mineral Resources, Australia 1:100 000 Map Commentary, 29pp

BLAKE D.H. & STEWART A.J. 1992; Stratigraphic and tectonic framework, Mt Isa
Inlier p 1-11. *In:*-Stewart A.J. and Blake D.H. eds:- *Detailed Studies of the Mt Isa
Inlier*, , *Bureau of Mineral Resources Bulletin* **243**

BODON S.B. 1996; Genetic implications of the paragenesis and rare-earth
geochemistry at the Cannington Ag-Pb-Zn deposit, Mt Isa Inlier, northwest
Queensland. In:- New Developments in Broken Hill-type deposits. Pongratz J. &
Davidson G.J. eds. pp.133-144. *CODES Special Publication No.1*

BODON S.B. 1998; Paragenetic relationships and their implications for ore genesis at
the Cannington Ag-Pb-Zn deposit, Mount Isa Inlier, Queensland, Australia.
Economic Geology, **93**, 1463-1488

BODON S.B. 2002, Geodynamic evolution and genesis of the Cannington Broken
Hill-type Ag-Pb-Zn deposit, Mount Isa Inlier, Queensland. Unpublished PhD
thesis, Centre for Ore Deposit Research, University of Tasmania, 373p.

BOUMA A.H. 1962; Sedimentology of some flysch deposits; Elsevier Amsterdam,
168 pp.

BOYNTON W.V. 1984; Geochemistry of the rare earth elements. *In:*- Lipin B.R. and
McKay G.A. (eds). *Rare earth element geochemistry*, Elsevier, pp.63-114

BRADSHAW B.E., LINDSAY J.E., KRASSAY A.A & WELLS A.T. 2000;
Attenuated basin-margin sequence stratigraphy of the Palaeoproterozoic Calvert
and Isa Superbasins: the Fickling Group, southern Murphy Inlier, Queensland.
Australian Journal of Earth Sciences, **47**, 599-624

BRANNEY M.J. & SUTHREN R.J. 1988; High-level peperitic sills in the English
Lake District: Distinction from block lavas and implications for Borrowdale
Volcanic Group stratigraphy, *Geological Journal*, **23**, 171-187

BROADBENT G.C., MYERS R.E. & WRIGHT J.V. 1998; Geology and origin of
shale hosted mineralization at the Century Zn-Pb-Ag deposit, northwest
Queensland. *Economic Geology*, **93(8)**, pp.1264-1294

BROOKS C.K., LARSEN L.M. & NIELSEN T.F.D. 1991; Importance of iron-rich
tholeiitic magmas at divergent plate margins. *Geology*, **19**, 269-272

BROOKS E.R. 1995; Palaeozoic fluidization, folding and peperite formation,
northern Sierra Nevada, California. *Canadian Journal of Earth Science*, **32**, 314-
324

BULL S.W. & CAS R.A.F 1989; Volcanic influences in a storm and tide dominated
shallow marine depositional system: the Late Permian Broughton Formation,
southern Sydney Basin, Kiama, NSW, Australia. *Australian Journal of Earth
Sciences*, **36**, 569-584

BULTITUDE R.J. & WYBORN L.A.I 1982; Distribution and geochemistry of volcanic rocks in the Duchess-Urandangi region, Queensland. *BMR Journal of Geology and Geophysics,* **7,** p.99-112

BUSBY-SPERA C.J. & WHITE J.D.L. 1987; Variation in peperite textures associated with differing host-sediment properties. *Bulletin of Volcanology,* **49,** 765-775

CARR G.R. & SUN S-s 1996; Lead isotope models applied to Broken Hill-style terrains syngenetic vs. epigenetic metallogenesis. *In:-* New Developments in Broken Hill-type Deposits. *CODES Special Publication* **No.1.** G.J. Davidson & J Pongratz eds.

CARTER E.K., BROOKS J.H. & WALKER K.R. 1961; The Precambrian mineral belt of northwestern Queensland. *Bureau of Mineral Resources Bulletin* **no.61**

CAWOOD P.A., NEMCHIN A.A. LEVERENZ A. SAEED A., BALANCE P.F 1999; U/Pb dating of detrital zircons: Implications for the provenance record of Gondwana margin terranes. *Geological Society of America Bulletin,* **111,** 1107-1119

CHOWN E.H., N'DAH E. & MUELLER W.U. 2000; The relation between iron-formation and low temperature hydrothermal alteration in an Archaean volcanic environment. *Precambrian Research,* **101,** 263-275

CLAGUE D.A., HOLCOMB R.T., SINTON J.M., DETRICK R.S & TORRESAN M.E., 1990; Pliocence and Pleistocene alkalic flood basalts from the seafloor north of the Hawaiian islands, *Earth and Planetary Science Letters,* **98(2),** 175-191

CLOUGH P.W.L & FIELD D. 1980; Chemical variations in metabasites from a Proterozoic amphibolite-granulite transition zone, south Norway. *Contributions to Mineralogy and Petrology,* **73,** 277-286

COLLINS W.J. 1998; Evaluation of petrogenetic models for Lachlan Fold Belt granitoids: implications for crustal architecture and tectonic models. *Australian Journal of Earth Sciences,* **45,** 483-500

COOKE D.R., BODON S.B. and BULL S.W. 1998; Element associations and depositional processes for McArthur-Type and Selwyn-type sediment-hosted Pb-Zn deposits. Sediment hosted base metal deposits Vol. 2: Research Projects for 1998, Final Report AMIRA P384A, December 1998

CORSARO R.A. & MAZZOLENI P. 2002 ; Textural evidence of peperites inside pillow lavas at Acicastello Castle Rock (Mt. Etna Sicily), *Journal of Volcanology and Geothermal Research,* **114,** 219-229

COURTOIS C. & TREUILL M. 1977; Distribution des terres rares et de quelques elements en trace dans les sediments recents des fosses de la Mer Rouge. *Chemical Geology,* **20,** 57-72

COX K.G. & HAWKESWORTH C.J. 1985; Geochemical stratigraphy of the Deccan Traps at Mahabaleshwar, Western Ghats, India, with implications for open system magmatic processes. *Journal of Petrology,* **15,** 269-301

CUMMINGS G.L. & RICHARDS J.R., 1975; Ore lead isotope ratios in a continuously changing Earth, Earth and Planetary Science Letters, **28(2)**,155-171

DADD K.A. & van WAGONER N.A. 2002; Magma composition and viscosity as controls on peperite texture: an example from Passamaquoddy Bay, southeastern Canada, *Journal of Volcanology and Geothermal Research,* **114,** 63-80

DAVIDSON G.J. 1991; Starra and Trough Tank: iron formation-hosted gold-copper deposits of northwest Queensland, Australia. Unpublished PhD. Thesis University of Tasmania.

DAVIDSON G.J. 1994; A geochemical and geological reconnaissance study of alteration, copper-gold ores, and iron-rich lithologies in the Cloncurry area, Mt Isa Inlier. Centre for Ore Deposit and Exploration Studies (University of Tasmania) Unpublished report for BHP World Minerals, 115 p.

DAVIDSON G.J. 1996; Styles and timing of iron enrichment in the Mt Isa Eastern Succession. In:- MIC '96- New Developments in Metallogenic Research-The McArthur-Mt Isa-Cloncurry Province, p.40-43. Compiled and edited by T.Baker, J.F. Rotherham, J.M. Richmond, G.Mark, P.J. Williams, pp.161

DAVIDSON G.J., 1998; Variation in copper-gold styles through time in the Proterozoic Cloncurry goldfield, Mt Isa Inlier: a reconaissance view. *Australian Journal of Earth Sciences,* **45(3),** 445-462

DAVIDSON G.J. AND DAVIS B.K. 1997; Characteristics of the Monakoff Cu-Au-F-Ba-Mn deposit, Mt. Isa Eastern Succession. AMIRA Final Report 1997, Volume 2, Section 13.

DAVIDSON G.J., STOLZ A.J. & EGGINS S.M. 2001; Geochemical anatomy of silica iron exhalites: evidence for hydrothermal oxyanion cycling in response to vent fluid redox and thermal evolution (Mt. Windsor Subprovince, Australia). *Economic Geology,* **96,** 1201-1226

DAVIDSON G.J., DAVIS B.K. & GARNER A. 2002; Structural and geochemical constraints on the emplacement of the Monakoff oxide Cu-Au (Co-U-REE-Ag-Pb-Zn) deposit, Mt Isa Inlier Australia. "Hydrothermal iron oxide copper-gold & related deposits, a global perspective' vol. 2. Porter GeoConsultancy Pty Ltd. Page numbers at this stage unknown.

DeCELLES P.G. & CAVAZZA W. 1991: Constraints on the formation of Pliocene Hummocky Cross-Stratification in Calabria (Southern Italy) from consideration of hydraulic and dispersive equivalence, grain-flow theory, and suspended-load fallout rate. *Journal of Sedimentary Petrology,* **62(4),** 555-568

DEER W.A., HOWIE R.A. & ZUSSMAN J. 1992; An introduction to the rock forming minerals-2nd Edition, 687 p.

DERRICK G.M., WILSON I.H. & HILL R.M. 1976(b);Revision of stratigraphic nomenclature in the Precambrian of northwest Queensland. II: Haslingden Group. *Queensland Government Mining Journal,* **no.77,** 300-306

DERRICK G.M., WILSON I.H. & HILL R.M. 1976(c);Revision of stratigraphic nomenclature in the Precambrian of northwest Queensland. III: Mount Isa Group. *Queensland Government Mining Journal,* **no.77,** 402-405

DERRICK G.M., WILSON I.H. & HILL R.M. 1976(d);Revision of stratigraphic nomenclature in the Precambrian of northwest Queensland. IV: Malbon Group. *Queensland Government Mining Journal,* **no.77,** 515-517

DERRICK G.M., WILSON I.H. & HILL R.M. 1976(e);Revision of stratigraphic nomenclature in the Precambrian of northwest Queensland. V: Soldiers Cap Group. *Queensland Government Mining Journal.* **no.77,** 601-604

DERRICK G.M., WILSON I.H. & HILL R.M. 1977(a); Revision of the stratigraphic nomenclature of the Precambrian of northwestern Queensland. VI: Mary Kathleen Group. *Queensland Government Mining Journal,* **no.78,** 15-23

DERRICK G.M., WILSON I.H. & HILL R.M. 1977(b); Revision of the stratigraphic nomenclature of the Precambrian of northwestern Queensland. VII: Mount Albert Group. *Queensland Government Mining Journal,* **no.78,** 113-116

DERRICK G.M. 1982; A Proterozoic rift zone at Mount Isa, Queensland and implications for mineralisation. *BMR Journal of Geology and Geophysics,* **no.7,** 81-92

DIMROTH E, COUCINEAU P., LEUDU M. & SANGCHARGRIN Y. 1987; Structure and organisation of Archaean basalt flows, Rouyn-Noranda area, Quebec, Canada, *Canadian Journal of Earth Sciences,* **15,** 902-918

DeJONG G. and WILLIAMS P.J. 1995; Evolution of the metasomatic features during exhumation of the mid-crustal Proterozoic rocks in the vicinity of the Cloncurry Fault, NW Queensland. *Australian Journal of Earth Sciences,* **42,** 281-290

DOLOZI M.B. & AYRES L.D. 1991; Early Proterozoic basaltic-andesite tuff breccia: downslope subaqueous mass transport of phreatomagmatically-generated tephra. *Bulletin of Volcanology,* **53,** 477-495

DOMAGALA J., SOUTHGATE P.N., McCONACHIE B.A. & PIDGEON B.A. 2000; Evolution of the Palaeoproterozoic Prize, Gun and lower Loretta Supersequences of the Surprise Creek Formation and Mount Isa Group. *Australian Journal of Earth Sciences,* **47,** 485-508

DOTT R.H. & BOUERGOIS J, 1982; Hummocky cross stratification: Significance of its variable bedding sequences. *Geological Society of America Bulletin,* **93,** 663-680

DRIESE S.G., FISCHER M.W., EASTHOUSE K.A., MARKS G.T., GOGOLA A.R. & SCHONER A.E. 1991; Model for genesis of shoreface and shelf sandstone sequences, southern Appalachians: palaeoenvironmental reconstruction of an Early Silurian shelf system. *In:-* Shelf sand and sandstone bodies D.J.P Swift, G.F. Oertel, R.W. William & J.A. Thorne (*eds*). *International Association of Sedimentologists, Special Publication,* **No. 14,** 309-338

DUFFIELD W.A., BACON C.R. & DELANEY P.T. 1986; Deformation of poorly consolidated sediment during shallow emplacement of a basalt sill, Coso Range California. *Bulletin of Volcanology,* **48,** 97-107

DUKE W.L. 1990: Geostrophic circulation or shallow marine turbidity currents? The dilemma of palaeoflow patterns in storm-influenced prograding shoreline systems. *Journal of Sedimentary Petrology,* **60,** 870-883

DUKE W.L., ARNOTT R.W.C. & CHEEL R.J., 1991; Shelf sandstones and hummocky cross stratification: New insights on a stormy debate. *GEOLOGY,* **19,** 625-628

DYMOND J., CORLISS J.B., HEATH G.R., FIELD C.W., DASCH E.J. & VEEH E.H. 1973; Origin of metalliferous sediments from the Pacific Ocean. *Geological Society of America Bulletin,* **84,** 3355-3372

EBINGER C.J. 1989; Geometric and kinematic development of border faults and accommodation zones, Kivi-Rusizi rift, Africa. *Tectonics,* **8,** 117-133

EBINGER C.J., KARNER G.D. & WEISSEL J.K. 1991; Mechanical strength of the continental lithosphere: constraints from the western rift system, East Africa. *Tectonics,* **10,** 1239-1256

EINSELE G., GIESKES J.M. & CURRAY J.R. 1980; Intrusion of basaltic sills into highly porous sediments and resulting hydrothermal activity. *Nature,* **283,** 441-445

EINSELE G. & SEILACHER A. 1982; Distribution of tempestites and turbidites, p.377-382. *In:-* Cycles and Events in Stratigraphy, Einsele G., Ricken W. Seilacher A. (*eds.*)

ELDERFIELD H. & GREAVES M.J. 1981; Negative cerium anomalies in the rare-earth element patterns of oceanic ferromanganese nodules. *Earth and Planetary Science Letters,* **55,** 163-170

ELDERFIELD H. & GREAVES M.J. 1982; The rare earth elements in seawater. *Nature,* **296,** 214-219

ERLANK A.J. & KABLE E.J.D. 1976; The significance of incompatible elements in Mid-Atlantic Ridge basalts from 45°N, with particular reference to Zr/Nb. *Contributions to Mineralogy and Petrology,* **48,** 281-291

ETHERIDGE M.A., RUTLAND R.W.R & WYBORN L.A.I. 1987; Orogenesis and tectonic process in the Early to Middle Proterozoic of northern Australia. *In:-* Kroner A. *ed. Proterozoic Lithosphere Evolution,* pp. 131-147. American Geophysical Union and Geological Society of America Geodynamics Series **No. 17.**

ETHIER V.G., CAMPBELL F.A., BOTH R.A. & KROUSE H.R. 1976; Geological setting of the Sullivan orebody and estimates of temperatures and pressures of metamorphism, *Economic Geology,* **71,** 1570-1588

FENG, R., MACHADO, N., and LUDDEN, J., 1993, Lead Geochronology of Zircon By Laserprobe-Inductively Coupled Plasma Mass Spectrometry (Lp-ICP-MS): Geochimica et Cosmochimica Acta, **57,** 3479-3486.

FINLOW-BATES T. & STUMPFL E.F. 1981; The behaviour of so-called immobile elements in hydrothermally altered rocks associated with volcanogenic submarine exhalative ore deposits. *Mineralium Deposita,* **16,** 319-328

FLEET A.J. 1984; Aqueous and sedimentary geochemistry of the rare-earth elements. *In:-*Henderson P. (ed.), *Rare Earth Element Geochemistry.* Elsevier pp.343-373

FLOYD P.A. & WINCHESTER J.A. 1978; Identification and discrimination of altered and metamorphosed volcanic rocks using immobile elements. *Chemical Geology,* **v.21(3-4),** pp.291-306.

FORNARI D.J., PERFIT M.R., MALAHOFF A. & EMSLEY R. 1983; Geochemical studies of abyssal lavas recovered by DSRV Alvin from the Eastern Galapagos Rift, Inca Transform and Ecuador Trough. 1. Major element variations in natural glasses and spatial distribution of lavas. *Journal of Geophysical Research,* **88,** 10519-10529

FRIETSCH R. & PERDAHL J.A. 1995; Rare earth elements in apatite and magnetite in Kiruna-type ores and some other iron ore types. *Ore Geology Reviews,* **9(6),** 489-510

FRYER B.J., SIMON E., JACKSON H. & LONGERICH P., 1993; The application of Laser Ablation Microprobe Inductively Coupled Plasma Mass Spectrometry (LAM-ICPMS) to in-situ (U)-Pb geochronology. Chemical Geology, **109,** 1-8

GARBENSCHONBERG, C. D., and ARPE, T., 1997, High Resolution ICPMS in Fast Scanning-Mode - Application For Laser Ablation Analysis of Zircon. Fresenius Journal of Analytical Chemistry, **359,** 462-464.

GAWTHORPE R.L. & LEEDER M.R. 2000; Tectono-sedimentary evolution of active extensional basins. *Basin Research,* **12,** 195-218

GERMAN C.R., CAMPBELL A.C. & EDMOND J.M. 1991; Hydrothermal scavenging at the Mid-Atlantic ridge: Modification of trace element dissolved fluxes. *Earth and Planetary Science Letters,* **107,** 101-114

GILES D. & MacCREADY T. 1997; The structural and stratigraphic position of the Soldiers Cap Group in the Mount Isa Inlier p. 61-74. *In:-* Ailleres L. & Betts P. eds- *Structural Elements of the Eastern Successions,* Australian Geodynamics Research Centre Technical Publication, **63,** pp.175

GILES D., 2000; Tectonic setting of Broken Hill-type mineralisation; the Cannington perspective. Unpublished PhD Thesis, Monash University, Melbourne, Victoria.

GILES D. & BETTS P. G. 2000a; The Early to Middle Proterozoic configuration of Australia and its implications for Australian-US relations. *Geological Society of Australia Abstracts* **59,** 174.

GILES D. & BETTS P. G. 2000b; Beyond Rodinia: the Early to Middle Proterozoic amalgamation of Australia and North America. *Australian Crustal Research Centre Technical Report* **85**

GILES D., BETTS P. G. & LISTER G. S. 2001; A continental backarc setting for Early to Middle Proterozoic basins of north-eastern Australia. *Geological Society of Australia Abstracts* **64,** 55-56

GILES D, BETTS P.G. & LISTER G.S. 2002; Far-field continental backarc setting for the 1.80-1.67 Ga basins of northeastern Australia. *Geology,* **30(9),** 823-826

GILES D. & NUTMAN A.P. 2003; SHRIMP U-Pb dating of the host rocks of the Cannington Ag-Pb-Zn deposit, southeastern Mt Isa Block, Australia. *Australian Journal of Earth Sciences,* **50,** 295-309

GLIKSON A.Y. 1972; Structural setting and origin of Proterozoic calc-silicate megabreccias, Cloncurry region, Northwestern Queensland, *Journal of the Geological Society of Australia,* **19(1),** 53-63

GLIKSON, A.Y. & DERRICK G.M. 1970; The Proterozoic metamorphic rocks of the Cloncurry 1:100 000 Sheet area, (Soldiers Cap Belt) northwestern Queensland. Bureau of Mineral Resources, Australia.

GLIKSON A.Y & DERRICK G.M. 1978; Geology and geochemistry of Middle Proterozoic basic volcanic belts, Mt Isa/ Cloncurry, northwestern Queensland. *Bureau of Mineral Resources Record,* **1978/48**

GLIKSON A.Y., DERRICK G.M., WILSON I.H., & HILL R.M., 1976; Tectonic evolution and crustal setting of the middle Proterozoic Leichardt River Fault Trough, Mt Isa region, northwestern Queensland. *Bureau of Mineral Resources Journal of Australian Geology and Geophysics,* **1,** 115-129

GONCHAROV A.G., COLLINS C.D.N., GOLEBY B.R. & DRUMMOND B.J. 1996; Anomalous structure of the Mount Isa Inlier crust and crust-mantle

transition zone in the global context, from refraction wide-angle seismic transects. *Geological Society of Australia, Abstracts,* **41,** 159

GOODFELLOW W.D. 1998; SEDEX Pb-Zn-Ag deposits of North America, CODES Short Course Manual No. 3, Sediment-hosted Zn-Pb deposits: North American SEDEX deposits, Genetic considerations

GOODFELLOW W.D 1999; Sediment hosted Zn-Pb-Ag deposits of North America. In:- *Basins, Fluids and Zn-Pb ores,* CODES Special Publication No. 2, Holm.O, Pongratz J. & McGoldrick P. *(eds),* pp. 168

GOODFELLOW W.D. 2000; Anoxic conditions in the Aldridge basin during formation of the Sullivan Zn-Pb deposit: implications for the genesis of massive sulphides and distal hydrothermal sediments. *In:-* . In:- The Geological Environment of the Sullivan Deposit , British Columbia, (eds) J.W. Lydon, J.F. Slack, T Höy and M.E. Knapp; *Geological Association of Canada, Mineral Deposits Division,* **MDD Special Publication No.1,** pp.159-191

GOODFELLOW W.D., LYDON J.W. & TURNER R.J.W. 1993; Geology and genesis of stratiform sediment-hosted (SEDEX) zinc-lead-silver sulphide deposits. In:- Kirkham R.V., Sinclair W.D., Thorpe R.I. and Duke J.M. eds., *Mineral Deposit Modelling: Geological Association of Canada, Special Paper,* **no.40,** p.201-251

GORTON M.P., SCHANDL E.S. & HÖY T. 2000; Mineralogy and Geochemistry of the Middle Proterozoic Moyie Sills in southeastern British Columbia. *In:-*The Geological Environment of the Sullivan Deposit, British Columbia. J.W. Lydon, J.F. Slack, T. Hoy and M.E. Knapp *(eds.). Geological Association of Canada, Mineral Deposits Division,* **MDD Special Volume No.1**

GROSS G.A. 1965; Geology of iron ore deposits in Canada. I-General Geology and evaluation of iron deposits. *Geological Survey of Canada Economic Geology Report* **22**

GROSS G.A. 1993; Element distribution patterns as metallogenetic indicators in siliceous metalliferous sediments. Proceedings of the 29th International Geological Congress-Resource Geology Special Issue, **17(C), 96-106**

HAINES P.W., BAGO J.B. & GUM J.C. 2001; Turbidite deposition in the Cambrian Kanmantoo Group, South Australia. *Australian Journal of Earth Sciences,* **48,** 465-478

HAMBLIN A.P. & WALKER R.G., 1979; Storm dominated shallow marine deposits: The Fernie-Kootenay (Jurassic) transition, southern Rocky Mountains. *Canadian Journal of Earth Sciences,* **16,** 1673-1690

HAMILTON J.M. 1984; The Sullivan deposit, Kimberley, British Columbia- a magmatic component to genesis?: In:- The Belt, Belt Symposium II, Abstracts with Summaries. *(ed.)* S.W. Hobbs. *Montana Bureau of Mines and Geology, Special Publication* **No. 90,** p.58-60

HARMS J.C., SOUTHARD J.B. & WALKER R.G., 1982; Structures and sequences in clastic rocks. *Society of Economic Palaeontologists and Mineralogists, Short Course No.9.*

HATTON O.J., BULL S.W. & DAVIDSON G.J. 2000; A review of the geological setting and sedimentology of the Proterozoic upper Soldiers Cap Group, Eastern Succession, rift fill in a Pb-Zn rich basin (Mt Isa Inlier, NW Qld). Proceedings of New Ideas for a New Millenium, Cranbrook Workshop, May 6-7 2000.

HELVACI C. 1984; Apatite-rich iron deposits of the Avnik (Bing¬l) Region southeastern Turkey. *Economic Geology,* **79,** 354-371

HENDERSON R.A. 1980; Structural outline and summary geological history for northeastern Australia p.1-26. *In:-* The Geology and Geophysics of Northeastern Australia. R.A. Henderson and P.J. Stephenson *(eds.). Geological Society of Australia, Queensland Division.*

HILL E.J., LOOSVELD R.J.H. & PAGE R.W. 1992; Structure and geochronology of the Tommy Ck Block, Mt Isa Inlier. In:- Stewart A.J. & Blake D.H. (eds). Detailed Studies of the Mount Isa Inlier, *Australian Geological Survey Bulletin,* **243,** 329-348

HIRATA, T., and NESBITT, R. W., 1995, U-Pb isotope geochronology of zircon - evaluation of the laser probe-inductively coupled plasma mass spectrometry technique. *Geochimica et Cosmochimica Acta,* **59,** 2491-2500.

HOGG A.J.C., FAWCETT J.J., GITTINS J. & GORTON M.P. 1988; Cyclical tholeiite volcanism and associated magma chambers: Eruptive mechanisms in East Greenland. *In-* Morton A.C. and Parson L.M. *eds,* Early Tertiary volcanism and the opening of the North Atlantic. *Geological Society of London, Special Publication,* **39,** 197-200

HOGG A.J.C., FAWCETT J.J., GITTINS J. & GORTON M.P. 1989; Cyclical variation in composition in continental tholeiites of East Greenland. *Canadian Journal of Earth Sciences,* **26,** 534-543

HOLCOMBE R.J., PEARSON P.J. & OLIVER N.H.S 1991; Geometry of a Middle Proterozoic extensional decollement in northeastern Australia. *Tectonophysics,* **191,** 255-274.

HOLLAND H.D. 1973; The oceans: a possible source of iron in iron-formation. *Economic Geology,* **68,** 1169-1172

HOLLAND H.D. 1984; The chemical evolution of the atmosphere and oceans. Princeton University Press, Princeton, New Jersey, pp.351

HOLM O.H., PONGRATZ J. McGOLDRICK P.M. 1998; Basins, fluids and Zn-Pb ores. Proceedings of an International Conference at CODES, July 1998. *CODES Special Publication,* **No.2**

HORN I., RUDNICK R.L., McDONOUGH W.F. 2000; Precise elemental and
isotopic determinaton by simultaneous solution nebulization and laser
ablation ICPMS: application to U-Pb geochronology. *Chemical Geology*, **164,**
281-301

HÖY T. 1982; Stratigraphic and structural setting of stratabound lead-zinc deposits in
southeastern B.C. *Canadian Institute of Mining and Metallurgy, Bulletin*. **v.75,**
No. 840, 114-134

HÖY T. 1989; The age, chemistry and tectonic setting of Middle Proterozoic Moyie
sills, Purcell Supergroup, southeastern British Columbia. *Canadian Journal of*
Earth Sciences. **26,** 2305-2317

HÖY T., ANDERSON D., TURNER R.J.W. & LEITCH C.H.B. 2000: Tectonic,
Magmatic and Metallogenic History of the early synrift phase of the Purcell
Basin, southeastern British Columbia. *In:*-The Geological Environment of the
Sullivan Deposit, British Columbia. J.W. Lydon, J.F. Slack, T. Hoy and M.E.
Knapp *(eds.)*. *Geological Association of Canada, Mineral Deposits Division,*
MDD Special Volume No.1

HUNTER R.E. & CLIFTON H.E. 1982; Cyclic deposits and hummocky cross-
straitification of probable storm origin in Upper Cretaceous rocks of the Cape
Sebastian area, southwestern Oregon. *Journal of Sedimentary Petrology*, **52,** 127-
143

ISLEY A.E. 1995; Hydrothermal plumes and the delivery of iron to banded iron
formations. *Journal of Geology,* **103,** 169-185

JACKSON J.A., WHITE N.J., GARFUNKEL Z., Anderson H., 1988; Relationships
between normal fault geometry, tilting and vertical motions in extensional
terrains: an example from the southern Gulf of Suez. Journal of Structural
Geology, **10,** 155-170

JACKSON M.J., SIMPSON E.L. & ERIKSSON K.A. 1990; Facies and sequence
stratigraphy analysis in an intracratonic, thermal relaxation basin; the early
Proterozoic lower Quilalar Formation and Ballara Quartzite, Mount Isa Inlier,
Australia. *Sedimentology,* **37,** 1053-1078

JAMES S.D., PEARCE J.A. & OLIVER R.A. 1987; The geochemistry of the Lower
Proterozoic Willyama Complex volcanics, Broken Hill Block, New South Wales.
In: Pharaoah T.C., Beckinsale R.D. & Rickard D. eds. *Geochemistry and*
mineralisation of the Proterozoic volcanic suites. pp.395-408, Geological Society
of London Special Publication **No.33**

JAQUES A.L., BLAKE D.H. & DONCHAK P.J.T., 1982; Regional metamorphism in
the Selwyn Range area, northwest Queensland. *Bureau of Mineral Resources*
Journal of Geology and Geophysics, **7,** 181-196

JAQUES A.L., BLAKE D.H. & DONCHAK P.J.T., 1982; Regional metamorphism in the Selwyn Range area, northwest Queensland. *Bureau of Mineral Resources Journal of Geology and Geophysics,* **7,** 181-196

JIANG S-Y, PALMER M.R., SLACK J.F., YANG J-H & SHAW D.R. 2000; Trace element and rare-earth element geochemistry of tourmalinites and related rocks and ores from the Sullivan deposit and vicinity, southeastern British Columbia. *In:-*The Geological Environment of the Sullivan Deposit, British Columbia. J.W. Lydon, J.F. Slack, T. Hoy and M.E. Knapp *(eds.). Geological Association of Canada, Mineral Deposits Division,* **MDD Special Volume No.1**

KLEIN C (Jr.) 1973; Changes in mineral assemblages with metamorphism of some Precambrian iron-formations. *Economic Geology,* **68,** 1075-1088

KLINKHAMMER G. ELDERFIELD J.M., EDMOND J.M. and MITRA A. 1994; Geochemical implications of rare-earth element patterns in hydrothermal fluids from mid-ocean ridges. *Geochimica Cosmochima et Acta,* **58,** 5105-5113

KNELLER B.C., EDWARDS D., McCAFFREY W. & MOORE R. 1991; Oblique reflection of turbidity currents. *Geology,* **19,** 250-252

KNELLER B.C, 1995; Beyond the turbidite paradigm: physical models for deposition of turbidites and their implications for reservoir prediction. In:-*Reservoir Characterisation of Deep Marine Clastic Systems*(Eds- D.J. Prosser & A Hartley) *Geological Society Special Publication* **No.94**

KNELLER B.C. & BRANNEY M.J., 1995; Sustained high-density turbidity currents and the deposition of thick massive sands. *Sedimentology,* **42,** 607-616

KNUDSEN T.L., ANDERSEN T., WHITEHOUSE M.J. & VESTIN J. 1997; Detrital zircon ages from southern Norway-implications for the Proterozoic evolution of the southwestern Baltic Shield. *Contributions to Mineralogy and Petrology,* **130,** 47-58

KOKELAAR B.P.1982; Fluidization of wet sediments during the emplacement and cooling of various igneous bodies. *Geological Society of London.* **139,** 21-33

KOKELAAR P. 1986; Magma-water interactions in subaqueous and emergent basaltic volcanism. *Bulletin of Volcanology,* **48,** 275-291

KRONER A 1983; Proterozoic mobile belts compatible with the plate tectonics concept. In:- G.M Medaris, C.W. Byers, D.M. Mikelson and W.G. Shanks *eds.* Proterozoic Geology: Selected Papers from an International Proterozoic Symposium. *Geological Society of America, Memoir,* **No.161,** 59-74

KUSZNIR N.J. & EGAN S.S. 1990; Simple-shear and pure shear models of extensional sedimentary basin formation: application to the Jeanne d'Arc Basin, Grand Banks of Newfoundland. *In:-* Extensional Tectonics and Stratigraphy of the North Atlantic Margin, A.J. Tankard and H.R. Balkwill *(eds).* American Association of Petroleum Geologists Memoir, **46,** 305-322

LAAJOKI K. 1986; Main features of Precambrian Banded Iron-Formations of Finland. *Journal of the Geological Society of India,* **28,** 251-270

LAAJOKI K. & KORKIAKOSKI E., 1988; The Precambrian tempestite-turbidite transition as displayed by the amphibolite facies Puolankajarvi Formation, Finland. *Sedimentary Geology,* **58,** 195-216.

LaBERGE G.L 1973; Possible biological origin of Precambrian iron-formations. *Economic Geology,* **68,** 1098-1109

LAING W.P. 1990; The Cloncurry terrane: an allocthon of the Diamantina orogen rafted onto the the Mt Isa Orogen, with its own distinctive metallogenic signature. *In: Mount Isa Inlier Geology Conference,* p.19-22. Victorian Insitute of Earth and Planetary Sciences, Monash University, Melbourne.

LAING W.P. 1996; The Diamantina Orogen linking the Willyama and Cloncurry terranes, eastern Australia. In:- New developments in Broken Hill-type deposits, p.67-72, *In:-* New Developments in Broken Hill-type deposits. Pongratz J. & Davidson G. *(eds) CODES Special Publication No.1.*

LAING W.P. 1998; Structural-metasomatic environment of the East Mt Isa Block base-metal gold province. *Australian Journal of Earth Sciences,* **45,** 413-428

LAMBIASE J.J. & BOSWORTH W. 1995; Structural controls on rift sedimentation. In:- Hydrocarbon Habitat in Rift Basins, J.J. Lambiase ed. *Geological Society, Special Publication,* **80,** 117-144

LARGE R.R., BODON S.B., DAVIDSON G.J. & COOKE D. 1996; The chemistry of BHT ore formation- one of the keys to understanding the differences between SEDEX and BHT deposits p.105-112. *In:-* New Developments in Broken Hill-type deposits. Pongratz J. & Davidson G. *(eds),. CODES Special Publication No.1*

LEE J.K.W., WILLIAMS I.S. and ELLIS D.J. 1997; Pb, U and Th diffusion in natural zircon. Nature, **390,** 159-162

LEEDER M.R. & GAWTHORPE R.L. 1987; Sedimentary models for extensional tilt block/half graben basins. *In:-* Coward M.P., Dewey J.F. & Hancock P.L. (eds) *Continental Extensional Tectonics.* Geological Society of London Special Publication **28,** 139-152

LEEDER M.R. & JACKSON J.A. 1993; The interaction between normal faulting and drainage in active extensional basins, with examples from the western United States and central Greece. *Basin Research,* **5,** 79-102

LI Xian-Hua, LIANG X., SUN M., LIU Y., TU X. 2000; Geochronology and geochemistry of single grain zircons: simultaneous in-situ analysis of U-Pb age

and trace elements by LAM-ICP-MS. *European Journal of Mineralogy* **12**, 1015-1024

LISTER G.S., O'DEA M.G., MacCREADY T. & BETTS P.G. 1996; Evolution of the Isan Orogeny. In:- Baker T., Rotherham J., Richmond G., Mark G. & Williams P *eds.* New developments in metallogenic research: The McArthur, Mount Isa and Cloncurry minerals province. *Contributions of the Economic Geology Research Unit,* **55,** 75-76

LISTER G.S., BETTS P.G., GILES D. & MacCREADY T. 1997; The active tectonic environment of ore deposition in the Mt Isa Terrane p.117-130. *In*: Structural Elements of the Eastern Succession: A field guide illustrating the Structural Geology of the Eastern Mt Isa Terrane, Australia. Ailleres L. & Betts P.G. *(eds)*

LISTER G.S., O'DEA M.G. & SOMAIA I. 1999; A tale of two synclines: rifting, inversion and transpressional popouts at Lake Julius, northwestern Mt Isa terrane, Queensland. *Australian Journal of Earth Sciences,* **46,** 233-250

LISTER J.R. & KERR R.C. 1990; Fluid-mechanical models of dyke propagation and magma transport p.69-80. In:- Mafic Dykes and Emplacement Mechanisms, A.J. Parker, P.C. Rickwood and D.H. Tucker *(eds), Proceedings of the International Dyke·Conference,* **vol.2**

LOOSVELD R.J.H. 1988; Structure and tectonothermal history of the eastern Mt Isa Inlier, Australia. PhD thesis (unpubl.) Australian National University, Canberra.

LOOSVELD R.J.H. 1992; Structural geology of the central Soldiers Cap Belt, Mount Isa Inlier, Australia. In:- AGSO Bulletin 243- Detailed Studies of the Mount Isa Inlier- Stewart A.J. & Blake D.H. eds.

LOTTERMOSER B.G. 1989; Rare-earth element study of exhalites within the Willyama Supergroup, Broken Hill Block, Australia. *Mineralium Deposita,* **24,** 92-99

LOTTERMOSER B.G., ASHLEY P.M. & PLIMER I.R. 1994; Iron formations, barite rocks and copper-gold mineralisation within the Willyama Supergroup, Olary Block, South Australia. *In-* Australian Research on Ore Genesis Symposium. Australian Mineral Foundation, Adelaide, 8.1-8.5

LOTTERMOSER B.G. & ASHLEY P.M. 1995; Geochemistry and exploration significance of ironstones and barite rich rocks in the Proterozoic Willyama Supergroup. *Journal of Geochemical Exploration,* **57(1-3),** 57-73

LOWE D.R. 1982; Sediment gravity flows II. Depositional models with special reference to the deposits of high-density turbidity currents. *Journal of Sedimentary Petrology* **52**, 279-297

LYDON J.W. 2000; Sediment-sill sulphur interaction and Sullivan.
In:- *Technical Volume-New Ideas for a New Millenium, Cranbrook, 2000,* Walker R. *(ed)*

LYDON J.W. & PAAKKI J. 2000; An overview of the geology of the Sullivan Pb-Zn deposit. *In:*-The Geological Environment of the Sullivan Deposit, British Columbia. J.W. Lydon, J.F. Slack, T. Hoy and M.E. Knapp *(eds.)*. *Geological Association of Canada, Mineral Deposits Division*, **MDD Special Volume No.1**

LYDON J.W., SLACK T., HOY T., KNAPP M.E. 2000; The Geological Environment of the Sullivan Deposit, British Columbia. *In:*-The Geological Environment of the Sullivan Deposit, British Columbia. J.W. Lydon, J.F. Slack, T. Hoy and M.E. Knapp *(eds.)*. *Geological Association of Canada, Mineral Deposits Division*, **MDD Special Volume No.1**

LUDWIG K. R. 1999. *Users Manual for Isoplot/Ex, Version 2.05, a Geochronological Toolkit for Microsoft Excel.* Berkeley Geochronological Center, Berkeley

MacCREADY T., GOLEBY B.R., GONCHAROV A., DRUMMOND B.J. & LISTER G.S., 1998; A framework of overprinting orogens based on interpretation of the Mount Isa Deep Seismic Transect. *Economic Geology*, **93**, 1422-1434

MacGEEHAN P.J. & MacLEAN W.H. 1980; An Archaean sub-seafloor geothermal system, calc-alkali trends and massive sulphide genesis. *Nature*, **286**, 767-771

MACHADO, N., and GAUTHIER, G., 1996, Determination of Pb207/Pb206 ages on zircon and monazite by laser-ablation ICPMS and application to a study of sedimentary provenance and metamorphism in southeastern Brazil: *Geochimica et Cosmochimica Acta*, **60**, 5063-5073.

MACHADO, N., SCHRANK, A., NOCE, C. M., and GAUTHIER, G., 1996, Ages of Detrital Zircon From Archean-Paleoproterozoic Sequences - Implications For Greenstone Belt Setting and Evolution of a Transamazonian Foreland Basin in Quadrilatero Ferrifero, Southeast Brazil: *Earth & Planetary Science Letters*, **141**, 259-276.

MARES V.M 1998; Structural development of the Soldiers Cap Group in the Eastern Fold Belt of the Mt Isa Inlier: a succession of horizontal and vertical deformation events and large-scale shearing. *Australian Journal of Earth Sciences*, **45**, 373-388

MARK G. 1999; Petrogenesis of Mesoproterozoic K-rich granitoids, southern Mt Angelay igneous complex, Cloncurry district northwest Queensland. *Australian Journal of Earth Sciences*, **46**, 933-950

MARK G. 1998; Albitite formation by selective pervasive sodic-calcic alteration of tonalite plutons in the Cloncurry district, NW Queensland. *Australian Journal of Earth Sciences*, **45**, 765-774

MAYNARD J.B. 1983; Geochemistry of Sedimentary Ore Deposits-Chapter 2: Iron, p.9-37.

McBIRNEY A.R., 1963; Factors governing the nature of submarine volcanism. *Bulletin of Volcanology,* **26,** 455-469.

McDONALD G.D., COLLERSON K.D. & WENDT J.I. 1996; New field and Sm-Nd isotopic constraints on the early evolution of the Mt. Isa Block. *Geological Society of Australia Abstracts,* **41,** 285

McDONALD G.D., COLLERSON K.D. & KINNY P.D. 1997; Late Archaean and early Proterozoic crustal evolution of the Mount Isa Block, northwest Queensland, Australia. *Geology,* **25(12),** 1095-1098

McKENZIE D. & WEISS N. 1975. Speculations on the thermal and tectonic history of the Earth. *Geophysical Journal of the Royal Astronomical Society* **42,** 31-174

McLENNAN S.M. 1989; Rare earth elements in sedimentary rocks: Influence of provenance and sedimentary processes. *Reviews in Mineralogy,* **21,** 169-200

McPHIE J. 1993; The Tennant Creek porphyry revisited: A synsedimentary sill with peperite margins, Early Proterozoic, Northern Territory. *Australian Journal of Earth Sciences,* **40,** 545-558

McPHIE J., DOYLE M. & ALLEN R.L. 1993; Volcanic textures: A guide to the interpretation of textures in volcanic rocks. Printed by Tasmanian Government Printing Office, 198pp.

McPHIE J. & HOUGHTON B. 1998; Volcanology: An outline of eruption processes and products, volcanic facies and facies associations in modern terrains. Centre for Ore Deposit Research, Master of Economic Geology, Course Work Manual No.7, Fifth Edition, pp. 230

MEZGER K. & KROGSTAD E.J., 1997; Interpretation of discordant U-Pb ages: an evaluation. *Journal of Metamorphic Geology,* **15,** 127-140

MIALL A.D. 1990; Principles of Sedimentary Basin Analysis, 2nd edition. Springer-Verlag New York, 668 pp.

MICHARD A. & ALBERADE F. 1986; The REE content of some hydrothermal fluids. *Chemical Geology,* **55,** 51-60

MICHARD A. 1989; Rare earth element systematics in hydrothermal fluids. *Geochimica Cosmochima et Acta,* **53,** 745-750

MICHARD A, ALBERADE F., MICHARD G., MINSTER J.F. & CHARLOU J.L. 1983; Rare earth elements and uranium in high-temperature solutions from the East Pacific Rise hydrothermal vent field (13°N). *Nature,* **303,** pp.43-65

MIDDLETON G.V 1967; Experiments on density and turbidity currents III. Deposition of sediment. *Canadian Journal of Earth Sciences,* **3,** 475-505

MIDDLETON G.V. & HAMPTON M.A. 1976; Subaqueous sediment transport and deposition by sediment gravity flows p.197-218. In *Marine Sediment Transport and Environmental Management*, D.J Stanley & D.J.P. Swift *(eds)*

MILLS A.A. 1984; Pillow lavas and the Leidenfrost effect. *Journal of the Geological Society of London*, **141**, 183-186

MILLS R.A. & ELDERFIELD H. 1995; Rare-earth element geochemistry of hydrothermal deposits of the active TAG Mound, 26°N Mid-Atlantic Ridge. *Geochimica Cosmochima et Acta*, **59**, 3511-3524

MOODY J.B, MEYER D. & JENKINS J.E. 1983; Experimental characterisation of the greenschist/amphibolite boundary in mafic systems. *American Journal of Science*, **283**, 48-92

MOORE J.G. 1975; Mechanism of formation of pillow lava. *American Scientist*, **63**, 269-277

MOORE J.G., PHILLIPS R.L., GRIGG R.W., PETERSON D.W. & SWANSON D.A. 1973; Flow of lava into the sea, 1969-1971, Kilauea Volcano, Hawaii. *Geological Society of America Bulletin*, **84**, 537-546

MORRIS R.C. 1985; Genesis of iron ore in banded iron formations by supergene and supergene-metamorphic enrichment processes: A conceptual model p.73-225. *In-* Handbook of stratabound and stratiform ore deposits, Wolf K.H. *(ed.)* **Volume 13**, Elsevier, Amsterdam

MORRIS R.C. 1993; Genetic modelling for banded iron-formation of the Hamersley Group, Pilbara Craton, Western Australia. *Precambrian Research*, **60**, 243-286

MOTTL M.J. 1983; Metabasalts, axial hot springs, and the structure of hydrothermal systems at mid-ocean ridges. *Geological Society of America Bulletin*, **94**, 161-180

MOTTL M.J., WHEAT G.C. & BOULEGUE J. 1994; Timing of ore deposition and sill intrusion at Site 856: Evidence from stratigraphy, alteration and sediment pore-water composition. In *Proceedings of the Ocean Drilling Program, Scientific Results*, Mottl *et al.* (Eds.), **vol. 139**, 679-693

MUIR R.J., IRELAND T.R., WEAVER S.D. & BRADSHAW J.D. 1994; Ion microprobe U-Pb zircon geochronology of granitic magmatism in the Western Province of the South Island New Zealand. *Chemical Geology* **113**, 171-189

MUTTI E. & RICCHI-LUCCHI F., 1972; Turbidites of the northern Appenines: Introduction to Facies Analysis (English translation by T.H. Nilsen 1978) *International Geology Review*, **20**, 125-166.

MYROW P.M. & SOUTHARD J.B., 1996; Tempestite deposition. *Journal of Sedimentary Research*, **66(5)**, 875-887

NEW B. 1993; Multiple deformation and metamorphism at the Snake Ck Anticline, northwest Queensland. Unpublished BSc (Hons) thesis, James Cook University.

NEWBERY S.P. 1990; The middle Proterozoic Maronan Supergroup, Soldiers Cap Belt, eastern Mount Isa Inlier; a rationalisation of the geology and mineralisation of a complexly deformed and metamorphosed terrane. PhD thesis, James Cook University, Townsville (unpubl).

NEWBERY S.P. 1991; Iron Formation hosted base-metal mineralisation of the Cloncurry terrane, Mount Isa Inlier. James Cook University Economic Geology Research Unit Contribution, **38,** *Base Metal Deposits Symposium, Townsville, April 1991*

NIJMAN W., VAN LOCHEM J.H., SPLIETHOFF H. & FEIJTH J. 1992; Deformation model and sedimentation patterns of the Proterozoic of the Paroo Range, Mt Isa Inlier, Queensland p.75-110. *In:-* Stewart A.J. and Blake D.H. eds, *Detailed Studies of the Mt Isa Inlier, , Australian Geological Survey Bulletin,* **243.**

NOTTVEDT A & KREISA R.D., 1987; Model for the combined flow origin of hummocky cross-stratification. *Geology,* **15,** 357-361.

O'DEA M.G. & LISTER G.S. 1995; The role of ductility contrast and basement architecture in the structural evolution of the Crystal Creek block, Mount Isa Inlier, Australia. *Journal of Structural Geology,* **17,** 949-960

O'DEA M.G., LISTER G.S., MacCREADY T., BETTS P.G., OLIVER N.H.S, POUND K.S, HUANG W. & VALENTA R.K. 1997; Geodynamic evolution of the Proterozoic Mount Isa terrane, *In:-* Orogeny through time, Burg J.P. & Ford M. *(eds.) Geological Society of London Special Publication,* **121,** 99-122

O'HARA M.J. 1977; Geochemical evolution during fractional crystallisation of a periodically refilled magma chamber. *Nature,* **266,** 503-507

O'HARA M.J. & MATTHEWS R.E. 1981; Geochemical evolution during fractional crystallisation of a periodically tapped, continuously fractionated magma chamber. *Geological Society of London Journal,* **138,** 237-277

OLIVER N.H.S., HOLCOMBE R.J., HILL E.J. & PEARSON P.J. 1991; Tectono-metamorphic evolution of the Mary Kathleen Fold Belt, northwest Queensland: a reflection of mantle plume processes? *Australian Journal of Earth Sciences,* **38,** 425-455

OLIVER N.H.S 1995; Hydrothermal history of the Mary Kathleen Fold Belt, Mount Isa Block, Queensland. *Australian Journal of Earth Sciences,* **42,** 267-279

PAGE R.W. 1978; Response of U-PB zircon and Rb-Sr total rock and mineral systems to low-grade regional metamorphism, Mt Isa Belt , Queensland. *Journal of Geochemical Exploration,* **12,** 259-264

PAGE R.W. 1981; Depositional ages of the stratiform base metals deposits at Mt Isa and McArthur River, based on U-Pb zircon dating of concordant tuff horizons. *Economic Geology*, **76,** 648-658

PAGE R.W. 1983; Timing of superposed volcanism in the Proterozoic Mount Isa Inlier. *Precambrian Research,* **21,** 223-245

PAGE R.W. & BELL T.H. 1986; Isotopic and structural responses of granite to successive deformation and metamorphism. *Journal of Geology*, **94,** 365-379

PAGE R.W. & LAING W.P. 1992; Felsic metavolcanic rocks related to the Broken Hill Pb-Zn-Ag orebody, Australia: geology, depositional age and timing of high grade metamorphism. *Economic Geology,* **87,** 2138-2168

PAGE R.W. & MACCREADY T. 1997; Rocks of Mount Isa Group age in the Eastern Fold Belt. *AGSO Research Newsletter,* **26,** 16-17

PAGE R.W. & SWEET I.P. 1998; Geochronology of basin phases in the western Mount Isa Inlier, and correlation with the McArthur Basin, *Australian Journal of Earth Sciences,* **45,** 219-322

PAGE R.W. & SUN S-S 1997; New geochronological results in the central and eastern Mount Isa Inlier and implications for mineral exploration. *In:- Abstracts, Geodynamics and Ore Deposits Conference,* Australian Geodynamics Cooperative Research Centre.

PAGE R.W., SUN S-s & MacCREADY T. 1997; New geochronological results in the central and eastern Mount Isa Inlier and implications for mineral exploration p.46-48. *Abstracts, Geodynamics and Ore Deposits Conference, Geodynamics Cooperative Research Centre, Ballarat, Victoria, Australia.*

PAGE R.W. & SUN S-S 1998; Aspects of geochronology and crustal evolution in the Eastern Fold Belt, Mount Isa Inlier. *Australian Journal of Earth Sciences,* **45,** 343-362

PAGE R.W. & WILLIAMS I.S. 1988; Age of the Barramundi Orogeny in northern Australia by means of ion microprobe and conventional U-Pb zircon studies. *Precambrian Research,* **40/41,** 21-36

PAGE R.W., SUN S-s, BLAKE D.H., EDGECOMBE D.R. & PEARCEY D.P. 1996; Exposed late-Archaean basement terrains in the Granites-Tanami region, Northern Territory. *Geological Society of Australia Abstracts,* **41,** 334

PAGE R.W., STEVENS B.P.J. & GIBSON G.M. 2000, New SHRIMP zircon results from Broken Hill: towards robust stratigraphic and event timing, p.375. *Geological Society of Australia, Abstracts,* **59**

PAGE R. W., STEVENS B. P. J., GIBSON G. M. & CONOR C. H. H. 2000b; Geochronology of the Willyama Supergroup rocks between Olary and Broken

Hill, and comparisons to northern Australia. *In:* Broken Hill Exploration Initiative Meeting, pp. 72-75. Australian Geological Survey Organisation Record **2000/10**.

PALIN J.M., CAMPBELL I.H., BALLARD J. & ALLEN C, 2000; To see a world in a grain of sand-zirconology by excimer laser ablation ICP-MS, 290. *Geological Society of America Abstracts and Programs* **32**

PARAK T. 1985; Phosphorus in different types of ore, sulfides in the iron deposits, and the type and origin of ores at Kiruna. *Economic Geology,* **80,** 646-665

PARR J.M. 1992; Rare-earth element distribution in exhalites associated with Broken Hill-type mineralisation at the Pinnacles deposit, New South Wales, Australia. *Chemical Geology,* **93,** 219-230

PASSCHIER C.W. 1986; Evidence for early extensional tectonics in the Proterozoic Mount Isa Inlier, Australia. *Geology,* **14,** 1008-1011

PASSCHIER C.W. & WILLIAMS P.R. 1989; Proterozoic extensional deformation in the Mount Isa Inlier, Queensland, Australia. *Geological Magazine,* **126,** 43-53

PEARCE J.A. & CANN J.R. 1973; Tectonic setting of basic volcanic rocks determined using trace element analysis. *Earth and Planetary Science Letters,* **19,** 290-300

PEARCE J.A. 1983; Role of the sub-continental lithosphere in magma genesis at destructive plate boundaries p.230-249. *In:- Continental basalts and mantle xenoliths,* Hawkesworth C.J. and Norry M.J. *(eds)* Shiva, Nantwich,

PEARSON P.J., HOLCOMBE R.J. & PAGE R.W. 1992; Syn-kinematic emplacement of the Middle Proterozoic Wonga Batholith into a mid-crustal extension shear zone, Mount Isa Inlier, Queensland, Australia p.289-328. *In:-* Detailed Studies of the Mount Isa Inlier, Stewart A.J. and Blake D.H. *(eds) Australian Geological Survey Organisation Bulletin* **243**

PERKINS C. & WYBORN L.A.I. 1996; The age of Cu-Au mineralisation, Cloncurry district, Mount Isa Inlier, as determined by Ar^{40}/Ar^{39} dating. *AGSO Research Newsletter,* **25,** 8-10

PETER J.M. & GOODFELLOW 1996; Mineralogy, bulk and rare earth geochemistry of massive sulphide-associated hydrothermal sediments of the Brunswick Horizon, Bathurst Mining Camp, New Brunswick. *Canadian Journal of Earth Sciences,* **33,** 252-283

PICKERING K.T. & HISCOTT R.N. 1985; Contained (reflected) turbidity currents from the Middle Ordovician Cloridorme Formation, Quebec, Canada: an alternative to the antidune hypothesis. *Sedimentology,* **32,** 373-394

PLUMB K.A., DERRICK G.M. & WILSON I.H. 1980; Precambrian geology of the McArthur River-Mount Isa region northern Australia. *In:-* The Geology and

Geophysics of Northeastern Australia, 71-88, Henderson R.A. & Stephenson P.J. *eds.* Geological Society of Australia Queensland Division.

POLDEVAART A. 1956; Zircon in rocks:2 Magmatic Rocks. *American Journal of Science,* **254,** 531-554

POLLARD P. 1995; Cloncurry Base Metals and Gold 1995 Annual Report, AMIRA Project P438, Pollard.P *(compiler).*

POTMA W.A. 1996; The structures of the Mitakoodi Culmination, eastern Mount Isa Inlier, Queensland, Australia. Unpublished MSc thesis, Monash University, Melbourne.

POTMA W.A. & BETTS P.G. 1997; The role of basin inversion in the evolution of the Mitakoodi Culmination; *In:-* L.Ailleres & P.Betts (eds) Structural elements of the Eastern Successions. *Australian Crustal Research Centre-Technical Publication,* **63,** 75-90

POTTER P.E. & PETTIJOHN F.J. 1977; Palaeocurrents and basin analysis. 2nd edition. Academic Press New York, 425 pp.

POWELL C. McA, OLIVER N.H.S., ZHENG-XIANG L., MARTIN D. McB. & RONASEZKI J. 1999; Synorogenic hydrothermal origin for giant Hamersley iron oxide ore bodies. *Geology,* **27(2),** 175-178

PRICE R.A. 1981; The Cordilleran Foreland thrust and fold belt in the southern Rocky Mountains; *In:-* Thrust and Nappe Tectonics, K.R. McClay & N.J. Price (eds). *Geological Society of London Special Publication,* **No.9,** pp.427-448

PRICE R.A. & SEARS J.W. 2000; A preliminary palinspastic map of the Mesoproterozoic Belt-Purcell Supergroup, Canada and USA: Implications for the tectonic setting of the Purcell Anticlinorium and the Sullivan deposit. *In:-*The Geological Environment of the Sullivan Deposit, British Columbia. J.W. Lydon, J.F. Slack, T. Hoy and M.E. Knapp *(eds.). Geological Association of Canada, Mineral Deposits Division,* **MDD Special Volume No.1**

PUPIN J.P. 1980; Zircon and granite petrology. *Contributions to Mineralogy and Petrology,* **73,** 207-220

RAETZ M., KRABBENDAM M. & GILES D 2000; Three tectonostratigraphic cycles in the Broken Hill terrane based on a review of SHRIMP ^{207}Pb/^{206}Pb zircon dates comparison with northern Australia pp. 403. *Geological Society of Australia, Abstracts,* **59**

RAETZ M., KRABBENDAM M. & DONAGHY A.G. 2002; Compilation of U-Pb zircon data from the Willyama Supergroup, Broken Hill region, Australia: evidence for three tectonostratigraphic successions and four magmatic events. *Australian Journal of Earth Sciences,* **49,** 965-983

RAMSAY J.G. 1961; The effects of folding upon the orientation of sedimentary structures. *Journal of Geology* **69,** 84-100

RAWLINGS D.J. 1993; Mafic peperite from the Gold Creek Volcanics in the Middle Proterozoic McArthur Basin, Northern Territory. *Australian Journal of Earth Science,* **40,** 109-113

ROBERTSON B.T. 1982; Occurrence of epigenetic phosphate minerals in a phosphatic iron formation, Yukon Territory. *Canadian Mineralogist,* **20,** 177-187

ROBSON D. & CANN J.R. 1982; A geochemical model of mid-ocean ridge magma chambers. *Earth and Planetary Science Letters,* **60,** 93-104

ROEP Th.B. & LINTHOUT K., 1989; Precambrian storm wave-base deposits of Early Proterozoic age (1.9 Ga), preserved in andalusite-cordierite rich granofels and quartzite (Ramsberg area, Varmland Sweden), *Sedimentary Geology,* **61,** 239-251

le ROEX A.P., DICK H.J.B., REID A.M. & ERLANK A.J. 1982; Ferrobasalts from the Speiss Ridge segment of the Southwest Indian Ridge. *Earth and Planetary Science Letters,* **60,** 437-451

ROLLINSON H 1993; Using geochemical data: Evaluation, Presentation and interpretation, pp.352

RUBENACH M.J. & FOSTER D.R.W 1997; Metamorphism and metasomatism in the Mount Isa Inlier, *In*-Structural Elements of the Eastern Successions, Ailleres L. & Betts P.G. *eds.* Australian Geodynamics Cooperative Research Centre.

RUBENACH M.J., & BARKER A.J., 1998; Metamorphic and metasomatic evolution of the Snake Creek Anticline, Eastern Succession, Mt Isa Inlier. *Australian Journal of Earth Sciences,* **45(3)** 363-372

RUBIN J.N., HENRY C.D. & PRICE J.G. 1989; Hydrothermal zircons and zircon overgrowths, Sierra Blanca Peaks, Texas. *American Mineralogist,* **74,** 865-869

RYBURN R.B., GRIMES K.G. & OTHERS 1987; Cloncurry 1:100 000 geological sheet. *Bureau of Mineral Resources, Canberra.*

SAMBRIDGE M.S. & COMPSTON W. 1994; Mixture modeling of multi-component datasets with application to ion-probe zircon ages. *Earth and Planetary Science Letters,* **128,** 373-390

SANGSTER D.F. 1993; Evidence for, and implications of , a genetic relationship between MVT and SEDEX zinc-lead deposits. *Australasian Institute of Mining and Metallurgy,* International Symposium: World Zinc '93, 131-149

SCOTT D.J. and GAUTHIER G. 1996; Comparison of TIMS (U-Pb) and laser ablation microprobe ICPMS (Pb) techniques for age determination of detrital zircons from Palaeoproterozoic from northeastern Laurentia, Canada, with tectonic implications. *Chemical Geology,* **131,** 127-142

SCOTT D.L., RAWLINGS D.J., PAGE R.W., TARLOWSKI C.Z., IDNURM M., JACKSON M.J. & SOUTHGATE P.N. 2000; Basement framework and geodynamic evolution of the Palaeoproterozoic superbasins of north-central Australia: an integrated view of geochemical, geochronological and geophysical data. *Australian Journal of Earth Sciences,* **47,** 341-380

SEILACHER A. 1982; Distinctive features of tempestites, p. 333-349. *In:-* Cyclic and Event Stratification-Symposium, Einsele G. & Seilacher *(eds.).* Tuebingen, Federal Republic of Germany, April 25-27 1982

SHANMUGAM G. 1997; The Bouma sequence and the turbidite mind set, *Earth Science Reviews,* **42,** 201-229

SHANMUGAM G. 2002; Ten Turbidite myths. *Earth Science Reviews,* **58(3-4),** pp.311-341.

SHANMUGAM G & MOIOLA, R.J. 1991; Types of submarine fan lobes: models and implications. *American Association of Petroleum Geologists Bulletin,* **75(1),** 156-179.

SHARPE I.R., GAWTHORPE R.L., ARMSTRONG B. & UNDERHILL J.R. 2000; Propagation history and passive rotation of mesoscale normal faults: implications for synrift stratigraphic development. *Basin Research,* **12,** 285-305

SINTON J.M., WILSON D.S., CHRISTIE D.M., HEY R.N. & DELANEY J.R. 1983; Petrologic consequences of rift propagation on oceanic spreading ridges. *Earth and Planetary Science Letters,* **62,** 193-207

SIRCOMBE K.N.; 1999, Tracing provenance through isotope ages of littoral and sedimentary detrital zircons, eastern Australia. *Sedimentary Geology* **124,** 47-67

SIVELL W.J. 1988; Geochemistry of metatholeiites from the Harts Range, central Australia: Implications for mantle source heterogeneity in a Proterozoic mobile belt. *Precambrian Research,* **40/41,** 261-275

SLACK J.F., SHAW D.R., LEITCH C.H.B., TURNER R.J.W. 2000; Tourmalinites and coticules from the Sullivan Pb-Zn-Ag deposit and vicinity, British Columbia: Geology, Geochemistry and Genesis. *In:-*The Geological Environment of the Sullivan Deposit, British Columbia. J.W. Lydon, J.F. Slack, T. Hoy and M.E. Knapp *(eds.). Geological Association of Canada, Mineral Deposits Division,* **MDD Special Volume No.1**

SMITH M.J. 1999: Geochemical and paragenetic characterisation of the "Core Amphibolite", Cannington Ag-Pb-Zn mine, northwestern Queensland. Unpublished B.Sc. Hons thesis, James Cook University of North Queensland

SNEDDEN J.W. & NUMMEDAL D. 1991; Origin and geometry of storm-deposited sand beds in modern sediments of the Texas continental shelf. *In:-* Shelf sand and sandstone bodies D.J.P Swift, G.F. Oertel, R.W. William & J.A. Thorne *(eds).*

International Association of Sedimentologists, Special Publication, **No. 14,** 283-308

SOLOMON M.J. & SUN S-s 1997; Earth's evolution and mineral resources, with particulat emphasis on volcanic-hosted massive sulphide deposits and banded iron formations. *AGSO Journal of Geology and Geophysics,* **17(1),** 33-48

SOUTHGATE P.N., SCOTT D.L., SAMI T.T., DOMAGALA J., JACKSON M.J., JAMES N.P. & KYSER T.K. 2000; Chronostratigraphic basin framework for Palaeoproterozoic rocks (1730-1575 Ma) in northern Australia and implications for base-metal mineralisation. *Australian Journal of Earth Sciences,* **47,** 461-484

SPRY P.G., PETER J.M. and SLACK J.F. 2000; Meta-exhalites as exploration guides to ore. *Reviews in Economic Geology,* **11,** 163-201

SQUIRE R.J. & McPHIE J. 2002 ; Characteristics and origin of peperite involving coarse-grained host sediment. *Journal of Volcanology and Geothermal Research,* **114,** 45-61

STANTON R.L. 1976a; Petrochemical studies of the ore environment at Broken Hill New South Wales, 2, Regional metamorphism of banded iron formations and their immediate associates. *Transactions of the Institute of Mining and Metallurgy* **B85,** 118-131

STANTON R.L. 1976b; Petrochemical studies of the ore environment at Broken Hill New South Wales, 3, Banded iron formations and sulfide orebodies, constitutional and genetic ties. *Transactions of the Institute of Mining and Metallurgy,* **B85,** 132-141

STANTON R.L. & VAUGHAN J.P. 1979; Facies of ore formation: a preliminary account of the Pegmont deposit as an example of potential relations between small "iron formations" and stratiform sulphide ores. *Proceedings of the Australian Institute of Mining and Metallurgy,* **270,** 25-38

SVERJENSKY D.A. 1984; Europium equilbria in aqueous solution. *Earth and Planetary Science Letters,* **67,** 70-78

SWIFT D.J.P. and THORNE J.A. 1991; Sedimentation on continental margins, I: a general model for shelf sedimentation. In:- Shelf sand and sandstone bodies-Geometry, Facies and sequence stratigraphy. Eds- D.J.P. Swift, G.F. Oertel, R.W. Tillman & J.A. Thorne. *International Association of Sedimentologists, Special Publication,* **14,** pp 3-32

TAYLOR B.E., TURNER R.J.W, LEITCH C.H.B. WATANABE D.H. & SHAW D.R. 2000; Oxygen and Hydrogen isotope evidence for the origins of the mineralising and alteration fluids, Sullivan Pb-Zn mine and vicinity, British Columbia. *In:*-The Geological Environment of the Sullivan Deposit, British Columbia. J.W. Lydon, J.F. Slack, T. Hoy and M.E. Knapp *(eds.). Geological Association of Canada, Mineral Deposits Division,* **MDD Special Volume No.1**

THOMPSON R.N., MORRISON M.A., DICKIN A.P. & HENDRY G.L. 1983; Continental flood basalts... Arachnids rule O.K.? p.158-185 *In:-* Hawkesworth C.J. and Norry M.J. *(eds) Continental Basalts and Mantle Xenoliths.* Shiva Publishing Ltd. Norwich,

TOYODA J. & MASUDA A. 1991: Chemical leaching of pelagic sediments: Identification of the carrier of the Ce anomaly. *Geochemical Journal,* **25,** 95-119

TRELOAR P.J. & COLLEY H. 1996; Variations in F and Cl contents in apatites from magnetite-apatite ores in northern Chile, and their ore-genetic implications. *Mineralogical Magazine,* **60,** 285-301

TURNER R.J.W., LEITCH C.H.B, KIKA R., HÖY T. & DELANEY G.D 1995; District scale rift-hosted hydrothermal field associated with the Sullivan stratiform lead-zinc deposit, British Columbia, Canada. In:- *Course Notes: extended abstracts and figures, Metallogeny of Proterozoic Basins Short Course.* Mineral Deposits Research Unit, University of British Columbia.

TURNER R.J.W, LEITCH C.H.B., ROSS K., HOY T., DELANEY G.D. & HAGEN 1996; Sullivan stratiform lead-zinc deposit British Columbia, Canada: rift setting associated district scale hydrothermal field, and comparison to BHT deposits. *In:-* New·Developments in Broken Hill-type Deposits. G.J. Davidson & J. Pongratz *(eds.), CODES Special Publication,* **No.1,** pp.153-163

TURNER R.J.W, LEITCH C.H.B & DELANEY G.D. 2000a; Syn-rift structural controls on the Palaeoenvironmental Setting and Evolution of the Sullivan Orebody. *In:-*The Geological Environment of the Sullivan Deposit, British Columbia. *(eds.)* J.W. Lydon, J.F. Slack, T.Höy and M.E. Knapp. *Geological Association of Canada,* **Mineral Deposits Division, MDD Special Volume No.1**

TURNER R.J.W., LEITCH C.H.B., HOY T., RANSOM P.W., HAGEN A. & DELANEY G.D. 2000b; Sullivan Graben System: District scale setting of the Sullivan deposit. *In:-*The Geological Environment of the Sullivan Deposit, British Columbia. *(eds.)* J.W. Lydon, J.F. Slack, T.Höy and M.E. Knapp. *Geological Association of Canada,* **Mineral Deposits Division, MDD Special Volume No.1**

VAUGHAN J.P. & STANTON R.L. 1984; Stratiform Pb-Zn mineralisation in the Kuridala Formation and Soldiers Cap Group, Mount Isa Block, NW Queensland p.307-317. *Australian Institute of Mining and Metallurgy Conference, Darwin, N.T.,*

VINCENT C.E. 1986; Processes affecting sand transport on a storm dominated shelf. In-*Shelf Sands and Sandstones.* R.J. Knight & J.R. McLean *(eds). Canadian Society of Petroleum Geologists Memoirs,* **11,** 121-132

WALKER G.P.L. 1992; Morphometric study of pillow-size spectrum along pillow lavas, *Bulletin of Volcanology,* **54,** 459-474

WALKER, R.G., 1978; Deep water sandstone facies and ancient submarine fans: models for for exploration for stratigraphic traps, *American Association of Petroleum Geologists Bulletin*, **62**, 932-966

WALKER R.G., 1984; Shelf and shallow marine sands *in:*- Facies Models (second edition), *Geoscience Canada, reprint series* **1**, 141-170.

WALKER R.G., DUKE W.L. & LECKIE D.A., 1983; Hummocky stratification: Significance of its variable bedding sequences: Discussion. *Geological Society of America Bulletin*, **94**, 1245-1251

WALTERS S.J. 1996; An overview of Broken Hill-type deposits p.1-10. In:- New Developments in Broken Hill-type deposits. Pongratz J. & Davidson G.J. *(eds)*,. *CODES Special Publication No.1*

WAYNE D.M., SINHA A.K. & HEWITT D.A. 1992; Differential response of zircon U-Pb systematics to metamorphism across a lithologic boundary: an example from the Hope Valley Shear Zone, southeastern Massachusetts, USA. *Contributions to Mineralogy and Petrology*, **109**, 408-420

WEISSEL J.K. & KARNER G.D. 1989; Flexural uplift of rift flanks due to mechanical unloading of the lithosphere during extension. Journal of Geophysical Research, **94**, 13919-13950

WETHERILL G.W. 1956; Discordant uranium-lead ages. *Transactions of the American Geophysical Union*, **37**, 320-327

WILLIAMS H. & McBIRNEY A.R. 1979; *Volcanology,* Freeman Cooper and Co., San Francisco, pp.397

WILLIAMS P.J. 1989; Nature and timing of early extension structures in the Mitakoodi Quartzite, Mount Isa Inlier, northwest Queensland. *Australian Journal of Earth Sciences,* **36**, 283-296

WILLIAMS P.J. 1997; Notes to accompany the 1:25 000 scale geological map of the western Pumpkin Gully Syncline, Cloncurry district, NW Queensland. AMIRA P438 Final Report Vol.2.

WILLIAMS P.J. 1998; Magmatic iron enrichment in high iron metatholeiites associated with 'Broken Hill-type' Pb-Zn-Ag deposits, Mt Isa Eastern Succession. *Australian Journal of Earth Sciences,* **45(3)** 389-396

WILLIAMS P.J. & BLAKE K.L. 1993; Alteration in the Cloncurry District; roles of recognition and interpretation in exploration for Cu-Au and Pb-Zn-Ag deposits. *Contributions of the Economic Geology Research Unit, James Cook University* **No.49,** pp.74

WILLIAMS P.J. & BAKER T. 1995; A regional-scale association of skarn alteration and base metal deposits in the Cloncurry district, Mt Isa Inlier, Queensland, Australia. *Transactions of the Institute of Mining and Metallurgy,* **104,** B187-196

WILLIS I.L. 1996; Exploration for Broken Hill-type Pb-Zn-Ag deposits p.145-152.
In:- New Developments in Broken Hill Type Deposits, Pongratz J. & Davidson G.J.
(eds) CODES Special Publication No.1

WILSON I.H. 1982; Petrology and geochemistry of selected Proterozoic volcanics
from the Mt Isa Inlier. Unpublished PhD thesis, University of Queensland

WILSON I.H. 1987; Geochemistry of Proterozoic volcanics, Mt Isa Inlier, Australia
p.395-408. *In: Geochemistry and mineralisation of the Proterozoic volcanic
suites* Pharaoah T.C., Beckinsale R.D. & Rickard D. *(eds)..*, Geological Society of
London Special Publication **No.33**

WILSON I.H. & GRIMES K.G. 1986; Coolullah, Queensland 1:100 000 Geological
map commentary. Bureau of Mineral Resources, Canberra

WILSON I.H., DERRICK G.M. & PERKIN D.J. 1985; Eastern Creek Volcanics:
their geochemistry and possible role in copper mineralisation at Mount Isa,
Queensland. *BMR Journal of Geology and Geophysics,* **9,** 317-328

WITHNALL I.W. 1983; The Robertson River Subgroup and Cobbold Metadolerite-
revised stratigraphic units in the Georgetown Inlier, north Queensland.
Queensland Government Mining Journal, **84,** 182-190

WITHNALL I.W. 1985a; Geochemistry and tectonic significance of Proterozoic
mafic rocks from the Georgetown Inlier, north Queensland. *BMR Journal of
Australian Geology and Geophysics,* **9,** 339-351

WITHNALL I.W. 1985b; Suspect terranes along the Precambrian/Palaeozoic margin,
Greenvale area, north Queensland. In: E.Leitch (ed) Third Circum-Pacific
Conference, extended abstracts. *Geological Society of Australia Abstracts,* **14,**
247-250

WITHNALL I.W., BAIN J.H.C & OVERSBY B.S. 1976; New and revised names for
intrusive rock units in the Georgetown and Forsayth 1:100 000 Sheet areas,
Georgetown Inlier, north Queensland. *Queensland Government Mining Journal,*
77, 228-231

WITHNALL I.W., BAIN J.H.C. & RUBENACH M.J. 1980; The Precambrian
geology of northeastern Queensland. *In:-* The Geology and Geophysics of
northeastern Australia, R.A. Henderson & P.J.Stephenson *eds.; Geological
Society of Australia, Queensland Division, pp.*109-127

WITHNALL I.W., BAIN J.H.C, DRAPER J.J., MacKENZIE D.E., OVERSBY B.S.
1988; Proterozoic stratigraphy and tectonic history of the Georgetown Inlier,
Northeastern Queensland. *Precambrian Research* **40/41,** 429-446

WOHLETZ K. 2002; Water/magma interaction: some theory and experiments on
peperite formation. *Journal of Volcanology and Geothermal Research,* **114,** 19-35

WYBORN L.A.I. & BLAKE D.H. 1982; Reassessment of the tectonic setting of the Mt Isa Inlier in the light of new field, petrographic and geochemical data. *Abstracts 11ᵗʰ BMR Symposium, BMR Journal of Australian Geology and Geophysics,* **7**, 143

WYBORN L.A.I., PAGE R.W. & McCULLOCH M.T. 1988; Petrology, geochronology and isotope geochemistry of the post-1820 Ma granites of the Mt Isa Inlier: mechanisms for the generation of Proterozoic anorogenic granites. *Precambrian Research,* **40/41**, 509-541

WYBORN L.A.I. 1998; Younger ca. 1500Ma granites of the Williams and Naraku Batholiths, Cloncurry district, eastern Mt Isa Inlier, geochemistry, origin, metallogenic significance and exploration indicators. *Australian Journal of Earth Sciences,* **45**, 397-412

YAMAGISHI H. 1979; Classification and features of subaqueous volcaniclastic rocks of Neogene age in southwest Hokkaido. *Geological Survey of Hokkaido Report,* **51**, 1-20

YAMAGISHI H. 1987; Studies on Neogene subaqueous lavas and hyaloclastites in southwest Hokkaido, *Geological Survey Hokkaido Report,* **59**, 55-117

YANG W. & ZENG Y. 1993 ; On the origin of Precambrian phosphorites in Central Guizhou, China. *Proceedings of the 29ᵗʰ International Geological Congress- Resource Geology Special Issue,* **17, vol.C**, 138-142

Soldiers Cap Group iron-formations, Mt Isa Inlier, Australia, as windows into the hydrothermal evolution of a base-metal-bearing Proterozoic rift basin

O. J. HATTON* AND G. J. DAVIDSON

Centre for Ore Deposit Research (CODES SRC), University of Tasmania, Private Bag 79, Hobart, Tas. 7001, Australia.

The Proterozoic Soldiers Cap Group, a product of two major magmatic rift phases separated by clastic sediment deposition, hosts mineralised (e.g. Pegmont Broken Hill-type deposit) and barren iron oxide-rich units at three main stratigraphic levels. Evaluation of detailed geological and geochemical features was carried out for one lens of an apatite–garnet-rich, laterally extensive (1.9 km) example, the Weatherly Creek iron-formation, and it was placed in the context of reconnaissance studies of other similar units in the area. Chemical similarities with iron-formations associated with Broken Hill-type Pb–Zn deposit iron-formations are demonstrated here. Concordant contact relationships, mineralogy, geochemical patterns and pre-deformational alteration all indicate that the Soldiers Cap Group iron-formations are mainly hydrothermal chemical sediments. Chondrite normalised REE patterns display positive Eu and negative Ce anomalisms, are consistent with components of both high-temperature, reduced, hydrothermal fluid ($\geq 250°C$) and cool oxidised seawater. Major element data suggest a largely mafic provenance for montmorillonitic clays and other detritus during chemical sedimentation, consistent with westward erosion of Cover Sequence 2 volcanic rocks, rather than local mafic sources. Ni enrichment is most consistent with hydrogenous uptake by Mn-oxides or carbonates. Temperatures inferred from REE data indicate that although they are not strongly enriched, base metals such as Pb and Zn are likely to have been transported and deposited prior to or following iron-formation deposition. Most chemical sedimentation pre-dated emplacement of the major mafic igneous sill complexes present in the upper part of the basin. Heating of deep basinal brines in a regional-scale aquifer by deep-seated mafic magma chambers is inferred to have driven development of hydrothermal fluids. Three major episodes of extension exhausted this aquifer, but were succeeded by a final climactic extensional phase, which produced widespread voluminous mafic volcanism. The lateral extent of the iron-formations requires a depositional setting such as a sea-floor metalliferous sediment blanket or series of brine pools, with iron-formation deposition likely confined to much smaller fault-fed areas surrounded by Fe–Mn–P-anomalous sediments. These relationships indicate that in such settings, major sulfide deposits and their associated chemical sediment marker horizons need not overlie major igneous sequences. Rather, the timing of expulsion of hydrothermal fluid reflects the interplay between deep-seated heating, extension and magmatism.

KEY WORDS: chemical sediment, garnet quartzite, hydrothermal, iron-formations, mafic magmatism, Mt Isa Inlier, rare-earth elements, rifting, Soldiers Cap Group.

INTRODUCTION

The volcano-sedimentary sequence of the Soldiers Cap Group contains the easternmost exposure of the informal Maronan Supergroup of Beardsmore et al. (1988), in the metallogenically endowed Eastern Succession of the Proterozoic Mt Isa Inlier, northwest Queensland, Australia (Figure 1). The Maronan Supergroup is perhaps best known as the host sequence for the massive Broken Hill-type Ag–Pb–Zn Cannington deposit, but it also hosts numerous barren and mineralised iron oxide-rich meta-sediments, commonly referred to as 'iron-formations' (Newbery 1991) and, where unbanded, as 'ironstones' (Davidson 1998; Laing 1998; Davidson et al. 2002).

The main aim of the present study was to determine the geological nature and genesis of the problematic Soldiers Cap Group iron-formations and determine their relationships to their host units. Iron-formations of Soldiers Cap

Group age are generally rare in the rock record (Solomon & Sun 1997). They are also commonly base- or precious-metals mineralised and so may have significant vector potential for mineral exploration. Last, if these iron-formations formed locally through hydrothermal activity, then they may provide a window into the hydrothermal history of this metallogenically important basin. Our approach was to study several typical examples in detail, and place these results in the context of wider regional and global studies.

We use the nomenclature of Gross (1965), which defines an iron-formation as a banded-laminated ferruginous unit, containing 15wt% or more Fe_2O_{3tot}, that is broadly conform-

---

*Corresponding author and present address: C/- Lionore Australia Pty Ltd, Level 2, 10 Ord Street, West Perth, WA 6005, Australia (owen.hatton@lionore.com.au).
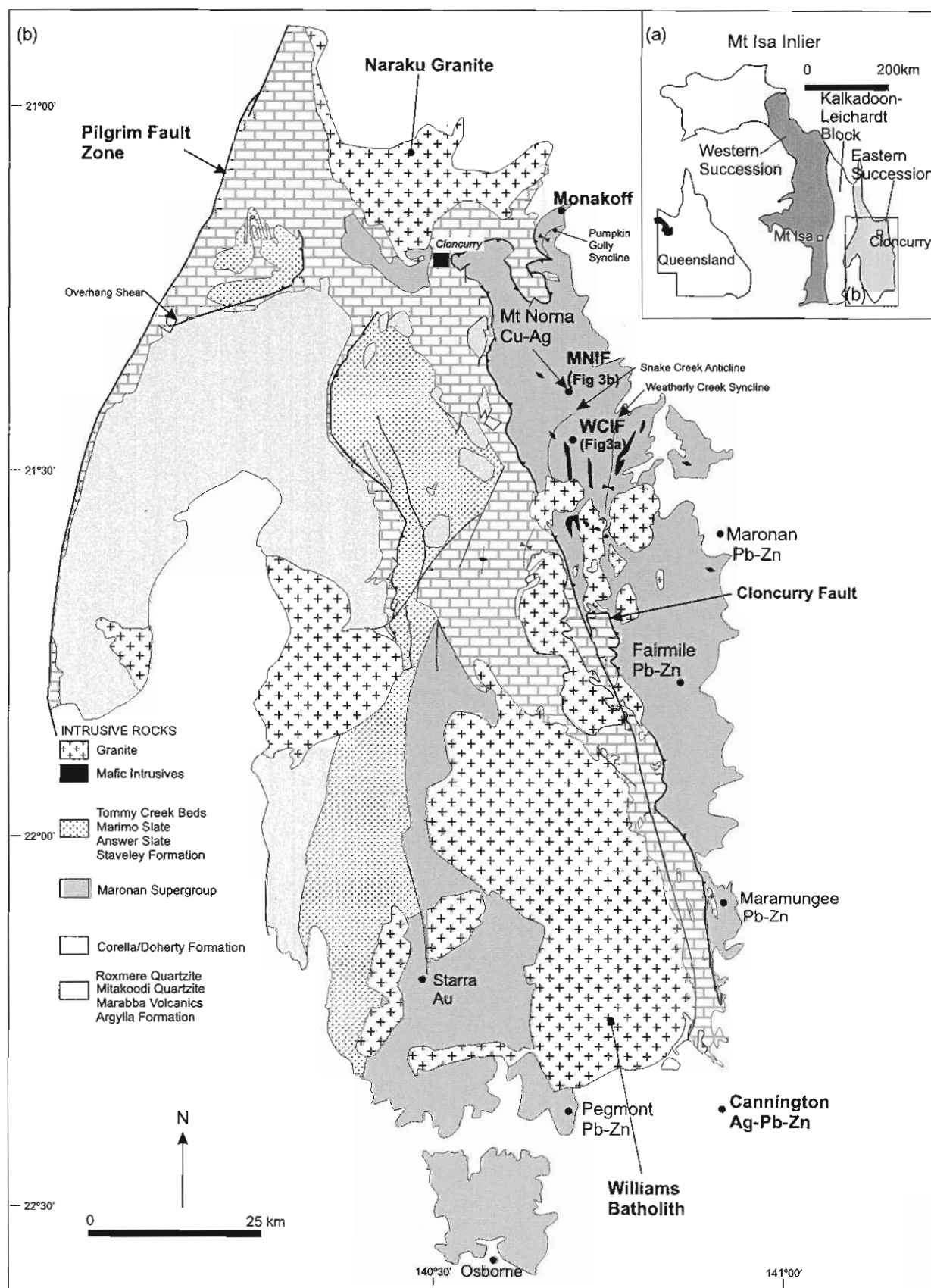
Table 1   Analyses from the Weatherly Creek iron-formation.

(wt%)	WC-78 GTQ	WC81 IF	WC86 TF	WC89 IF	WC91 IF	WC92 IF	WC95 TF	WC97 GTQ	WC98 TF	WC99 TF	WC02 GTQ	WC10 GTQ	WC27 TF	WC28 TF	WC29 TF
SiO_2	30.24	28.80	33.46	41.74	48.36	21.72	26.15	53.46	29.90	25.5	24.16	33	29.16	15.81	6.16
TiO_2	0.07	0.02	0.03	0.02	0.03	0.11	0.24	0.06	0.4	0.06	0.02	0.08	0.02	0.02	0.03
Al_2O_3	1.54	0.29	0.64	0.36	0.69	1.82	5.13	1.68	8.94	0.96	0.4	2.48	0.25	0.77	0.29
$Fe_2O_{3(tot)}$	40.85	69.66	32.18	56.42	49.34	53.66	47.66	6.39	46.29	36.61	73.12	40.44	68.32	81.02	91.89
Fe_2O_3	4.08	6.97	3.22	5.64	4.93	5.37	4.77	0.64	4.63	3.66	7.31	4.04	6.83	8.10	9.19
FeO	36.76	62.69	28.96	50.78	44.41	48.29	42.89	5.75	41.66	32.95	65.81	36.40	61.49	72.92	82.70
MnO	1.99	0.02	3.35	0.07	0.05	1.82	6.97	1.62	5.58	27.49	0.04	3.73	0.02	0.08	0.01
MgO	0.38	<0.01	0.57	0.02	0.11	0.26	0.2	0.4	0.38	0.16	0.05	0.39	0.04	0.06	0.07
CaO	13.26	0.03	13.25	0.2	0.37	10.24	6.17	19.96	5.00	1.29	0.01	10.72	0.01	0.03	0.03
Na_2O	0.06	<0.05	0.15	<0.05	<0.05	0.09	0.09	0.12	<0.05	0.08	0.05	0.15	0.05	0.05	0.05
K_2O	0.01	0.08	0.07	0.08	0.15	0.01	0.07	0.01	0.10	0.58	0.03	0.04	0.01	0.02	0.02
P_2O_5	7.8	0.2	9.75	0.31	0.3	7.79	4.5	14.82	2.56	1.29	0.48	4.92	0.18	0.29	0.06
Total	99.34	99.79	99.37	100.18	100.01	100.20	100.04	99.68	99.79	99.18	99.90	100.02	99.54	100.07	99.36
ppm															
Ba	55	61	74	251	20	276	15	21	28	18	150	276	11	10	30
Sc	1	1	3	3	1	1	4	3	7	1	<3	6	<3	<3	4
V	127	90	105	566	480	588	295	358	163	74	41	810	22	49	630
Co	10	10	n.d.	19	7	n.d.	9	6	9	11	n.d	n.d	n.d	n.d	n.d
Ni	8	8	8	63	35	77	56	16	42	146	26	95	11	<2	144
Cu	71	63	96	132	73	128	50	43	125	39	1074	100	1286	1790	23
As	232	1	418	11	<5	130	n.d.	20	17	211	121	194	94	217	10
Zn	6	<2	<2	33	121	87	221	12	8	214	147	117	462	100	12
Pb	9	8	3	9	10	8	18	7	13	<2	14	10	4	15	5
Zr	7	7	4	18	11	13	56	14	87	8	2	22	2	2	2
Y	14	4	3	67	31	37	22	29	29	12	13	40	5	10	80
U	6	7	4	29	36	14	35	38	25	32	5	14	5	5	<3
Th	1	0	<2	11	2	4	6	2	10	1	<3	4	5	3	<3

GTQ, garnet quartzite; TF, transitional iron-formation; IF, iron-formation. See Appendix 1 for sample locations.

able with the surrounding rocks. Ironstones are defined as massive, ferruginous units that can be both concordant and discordant with the surrounding units. However, although Cu–Au enriched and barren examples of the latter are common in parts of the Soldiers Cap Group, including examples that texturally overprint iron-formations, they are interpreted as products of structurally controlled metasomatism (Davidson 1996) and fall outside the scope of the present study.

Iron-formations from three stratigraphic levels were the basis of the present study: (i) detailed geological and whole-rock geochemical data were collected from the well-exposed, laterally extensive and weakly mineralised Weatherly Creek iron-formation; (ii) more limited data were collected from the Cu–Ag mineralised Mt Norna iron-formation; and (iii) limited data were collected from local weakly Cu–Au mineralised and barren iron-formations in the Pumpkin Gully Syncline on the Mt Norna Quartzite upper contact (Figure 1b). The terms 'Weatherly Creek iron-formation' and 'Mt Norna iron-formation' are informal names given here to these two distinctive units (Figure 3).

◄
Figure 1   (a) Tectonostratigraphic divisions of the Mt Isa Inlier, Queensland. (b) Simplified Eastern Succession regional geology (modified after Betts et al. 2000). Locations of relevant iron-formations and ironstones in the region as well as major structural features depicted.

SAMPLING AND ANALYTICAL TECHNIQUES

Detailed mapping at 1:10 000 scale and focused rock-chip sampling of the Weatherly Creek and Mt Norna iron-formations and several iron-formation lenses in the Pumpkin Gully Syncline (Figure 1b; Appendix 1) were undertaken during two field seasons as part of a broader study of the sedimentology, volcanology and geochemistry of the upper Soldiers Cap Group. Company aeromagnetic data tied to detailed logging of exploration drillcore were used to determine the extent of iron-formations under cover. Three iron-formation lenses were selected for study on the basis of their relative lack of complex regional alteration overprint, and their moderate deformation, lateral continuity, well-defined stratigraphic positions and local geological environment.

Representative samples from the Weatherly Creek iron-formation ($n = 16$) and Mt Norna iron-formation ($n = 6$) were thin-sectioned, slabbed, and their petrography examined in detail. The lenses were sampled as uniformly as possible (because of their heterogeneity) and individual hand samples ranged in size from 1.5 to 8 kg, taken from laterally equivalent segments of the iron-formations defined by mapping. Samples from the Weatherly Creek iron-formation were analysed for major and selected trace elements ($n = 16$: Table 1) and rare-earth elements (REE) ($n = 10$: Table 2), while only REE and selected trace elements were determined from the Mt Norna iron-formation (Table 3). Major element data used to compare

our study sites with regional equivalents were taken from an unpublished report written by G. J. Davidson for BHP Minerals in 1994 (data available on request).

Unweathered samples were crushed and then milled in a tungsten carbide mill. Major elements were determined on fused discs; Zr, Nb, Sr, Y and Mo were determined from pressed pills at the University of Tasmania. Other trace elements and REE compositions were determined by inductively coupled plasma-mass spectrometry (ICPMS) solution analysis after HF/H_2SO_4 digestion. Analyses of randomly selected duplicates were within 5–10% of each other. Possible incomplete dissolution of refractory phases was monitored by comparison of ICPMS results with values obtained for Zr, Y and Nb by XRF. These values agreed throughout the sample set to within 5%, suggesting that refractory phases were completely dissolved.

The REE values were normalised to the values of chondrite recommended by Boynton (1984). The Eu anomaly (Eu/Eu*) was calculated using the formula of McLennan (1989). Ce anomalies (Ce/Ce*) were calculated using the formula of Toyoda and Masuda (1991), and only values <0.9 were considered geologically significant (Davidson *et al.* 2001).

REGIONAL GEOLOGY

The Mt Isa Inlier of northwest Queensland is interpreted as the product of Palaeoproterozoic–Mesoproterozoic intracontinental rifting (Etheridge *et al.* 1987; O'Dea *et al.* 1997). The inlier is separated into three major tectono-stratigraphic zones on the basis of bounding faults, lithology, metamorphic grade and deformation style. These are the Western Succession, the oldest Kalkadoon–Leichardt Block, and the youngest Eastern Succession, in which the informal but widely recognised Maronan Super-group, including the 1690–1670 Ma Soldiers Cap Group, occurs (Figure 1) (Beardsmore *et al.* 1988; Page & Sun 1998). The Maronan Supergroup is a thick volcano-sedimentary sequence interpreted to represent rift–sag development during thermal relaxation of the crust (Blake 1987; Etheridge *et al.* 1987; Beardsmore *et al.* 1988; O'Dea *et al.* 1997).

Table 2 Rare-earth element values from the Weatherly Creek iron-formation.

(ppm)	WC-78	WC81	WC86	WC89	WC91	WC92	WC95	WC97	WC98	WC99
La	48.5	8.6	55.9	8.7	20.2	36.3	30.5	52.4	42.4	15.7
Ce	46.9	12.1	76.4	13.3	22.1	41.2	38.7	60.0	66.6	17.7
Pr	5.8	1.2	10.3	1.5	4.0	5.4	5.2	7.5	9.0	2.8
Nd	23.9	3.3	49.2	5.6	16.6	22.2	21.3	27.3	33.1	11.0
Sm	5.0	0.6	12.2	1.2	3.5	4.4	4.2	5.1	6.5	1.9
Eu	3.3	0.2	8.6	0.6	1.2	2.9	3.5	4.3	2.8	0.8
Gd	6.7	0.6	14.0	1.2	3.2	5.1	4.3	5.7	5.6	2.0
Tb	0.8	0.1	1.9	0.2	0.5	0.7	0.6	0.7	0.8	0.3
Dy	3.9	0.6	9.4	0.9	2.2	3.8	3.1	3.3	4.3	1.4
Ho	0.7	0.1	1.7	0.2	0.4	0.8	0.6	0.7	0.9	0.3
Er	1.7	0.3	4.2	0.4	1.1	2.0	1.7	1.7	2.5	0.8
Tm	0.0	0.0	0.5	0.5	0.0	0.1	0.2	0.2	0.4	0.1
Lu	0.1	0.0	0.4	0.1	0.1	0.2	0.2	0.1	0.3	0.1
ΣREE	147.4	27.7	244.7	34.4	75.1	125.1	114.1	169.0	175.2	54.9

Analysed at Analabs, Cloncurry. See Figure 3a for detail on sample locations.

Table 3 Rare-earth element values from the Mt Norna iron-formation.

ppm	WC110	WC112	WC114	WC117	WC119	WC120
La	1.5	3.7	5.8	13.8	7.8	6.9
Ce	2.3	7.1	8.7	25.8	11.4	11.4
Pr	0.3	1.0	1.1	3.5	1.8	1.5
Nd	1.2	4.7	4.5	13.9	7.1	5.7
Sm	0.4	1.4	1.3	3.8	1.7	1.7
Eu	0.5	1.5	1.3	2.2	0.7	1.2
Gd	0.5	1.8	2.0	4.0	1.4	1.8
Tb	0.1	0.3	0.4	0.6	0.2	0.3
Dy	0.8	2.0	2.8	3.4	1.0	1.7
Ho	0.2	0.4	0.6	0.7	0.2	0.3
Er	0.6	1.1	1.8	1.8	0.4	0.9
Tm	0.0	0.1	0.3	0.3	0.0	0.1
Lu	0.1	0.1	0.3	0.2	0.1	0.1
ΣREE	8.5	25.2	30.9	74.0	33.8	33.6

Analysed at Analabs, Cloncurry. See Figure 3b for detail on sample locations.

Isan Orogeny deformation in the Eastern Succession involved four major stages: large-scale east–west thrusting and smaller scale isoclinal folding (D_1); further compression resulting in large-scale upright to inclined north–south-orientated folds (D_2); brittle–ductile northwest-northeast-trending faulting and folding (D_3); and $D_{2.5}$, proposed by Bell and Hickey (1996) and lying between D_2 and D_3, which produced structures at a high angle to D_2 and later D_3 deformations. Notable features of $D_{2.5}$ deformation are that it is not homogeneous over the Eastern Fold Belt and may be recognisable only where favourably oriented. $D_{2.5}$ in the Soldiers Cap Group refolded D_2 folds, and produced a shallowly dipping crenulation cleavage. High-grade metamorphism characterises the Eastern Succession, with the peak high-T/low-P, upper greenschist to amphibolite facies event dated at 1584 ± 17 Ma (Jaques *et al.* 1982; Page & Sun 1998; Rubenach & Barker 1998). Syn- to post-orogenic granitoids of the Williams and Naraku Batholiths (Figure 1b) intruded at *ca* 1500 Ma (Wyborn *et al.* 1988; Wyborn 1998). Concomitant with this felsic magmatic episode was an extensive regional-scale sodic-calcic metasomatism event (De Jong & Williams 1995; Mark 1998).

Within the Eastern Succession there are numerous mineralised and barren iron oxide-rich metasediment units including the Overhang Jaspilite, Staveley Formation banded iron-formations and the Cu–Au mineralised ironstones at Osborne and Starra. Mineralised chemical sediments in the Maronan Supergroup fall into either iron oxide Cu–Au (polymetallic) or Pb–Zn stratiform mineralisation associations (Davidson 1996). Maronan Supergroup iron-formations host Pb–Zn mineralisation at Pegmont and Maramungee (Figure 1b), with the former interpreted by Newbery (1991; see also Stanton & Vaughan 1979; Vaughan & Stanton 1984) as laterally equivalent to the Mt Norna iron-formation, i.e. stratigraphically below the Weatherly Creek iron-formation. Mineralised portions of these iron-formations in the Maronan Supergroup include the subeconomic Fairmile and Maronan Pb–Zn prospects (Figure 1b), Cu–Ag ores of the Mt Norna mine, a Cu–Au (polymetallic) association at Monakoff mine, Hot Rocks prospect, and other subeconomic occurrences (Williams 1997).
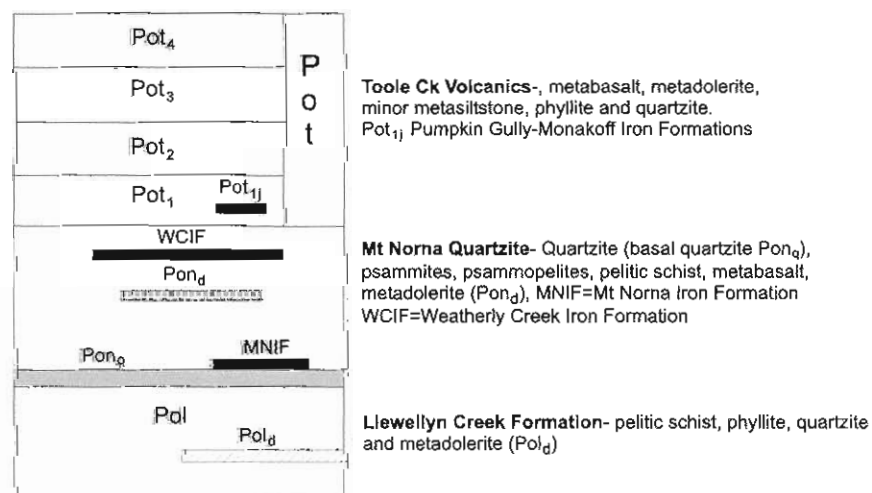
LOCAL GEOLOGY

Soldiers Cap Group geology

The Soldiers Cap Group comprises three conformable lithostratigraphic units (Figure 2) (Derrick *et al.* 1976). The basal Llewellyn Creek Formation comprises a ~2200 m-thick pile of turbiditic pelite. This unit is conformably overlain by the Mt Norna Quartzite (Figure 2), which consists of a 1300–2700 m-thick sequence of massive, swaly–hummocky and cross-bedded quartzite, laminated and rippled psammopelite and pelite, intercalated with metadolerite and lesser metabasalt. It is interpreted as a sequence of storm-current-influenced density flows (Hatton *et al.* 2000). The Mt Norna Quartzite is conformably overlain by the youngest stratigraphic unit, the Toole Creek Volcanics (Figure 2), a 2800 m-thick sequence of interbedded quartzite, pelite, minor carbonaceous pelite, metadolerite and metabasalt, ironstone and iron-formation, deposited in a broadly similar environment to the Mt Norna Quartzite (Derrick *et al.* 1976; Ryburn *et al.* 1987; Davidson & Davis 1997; Hatton *et al.* 2000). The voluminous Soldiers Cap Group mafic units, including those associated with iron-formations and ironstones, are defined as high-Fe metatholeiites, containing between 12 and 19 wt% Fe_2O_{3tot}, with an intracontinental rift signature (Glikson & Derrick 1978; Williams 1998). Throughout the Soldiers Cap Group many of these metatholeiitic units have distinctive brecciated contacts (peperite, hyaloclastite), concordant alteration haloes, and disturbed local bedding providing strong evidence for a synsedimentary to late diagenetic origin. These sills underlie subaqueous pillowed and vesicular basalts (Davidson & Davis 1997). The thickest accumulation of these sills and flows occurs some 200 m stratigraphically above the Weatherly Creek iron-formation, and the Monakoff/Pumpkin Gully Syncline horizons.

Geology of the study area

The Mt Norna iron-formation (Figures 1b, 2, 3b) occurs in massive quartzites at the Mt Norna Quartzite – Llewellyn Creek Formation contact and has several smaller lateral

Figure 2 Detailed lithostratigraphy of the Soldiers Cap Group, outlining the stratigraphic positions of the three iron-formations in the present study.

Toole Ck Volcanics-, metabasalt, metadolerite, minor metasiltstone, phyllite and quartzite. Pot_{1j} Pumpkin Gully-Monakoff Iron Formations

Mt Norna Quartzite- Quartzite (basal quartzite Pon_q), psammites, psammopelites, pelitic schist, metabasalt, metadolerite (Pon_d), MNIF=Mt Norna Iron Formation WCIF=Weatherly Creek Iron Formation

Llewellyn Creek Formation- pelitic schist, phyllite, quartzite and metadolerite (Pol_d)

equivalents along-strike (e.g. Mt Norna South: Arnold 1983). The Weatherly Creek iron-formation (Figures 1b, 2, 3a) occurs in the middle of the Mt Norna Quartzite. The Monakoff iron-formation and lateral equivalents are located at the Mt Norna Quartzite – Toole Creek Volcanics

contact in the Pumpkin Gully Syncline (Figures 1b, 2). The Weatherly Creek and Mt Norna iron-formations are the focus of the present study because they lie within a ~10 km strike length of rocks along the western limb of the Weatherly Creek Syncline, which has been mapped in
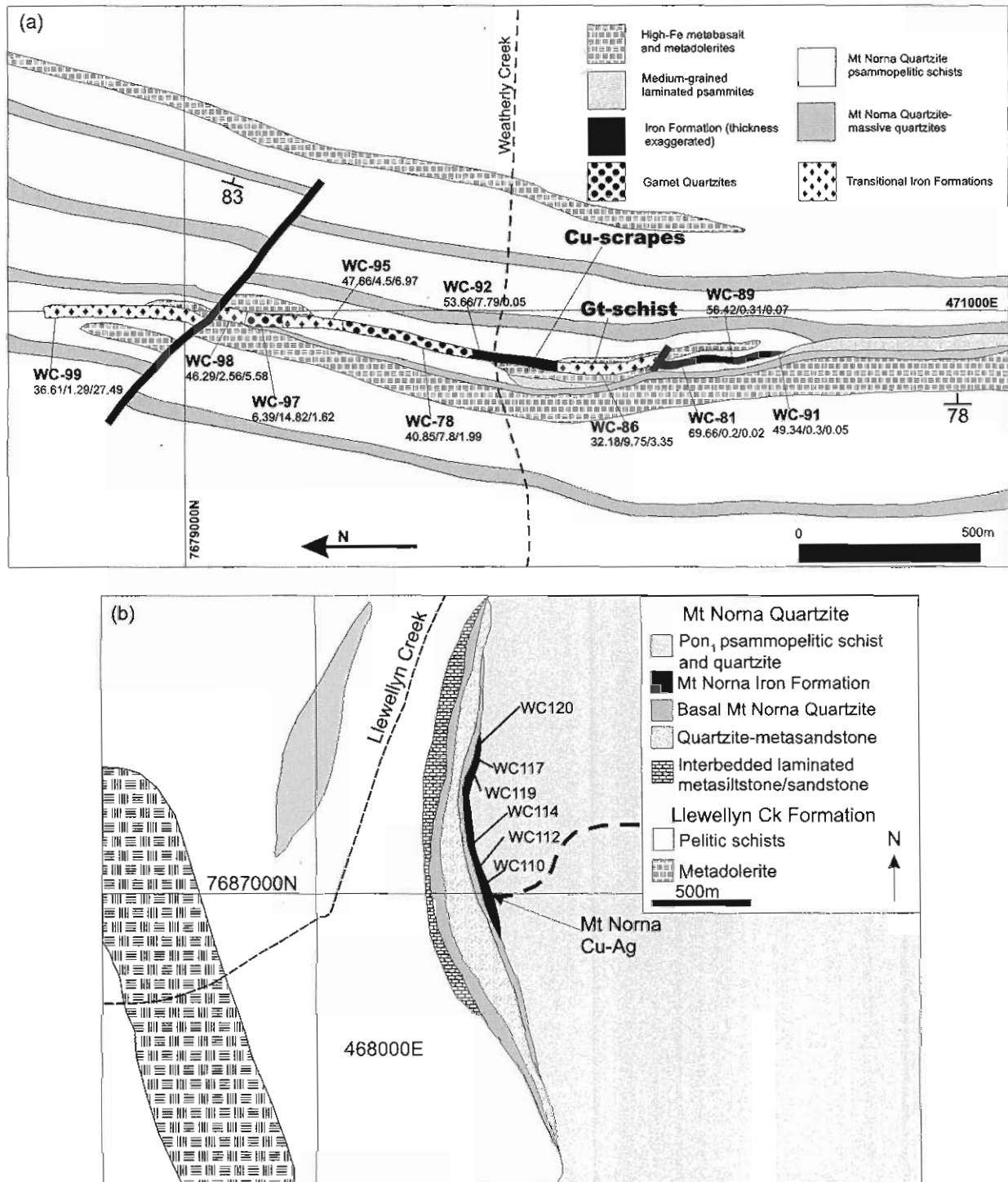

Figure 3 (a) Simplified geological fact map of the Weatherly Creek iron-formation and surrounding units. Locations of samples used in the present study (e.g. WC-99) are displayed in the figure, which are $Fe_2O_3/P_2O_5/MnO$ values in wt%; (b) Simplified geological fact map of the Mt Norna iron-formation and adjacent units; samples analysed in the present study are depicted. The datum used for grid references is AGD 94.

detail by the authors. Well-studied (Davidson 1996, 1998; Davidson & Davis 1997; Davidson *et al.* 2002) iron-formations in the Pumpkin Gully Syncline were also mapped in detail to provide data on the often complex contact relationships with adjacent units. Aeromagnetic anomalies are common at each of the stratigraphic levels of outcropping iron-formation. Hence, aeromagnetics has helped to constrain the extent and stratigraphic location of the three main iron-formations, and establish that magnetic material occurs at these levels for tens of kilometres under Mesozoic cover to the east; this has been verified by exploration drilling.

Major deformational structures in the study area include the north–south-striking, steep to moderately plunging, D_2 Weatherly Creek Syncline (Figure 1b), and the complexly refolded Snake Creek Anticline (Figure 1b). D_3–D_4 east-directed reverse faults parallel stratigraphy at some localities and are temporally associated with Cu introduction at dilational sites such as Mt Freda and Cu–Ag at Mt Norna (Davidson 1998). Metamorphic grade varies from upper greenschist to lower amphibolite facies, and folded isograds have been identified in the Snake Creek Anticline (Rubenach & Barker 1998). The Mt Norna iron-formation is located to the east of the composite garnet–andalusite–staurolite isograd of Rubenach and Barker (1998). It is also located ~700 m from the nearest of the albitites related to regional sodic–calcic metasomatism in the core of the Snake Creek Anticline (Rubenach & Barker 1998).

The Pumpkin Gully Syncline (Figure 1b) is a complex synformal structure with successive overprinting D_1–D_3 fabrics and a major tectonic contact with stratigraphically lower calc-silicate breccias of the Mary Kathleen Group (Williams 1997). Along the northern limb of the Pumpkin Gully Syncline, units of the Mt Norna Quartzite and Toole Creek Volcanics outcrop and comprise a conformable, albeit structurally complex, southward-younging sequence.

DETAILED GEOLOGY OF THE SOLDIERS CAP GROUP IRON-FORMATIONS

Weatherly Creek iron-formation

The Weatherly Creek iron-formation (Figure 3a), the main focus of the present study, is a discrete concordant lens, 2–5 m wide, approximately 1900 m long, that subparallels adjacent rocks (Figure 3a). These include massive quartzite, laminated to thinly bedded and rippled psammopelites, metadolerite sills and minor, discontinuous and thin ($\leq$0.5 m) garnetiferous schists. The mapped contacts show that the Weatherly Creek iron-formation is broadly conformable and hosted in a generally northward thickening psammopelite lens, and is in gradational contact at the southern end with a medium-grained, thinly laminated to cross-bedded psammite (Figure 3a). Although the northern end of the Weatherly Creek iron-formation outcrops poorly, a sharp contact with laminated to thinly bedded psammopelitic schist was observed. The nature of the host psammopelite and psammite suggests that the Weatherly Creek iron-formation was deposited during more quies-

cent sedimentation compared to the underlying and overlying massive quartzites; these are interpreted as the products of high-density turbidity currents (Hatton *et al.* 2000). High-Fe metatholeiite (Williams 1998) conformably underlies much of the Weatherly Creek iron-formation (Figure 3a). Several small scrapes containing Mt Freda-style supergene Cu oxides (malachite–azurite: Arnold 1983; Davidson 1998), ankerite veins and minor sulfides (pyrite–arsenopyrite) occur at the southern end of the Weatherly Creek iron-formation and post-date the pervasive fabrics.

Structure within the Weatherly Creek iron-formation is locally quite variable, although early Fe–Mn–P-rich laminae, which subparallel S_0 in the adjacent metasediments, are preserved throughout the deformational history (Figure 4b). Fabrics, including S_2, are easily traceable across mappable contacts in the study area. At the localities of samples WC-78 and WC-95 (Figure 4h) the Weatherly Creek iron-formation has undergone a high degree of structural deformation with rare tight isoclinal D_1 folds (Figure 4b), which have folded original laminae and are overprinted by S_2 and later fabrics. However, these structures are anomalous in the Weatherly Creek iron-formation. No cataclastic textures indicative of mylonites, as suggested by Laing (1990, 1998), were observed at the hand-specimen or thin-section scale elsewhere in the Weatherly Creek iron-formation or other study sites in the Soldiers Cap Group.

Garnet–epidote±quartz±carbonate alteration zones are associated commonly associated with the chemical sediments in metabasaltic and metasedimentary units. Zones of massive, very fine-grained epidote–quartz studded with subhedral garnets 1–2 mm in diameter have grown preferentially within S_2, forming asymmetric 2–15 m-wide haloes on the stratigraphically lower side, subparallel to the adjacent iron-formation. In metadolerites adjacent to iron-formation, this alteration assemblage is characterised by small (>1 mm), subhedral epidote–garnet and rare siderite grains overgrown by peak metamorphic (ferro)amphiboles, which define the dominant peak metamorphic structural fabric S_2 (Figure 4g). A similar pre-D_1 alteration assemblage was noted by Williams (1997) to be associated with iron-formations in the Pumpkin Gully Syncline. Similar pre-deformational alteration was also noted by Davidson *et al.* (2002) to be associated with the polymetallic Monakoff deposit.

In detail, the Weatherly Creek iron-formation consists mainly of garnet-dominated 'garnet quartzites'. (Garnet quartzite is a commonly used field term by workers in the Australian Proterozoic but does not indicate a clastic origin in this case.) This comprises fine to very fine (>0.5–3 mm) garnet (calcic almandine)–quartz–apatite±stilpnomelane laminae, and laminae of uniform magnetite–hematite–quartz±grunerite laminae (Figure 4c, d). The garnet quartzites are defined by their high modal percentages of garnet (60%) and apatite (10–15%). Relationships between the alternating laminae in garnet quartzites are complex at the microscale. Internally, the garnetiferous (gt_l and ap_l) layers have sharp contacts with magnetite–hematite–quartz±grunerite layers (Figure 4c, d). Primary sedimentary laminations may be preserved as 'dirty' inclusion trails of quartz–magnetite

(Figure 4c, d). These laminae are commonly overgrown by later, coarse apatite (ap$_2$: Figure 4c, d), which is in turn overgrown by a garnet–grunerite–stilpnomelane metamorphic assemblage indicative of upper greenschist to amphibolite-grade metamorphism (Klein 1973; Maynard 1983; Deer *et al.* 1992). Dennisonite (6CaOAl$_2$O$_3$.2P$_2$O$_5$.5 H$_2$O), is present as rare (<1%), small, acicular randomly oriented crystals throughout the garnetiferous laminae, commonly overgrown by subhedral garnets, suggesting that it developed prior to peak metamorphism. No
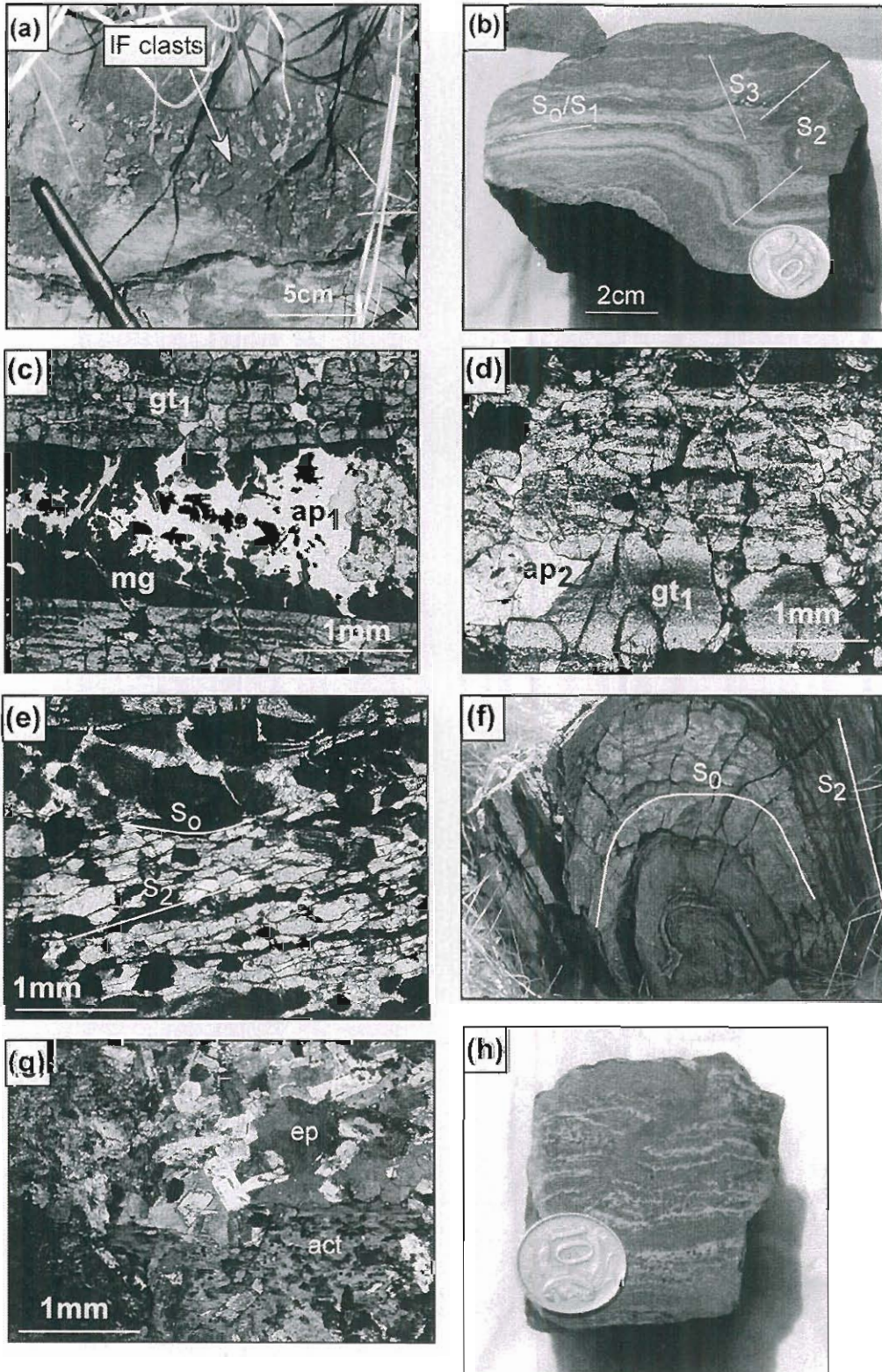
stromatolitic or other structures indicative of biogenic activity were observed in the iron-formations or adjacent units during the present study. Later (D_2–D_3) magnetite–hematite regional retrogression occasionally occurs preferentially within S_2 foliations as coarse and acicular grains that overprint earlier magnetite–apatite. Alignment of quartz-rich laminae defines a mineral lineation within S_2 that fans into the adjacent garnetiferous and iron oxide-rich laminae and can also be traced into adjacent host rocks (Figure 4e).

Small selvedges of garnetiferous pelitic schist <0.5 m thick, which extend for a lateral distance of 5–7 m, are commonly associated with garnet quartzites. These comprise muscovite–plagioclase–quartz schists with S_2 foliations wrapping around the garnets, indicating a pre-D_2 timing.

Garnet quartzites have diffuse contacts with transitional iron-formations, which have greater amounts of magnetite–hematite–quartz–grunerite laminae and lower garnet–apatite contents (20–30% gt; ~5% ap: Figure 4a). These transitional iron-formations have diffuse contacts with iron oxide-silicate banded-laminated iron-formations (Figure 4h), which have interlaminated monotonous hematite–magnetite±quartz±garnet and magnetite–hematite–grunerite layers with apatite largely absent and garnet a minor component (~10%).

Klein (1973) noted that original iron oxide and silicate laminae are present in some iron-formations up to and including amphibolite-facies metamorphism, with the only effect being an increase in the original grainsize of the constituent quartz and magnetite grains present in laminae. The absence of martitisation in the Soldiers Cap Group suggests that during regional metamorphism little to no mobilisation of oxygen occurred in iron-formations (Klein 1973; Morris 1985; Powell et al. 1999).

Mt Norna iron-formation

The Cu–Ag mineralised Mt Norna iron-formation (Figure 3b) (Arnold 1983) is ~800 m long, outcrops on the

Figure 4 (a) Erosional contact between metasandstone and iron-formation with basal rip-up clasts, upper Mt Norna Quartzite, Pumpkin Gully Syncline (AMG 466100mE, 7717903mN). (b) Laminated iron-formations from the Weatherly Creek iron-formation displaying the evolution of some of the structural fabrics; coin is 24 mm in diameter (WC-86: 470837mE, 7677920mN). (c) Photomicrograph of garnet quartzite, Weatherly Creek iron-formation (crossed polars), depicting early garnetiferous laminae (gt₁) with relict sedimentary features and later magnetite (WC-78: 470863mE, 7678423mN). (d) Photomicrograph of same sample as (c), depicting early garnet overgrowing sedimentary laminae, defined by 'dirty' inclusions of quartz and feldspar overgrown by later apatite (ap₂). (e) Photomicrograph (crossed polars), depicting the growth of elongate quartz and overprinting grains parallel to S_2 in Mt Norna iron-formation (WC-97: 470988mE, 7678738mN). (f) Early D_1/S_1 fabrics in Pumpkin Gully iron-formation overprinted by later D2 fabrics (464438mE, 7717167mN). (g) Photomicrograph (crossed polars), depicting the overprinting epidote dominant alteration (PG-79: 465302mE, 7717644mN). (h) Sample of transitional iron-formation from the Weatherly Creek iron-formation with later cross-cutting quartz–magnetite vein; coin is 24 mm in diameter (WC-86: 470837mE, 7677920mN).

eastern slopes of Mt Norna itself (Figure 3b), and comprises a 1–7 m-thick iron-formation with very minor garnet quartzites. It occurs near the base of the Mt Norna Quartzite and is in conformable contact with underlying massive and extremely thickly bedded (~25 m) hematitic quartzite, psammopelite, polymict breccia and phyllite with no evidence for erosional contact. Several smaller lateral equivalents are evident on regional aeromagnetic images and aerial photographs (e.g. Mt Norna South: Arnold 1983). These are hosted along-strike to the south of Mt Norna in geologically similar and stratigraphically equivalent pods of massive quartzite.

The Mt Norna iron-formation is thickest in the centre and tapers out at both ends (Figure 3b). It comprises a hematite–magnetite±quartz±garnet and magnetite–hematite, thinly laminated to massive iron-formation. A small pit and several deep shafts are located at the thickest part of the outcrop concurrent with the occurrence of rare garnetiferous 1–10 × 0.5–7 m 'pods' in the Mt Norna iron-formation. These garnetiferous bodies are controlled by localised shear fabrics running subparallel to the surfaces of the Mt Norna iron-formation; their contacts overprint earlier D_1–D_4 fabrics. These 'pods' contain disseminated chalcopyrite–arsenopyrite–malachite–azurite and are interpreted to host the Mt Norna Cu–Ag mineralisation.

Pre-mineralisation structure observed in the shafts and pits at Mt Norna is the most complex observed during the present study. The fabrics here include tight isoclinal–rootless intrafolial folds of primary laminae overprinted by later deformations. To the north of the workings and stratigraphically above and below outcropping massive and laminated iron-formation, there are several small polymictic breccia pods, 1–3 m thick and of uncertain length. This breccia comprises angular clasts of the underlying psammopelite and quartzite in a phyllosilicate matrix. S_2 foliation is traceable into the surrounding units, wrapping around the elongated clasts. Contacts between this breccia and the Mt Norna iron-formation, where mappable, are sharp and conformable. The limited lateral and stratigraphic extent combined with poor outcrop and steep local topography makes confident interpretation of this unit difficult. Overprinting relations outlined here show that the breccia pre-dated D_2, and the conformable contacts with the Mt Norna iron-formation suggest a possible earlier timing. Elsewhere along the Mt Norna iron-formation structural overprints are largely similar to that in the Weatherly Creek iron-formation, with D_2 fabrics dominating and traceable into adjacent metasediments. As with the Weatherly Creek iron-formation, early laminae, equivalent and subparallel to S_0 in adjacent units, are preserved and overprinted by later crenulations and cleavages ranging from D_1–D_4.

Pumpkin Gully iron-formations

Polymetallic, metasomatised iron-formations and structurally controlled ironstones at Monakoff, and related prospects and unmineralised occurrences in the Pumpkin Gully Syncline (Figure 1b), have been well studied (Ashley 1983; Davidson & Davis 1997; Williams 1997; Davidson 1998; Davidson et al. 2002). The main iron-formation at Monakoff has some features in common with the Mt Norna

and Weatherly Creek iron-formations, but is complexly overprinted by syn-$D_{2.5}$ metasomatic products (biotite), currently dated using Ar–Ar at 1508 ± 10 Ma (Pollard & Perkins 1997; Davidson & Davis 1997). Mineralisation is not hosted directly in the iron-formation but is focused in an adjacent shear zone (Davidson & Davis 1997). The Monakoff iron-formations are banded, quartz–magnetite–hematite±(barite–garnet) horizons associated with laminated fine- to medium-grained metasediments, and syn-sedimentary basalt–andesite sills (Davidson & Davis 1997). The paragenesis and relations of complex carbonate–barite and garnet alteration assemblages associated with polymetallic mineralisation and minor localised pre-deformational Mn–Al–K–Fe metasomatism at Monakoff, are described in detail by Davidson *et al.* (2002).
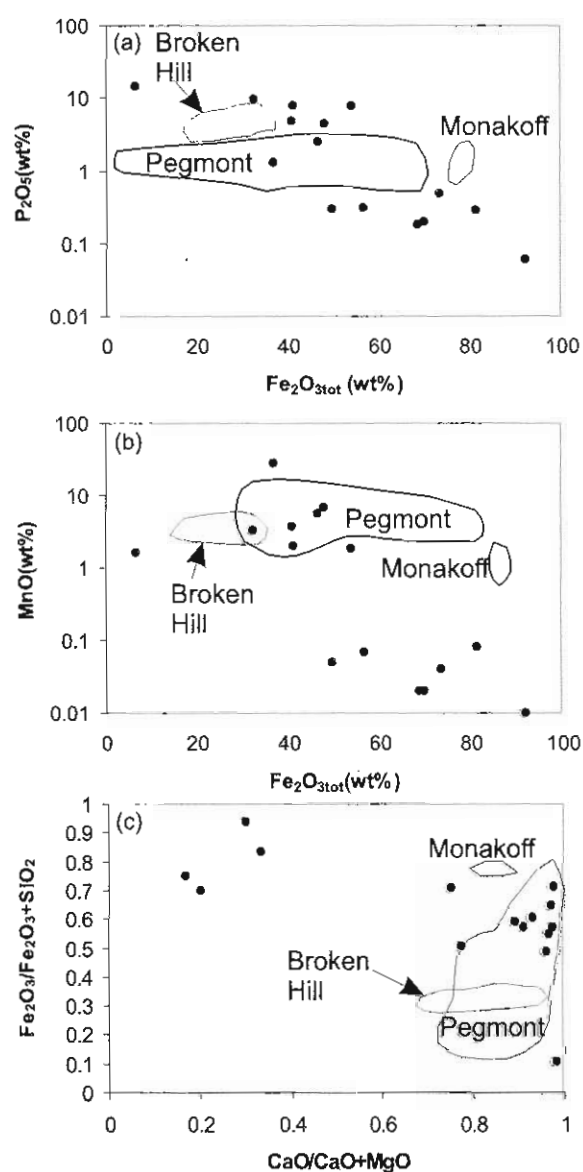

Figure 5 Selected major element fields for Maronan Supergroup iron-formations. Pegmont and Broken Hill iron-formation compositions taken from Newbery (1991), Stanton (1976a) and authors' unpublished data.

Away from the Monakoff horizon there are several other outcropping iron-formations that were the focus of the present study. Aeromagnetic images show these horizons to be very extensive (1–5 km along strike), forming a geophysical marker horizon above and/or close to the Mt Norna Quartzite – Toole Creek Volcanics contact in the Pumpkin Gully and Cloncurry Synclines. However, these horizons have only sporadic outcrop expression. Well-exposed examples are cited below, in which two differing styles of contacts allow determination of the relationships to surrounding units.

To the west of the Monakoff pit (GR 466100E 7717900N), a 1–2 m-thick magnetite–hematite–quartz laminated (1–20 mm bands) iron-formation is in direct contact with metasediments of the uppermost Mt Norna Quartzite, ~800 m down-stratigraphy from the mapped contact with Toole Creek Volcanics, i.e. not directly equivalent to the aforementioned Pumpkin Gully iron-formation. Here, a 1–3 m-thick psammitic bed has an erosional base, which contains clasts of the underlying iron-formation (Figure 4a). These clasts are angular and elongate (1–2 cm), chaotically arranged and have distinctive relict magnetite–garnet–quartz laminae. The adjacent psammite is medium-bedded and the underlying iron-formation retains magnetite–garnet–quartz laminae on a similar scale to the clasts. Along strike, relationships are obscured.

Approximately 350 m southeast of this occurrence, close to the mapped Mt Norna Quartzite – Toole Creek Volcanics contact (GR 469500E 7718150N) a thin (1–3 m), laterally restricted (10–20 m), laminated (1–20 mm) iron-formation occurs. This horizon is interleaved with metabasalt flows and metadolerite sills, and in hand specimen comprises bands of magnetite–hematite±garnet hosted by laminated pelite overprinted by the distinctive garnet–epidote±quartz±carbonate alteration halo. This pre-deformational alteration halo was first noted in the Pumpkin Gully Syncline by Williams (1997) and has been mapped by us elsewhere as being associated with other local iron-formations as conformable, broadly symmetric haloes up to 15 m wide in host mafic rocks and metasediments.

GEOCHEMISTRY OF SOLDIERS CAP GROUP IRON-FORMATIONS

Major and trace-element geochemistry

Geochemical data collected during the present study were used to define geochemical signatures of the iron-formations and compare these to others in the Maronan Supergroup (Newbery 1991), and similar age iron-formations in the Broken Hill Block (Stanton 1976a,b). Tables 1 and 2 present analyses of garnet quartzite, transitional iron-formation, and iron-formation from the Weatherly Creek iron-formation, and Table 3 presents the results of ICPMS analyses of the REE content of the Mt Norna iron-formation.

Other well-studied iron-formations in the Maronan Supergroup (Pegmont, Monakoff) fall into several distinctive compositional groupings (Figure 5). Si, Fe, Mn, P and Ca are the major components of the Weatherly Creek

iron-formation, and Ba and V are present as minor but important components (Table 1). Compared to other iron-formations in the Maronan Supergroup (Pegmont and Monakoff–Pumpkin Gully Syncline examples), major elements such as Fe, Mn, Ca and P oxides in the Weatherly Creek iron-formation are more variable (Figure 5): CaO/CaO+MgO) in particular extends to lower values than in the other iron-formations (Figure 5c). Compared to iron-formations from the similarly aged Broken Hill Block, the Weatherly Creek iron-formation is generally higher in Fe_2O_3 and SiO_2 (Figure 5a, c), and broadly equivalent in P_2O_5 (Figure 5a) and MnO (Figure 5b).

Spatially, P_2O_5 is elevated at the centre of the Weatherly Creek iron-formation, directly associated with garnet quartzite, and decreases sharply at the edges (Figures 3a,6c). MnO behaves similarly and varies widely across the Weatherly Creek iron-formation, with the highest values being associated with transitional iron-formations (Figures 3a, 6c). Elevated Al_2O_3 occurs at the

northern end of the Weatherly Creek iron-formation adjacent to the fault and is associated with garnet quartzites, transitional iron-formations and elevated MnO values.

Among the local and regional iron-formation data (authors' unpubl. data; Arnold 1983; Newbery 1991), the trace-element signature of the Weatherly Creek iron-formation is distinctive. It includes elevated Ni, Co, Cr, U and Sc that are particularly associated with Mn-rich garnet quartzites and transitional iron-formations, high values of other trace elements including Y, La and Ce, and slightly

Table 4 (a) Eigenvectors (component loadings) and (b) principal component scores for the major elements in the Weatherly Creek Iron Formation.*

|	Axis 1	Axis 2
(a) Eigenvectors (component loadings)		
SiO_2	0.227	−0.135
TiO_2	0.102	−0.075
Al_2O_3	0.054	−0.088
$Fe_2O_{3(T)}$	0.436	−0.119
MnO	−0.424	0.596
MgO	−0.054	−0.211
CaO	−0.604	−0.151
Na_2O	0.19	−0.167
K_2O	0.318	0.645
P_2O_5	−0.245	−0.295
(b) Sample		
WC78	−0.99	−0.336
WC81	1.05	0.102
WC86	−0.912	0.056
WC89	0.546	0.141
WC91	0.528	0.05
WC92	−0.882	−0.347
WC97	−1.234	−0.434
WC98	−0.589	0.304
WC99	−0.436	1.131
WC02	0.982	−0.081
WC10	−0.812	0.001
WC27	1.033	−0.292
WC28	0.707	−0.058
WC29	1.009	−0.236

*Represented graphically in Figure 7.
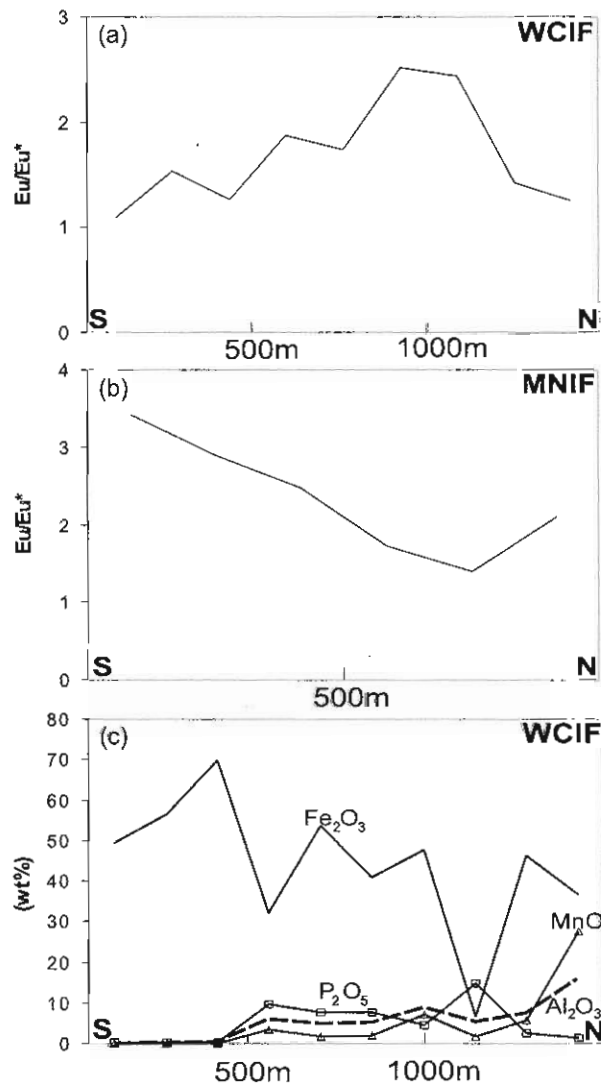
Figure 6 Along-strike chemical variations. (a) Eu/Eu* Weatherly Creek iron-formation. (b) Eu/Eu* Mt Norna iron-formation (c) P, Fe, Mn, Al Weatherly Creek iron-formation.
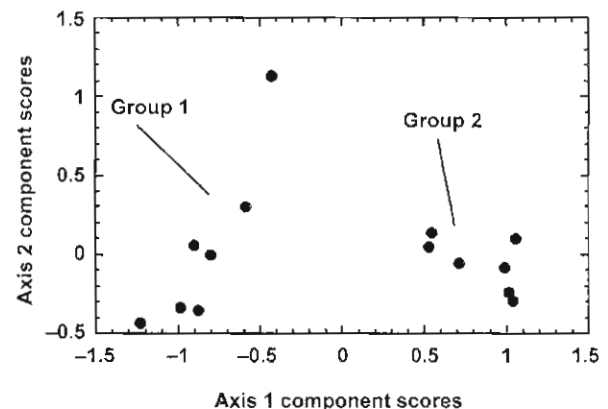

Figure 7 Component scores developed using Aitchison principal component analysis in the software package SMVP version 2.2j. Axis values are presented in Table 4.

elevated Pb, and Zn. Several high Cu values occur, but this is an inconsistent feature. When compared to local and regional values, the Mt Norna iron-formation is enriched in Cu, Ag, As and Zn but depleted in Pb and V; however, this element suite is highly likely to have been introduced during adjacent epigenetic ore formation at Mt Norna mine (Davidson 1998), because it is similar to the epigenetic ores, and is not addressed further here.

Interelement relationships in iron-formations are complex, commonly reflecting the contributions of several sources, including clastic, hydrogenous and evolving hydrothermal fluid sources (Parr 1992; Peter & Goodfellow 1996; Davidson *et al.* 2001). For the Weatherly Creek iron-formation, principal component analysis (well detailed in Le maitre 1982) and binary scatter plots of major elements has proven most useful for defining graphical interelement relationships in the dataset. For the purposes of analysis, the major element data in Table 1 were converted to centre log ratios using the software package MVSP version 2.2j (Rockware 2003), with those values below detec-
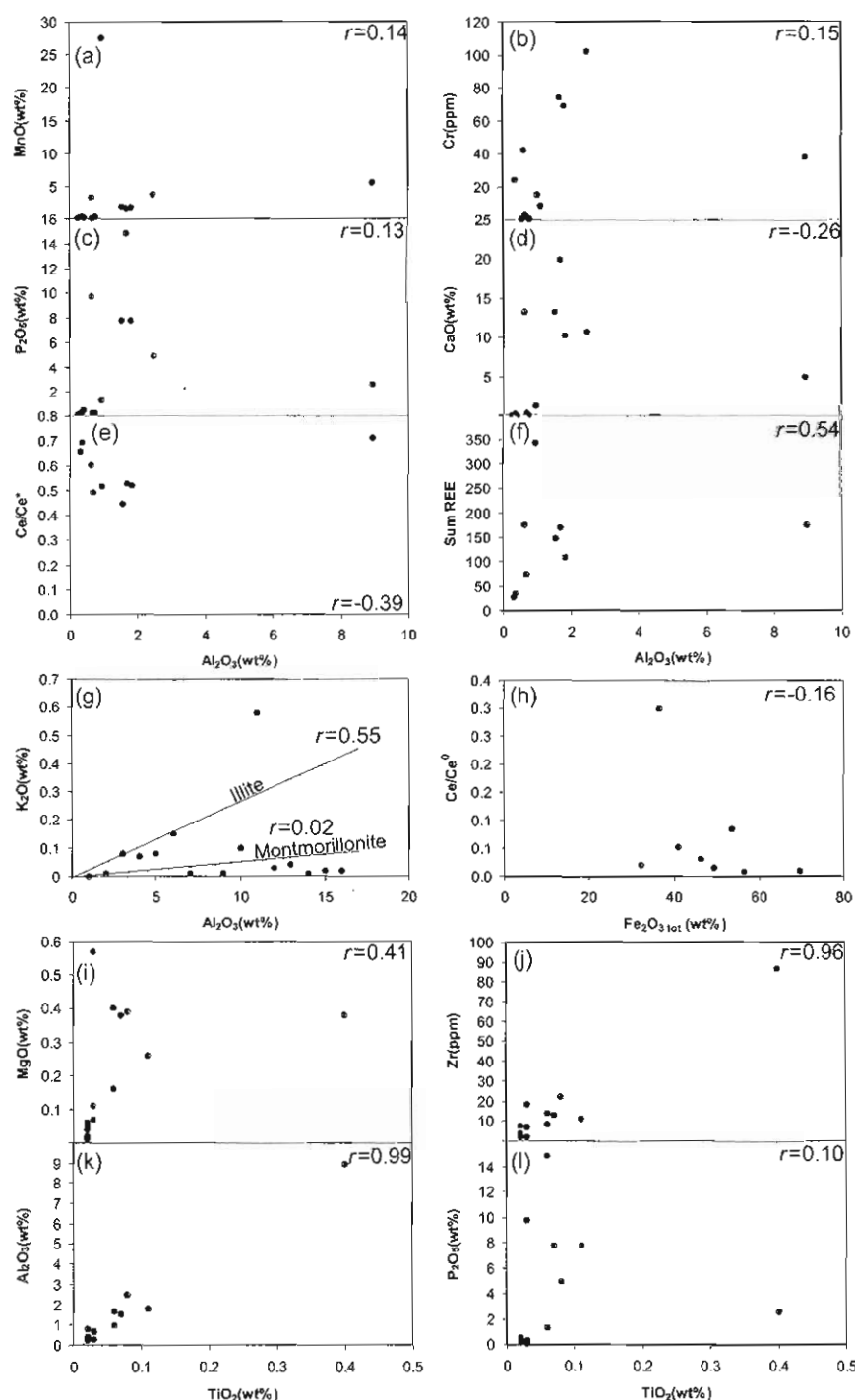

Figure 8   Bivariate scatter plots of major indicator elements from the Weatherly Creek iron-formation used to define detrital components. Correlation coefficients are quoted at the 95% confidence level; with $n = 16$, these are statistically significant above 0.400.

tion being assigned a value of one-third of the detection limit (trace-element data were not used in the analysis because some elements were not analysed for all samples). These ratios were used to construct an Aitchison covariance matrix. This approach was taken to determine interelement correlations in a way that addresses the effects of closure, which are likely to be profound in these Fe–Si-dominated rocks. The software was used to calculate principal component coordinates. Two eigenvectors, i.e. the coefficients of the discriminant functions, were suffi-

cient to account for 84.5% of the variance in the major element data. The scaled principal component scores are show in Table 4 and plotted in Figure 7 and show that the iron-formations consist of two main chemical components: (i) a high Ca–P–Mn–Na–Mg correlated group; and (ii) a Si–Fe correlated group. These groupings indicate that there is no clear positive correlation between Fe and Mn or Fe and P. Concentration of these two element groups apparently occurred by separate processes or from different sources.
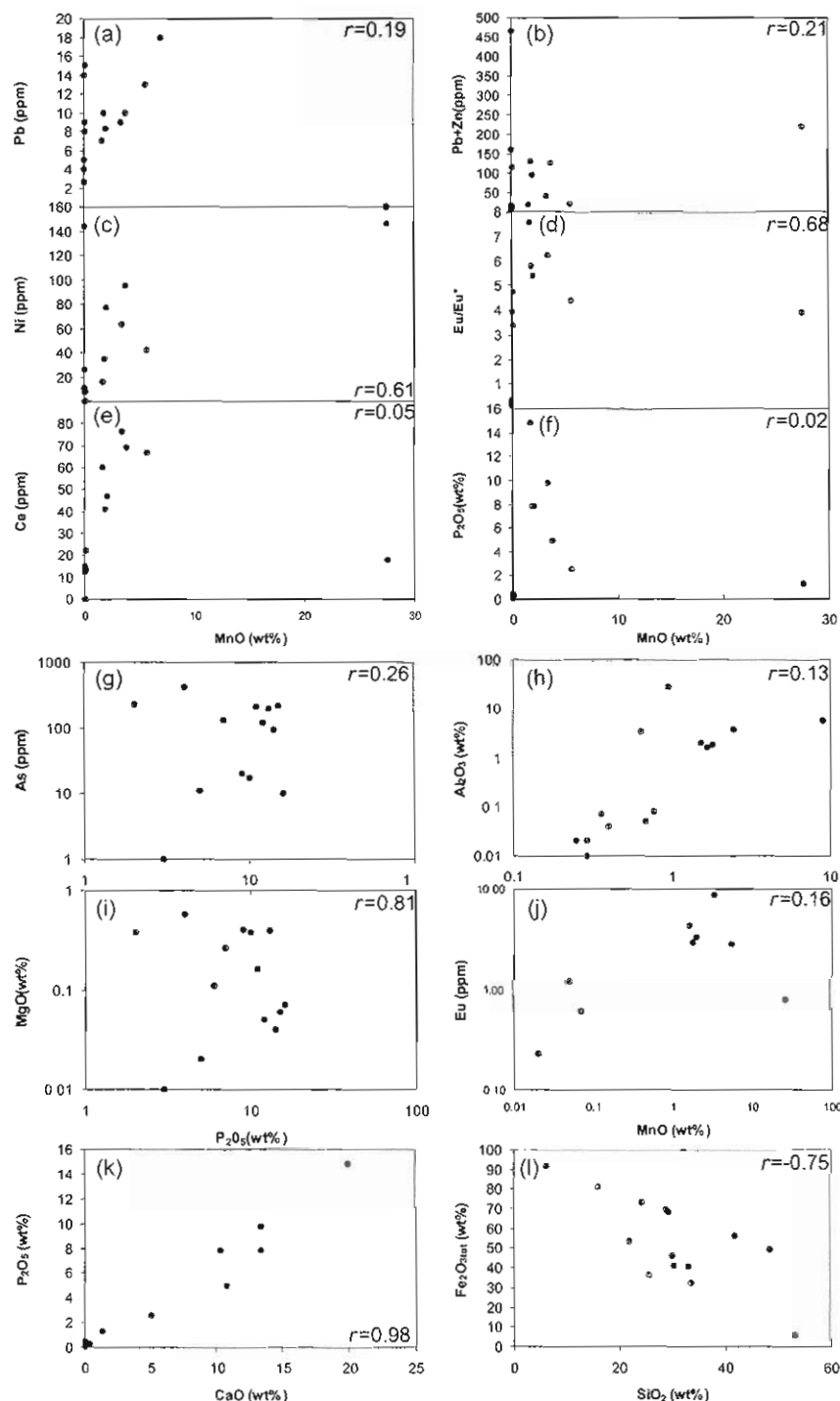

Figure 9 Bivariate scatter plots of major elements used to define hydrothermal and hydrogenous components. Correlation coefficients are quoted at the 95% confidence level; with $n = 16$, these are statistically significant above 0.400.

The element groupings were further refined using bivariate plots, which were useful for addressing a greater level of detail than was possible through multivariate analysis. The resulting plots, combined with the principal component analysis, show that two main groups of elements have positive graphical and statistical interelement correlations (Figures 8, 9): (i) Mn, P, Al, Ti, Zr, Mg, Ca, Na, K, As, Pb, Ni, U, SREE, Eu, Eu/Eu*; and (ii) Fe, Si, Ce/Ce*.

Rare-earth element geochemistry

The REE/chondrite-normalised plots such as those presented here (Figure 10) are commonly used in geochemical studies of chemical sediments (Lottermoser 1989; Parr 1992; Peter & Goodfellow 1996). The REE are generally considered to be immobile through low fluid–rock interaction metamorphic and alteration events (Michard & Alberade 1986; Michard 1989; Bau 1991; Rollinson 1993; Bingen et al. 1996). There is no clear evidence in outcrop, hand specimen, petrography or major element geochemistry that the sodic–calcic metasomatism that is prevalent in parts of the Soldiers Cap Group (de Jong & Williams 1995) affected the Weatherly Creek and Mt Norna iron-formations or local host rocks. However, the Mt Norna iron-formation, like the Monakoff iron-formation, probably experienced epigenetic metal addition. Rare-earth element data were collected from the Mt Norna iron-

formation to assess the effects on iron-formation chemistry of an overprinting Cu–Ag mineralising event.

Normalised REE patterns for the Weatherly Creek iron-formation are LREE enriched (Figure 10a; Table 2) and possess positive Eu and negative Ce anomalies (Figure 10a). Eu/Eu* is relatively consistent across the Weatherly Creek iron-formation, with elevated anomalies associated with apatite-rich garnet quartzites, transitional iron-formations and elevated Fe, Mn and P values (Figure 5a). The LREE are particularly elevated (Table 3) in samples of garnet quartzite and transitional iron-formation.

Although normalised data for the Mt Norna iron-formation have overall lower values ($\Sigma REE = 8$–74 ppm) than the Weatherly Creek iron-formation ($\Sigma REE = 27.7$–244.7) and are less LREE-enriched, the Mt Norna iron-formation has a similar chondrite-normalised pattern, with consistent positive Eu (Figures 5b, 10b) and negative Ce (Figure 10b) anomalies.

The REE patterns documented here are similar to those in base-metal mineralisation from the Cannington Pb–Zn deposit (Bodon 1996), and also in iron-formations from the Broken Hill Block that are closely associated with Broken Hill-type mineralisation (Figure 10) (Parr 1992; Bierlein 1995). The broad similarity of REE patterns in the detailed sampling of a single Soldiers Cap Group iron-formation (Weatherly Creek iron-formation) provides evidence that
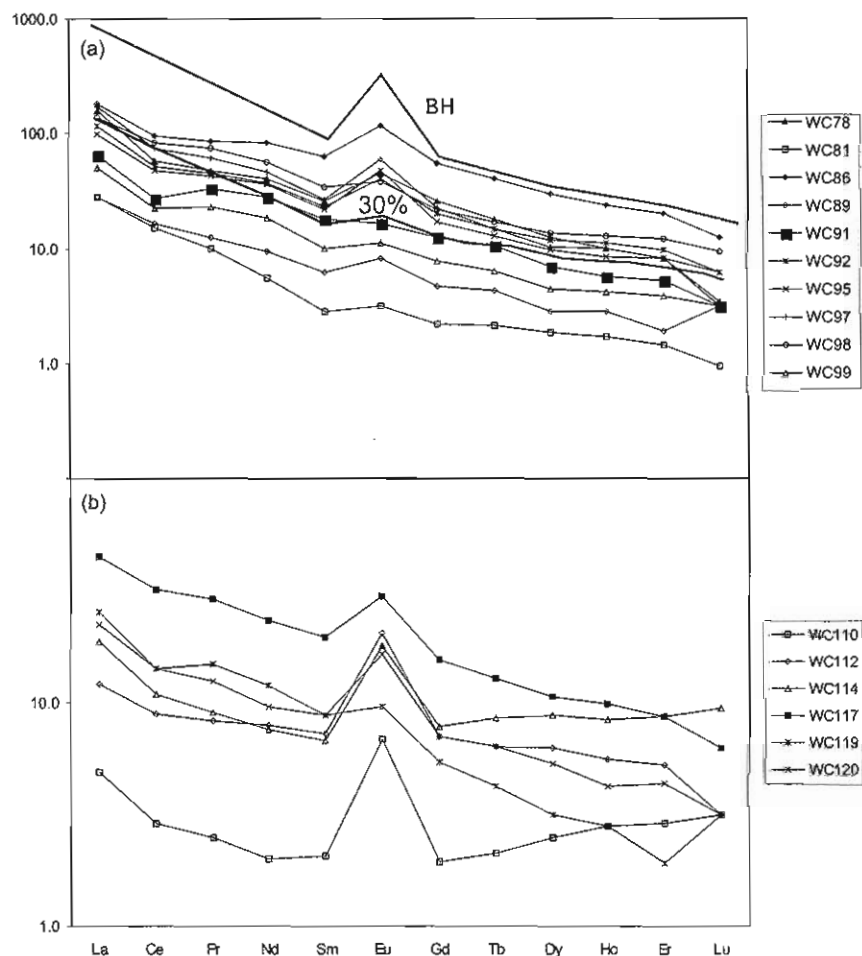

Figure 10 Chondrite-normalised REE plots for: (a) Weatherly Creek iron-formation (BH, average of Broken Hill exhalites proximal to ore from Lottermoser 1989); (b) Mt Norna iron-formation. See Figure 3 for location of samples.

only a small number of samples is necessary within a long strike length (~2 km) for adequate REE geochemical characterisation.

DISCUSSION

Previous models for the Soldiers Cap Group iron-formations

Newbery (1991) (see also Stanton & Vaughan 1979; Vaughan & Stanton 1984) studied in detail the petrography, host relationships and textures of the base-metal mineralised Maramungee and Pegmont iron-formations in the lower Maronan Supergroup; he interpreted the Pegmont iron-formations as laterally equivalent to the Mt Norna iron-formation. The Pegmont iron-formation is a stratiform body, hosted by metasediments adjacent to the Llewellyn Creek Formation – Mt Norna Quartzite contact. It grades laterally from a P–Fe–Mn centre to an Al–Si-rich margin and has a close spatial and genetic relationship with nearby quartz–gahnites and tourmalinites, which are absent from the Soldiers Cap Group chemical sediments studied here. Newbery (1991) proposed that, based on textural and geochemical characteristics including the presence of a significant detrital component and the lack of an alteration halo, Pegmont represented precipitation from mixing of exhalative brines and descending oxic waters in restricted basins. He proposed a medial–distal turbidite fan environment distal from volcanic activity and hydrothermal vents. The Weatherly Creek, Mt Norna and Pumpkin Gully iron formations, while broadly similar to Pegmont, differ in being deposited in a storm-influenced shelf sequence (Hatton *et al.* 2000), are proximal to igneous activity, and have common and well-defined syndepositional alteration haloes.

Laing (1990, 1998) proposed that some 'quartz+iron-oxide (magnetite dominant)-massive to laminated' 'ironstones' in the Soldiers Cap Group (Pumpkin Gully–Monakoff; Hot Rocks) are syntectonic D_1 or D_2 overprinted

mylonites, and also that many of the banded iron-formations found in the Maronan Supergroup may have been the result of alteration of existing calc-silicate sediments. In our study, clastic reworking (Figure 4a), synsedimentary alteration haloes, relationships with synsedimentary mafic sills, and detrital and hydrothermal geochemical signatures (Figures 7–11) provide strong evidence that the Mt Norna iron-formation, Weatherly Creek iron-formation and at least two Pumpkin Gully Syncline iron-formations, are the product of synsedimentary and not syntectonic processes.

Origin of major and trace-element variations in the Soldiers Cap Group iron-formations

The use of suites of indicator elements is common in studies of iron-formations to determine their various sources (clastic, hydrothermal, hydrogenous). The dataset from the Weatherly Creek iron-formation defined at least three distinct sources, discussed in detail below.

Data for the Weatherly Creek iron-formation, Mt Norna Quartzite and Toole Creek Volcanics clastic host rocks (O. J Hatton unpubl. data), and Soldiers Cap Group Fe-metatholeiites, were plotted with several other relevant lithologies on an Fe/Ti *vs* Al/(Al+Fe+Mn) diagram (Figure 11). On this plot, hydrothermal components are represented by elevated Fe and Mn, and clastic input by Al and Ti. The limited data from the Weatherly Creek iron-formation plots on a mixing line, with the Pegmont iron-formation, between a modern metalliferous sea-floor hydrothermal sediment component and a terrigenous sediment component. This terrigenous component is distinctly separated from the fields of Soldiers Cap Group Fe-metatholeiites and modern pelagic sediments. Instead it trends towards the Soldiers Cap Group metasediment field, strongly implying that both the Weatherly Creek iron-formation and, to a greater extent, the Pegmont iron-formation, had a significant Soldiers Cap Group clastic input. Percentages of detrital and hydrothermal components can be qualitatively assessed using arbitrary
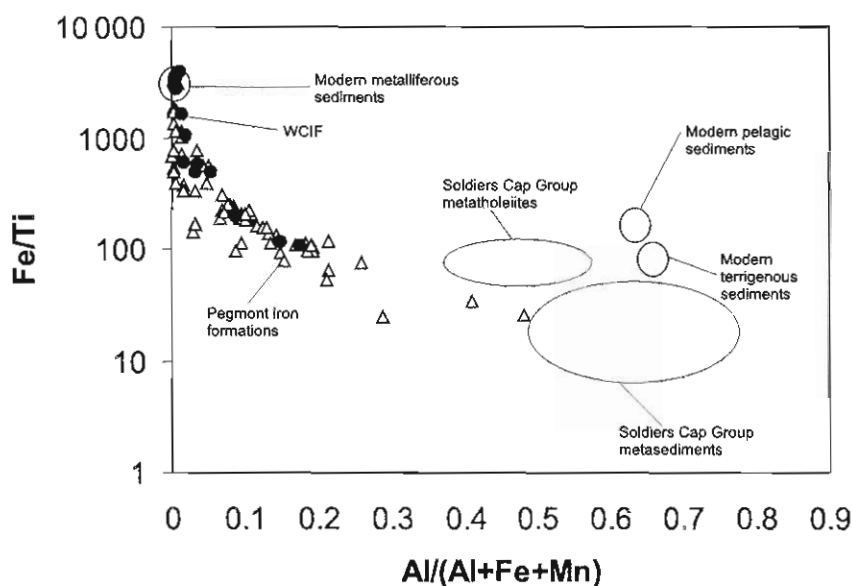

Figure 11 Diagram after Peter and Goodfellow (1996) used to determine the detrital *vs* hydrothermal component based on Al/Ti and Fe–Mn content. ●, Weatherly Creek iron-formations; △, Pegmont iron-formations. Values for metasediments and metatholeiites taken from authors' unpublished data; fields for metalliferous, clastic and terrigenous sediments from Peter and Goodfellow (1996).

end-members on Figure 10, with Fe/Ti >7000 representing hydrothermal processes and Al/(Al+Fe+Mn) >0.6 representing detrital end-members (Peter & Goodfellow 1996). Using this quantitative calculation for the Weatherly Creek iron-formation, detrital components range from 0.5 to 29 vol% and hydrothermal from 1.6 to 53 vol%.

The elements Al, Ti, Zr, Y, Nb, Si, Mg, Ca, Cr and K are accepted as commonly present in detrital sediments. They dominate the correlated group 1 identified by multivariate analysis and bivariate plots. Relatively low detrital mineral abundances may still significantly influence iron-formation geochemistry, as shown in the above analysis. More detailed analysis using bivariate diagrams can help determine the nature and provenance of the detrital component. Trends on Figure 8g favour a mixture of montmorillonite (K_2O/Al_2O_3 ~0.016) and muscovite (K_2O/Al_2O_3 ~0.22) for the original K-rich detrital phase in the Weatherly Creek iron-formation. A remnant mafic signature is evidenced by positive Al–Cr correlations (Figure 8b). The correlation of REE with other detrital elements provides evidence that much of the REE were also detrital (Peter & Goodfellow 1996). Uniform TiO_2/Zr (~0.008; $r = 0.96$) and TiO_2/Al_2O_3 ($r = 0.99$) (Figure 8j, k) ratios imply a relatively constant detrital source for the Weatherly Creek iron-formation. Assuming that Ti and Zr were not significantly fractionated from one another during transport and deposition (a proposition most favoured in shale and silt fractions: Taylor & McLennan 1985), possible Mt Isa Inlier sources, based upon TiO_2/Zr ratios from the Geoscience Australia Rockchem geochemical database, include volcanics of the Magna Lynn Metabasalt (TiO_2/Zr ~0.009) and the Marraba Volcanics (TiO_2/Zr ~0.006). Both units are located in the adjacent Eastern Succession and Kalkadoon–Leichardt Block. In contrast, the associated mafic rocks of the Soldiers Cap Group have average TiO_2/Zr ratios of 0.026.

The elements Fe, Mn, P, Pb, Sr and Eu are generally elevated in the silicates, Fe–Mn oxides, sulfides and carbonate minerals precipitated by active sea-floor hydrothermal systems (Gross 1993; Peter & Goodfellow 1996). They are a group of elements that do not normally concentrate by detrital processes, with the exception of immature magnetite–ilmenite heavy-mineral concentration. The multivariate analysis indicates that Fe was coprecipitated with Si in the Weatherly Creek iron-formation, whereas Mn and P showed an unusual positive correlation with detritally sourced elements such as Al. In general the very high abundances of Fe, Si, P and Mn are unlikely to be accounted for by pelagic detrital sedimentation. By analogy with other chemical sediment systems, it is likely that these elements in general reflect the precipitation of Fe–Mn oxides and silicates from hydrothermal solutions (Gross 1993; Peter & Goodfellow 1996), with iron oxides and cherts being separated in time but overlapping in space, with the deposition of Mn- and P-bearing phases. Speculatively, the deposition of the latter is likely to have required nucleation upon, or reaction with, detrital phases, or even have occurred in the subsurface porosity provided by clastic interbeds, to account for the positive Mn–P–Al–Ti correlations. Although most of the plots in Figures 8, 9 indicate consistent chemical relationships, many nevertheless display two populations, which broadly relate to the

banded iron-formations vs the transitional iron-formations and the garnet quartzites (Figure 9b, e, f, i, j).

A strong positive correlation exists between Mn and a range of other elements described above. For this reason it is difficult to separate the effects of hydrogenous Mn trace-scavenging from addition of elements via hydrothermal solutions. Several lines of evidence suggest that hydrogenous addition was active for some elements, but was mostly not important. For instance, REE are commonly scavenged by manganese crusts on the ocean floor, leading to very high REE concentrations. However, hydrogenous scavenging of seawater Ce^{4+} by Mn produces strong positive Ce anomalies under these conditions, and these are absent here. Consequently, positive Ca–P–Mn–REE correlations (Figure 9e, f, k) are more likely to have formed from hydrothermal precipitation with apatite as the main Ca–P phase, rather than through hydrogenous addition. The strong graphical and statistical correlation between Eu, Eu/Eu*, Mn and P (Figure 9d, j) can be accounted for by Eu preferentially entering apatite during hydrothermal precipitation.

The trace elements Ni, Th, U, V, Co, Fe, Ag, As, Pb, Zn, Mn and Ce are commonly adsorbed onto Fe–Mn coatings on the surface of detrital particles and hydrothermal precipitates and are an indicator of hydrogenous processes (Dymond et al. 1973; German et al. 1991). Input from such sources in iron-formations is defined by correlations of these trace elements internally and with Fe and Mn (Peter & Goodfellow 1996; Davidson et al. 2001). Some elements (As, Ni) do possess positive correlations with Mn (Figure 9b, c, g), and could be accounted for by hydrogenous uptake. As previously indicated, correlation between these elements and Mn–P is also consistent with their having a hydrothermal origin. A lack of correlation between Fe and U indicates that U did not coprecipitate with Fe oxyhydroxides, although this is commonly observed in modern iron oxide chemical and metalliferous sediments (German et al. 1991). Base metals such as Pb and Pb+Zn display a poor correlation to Mn (Figure 9a, b), and so are unlikely to have been enriched via hydrogenous Pb uptake (Davidson et al. 2001).

Origin of Soldiers Cap Group iron-formation REE patterns and Eu anomalies

A pattern of positive Eu anomalies and LREE enrichment–HREE depletion (Figure 10a, b) in chondrite-normalised Proterozoic iron-formations, similar to that of modern ocean-floor metalliferous sediments (Courtois & Treuill 1977; Michard et al. 1983; Michard & Alberade 1986; Michard 1989; Barrett et al. 1990) and sea-floor hydrothermal fluids (Klinkhammer et al. 1994; Mills & Elderfield 1995), has commonly been interpreted in ancient examples to be the product of exhalation proximal to a sea-floor hydrothermal centre (e.g. Broken Hill: Lottermoser 1989; Parr 1992; Bierlein 1995; Peter & Goodfellow 1996).

Production of a positive Eu anomaly occurs where Eu^{2+} is transported in solution preferentially to Eu^{3+}. Transport and precipitation of Eu complexes strongly depends on fluid temperature and to a lesser extent fO_2 and pH (Sverjensky 1984). Divalent Eu is stable in reduced hydrothermal fluids at temperatures ≥250°C and is commonly

mobilised during the hydrothermal breakdown of plagioclase in sediments and volcanics. Appropriate quartzofeldspathic quartzite source rocks, with up to 25–35% primary feldspar (O. J. Hatton unpubl. data), underlie the Soldiers Cap Group iron-formations in the lower Soldiers Cap Group and upper Fullarton River Group. The weaker Eu anomaly present in the Weatherly Creek iron-formation compared to the Mt Norna iron-formation may be a factor of mixing with a REE-rich sedimentary component, similar to detrital contamination proposed above for some major elements in the Weatherly Creek iron-formation. For example, Spry *et al.* (2000; Peter & Goodfellow 1996) proposed that a > ~30% detrital component is sufficient to mask hydrothermal Eu anomalies in chemical sediments. However, Weatherly Creek iron-formation samples with ≥30% detrital component still retained positive Eu anomalies (Figure 10a, b). Alternatively, studies of REE systematics at the Cannington Broken Hill-type deposit (Bodon 1998) indicate that Eu characteristics may be imposed during subsurface alteration; this could account for the presence of strong positive Eu anomalies in those Weatherly Creek iron-formation samples with high detrital contents. In summary, the positive Eu anomalies present here for Soldiers Cap Group iron-formations provide evidence that the Weatherly Creek and Mt Norna iron-formations were chemically influenced by reduced fluids with reservoir temperatures ≥250°C.

The most likely cause of the physicochemical change necessary for the precipitation of Eu and the associated silicates and oxides in the system studied here is the presence of cold, oxic seawater. Some evidence for this exists in the weak negative Ce anomaly present in all samples from both the Weatherly Creek iron-formation and Mt Norna iron-formation (Figure 10a, b); this appears to have been strongest during Fe precipitation, based upon the increasing strength of Ce depletion at higher Fe contents. Strong negative Ce anomalism in volcano-sedimentary systems is generally considered indicative of seawater mixing (Elderfield & Greaves 1981, 1982; Barrett *et al.* 1990; Davidson 1996; Large *et al.* 1996; Peter & Goodfellow 1996). Additionally, the negative correlation between Al_2O_3 and Ce/Ce^* (Figure 8d) indicates the presence in the system of detritus lacking a Ce anomaly (Peter & Goodfellow 1996).

Mafic magmatism and iron-formations

The metatholeiites of the upper Soldiers Cap Group are largely synsedimentary intrusive sills and flows that are associated with the main iron-formation positions, but were most voluminous following their deposition (forming the Toole Creek Volcanics). This is notably in contradiction to relationships in many volcano-sedimentary basins, where hydrothermal sediments conventionally accumulate in the wake of major volcanic episodes.

The synsedimentary sills and their source chambers in the Maronan Supergroup likely produced a significant increase in local and regional heat flow, providing a potential heat source for the generation of hydrothermal components in the iron formations, either through local heating around sills or larger scale basinal convection processes. Einsele *et al.* (1980) proposed that heating adjacent to dolerite sills in saturated sediments as shallow as 100 m below the surface, can be as high as 400°C at the sill–sediment contact. Conceivably, the temperatures of ≥250°C necessary for the production of the Weatherly Creek iron-formation Eu anomalies could have been attained by the intrusion of such sills into the wet, unconsolidated sediments of the Soldiers Cap Group, setting up local convection cells that leached local sediments and mobilised components to the sediment–water interface. However, two important factors preclude this interpretation. These are the lack of observed metal (Pb–Zn) sulfide assemblages expected through the exhalation of >250°C fluids, and, most importantly, local sill-driven convection should have produced chemical sediments close to but above the level of most sills, rather than at the three extensive stratigraphic levels outlined in the present study. Preferably, deep-seated basin-scale convection cells were driven by heating from large mafic magma chambers within and below the Fullarton River Group, producing regional over-pressured aquifers with temperatures ≥250°C. Breaching of one of these aquifers by a major extensional fault system, and expulsion via one or more of these faults, provided a mechanism to develop hydrothermal chemical sediments in sub-basins at similar stratigraphic levels across the basin (Figure 12).

Sources of anomalous phosphorus

P_2O_5 up to 15wt% is an anomalous feature of the Weatherly Creek iron-formation, compared to iron-formations both globally and elsewhere in the Soldiers Cap Group (Figure 6a). Phosphorus, probably as fine-grained apatite, could have been introduced into the Weatherly Creek iron-formation system by a number of processes, discussed here.

Biogenic processes are a common cause of P concentration on the sea floor but can be discounted here, based on a lack of evidence of any remnant biological activity in the Soldiers Cap Group apart from sporadic and poorly understood black shales in the Toole Creek Volcanics (not associated with iron-formation). Adsorption of P (orthophosphates) onto Fe-oxides related to biogenic activity and chemical precipitation from the water column (Bjerrum & Canfield 2002) is a possibility, but the lack of Fe–P positive correlation in the Weatherly Creek iron-formation precludes such a mechanism (Davidson *et al.* 2001).

An extrabasinal or local detrital Soldiers Cap Group source of P (Bjerrum & Canfield 2002) derived from temporally equivalent, felsic volcanics or sedimentary units is unlikely because the sedimentary conditions at the time of deposition were not appropriate for placer formation and there is no evidence in the whole-rock data for a component of detrital P. Adjacent metasediments of the Soldiers Cap Group generally have low modal apatite (<0.5%) and P_2O_5 of 0.01–0.21 wt% (O. J. Hatton unpubl. data). Mechanical reworking and 'winnowing' of components lighter than apatite by active sedimentary currents as suggested by Yang and Zeng (1993) is also discounted, because except for one of the Pumpkin Gully iron-formations, sedimentary reworking is generally absent. Enrichment through metamorphic P-metasomatism is a possibility. However, no metasomatic textures were observed associated with

apatite. Similarly, post-depositional diagenetic enrichment of phosphate as suggested by Robertson (1982) is also unlikely given the lack of phosphatic rocks nearby.

The positive correlation of Mn, Ca, P and Eu (Figure 9) in the Weatherly Creek iron-formation, combined with a positive Eu anomaly (Figure 10a), are features consistent with a sea-floor hydrothermal origin for P. Hence, a major component of the elevated P values in the Weatherly Creek iron-formation are interpreted here to have resulted from hydrothermal precipitation of apatite. Elevated P (+/-Fe–Mn–Ca) values are a common feature of Broken Hill-type deposits and associated chemical sediments (Stanton 1972, 1976a, b; Lottermoser 1989; Lottermoser et al. 1994; Lottermoser & Ashley 1995; Walters 1996) and have been noted at Cannington (Bodon 1998). This distinctive geochemical signature provides an important potential link between the Soldiers Cap Group iron-formations and Broken Hill-type mineralisation.

An insight into the source of hydrothermal P enrichment in both Broken Hill-type deposits and the Soldiers Cap Group iron-formations is afforded by comparison to other Fe–P ore types. A primary magmatic fluid, derived from intermediate–felsic intrusives, is suggested by Frietsch and Perdahl (1995) for the apatite-rich iron-formations of Kiruna, Sweden, and the comparable Avnik ores in Turkey (Helvaci 1984). However, these source rocks are not known in the Soldiers Cap Group. Additionally, the Weatherly Creek and Mt Norna iron-formations do not have the chondrite-normalised negative Eu anomaly that is characteristic of Kiruna-style deposits (Frietsch & Perdahl 1995). Treloar and Colley (1996) studied massive, magnetite–apatite ores hosted by a sequence of calc-alkaline andesites and basalts, associated with iron-enriched magmas in northern Chile. They proposed, based upon detailed mineral chemistry and paragenetic studies, that these deposits were produced by release of hot (sub-magmatic: 450–600°C), acidic and reduced Fe–P-enriched fluids from fractionated Fe-rich magmas in which

magnetite–apatite crystallisation was suppressed until late in the magmatic history (Brooks et al. 1991). These fluids mixed with meteoric fluids in the host rocks, providing the physicochemical changes necessary to deposit high concentrations of Fe-oxides and apatite.

While the overall tectonic environment, temperature of formation, and geochemistry differ from the epigenetic, structurally controlled, deposits described by Treloar and Colley (1996), the method of fluid genesis could be relevant to the genesis of the Soldiers Cap Group iron-formations. Williams (1998) interpreted metatholeiites of the Soldiers Cap Group as ferrobasalts produced in high-level magma chambers characterised by suppression of magnetite and apatite crystallisation, accounting for their distinct Fe-enrichments. Although the link is difficult to test, a potential source of P in the hot Soldiers Cap Group basinal aquifers (interpreted by us to have supplied hydrothermal fluid to the Weatherly Creek iron-formation) may therefore have been magmatic fluids exsolved from very fractionated underlying mafic magma chambers.

CONCLUSIONS

Despite the high metamorphic grade and polydeformational history, primary depositional features and geochemical signatures are preserved in the iron-formations studied in detail here. They are composed of petrographically and chemically distinct garnet quartzites, transitional iron-formations and banded iron-formations. Contact relations with surrounding lithologies show these, and other stratigraphically equivalent lenses, to be broadly contemporaneous to host sediments and metatholeiite intrusions.

Fe and Si phases were precipitated from lower temperature hydrothermal fluids, whereas Mn, P, Mg, REE and possibly As and U, were preferentially coprecipitated in apatite–Mn oxyhydroxide aggregates from higher temperature solutions, and shared a spatial relationship with
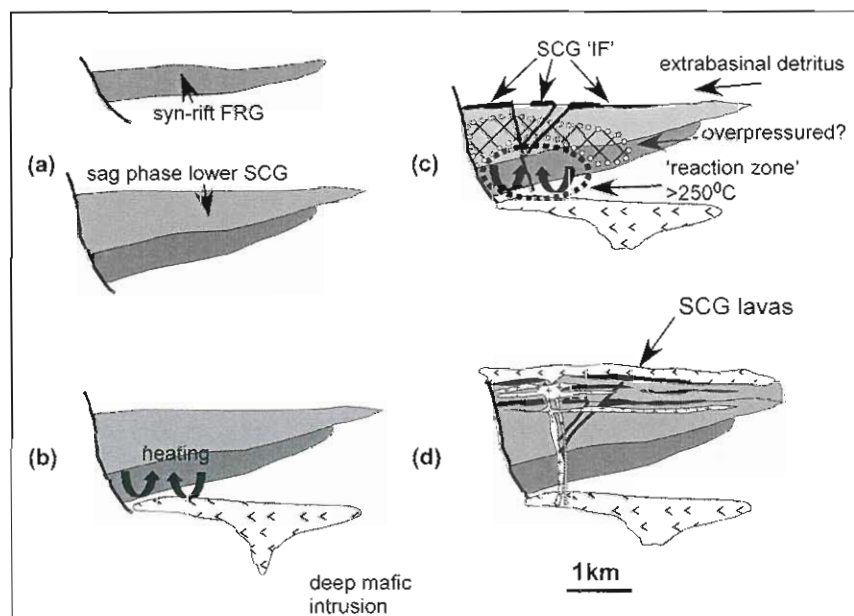

Figure 12 Schematic diagram of the evolution of the Soldiers Cap Group iron-formations. (a) deposition of the underlying Fullarton River Group (FRG) and deposition of the lower Soldiers Cap Group (SCG). (b) Intrusion of deep-seated mafic body, which causes heating in the lower basin levels. (c) Set-up of convection cells and breaching by extensional faults resulting in expulsion of hydrothermal fluids, which combine with extrabasinal detritus to produce the Soldiers Cap Group iron-formations. (d) Continued rifting and volcanism/magmatism and deposition of base-metal-enriched iron-formations.

detrital phases that is not understood, indicated by positive correlations between hydrothermal and detrital indicator elements. Al, Ti, Zr, Mg, Ca and K were mainly contributed to the iron-formations as mafic sedimentary detritus, the source of which is probably mixed Cover Sequence 1 and 2 units to the west and north in the Eastern Succession. Hydrogenous processes were responsible for deposition of Ni, but their role cannot be confidently distinguished for enriched elements such as As and U. Normalised REE patterns are remarkably similar to those of modern metalliferous sea-floor sediments and display anomalies controlled by high-temperature hydrothermal activity (Eu), seawater (Ce), and detrital minerals (LREE).

The favoured origin for the iron-formations of the upper Soldiers Cap Group is as products of the mixing and evolution of hydrothermal fluids and seawater at or near a sediment–water interface. Relevant genetic models for iron-formations commonly refer to processes involving: (i) sea-floor mounds/sinters in volcanogenic massive sulfide systems (Davidson *et al.* 2001); or (ii) precipitation from hydrothermal vents or vent fields on the sea floor into stratified sub-basins (Newbery 1991; Peter & Goodfellow 1996). The banded nature, lack of metal sulfides and the spatial restriction of Soldiers Cap Group iron-formations to more quiescent sedimentary environments, favour the latter depositional setting.

Following emplacement of Fe-tholeiite magma chambers into the base of the thick sedimentary pile of the Maronan Supergroup, hot, acidic Fe–P-rich fluids, possibly with a mafic-sourced Fe–P magmatic component, circulated in a regional aquifer, confined by a seal such as the clay-rich Llewellyn Creek Formation (Figure 12). Reaction of this fluid with feldspar at temperatures ≥250°C in the lower feldspathic Maronan Supergroup released Eu and, potentially, base metals. The fluids ascended to the surface along extensional faults to pond and mix with cold, oxic seawater in relatively quiescent segments of a storm-dominated shelf, precipitating Fe, P and Mn-rich minerals on the sea floor (Figure 12). Extrabasinal sources provided detritus deposited at the same time as the hydrothermal precipitates, which in places influenced the primary geochemical signature of the iron-formations. Tholeiitic magmas began to form the most voluminous sill complexes after the deposition of the Soldiers Cap Group iron-formations in the upper Mt Norna Quartzite and Toole Creek Volcanics. This provided evidence that large-scale fluid release and exhaustion of the deep aquifer occurred prior to the peak of magmatic activity (Figure 12).

The presence of the distinctive Broken Hill-type Ca–Fe–Mn–P and REE geochemical 'exhalite' signature, and the presence of numerous iron-formations, which are considered in some cases to be lateral markers but not direct vectors to ore (Walters 1996), suggests that the Soldiers Cap Group may host as yet unidentified base-metal mineralisation of this style. Further work is required to determine if lateral chemical zonation exists at >1 km scales within each of the three main iron-formations of the Soldiers Cap Group. For instance, a regional study of the isotopic characteristics of each horizon may provide vectors to hotter and/or more hydrothermally active areas with greater base-metal-forming potential, either at the same stratigraphic level, as appears to be the case at Pegmont

(Newbery 1991), or in subsurface pipes. Significantly, in targeting basins with two major rift stages, the Soldiers Cap Group provides evidence that metalliferous fluids with Broken Hill-type chemical signatures may be released prior to, rather than during or after, the second main tectonomagmatic event.

ACKNOWLEDGEMENTS

REFERENCES

ARNOLD G. 1983. The Cloncurry Authorities to Prospect. *BHP–Utah Development Co. Miscellaneous Report* 1117, April 1983.

ASHLEY P. M. 1983. *Recent Exploration Results from the Monakoff Prospect, Near Cloncurry, Northwest Queensland.* Minerals Department Esso Australia Ltd.

BARRETT T. J., JARVIS I. & JARVIS K. E. 1990. Rare earth element geochemistry of massive sulphides-sulphates and gossans on the Southern Explorer Ridge. *Geology* 18, 583–586.

BAU M. 1991. Rare-earth element mobility during hydrothermal and metamorphic fluid–rock interaction and the significance of the oxidation state or europium. *Chemical Geology* 93, 219–230.

BEARDSMORE T. J., NEWBERY S. P. & LAING W. P. 1988. The Maronan Supergroup: an inferred early volcanosedimentary rift sequence in the Mount Isa Inlier, and it's implications for ensialic rifting in the middle Proterozoic of northwest Queensland. *Precambrian Research* 40/41, 487–507.

BELL T. H. & HICKEY K. A. 1996. Multiple deformations with successive subvertical and subhorizontal axial planes: their impact on geometric development and significance for mineralisation and exploration in the Mt Isa region. *James Cook University Economic Geology Research Unit Contribution* 55, 14.

BETTS P. G., AILLERES L., GILES D. & HOUGH M. 2000. Deformation history of the Hampden Synform in the Eastern Fold Belt of the Mt Isa terrane. *Australian Journal of Earth Sciences* 47, 1113–1126.

BIERLEIN F. P. 1995. Rare-earth element geochemistry of clastic and chemical metasedimentary rocks associated with hydrothermal sulphide mineralisation in the Olary Block, South Australia. *Chemical Geology* 122, 77–98.

BINGEN B., DEMAIFFE D. & HERGOTEN J. 1996. Redistribution of rare earth elements, thorium, and uranium over accessory minerals in the course of amphibolite to granulite facies metamorphism: the role of apatite and monazite in orthogneisses from southeastern Norway. *Geochimica et Cosmochima Acta* 60, 1341–1354.

BJERRUM C. J. & CANFIELD D. E. 2002. Ocean productivity before about 1.9 Gyr ago limited by phosphorus adsorption onto iron oxides. *Nature* **417**, 159–162.

BLAKE D. H. 1987. Geology of the Mt Isa Inlier and environs, Queensland and Northern Territory. *Bureau of Mineral Resources Bulletin* **225**.

BODON S. B. 1996. Genetic implications of the paragenesis and rare-earth geochemistry at the Cannington Ag–pb–zn Deposit, Mt Isa Inlier, Northwest Queensland. *In*: Pongratz J. & Davidson G. eds. *New Developments in Broken Hill-type Deposits*, pp. 133–144. University of Tasmania, CODES Special Publication 1.

BODON S. B. 1998. Paragenetic relationships and their implications for ore genesis at the Cannington Ag–Pb–Zn deposit, Mount Isa Inlier, Queensland, Australia. *Economic Geology* **93**, 1463–1488.

BOYNTON W. V. 1984. Geochemistry of the rare-earth elements: meteorite studies. *In*: Henderson P. ed. *Rare Earth Element Geochemistry*, pp. 63–114. Elsevier, Amsterdam.

BROOKS C. K. & LARSEN L. M. & NIELSEN T. F. D. 1991. Importance of iron-rich tholeiitic magmas at divergent plate margins. *Geology* **19**, 269–272.

COURTOIS C. & TREUILL M. 1977. Distribution des terres rares et de quelques elements en trace dans les sediments recents des fosses de la Mer Rouge. *Chemical Geology* **20**, 57–72.

DAVIDSON G. J. 1996. Styles and timing of iron enrichment in the Mt Isa Eastern Succession. *In*: Baker T., Rotherham J., Richmond J., Mark G. & Williams P. eds. *MIC ''96 New Developments in Metallogenic Research: the Mcarthur, Mt Isa, Cloncurry Minerals Province*, pp. 40–43. James Cook University, Economic Geology Research Unit Contribution 55.

DAVIDSON G. J. 1998. Variation in copper-gold styles through time in the Proterozoic Cloncurry goldfield, Mt Isa Inlier: a reconnaissance view. *Australian Journal of Earth Sciences* **45**, 445–462.

DAVIDSON G. J. & DAVIS B. K. 1997. Characteristics of the Monakoff Cu–Au–F–Ba–Mn deposit, Mt. Isa Eastern Succession. *AMIRA Final Report* **2**, 13-1–13-53.

DAVIDSON G. J., DAVIS B. K. & GARNER A. 2002. Structural and geochemical constraints on the emplacement of the Monakoff oxide Cu–Au (Co–U–REE–Ag–Pb–Zn) deposit, Mt Isa Inlier Australia. *In*: Porter T. M. ed. *Hydrothermal Iron Oxide Copper–gold and Related Deposits, a Global Perspective*, Vol. 2, pp. 49–76. PGC Publishing, Adelaide.

DAVIDSON G. J., STOLZ A. J. & EGGINS S. M. 2001. Geochemical anatomy of silica iron exhalites: evidence for hydrothermal oxyanion cycling in response to vent fluid redox and thermal evolution (Mt. Windsor Subprovince, Australia). *Economic Geology* **96**, 1201–1226.

DE JONG G. & WILLIAMS P. J. 1995. Giant metasomatic system formed during exhumation of mid-crustal Proterozoic rocks in the vicinity of the Cloncurry Fault, northwest Queensland. *Australian Journal of Earth Sciences* **42**, 281–290.

DEER W. A., HOWIE R. A. & ZUSSMAN J. 1992. *An Introduction to the Rock-Forming Minerals* (2nd edition). Longman, Harlow.

DERRICK G. M., WILSON I. H. & HILL R. M. 1976. Revision of stratigraphic nomenclature in the Precambrian of northwest Queensland. V: Soldiers Cap Group. *Queensland Government Mining Journal* **77**, 601–604.

DYMOND J., CORLISS J. B., HEATH G. R., FIELD C. W., DASCH E. J. & VEEH E. H. 1973. Origin of metalliferous sediments from the Pacific Ocean. *Geological Society of America Bulletin* **84**, 3355–3372.

EINSELE G., GIESKES J. M. & CURRAY J. R. 1980. Intrusion of basaltic sills into highly porous sediments and resulting hydrothermal activity. *Nature* **283**, 441–445.

ELDERFIELD H. & GREAVES M. J. 1981. Negative cerium anomalies in the rare-earth element patterns of oceanic ferromanganese nodules. *Earth and Planetary Science Letters* **55**, 163–170.

ELDERFIELD H. & GREAVES M. J. 1982. The rare earth elements in seawater. *Nature* **296**, 214–219.

ETHERIDGE M. A., RUTLAND R. W. R. & WYBORN L. A. I. 1987. Orogenesis and tectonic process in the Early to Middle Proterozoic of northern Australia. *In*: Kroner, A., ed. *Proterozoic Lithosphere Evolution*, pp. 131–147. American Geophysical Union Geodynamics Series **17**.

FRIETSCH R. & PERDAHL J. A. 1995. Rare earth elements in apatite and magnetite in Kiruna-type ores and some other iron ore types. *Ore Geology Reviews* **9**, 489–510.

GERMAN C. R., CAMPBELL A. C. & EDMOND J. M. 1991. Hydrothermal scavenging at the Mid-Atlantic ridge: modification of trace element dissolved fluxes. *Earth and Planetary Science Letters* **107**, 101–114.

GLIKSON A. Y. & DERRICK G. M. 1978. Geology and geochemistry of the Middle Proterozoic basic volcanic belts, Mt Isa/Cloncurry northwestern Queensland. *Bureau of Mineral Resources Record* 1978/48.

GROSS G. A. 1965. Geology of iron ore deposits in Canada. I. General geology and evaluation of iron deposits. *Geological Survey of Canada Economic Geology Report* **22**.

GROSS G. A. 1993. Element distribution patterns as metallogenetic indicators in siliceous metalliferous sediments. *Proceedings of the 29th International Geological Congress: Resource Geology Special Issue* **17** (C), 96–106.

HATTON O. J., BULL S. W. & DAVIDSON G. J. 2000. A review of the geological setting and sedimentology of the Proterozoic upper Soldiers Cap Group, Eastern Succession, rift fill in a Pb-Zn rich basin (Mt Isa Inlier, NW Qld). *Proceedings of New Ideas for a New Millennium, Cranbrook Workshop, May 6–7 2000.* <http://www.cyberlink.bc.ca/-ekcm/Abstracts.htm >.

HELVACI C. 1984. Apatite-rich iron deposits of the Avnik (Bingol) Region southeastern Turkey. *Economic Geology* **79**, 354–371.

JAQUES A. L. & BLAKE D. H. & DONCHAK P. J. T. 1982. Regional metamorphism in the Selwyn Range area, northwest Queensland. *BMR Journal of Australian Geology & Geophysics* **7**, 181–196.

KLEIN C. Jr. 1973. Changes in mineral assemblages with metamorphism of some Precambrian iron-formations. *Economic Geology* **68**, 1075–1088.

KLINKHAMMER G., ELDERFIELD J. M., EDMOND J. M. & MITRA A. 1994. Geochemical implications of rare-earth element patterns in hydrothermal fluids from mid-ocean ridges. *Geochimica et Cosmochima Acta* **58**, 5105–5113.

LAING W. P. 1990. The Cloncurry terrane: an allochthon of the Diamantina orogen rafted onto the Mt Isa Orogen, with its own distinctive metallogenic signature. *In*: *Mount Isa Inlier Geology Conference*, pp. 19–22. Victorian Institute of Earth and Planetary Sciences, Monash University, Melbourne.

LAING W. P. 1998. Structural–metasomatic environment of the East Mt Isa Block base-metal–gold province. *Australian Journal of Earth Sciences* **45**, 413–428.

LARGE R. R., BODON S. B., DAVIDSON G. J. & COOKE D. 1996. The chemistry of BHT oreformation: one of the keys to understanding the differences between SEDEX and BHT deposits. *In*: Pongratz J. & Davidson G. eds. New *Developments in Broken Hill-type Deposits*, pp. 105–112. University of Tasmania, CODES Special Publication 1.

LE MAITRE R. W. 1982. *Numerical Petrology: Statistical Interpretation of Geochemical Data*. Elsevier, Amsterdam.

LOTTERMOSER B. G. 1989. Rare-earth element study of exhalites within the Willyama Supergroup, Broken Hill Block, Australia. *Mineralium Deposita* **24**, 92–99.

LOTTERMOSER B. G. & ASHLEY P. M. 1995. Geochemistry and exploration significance of ironstones and barite rich rocks in the Proterozoic Willyama Supergroup. *Journal of Geochemical Exploration* **57**, 57–73.

LOTTERMOSER B. G., ASHLEY P. M. & PLIMER I. R. 1994. Iron formations, barite rocks and copper–gold mineralisation within the Willyama Supergroup, Olary Block, South Australia. *In*: *Australian Research on Ore Genesis Symposium*, pp. 8.1–8.5. Australian Mineral Foundation, Glenside.

MARK G. 1998. Albitite formation by selective pervasive sodic alteration of tonalite plutons in the Cloncurry district, northwest Queensland. *Australian Journal of Earth Sciences* **45**, 765–774.

MAYNARD J. B. 1983. *Geochemistry of Sedimentary Ore Deposits*. Springer-Verlag, Berlin.

MCLENNAN S. M. 1989. Rare earth elements in sedimentary rocks: influence of provenance and sedimentary processes. *Reviews in Mineralogy* **21**, 169–200.

MICHARD A. 1989. Rare earth element systematics in hydrothermal fluids. *Geochimica et Cosmochima Acta* **53**, 745–750.

MICHARD A. & ALBERADE F. 1986. The REE content of some hydrothermal fluids. *Chemical Geology* **55**, 51–60.

MICHARD A., ALBERADE F., MICHARD G., MINSTER J. F. & CHARLOU J. L. 1983. Rare earth elements and uranium in high-temperature

solutions from the East Pacific Rise hydrothermal vent field (13°N). *Nature* 303, 43–65.

Mills R. A. & Elderfield H. 1995. Rare-earth element geochemistry of hydrothermal deposits of the active TAG Mound, 26°N Mid-Atlantic Ridge. *Geochimica et Cosmochima Acta* 59, 3511–3524.

Morris R. C. 1985. Genesis of iron ore in banded iron formations by supergene and supergene-metamorphic enrichment processes: a conceptual model. *In:* Wolf K. H. ed. *Handbook of Stratabound and Stratiform Ore Deposits,* Vol. 13, pp. 73–225. Elsevier, Amsterdam.

Newbery S. P. 1991. Iron formation hosted base-metal mineralisation of the Cloncurry terrane, Mount Isa Inlier. *In: Base Metal Deposits Symposium, Townsville, April 1991,* pp. 89–99. James Cook University Economic Geology Research Unit Contribution 38.

O'Dea M. G., Lister G. S., MacCready T., Betts P. G., Oliver N. H. S., Pound K. S., Huang W. & Valenta R. K. 1997. Geodynamic evolution of the Proterozoic Mount Isa Terrane. *In:* Burg J. P. & Ford M., eds. *Orogeny Through Time,* pp. 99–122. Geological Society of London Special Publication 121.

Page R. W. & Sun S-S. 1998. Aspects of geochronology and crustal evolution in the Eastern Fold Belt, Mt Isa Inlier. *Australian Journal of Earth Sciences* 45, 343–362.

Parr J. M. 1992. Rare-earth element distribution in exhalites associated with Broken Hill-type mineralisation at the Pinnacles deposit, New South Wales, Australia. *Chemical Geology* 93, 219–230.

Peter J. M. & Goodfellow W. D. 1996. Mineralogy, bulk and rare earth geochemistry of massive sulphide-associated hydrothermal sediments of the Brunswick Horizon, Bathurst Mining Camp, New Brunswick. *Canadian Journal of Earth Sciences* 33, 252–283.

Pollard P. J. & Perkins C. 1997. ⁴⁰Ar/³⁹Ar geochronology of alteration and Cu–Au–Co mineralization in the Cloncurry district, Mount Isa Inlier, Australia. *In: Cloncurry Base Metals and Gold.* AMIRA/ARC project P438, Section 3-1-3-40.

Powell C. McA., Oliver N. H. S., Zheng-Xiang L., Martin D. McB. & Ronasezki J. 1999. Synorogenic hydrothermal origin for giant Hamersley iron oxide ore bodies. *Geology* 27, 175–178.

Robertson B. T. 1982. Occurrence of epigenetic phosphate minerals in a phosphatic iron formation, Yukon Territory. *Canadian Mineralogist* 20, 177–187.

Rockware. 2003. *MVSP a multivariate statistical package for PCs.* RockWare, Golden, CO.

Rollinson H. 1993. *Using Geochemical Data: Evaluation, Presentation and Interpretation.* Longman Scientific & Technical, New York.

Rubenach M. J. & Barker A. J. 1998. Metamorphic and metasomatic evolution of the Snake Creek Anticline, Eastern Succession, Mt Isa Inlier. *Australian Journal of Earth Sciences* 45, 363–372.

Ryburn R. B., Wilson I. H., Grimes K. G. & Hill R. M. 1987. *Cloncurry 1:100 000 Geological Sheet.* Bureau of Mineral Resources, Canberra.

Solomon M. J. & Sun S-S. 1997. Earth's evolution and mineral resources, with particular emphasis on volcanic-hosted massive sulphide deposits and banded iron formations. *AGSO Journal of Australian Geology & Geophysics* 17, 33–48.

Spry P. G., Peter J. M. & Slack J. F. 2000. Meta-exhalites as exploration guides to ore: *Reviews in Economic Geology* 11, 163–201.

Stanton R. L. 1972. A preliminary account of the chemical relationships between sulfide lode and 'banded iron formation' at Broken Hill, New South Wales. *Economic Geology* 67, 1128–1145.

Stanton R. L. 1976a. Petrochemical studies of the ore environment at Broken Hill New South Wales, 2, Regional metamorphism of banded iron formations and their immediate associates. *Transactions of the Institution of Mining and Metallurgy* B85, 118–131.

Stanton R. L. 1976b. Petrochemical studies of the ore environment at Broken Hill, New South Wales, 3, Banded iron formations and sulfide orebodies, constitutional and genetic ties. *Transactions of the Institution of Mining and Metallurgy* B85, 132–141.

Stanton R. L. & Vaughan J. P. 1979. Facies of ore formation: a preliminary account of the Pegmont deposit as an example of potential relations between small 'iron formations' and stratiform sulphide ores. *Proceedings of the Australasian Institute Of Mining and Metallurgy* 270, 25–38.

Sverjensky D. A. 1984. Europium equilibria in aqueous solution. *Earth and Planetary Science Letters* 67, 70–78.

Taylor S. R. & McLennan S. 1985. *The Continental Crust: its Composition and Evolution.* Blackwell, Oxford.

Toyoda J. & Masuda A. 1991. Chemical leaching of pelagic sediments: identification of the carrier of the Ce anomaly. *Geochemical Journal* 25, 95–119.

Treloar P. J. & Colley H. 1996. Variations in F and Cl contents in apatites from magnetite–apatite ores in northern Chile, and their ore-genetic implications. *Mineralogical Magazine* 60, 285–301.

Vaughan J. P. & Stanton R. L. 1984. Stratiform Pb–Zn mineralisation in the Kuridala Formation and Soldiers Cap Group, Mount Isa Block, NW Queensland. *In: The Mineral Potential of Northern Australia and Changing Concepts of Development: Australasian Institute of Mining and Metallurgy 1984 Annual Conference, Darwin,* pp. 307–317. Australasian Institute Of Mining and Metallurgy Conference Series 13.

Walters S. J. 1996. An overview of Broken Hill-Type deposits. *In:* Pongratz J. & Davidson G. eds. *New Developments in Broken Hill-type Deposits,* pp. 1–10. University of Tasmania, CODES Special Publication 1.

Williams P. J. 1997. Notes to accompany the 1:25 000 scale geological map of the Western Pumpkin Gully Syncline, Cloncurry District, NW Queensland. *In:* Pollard P. J. ed. *Cloncurry Base Metals and Gold 1997 Annual Report,* pp. 13A-1–13A-9. AMIRA P438 Final Report, 2.

Williams P. J. 1998. Magmatic iron enrichment in high-iron metatholeiites associated with 'Broken Hill-type' Pb–Zn–Ag deposits, Mt Isa Eastern Succession *Australian Journal of Earth Sciences* 45, 389–397.

Wyborn L. A. I., Page R. W. & McCulloch M. T. 1988. Petrology, geochronology and isotope geochemistry of the post-1820 Ma granites of the Mt Isa Inlier: mechanisms for the generation of Proterozoic anorogenic granites *Precambrian Research* 40/41, 509–541.

Wyborn L. A. I. 1998. Younger ca 1500 Ma granites of the Williams and Naraku Batholiths, Cloncurry district, eastern Mt Isa Inlier, geochemistry, origin, metallogenic significance and exploration indicators. *Australian Journal of Earth Sciences* 45, 397–412.

Yang W. & Zeng Y. 1993. On the origin of Precambrian phosphorites in Central Guizhou, China. *Proceedings of the 29th International Geological Congress: Resource Geology Special Issue* 17 (C), 138–142.

APPENDIX 1: SAMPLE LOCATIONS

Sample no.	Easting	Northing
WC02	470869mE	7678171mN
WC10	470916mE	7680359mN
WC27	470817mE	7677623mN
WC28	470819mE	7677651mN
WC29	470823mE	7677543mN
WC-78	470863mE	7678423mN
WC-81	470934mE	7677762mN
WC-86	470837mE	7677920mN
WC-89	470924mE	7677640mN
WC-91	470941mE	7677514mN
WC-92	470953mE	7678243mN
WC-95	470982mE	7678623mN
WC-97	470988mE	7678738mN
WC-98	470985mE	7678852mN
WC-99	471003mE	7679349mN
WC110	468864mE	7687042mN
WC112	468843mE	7687123mN
WC114	468798mE	7687294mN
WC117	468829mE	7687732mN
WC119	468821mE	7687593mN
WC120	468822mE	7687843mN